

Spatial compartmentalisation of regulatory T cells within intestinal lymphoid tissue

Yisu Gu

University of Oxford
St. Anne's College

A Thesis Submitted for the Degree of Doctor of Philosophy
Michaelmas Term, 2020

Abstract

Gut tissue-associated lymphoid structures include a heterogenous spectrum of lymphoid clusters of varying size and maturity, however little is known about their functional relevance. We hypothesise that lymphoid structure may promote gut homeostasis through a number of potential local mechanisms that is currently unclear.

Firstly, signalling and subsequent repair of tissue injury is regulated by the alarmin IL-33, which has been shown to be expressed by non-immune cells within lymphoid structures. IL33 signals through its receptor ST2 which present on a subset of Tregs. Thus, IL-33 signalling to $ST2^+$ Tregs within lymphoid structures may constitute one important pathway that promotes gut health. Secondly, lymphoid structures have been reported to act as regional hubs of immunity. Local priming of commensal-reactive T cells within lymphoid structures could promote the activation and function of T cells, inducing their tolerance towards intestinal microbiota.

Using a combination of multi-parameter flow cytometry and histo-cytometry, we firstly characterised lymphoid structures of the murine gut, and report distinct differences in their architecture and complexity at different anatomical sites. We confirmed the presence of both IL-33-producing cells and $ST2^+$ Tregs at close proximity to each other within lymphoid structures. However, $ST2^+$ Tregs were not found to be spatially closer to IL-33-producing cells compared to the $ST2^-$ Treg subset during health and disease, indicating a close interaction may not be strictly necessary for optimal IL-33 cytokine function.

Next, we employed a T cell receptor transgenic mouse model specific to the pathobiont *Helicobacter hepaticus*, and used advanced *in vivo* live imaging techniques to study the compartmentalised induction, phenotype and function of commensal-reactive T cells within lymphoid structures as compared to the surrounding lamina propria tissue. Our results show a spatial compartmentalisation of regulatory IL-10 production by *Helicobacter hepaticus*- specific Tregs in the lamina propria tissue, distinct from lymphoid structures. Unique transcriptional differences in dendritic cells at these distinct spatial sites may drive IL-10 production at some, but not other locations within the tissue micro-environments.

Altogether, we highlight the complex cellular interactions that occur within intestinal tissue-associated lymphoid structures that promote gut health. We use advanced imaging techniques to further our understanding of the behaviour of T cells in response to microbial antigen *in vivo* and our findings show tissue-associated lymphoid structures and the lamina propria tissue support Treg functions in distinct ways.

Acknowledgements

First and foremost, I would like thank Professor Fiona Powrie for her excellent supervision and guidance throughout my DPhil. She continuously challenges me to ask questions and develop more independence in thinking and planning experiments. With her support, I have had many opportunities during my DPhil to attend and present my research at national and international meetings. In addition, I am grateful to Professor David Roberts who has acted as my clinical supervisor, providing translational guidance and invaluable career advice during my DPhil.

I would also like to give special thanks to my Post-Doc supervisor Dr Emily Thornton who has provided me with much day-to-day help. She has shown so much patience, particularly in the early days when I was new to science. I have particularly enjoyed our weekly 'catch up' meetings, where her enthusiasm for science has inspired me to pursue further scientific training after my DPhil. I am so grateful to Emily for her ongoing encouragement and belief in my abilities.

My DPhil training has been enriched by the guidance of so many members of the Powrie lab who have been incredibly helpful in showing me new lab techniques, providing feedback at lab meetings and general support during the more challenging times of the DPhil. In particular, I'd like to thank Drs Claire Pearson, Samuel Bullers, Natasha Whibley, Lilian Lam, Matthias Friedrich and Grigory Ryzhakov. I am also particularly grateful to Dr Agnieszka Chomka who taught me many lab techniques and animal handling procedures specific to the IL-33 project.

Finally, I would like to thank the Wellcome Trust for the generous DPhil funding, provided to me through the Wellcome Trust Clinical Research Training Fellowship. Additionally, the Academic Clinical Fellowship supported by OUCAGS and the starter fund from the OHSRC research grant gave me the opportunity to gather preliminary data to secure a Wellcome Trust funding.

Table of Contents

Abstract 2

Acknowledgements 4

Table of Contents 6

Abbreviations 9

..... 9

Chapter 1. General Introduction 12

..... 12

1.1 The mucosal immune system 12

1.2 Inflammatory bowel disease 14

1.3 Experimental models of colitis 16

1.3.1 *Helicobacter hepaticus*/anti-IL10R model of colitis 18

1.3.2 Dextran sodium sulfate model of colitis 20

1.4 Innate immune cells involved in the adaptive immune response 21

1.4.1 Mononuclear phagocytes 21

1.4.2 Innate lymphoid cells 24

1.5 The gut associated lymphoid tissue 25

1.6 Interleukin 33 27

1.6.1 IL-33 release, regulation and signalling 27

1.6.2 IL-33 in inflammatory disease 29

1.7 The mucosal adaptive immune system 30

1.7.1 B cells 30

1.7.2 T cells 32

1.7.2.1 $CD4^+$ T cell development and differentiation 33

1.7.2.2 Th1 cells 36

1.7.2.3 Th2 cells 37

1.7.2.4 Th17 cells 38

1.7.2.5 T follicular helper cells 40

1.7.2.6 T regulatory cells 42

1.8 Host T cell-microbial cross-talk 53

1.9 Aims of the thesis 62

Chapter 2. Materials and Methods 63

2.1 Mice 63

2.2 *In vivo* experiments 64

2.2.1 *Helicobacter hepaticus*/anti-IL10R induction of colitis 64

2.2.2 Dextran sulphate sodium induction of colitis 64

2.2.3 Lymph node lymphocyte egress blocking experiment 65

2.3 Cell isolation **65**
2.3.1 Isolation of leukocytes from blood 65
2.3.2 Isolation of leucocytes from spleens and mesenteric lymph nodes 65
2.3.3 Isolation of leukocytes from the colon, caecum, caecal patch and organised lymphoid structures 66

2.4 Flow cytometry and cell sorting **67**
2.4.1 PMA/Ionomycin re-stimulation of cells for intracellular cytokine staining 67
2.4.2 Cell surface staining 67
2.4.3 Intracellular staining 68
2.4.4 Sorting and adoptive transfer of HH7-2tg cells 69

2.5 *In vitro* co-culture **69**

2.6 Imaging of *ex vivo* and *in vivo* tissue **70**
2.6.1 Immunofluorescent ex vivo tissue imaging 70
2.6.2 Two-photon microscopy 72
2.6.3 Blood vessel labelling 72
2.6.4 *In vivo* Image analysis and histo-cytometry 72

2.7 Statistical analysis **73**

Chapter 3. Solitary Isolated lymphoid tissue as a regulatory T cell niche ***74***

3.1 Introduction **74**

3.2 Results **79**
3.2.1 $ST2^+$ $Foxp3^+$ Tregs are unevenly distributed across the lower GI tract 79
3.2.2 The gut is associated with a diverse range of lymphoid structures 84
3.2.3 SILT composition varies between young and old mice 88
3.2.4 OLS form germinal centres during Hh/anti-IL10R colitis 92
3.2.5 OLS contain IL-33^+ cells in close proximity to Treg subsets 96 99
3.2.6 Compartmentalisation of Rorγt^+ Tregs in OLS during steady state and colitis 100
3.2.7 Colitis drives changes in the spatial compartmentalisation of Treg subsets relative to IL-33^+ cells in OLS 104

3.3 Discussion **109**

Chapter 4. The role of the tissue in modulating the T cell response to pathobionts ***114***

4.1 Introduction **114**

4.2 Results **118**
4.2.1 Validation of the antigen specificity of HH7-2tg T cells to *H.hepaticus* 118
4.2.2 HH7-2tg are present in SLOs prior to localising to gut tissue 124
4.2.3 HH7-2tg adopt a Treg phenotype within tissue sites 128
4.2.4 HH7-2tg adopt a T follicular helper cell phenotype at SLO sites 131
4.2.5 The tissue is the site of strongest HH7-2tg TCR stimulation 135
4.2.6 Interactions within tissue promote the highest production of IL-10 by HH7-2tg 141
4.2.7 MLNs are critical for Treg differentiation 145

4.3 Discussion **149**

Chapter 5. The role of lymphoid aggregates in modulating the T cell response to pathobionts ***157***

5.1 Introduction **157**

5.2 Results **161**

5.2.1 Experimental set up of two photon in vivo live imaging 161
5.2.2 TCR stimulated pathobiont-reactive T cells are evenly distributed within local tissue micro-niches 164
5.2.3 TCR-stimulated pathobiont-reactive T cells exhibit uniform TCR signal strength between tissue micro-niches. 168
5.2.4 FTY720 treatment does not alter the spatial compartmentalisation of Nur77^{GFP+} HH7-2tg T cells 171
5.2.5 IL-10^{+} HH7-2tg cells are predominantly positioned in the lamina propria, away from lymphoid aggregates 174
5.3 Discussion 178
Chapter 6. General discussion 186
References 191

Abbreviations

AIRE	Autoimmune Regulator
CD	Cluster of Differentiation
CNS	Conserved Noncoding sequence
CP	Caecal Patch
DAPI	4',6-Diamidino-2-Phenylindole
DSS	Dextran Sulphate Sodium
FACS	Fluorescence -activated Cell Sorting
FMO	Fluorescence minus one
Foxp3	Forkhead Box P3
FRC	Fibroblastic Reticular Cells
GALT	Gut associated lymphoid tissue
GF	Germ Free
GFP	Green Fluorescent Protein
GI	Gastrointestinal
MFI	Mean Fluorescent Intensity
GVHD	Graft Versus Host Disease
GWAS	Genome Wide Association Studies
HEV	High Endothelial Venule
IBD	Inflammatory Bowel Disease
IEL	Intraepithelial Lymphocyte
IFN	Interferon
Ig	Immunoglobulin
IHC	Immunohistochemistry
IL	Interleukin

ILC	Innate Lymphoid Cell
ILF	Isolated lymphoid Follicles
IPEX	Immunodysregulation Polyendocrinopathy Enteropathy X-Linked Syndrome
KO	Knock Out
LN	Lymph node
LP	Lamina Propria
LPS	Lipopolysaccharide
M Cell	Microfold Cell
mAb	Monoclonal Antibody
MHC	Major Histocompatibility Complex
MLN	Mesenteric Lymph Node
MyD88	Myeloid Differentiation Primary Response Gene 88
NK	Natural Killer cell
OD	Optical Density
OLS	Organised lymphoid structures
PDGFR	Platelet-Derived Growth Factor Receptor
PSA	Polysaccharide A
RA	Retinoic Acid
Rorγt	RAR-related orphan receptor-γt
SCFA	Short Chain Fatty Acid
SD	Standard Deviation
SFB	Segmented Filamentous Bacteria
SILT	Solitary Isolated Lymphoid Tissue
SNP	Single Nucleotide Polymorphism
SPF	Specific Pathogen Free
sST2	Soluble ST2
STAT	Signal Transducer and Activator of Transcription
TCR	T cell Receptor
Tfh	T follicular Helper cell
TGF	Transforming Growth Factor
Th	T helper cell

TLR	Toll-Like Receptor
TNBS	Trinitrobenzene Sulfonic Acid
TNF	Tumour Necrosis Factor
Treg	T regulatory cell
UC	Ulcerative Colitis
VAT	Visceral Adipose Tissue
WT	Wild Type

Chapter 1. General Introduction

1.1 The mucosal immune system

The mucosal immune system is defined as the body surfaces covered by a layer of mucus-secreting epithelium, namely the gastro-intestinal tract, the respiratory tract and the urogenital tract. These sites form the interface between the host self, and the foreign non-self. In the gut, there exists a continuous dialogue between the host immune system and the food and/or microbial antigens from potentially pathogenic and commensal micro-organisms that reside there. The gut is therefore a site of great immunological challenge, having to both tolerate the large array of commensal bacteria and ingested food proteins, whilst at the same time mount an appropriate immune response to harmful pathogens. As such, the gut is home to a diverse community of innate and adaptive immune cells that tightly regulate these opposing responses. Chronic inflammatory disorders such as inflammatory bowel disease (IBD) occur secondary to excessive immune responses to the commensal bacterial population (reviewed in [1]).

In cross section, the large intestine is divided into a number of distinct compartments: the innermost mucosa (which contains the epithelium, lamina propria and the muscular mucosae), the submucosa, the muscularis propria and the serosa. The most functionally complex layer is the mucosa, which is covered in a thick layer of mucus with anti-microbial properties. The epithelium, a single cell layer, plays critical roles in providing a physical barrier between the microbial species from the host. The lamina propria is a layer

of connective tissue, and along with the epithelium, contain the majority of the cells of the colonic innate and adaptive immune system.

The intestinal microbiome is defined as the total collection of micro-organisms that colonises the gastrointestinal tract. Bacteria form the most abundant group, along with smaller numbers of viruses, fungi, protozoa and archaea. The total concentration of bacteria varies across the length of the intestinal tract, but is estimated in the order of 10^{14}, with at least 1000 different species [2]. The vast majority of bacterial species belong to the phyla Firmicutes and Bacteroidetes [3]. Interestingly, the sum of all the different genes contained within the gut microbiome, the metagenome, totals more than 3 million distinct genes and exceeds the number of human genes by 150 times [4].

A symbiotic relationship exists between the gut and the microbiota, with interactions between the host immune system and bacterial species providing beneficial effects. Indeed, germ free mice that are devoid of all microbial colonisation exhibit underdeveloped immune systems, including less mature lymphoid structures, and deficiencies in T cell and antibody diversity (reviewed in [5]). Additionally, distinct bacterial species promote the breakdown of complex food components into essential vitamins and amino acids, whilst preventing colonisation of potentially pathogenic species through competition for niches in the intestinal tract (reviewed in [6]). For example, fermentation of starch by the commensal *Clostridia* produces the short-chain fatty acid butyrate which promotes the generation of extrathymic regulatory T cells [7]. Novel technological advances in microbial sequencing methods have highlighted disruption to the microbiome, or dysbiosis, to have far-reaching effects, being associated with numerous systemic autoimmune and inflammatory diseases such as inflammatory bowel disease,

diabetes, cancer and obesity [8-10]. However, it is currently unclear whether dysbiosis is the cause or effect of such pathologies.

1.2 Inflammatory bowel disease

Inflammatory bowel disease (IBD) is an umbrella term used to define a chronic inflammatory disorder of the gastrointestinal tract, and includes Crohn's disease (CD) and ulcerative colitis (UC). Inflammation of the intestinal mucosa results in relapsing episodes of abdominal pain, diarrhoea, per rectum bleeding and weight loss. IBD occurs in early life, with a UK prevalence of 157 per 100,000 for CD and 240 per 100,000 for UC [11]. The histological hallmarks of the disease include immune cell infiltration, goblet cell depletion and crypt abscess formation [12, 13].

IBD is a complex disease with a multifactorial aetiology that combines genetic, microbial, environmental and host immune factors. The pathogenesis is not fully understood, but is thought to occur in genetically susceptible individuals that develop a dysregulated immune response against distinct populations of the intestinal microbiome [14].

$CD4^+$ T cells play a key role in the pathogenesis of human IBD, with their influx into the gut mucosa during inflammatory flares of the disease. Prior to the discovery of Th17, CD had been associated with an aberrant Th1 response with high levels of IFN-γ [15], whilst UC was thought to be a Th2-driven disease induced by high expression levels of IL-4 and IL-13 [16, 17]. However, with the recent understanding of Th17 responses promoting inflammatory disorders, the classical Th1/Th2 paradigm has been revised. The main Th17 cytokines, IL-17 and IL-22, have been found elevated in the gut mucosa of CD and UC

patients [18-20]. Furthermore, IL23, primarily secreted by macrophages and dendritic cells is an important pro-inflammatory cytokine functioning to the maintain the Th17 lineage. In experimental models, absence of IL23 was associated with reduced colonic expression of TNF-α, IFN-γ and IL-6 with minimal disease pathology [21, 22]. Finally, regulatory T cells (Tregs) are an essential $CD4^+$ T cell subset required for the maintenance of homeostasis, and their absence drives colitis in response to the heavy burden of foreign microbial and food antigens encountered here. In experimental models of Treg depletion, the gastrointestinal tract forms the major site of inflammation [23]. Additionally, reduced numbers of Tregs both in the sera and colon of IBD patients have been observed [24].

The role of an altered gut microbiome, or dysbiosis in driving IBD has been shown in numerous studies. The most common pattern of dysbiosis in patients with IBD is one of loss of commensal bacteria diversity, particularly of the phyla Firmicutes and Bacteroides, with a relative increase of *Enterobacteriaceae* [25-27]. Furthermore, animal studies support a role for the microbiota in contributing to disease as many murine models of colitis are less severe in germ -free mice [28], whilst enteric bacteria are strictly necessary for the development of spontaneous colitis in IL-10 deficient mice [29]. Nevertheless it is not clear whether dysbiosis is a cause or an effect of inflammation, although faecal transfer studies from colitic donor mice into healthy hosts were able to demonstrate dysbiosis as a driver of disease [30, 31].

Additionally, the host's immune system, determined by the genetic make-up of the individual, and its response to microbial and environmental factors plays a critical role in IBD pathogenesis. The earliest epidemiological studies demonstrated clear family clustering with high sibling risk ratios that were shown to be due to genetics rather than

shared environmental factors [32]. Crohn's disease was amongst the first diseases to be studied using GWAS, and was used to identify a strong protective variant in IL23R, which encodes a subunit of the receptor for the inflammatory cytokine IL-23 [33]. Further GWAS studies were then used in larger sample sizes to identify both the innate (CARD9, NKX2-3) and the adaptive (TNFSF15, PTPN2, IL12B) immune pathways in IBD [34]. Additionally, defective regulatory immune pathways have also been demonstrated to drive IBD development, the most notable being distinct homozygous mutations of the regulatory IL-10 receptor having a strong association with early onset IBD, highlighting a breakdown of the usual regulatory pathways can drive IBD pathology [35].

The major goal of successful IBD therapy involves changing the lifelong course of disease, improve the patient's quality of life and reducing disease-related disabilities. Although much progress has been made in understanding the molecular pathogenesis of IBD, however to date, no cure exists. Recent therapies include anti-TNF monoclonal antibody blockade which have improved the disease course of many patients with CD, although not all patients are responsive to anti-TNF therapy [36, 37]. Additional work has focussed on harnessing the immune suppressive function of Tregs, however efforts have been hampered by challenges in generating adequate numbers of Tregs as well as the sustained therapeutic effect of such infused Tregs *in vivo* [38, 39]. There is therefore an unmet need in the management of moderate to severe IBD, with ongoing efforts focussed on more targeted therapies tailored to individual patient's underlying molecular abnormalities.

1.3 Experimental models of colitis

Using animal models to study the pathogenesis of inflammatory bowel disease is essential to further our understanding of intestinal homeostasis and how this can break down to

cause disease. A number of robust murine models have been designed to study intestinal inflammation, although not a single model can recapitulate all the pathological and clinical features of IBD in patients. The ideal model, however, should exhibit characteristic histopathological features of disease, in addition to typical clinical symptoms similar to those seen in patients. The models can be either chronic or acute, focussing on either the innate or adaptive immune responses.

Experimental models of colitis are numerous, and can be broadly classified into four groups: genetically modified animals leading to immune dysregulation, chemical disruption of the gut epithelial barrier, adoptive transfer model of colitis and the administration of infectious agents.

Defect	**Model**	**References**
Immune dysregulation	IL-10 deficiency	[40, 41]
	TCRα deficiency	[42]
	IL-7 over-expression	[43]
Chemical disruption of epithelial barrier	DSS	[44]
	TNBS	[45]
	Oxazolone	[46]
Adoptive transfer	$CD4^+$ $CD45R^{high}$	[47, 48]
Infectious agents	*Citrobacter rodentium*	[49]
	Helicobacter hepaticus	[50]

The two experimental models used in this thesis include the *Helicobacter hepaticus*/anti-IL10R and DSS models of colitis, described in greater detail below. *Helicobacter hepaticus* (*H.hepaticus*) is a valuable model to understand the pathogenesis of colitis as it mimics the multi-factorial nature of inflammatory bowel disease, including immune dysregulation and dysbiosis. DSS promotes colitis through disruption of the physical epithelial barrier separating the microbiota from the host immune system. In comparison, the DSS model drives colitis most severely in the distal colon, whereas *H. hepaticus* infection causes inflammation of the caecum and proximal colon. As such, using both models allow us to interrogate the effects of tissue inflammation comprehensively across the length of the colon.

1.3.1 *Helicobacter hepaticus*/anti-IL10R model of colitis

H.hepaticus is a gram-negative spiral bacterium of the Helicobacteraceae family which can grow in both anaerobic and microaerophilic conditions. It was originally discovered in 1992 as the cause of liver cancer in susceptible A/JCr mice [51, 52]. Early studies confirmed *H.hepaticus* to also drive colitis in certain mouse strains, with the induction of colitis in specific pathogen free IL-10 deficient mice [53]. The inflammatory response was shown to be characterised by an IL-12 and Interferon-γ dependent Th1 like cytokine profile [54]. Recently, these results have been recapitulated in wild-type C57BL mice using an antibody directed against the IL-10 receptor (anti-IL10R), with the development of colitis upon infection with *H.hepaticus* [22]. Furthermore, colitis in host mice treated with anti-IL10R is driven by an increased expression of INF-γ and IL-17 mRNA in the colon and mesenteric lymph nodes [22]. Mice deficient in IL-12p40 (a heterodimer of IL-23), but not IL-12p35 (a heterodimer of IL-12, but not IL-23) were resistant to *H.hepaticus*

induced colitis. This study therefore show the Th1 and Th17 responses are driven by the pro-inflammatory cytokine IL-23. The production of IL-23 by $CD11c^+$ mononuclear phagocytes is thought to be responsible for driving the inflammation [55]. Histologically, inflammation is most severe in the caecum and proximal colon, with epithelial cell hyperplasia, loss of goblet cells, infiltration by inflammatory leukocytes and in very severe cases, abscess formation within crypts, and cellular infiltration of the submucosa causing tissue oedema.

One major advantage of the *H.hepaticus* model of colitis is it permits analysis of the immune response to a particular bacterial pathobiont within an immune-competent lymphocyte-replete host. In contrast to commensal bacteria that supply the host with essential nutrients and defend the host against opportunistic infections, pathobionts have the potential to induce disease under the optimum conditions within the host. Studies involving this mouse model have revealed for example, *H.hepaticus* infection alone in wild type mice induces the generation of Tregs that prevent the development of colitis [56]. The mechanism of tolerance is thought to protect healthy individuals from developing IBD. A TCR transgenic mouse model to *H.hepaticus* was recently generated and using this model, it was shown that *H.hepaticus* colonisation induced the production of antigen-specific IL-10 producing Tregs that were able to restrain pro-inflammatory Th17 responses [57]. Such *H.hepaticus* specific Tregs were dependent on the transcription factor c-MAF for optimal regulatory function. The non-physiologically high frequencies of antigen specific T cells within TCR transgenic mice mean most studies use adoptive transfer of a limited number of sorted naïve TCR transgenic T cells into syngeneic wild type hosts. This allows a small, but trackable population of antigen specific T cells in hosts colonised with the cognate bacteria to be studied. As such, TCR transgenic mouse models

can be used to interrogate current unknowns such as where and when T cells initially receive activation signals and how particular bacterial antigens may modulate these responses in the host.

1.3.2 Dextran sodium sulfate model of colitis

Dextran sodium sulfate (DSS) is a water-soluble sulphated polysaccharide that can be added to drinking water and acts as a direct chemical toxin, driving colonic epithelial cell injury. This disruption to the epithelial monolayer results in entry of luminal bacterial contents and antigens into the mucosa, with intestinal inflammation of the underlying tissue [44, 58-60]. This model of colitis is a popular choice due to its rapidity, simplicity and reproducibility of results. However, DSS treatment can result in severe weight loss in mice, with pronounced diarrhoea and rectal bleeding [61]. The effects of DSS occur rapidly, with changes in the expression of tight junction proteins within the intestinal epithelium appearing as early as one day after treatment is initiated [60]. Similar changes in tight junction proteins have also been observed in human patients with inflammatory bowel disease [62].

The typical histological features of DSS treatment include loss of mucin and goblet cells, epithelial erosion, ulcer formation and infiltration of granulocytes into the lamina propria tissue and submucosa [63]. Chronic models with repeated cycles of DSS administration results in dysplastic changes and the transepithelial migration of neutrophils that drives crypt abscess formation- common features of human UC and IBD respectively [64]. DSS treatment is also associated with increased production of numerous pro-inflammatory cytokines, including TNF-α, the hallmark of DSS colitis, IL-6, IL-10, IL-17 and IL-1β (reviewed in [65]). As previously discussed, the gut microbiome plays a critical role in

driving mucosal inflammation, and various DSS- induced models of colitis have highlighted changes in the composition of the microbiota, such as loss of diversity, occurring as early as 3 days after the onset of treatment. Specific changes include reductions in Bacteroidetes, Clostridium and Lactobacillus, with increases in pro-inflammatory genera such as Enterococcales and Enterobacteriaceae [66-68].

1.4 Innate immune cells involved in the adaptive immune response

1.4.1 Mononuclear phagocytes

The lamina propria of the intestine is home to a wide array of mononuclear phagocytes including dendritic cells and tissue resident macrophages, that play critical and complementary roles in sensing and driving appropriate immune responses against pathogens.

Pattern recognition receptors (PRRs) are a group of proteins expressed predominantly by cells of the innate immune system, including dendritic cells and macrophages, and function to recognise molecules associated with pathogens such as lipopolysaccharides and peptidoglycans. PPRs are sub-divided into four main subcategories, namely Toll-like receptors (TLR), nuclear oligomerisation domain (NOD)- like receptors (NLR), RIG-1 like receptors (RLRs), and the C-type lectin receptors (CLRs) (reviewed in [69]). Sensing by PRRs forms an important pathway in host-microbe cross-talk and the maintenance of intestinal homeostasis. Studies have shown the recognition of pathogen associated

molecules by TLRs expressed on dendritic cells and macrophages that trigger production of the regulatory cytokine IL-10. Such IL-10 engages with IL-10R on T cells resulting in the suppression of pro-inflammatory T cell responses, including production of IFN-γ [70, 71]. This forms an important mechanism in the gut to suppress chronic inflammation towards commensal bacteria.

Dendritic cells migrate from the intestinal tissue to draining lymph nodes where they prime and activate T cells that help B cell antibody generation and to differentiate into effector T cells equipped with gut-homing receptors such as CCR9 and α4β7 [72]. Meanwhile, macrophages promote local intestinal immunity through phagocytic destruction of invading bacteria, in addition to secreting cytokines necessary for T cell recruitment. Intestinal dendritic cells and macrophages, although distinct in their function, share several surface receptors which have led to confusion discriminating the two populations. It is now accepted that although both subtypes of mononuclear phagocytes can sense, process and present antigens on their major histocompatibility complex class I and II, intestinal dendritic cells express the surface receptors $CD11c^{+}$ $CD103^{+}$ CX_3CR1^{-}, whilst gut -resident macrophages are $CD11c^{low}$ CX_3CR1^{high} [73, 74].

Intestinal dendritic cells consist of a heterogenous population, with the majority expressing the integrin CD103. Once loaded with antigen, dendritic cells migrate from the lamina propria to the T cell area of draining mesenteric lymph nodes (MLN) where priming of naïve T cells occur. Dendritic cells express the chemokine receptor CCR7 which promotes homing to lymph nodes. Another unique property of $CD103^{+}$ dendritic cells is their ability to produce retinoic acid, through the metabolism of vitamin A by the enzyme retinol

dehydrogenases [75]. Along with TGF-β produced by immune cells (macrophages and dendritic cells) and non-haematopoietic cells (epithelial cells and fibroblasts), such $CD103^+$ dendritic cells are potent inducers of Tregs from naïve $CD4^+$ T cells within draining lymph nodes, supporting a tolerogenic environment in the gut under homeostatic conditions [76, 77]. Furthermore, dendritic cells in the gut also produce the enzyme indoleamine dioxygenase (IDO) that catabolises tryptophan, producing kynurenine metabolites. This mechanism results in the generation of inducible Tregs that strongly suppress naïve $CD4^+$ T cell proliferation in response to allo-antigens in a mixed lymphocyte reaction [78].

Intestinal resident macrophages can be distinguished from dendritic cells by the expression of F4/80 and FCγR1 (CD64) (reviewed in [79]). Such macrophages have cytoplasmic vacuoles and high phagocytic activity, and in contrast to dendritic cells, do not migrate within lymphatics, nor do they prime naïve T cells as efficiently [80, 81]. As such, compared with intestinal dendritic cells that initiate adaptive immune responses in lymph nodes, macrophages function to regulate immune responses locally in the mucosa and act as a first line of defence against invading pathogens. Interestingly, gut resident macrophages have been shown to generate surprisingly low levels of pro-inflammatory cytokines such as TNF-α and IL-6 during microbial stimulation [82]. However, intestinal macrophages do constitutively produce IL-10, the expression of which is further increased upon microbial stimulation, whilst germ-free mice have significantly reduced expression of IL-10 [83, 84]. The high production of IL-10 has also been shown to support the expansion of Tregs in the T cell transfer model of colitis [85] and is necessary for oral tolerance to ingested food antigens [86]. These studies therefore suggest resident macrophages can efficiently clear potential pathogens without the excessive generation of

a pro-inflammatory response. Novel single cell RNA sequencing of colonic MHCII^{high} myeloid cells confirm the heterogenous nature of intestinal macrophages and dendritic cells, with signals from the microbiota critically required for optimal macrophage, but not dendritic cell development [87].

1.4.2 Innate lymphoid cells

Innate lymphoid cells (ILCs) are a subtype of immune cells, that are often described as the innate counterparts to T cells. In contrast to T cells, they do not express the somatically recombined antigen specific T cell receptors (reviewed in [88]). Abundant in both lymphoid and non-lymphoid tissue, ILCs are most often found resident within mucosal sites such as the gut and lung. They exert their effects by secreting cytokines and modulating the functions of other innate and adaptive immune cells.

ILCs are classified into three main subsets dependent on their expression of transcription factors and cytokine expression. ILC1s, ILC2s and ILC3s express the transcription factor Tbet, GATA-3, and Rorγt, and the cytokines IL-12/18, IL-5 /13 and IL-17/22 respectively, as per the classification of $CD4^+$ Th1, Th2 and Th17 T cells (reviewed in [89]). Of particular interest, ILC3s, enriched within the intestinal mucosa, have been defined as the master regulators of intestinal homeostasis and health (reviewed in [90]). ILC3s directly interact with commensal bacteria, and loss of ILC3s in the gut results in diminished IL-22 production with reduced expression of antimicrobial peptides by intestinal epithelial cells with eventual host inflammation secondary to bacterial dissemination [91]. In addition, another study showed ILC3s regulated Th cell responses to bacterial antigen through an MHCII-TCR dependent interaction, with loss of ILC3s driving an enhanced Th17 response to commensal bacteria, promoting spontaneous intestinal inflammation [92]. Finally, ILCs

also have an important role to play in defence against pathogens, such as *Citrobacter rodentium* infections of the host [93].

Lymphoid tissue inducer cells (LTi) are a specialised subset of ILC3s that were originally identified in lymph nodes, and are now understood to have critical functions in the formation of the gut associated lymphoid structures (GALT), including Peyer's patches, isolated lymphoid follicles and cryptopatches [94, 95], described in further detail in section 1.5. Two populations of LTi cells have been described: conventional foetal LTi cells that are present prenatally and soon after birth that are critically required for secondary lymphoid tissue organogenesis, and a low frequency population of LTi-like cells in adults [94, 96]. Both populations of LTi express the interleukin 7 receptor (IL7R) α, lymphotoxin (LT) and the transcription factor RAR-related orphan receptor (ROR)γt [97, 98]. Rorγt is critically required for the development of LTi cells [98]. Lymphoid structure formation involves the signalling of LT on the surface to stromal cells that express LTβR. This process drives the expression of adhesion molecules including intercellular cell adhesion molecule (ICAM)1, and chemokines including CCL19 and CCL21 for the recruitment of T cells, and CXCL13 to attract B cells (reviewed in [99]). The pivotal role of LTi cells in the formation of gut associated isolated lymphoid follicles has been highlighted [100].

1.5 The gut associated lymphoid tissue

The gut associated lymphoid tissues (GALT) forms the largest collection of lymphoid tissue in the body, and plays a vital role in protection of the host from invading pathogens (reviewed in [101]). It is composed of organised lymphoid structures, including the draining MLNs Peyer's patch, caecal and colon patches, and solitary isolated lymphoid

tissues (SILTs), in addition to scattered lymphocytes in the lamina propria and epithelium. SILTs are dynamic tissue-associated lymphoid aggregates that are heterogenous in size and cellular makeup that may provide a platform for the initiation of immune responses in the gut (reviewed in [102]). They range from cryptopatches, commonly defined as small aggregates of principally lineage-negative cells, to larger and more structurally organised isolated lymphoid follicles (ILFs) that are rich in B cells. Finally, intestinal inflammation induces the formation of tertiary lymphoid structures (TLS), another subgroup of SILTs, that resemble isolated lymphoid follicles in structure but are larger in size. Comprehensive studies investigating the composition and function of SILTs show they are equipped to quickly respond to environmental challenges, with commensal bacteria shaping the population of SILTs present within a host [103]. Lymphoid follicles have been observed to form in experimental models, such as dextran sulphate sodium (DSS) induction of colitis [104] and in a Crohn's-like ileitis (TNFΔARE) model [105], in addition to their presence within biopsy samples from patients suffering from IBD [106-108]. However, it is not yet clear to what extent SILTs contribute to the initiation and progression of the inflammatory process, and whether disrupting their formation is a beneficial treatment strategy for inflammatory disorders. A more detailed discussion of the development and functional role of SILTs will be reviewed in chapter 3, 4 and 5.

Recently, our laboratory has identified a number of immune cells within SILTs that may play a critical role in the maintenance of intestinal homeostasis. In particular, the possible interaction between the alarmin interleukin-33 (IL-33) produced by stromal cells in SILTs and $CD4^+$ T cells has been highlighted [Chomka, unpublished]. We now discuss the role of IL-33 and the $CD4^+$ T cell adaptive immune response in the gut below and in chapter 3.

1.6 Interleukin 33

1.6.1 IL-33 release, regulation and signalling

IL-33 was identified in 2005 as a member of the IL-1 cytokine family, which includes other cytokines such as IL-1α, IL-1β and IL-18 (reviewed in [109]). It plays key roles in both the innate and adaptive immune system in modulating homeostasis at tissue sites and responses to environmental stresses [110]. Due to its high expression in endothelial and epithelial cells, particularly at barrier sites that are exposed to pathogens and tissue damage, IL-33 functions as an alarmin, and is released upon tissue injury or infection. IL-33 cytokine has dual functions, operating either as a cytokine extracellularly, or acting intracellularly as a nuclear factor that regulates gene expression. IL-33 was initially discovered to be a potent activator of Th2 immune responses [111, 112], although it has now been established to play a key role in initiating both innate and adaptive immune responses, with its receptor, suppression of tumorigenicity 2 (ST2) expressed on a variety of immune cells, including Th1, Th2, ILC2s, Tregs, mast cells, basophils, eosinophils and $CD8^+$ T cells (reviewed in [113]). Furthermore, IL-33 can also bind to the soluble form of its receptor, sST2, which acts as a decoy receptor that blocks intracellular signalling through the MyD88 pathway [114]. Because IL-33 is constitutively expressed by epithelial cells of mucosal sites, with ST2 expressed by a heterogenous population of immune cells, the IL-33/ST2 pathway acts as a connection between mucosal tissue damage and the host immune system. Thus, a greater insight into the IL-33/ST2 signalling pathway is critical in understanding barrier immunity.

IL-33 binds to surface ST2 receptor resulting in a conformational change, allowing recruitment and interaction of ST2 with the co-receptor, IL-1RAcP (IL-1R accessory

protein) [115]. The IL-1RAcP co-receptor is shared with other IL-1 family members of IL-1α, IL-1β and IL-36. The formed IL-33/ST2/IL-1RAcP complex then signals through the MYD88 adaptor, IRAK1 and 4 kinases and TRAF6. The signalling cascade results in the activation of the transcription factors MAP kinases and NFκB (reviewed in [116]). This IL-33 activated signalling pathway is similar to that activated by other IL-1 family members, including IL-1 and IL-18.

IL-33 was initially described as a nuclear protein, termed 'nuclear factor from high endothelial venules' (NF-HEV) [117]. IL-33 is an in vivo nuclear cytokine associated with chromatin, with its nuclear domain (amino acids 1-65) required for chromatin association and thus nuclear localisation [118]. The functional role of IL-33 as a nuclear factor is currently unclear, although studies have observed IL-33 to act as a transcriptional repressor through interacting with NFκB to either dampen pro-inflammatory responses or modulate endothelial cell activation [119, 120]. Critically, abolished nuclear localisation of IL-33 results in constitutive release of IL-33, with lethal inflammation via ST2 activation [121].

Different forms of IL-33 have been identified, dependent on the extrinsic environment of the host tissue. IL-33 can be released either cleaved or in a full-length form (containing three domains: N terminus domain necessary for nuclear function, central domain, and a C-terminus IL-1-like domain) [122]. Under homeostatic conditions, full-length IL-33 resides in the nucleus of cells. During apoptosis, IL-33 is cleaved by caspases 3 and 7 to allow release into the extracellular space as an inactive form with no cytokine activity [123, 124]. However, during inflammatory or cellular damage, a full-length active IL-33 cytokine is released into the extracellular space. The bioactivity of such released IL-33 can

be further cleaved by neutrophil-derived serine proteases cathepsin G and elastase, and mast cell-derived chymase and tryptase, further increasing the activity of IL-33 between 10 to 30-fold [125, 126]. In contrast to apoptosis, this confirms the role of IL-33 as an alarmin with its biological active form released uniquely during cell necrosis, tissue damage and mechanical stress [127, 128]. However, as expected, the bioactivity of IL-33 is tightly regulated with mechanisms in place to prevent an excessive inflammatory response. Such mechanisms include for example conformational change of IL-33 as a result of oxidation of cysteines leading to disulfide bond formation in the IL-1 like domain that disrupts the ST2 binding site [129]. Furthermore, the soluble ST2 receptor (sST2) acts as a decoy receptor for IL-33, preventing its binding to the surface ST2 receptor (reviewed in [130]). Indeed, the presence of sST2 was shown to inhibit IL-33 induced NFκB pathway activation and downstream Th2 cytokine production in allergic airway inflammation [114].

1.6.2 IL-33 in inflammatory disease

IL-33 is known to act in a variety of biological processes aside from immune responses, including homeostasis, repair and tissue growth. It has been reported to play a role in a number of autoimmune and inflammatory pathologies, including asthma, allergic rhinitis, rheumatoid arthritis, diabetes and inflammatory bowel disease (reviewed in [131]).

Much focus of the role of IL-33 has been in respiratory inflammation, with polymorphisms of both *Il33* and *IL1RL1* encoding the ST2 receptor identified as a susceptibility loci for asthma [132]. In murine models of asthma, administration of IL-33 induced a strong Th2 response with increased production of mucus, eosinophilic infiltration and epithelial cell hypertrophy [110]. Altogether, most studies have demonstrated a pathological role of IL-33 in asthma murine models, with Th2 cells, ILC2s and macrophages as the cellular targets

of IL-33 signalling [133-135]. The role of IL-33 has also been highlighted in numerous other inflammatory disorders, with both pathological and protective effects depending on the disease context. These include rheumatoid arthritis, whereby an sST2-Fc fusion protein or anti ST2 antibody that blocked IL-33 signalling attenuated disease severity with downregulation of IL-6, IL-12 and TNF-α in a collagen-induced arthritis disease model [136]. Inflammation is an emerging driver of cardiovascular disease, and IL-33 was found to be synthesised by cardiac fibroblasts. Furthermore, administration of exogenous IL-33 reduced cardiac hypertrophy and fibrosis, improving survival in wild type, but not $ST2^{-/-}$ littermate controls, demonstrating a previously unrecognised cardioprotective IL-33/ST2 signalling pathway [137].

Finally, elevated IL-33 and ST2 levels have been demonstrated in colonic mucosal samples from patients with IBD, particularly in those with active disease flares [138-141]. In addition, numerous murine studies have reported similar results, with increased IL-33 expression in distinct intestinal inflammation models [142-146]. The role of the IL-33/ST2 pathway in maintaining intestinal homeostasis will be further discussed in chapter 3.

1.7 The mucosal adaptive immune system

1.7.1 B cells

B cells are the key players of the adaptive humoral immune response, with long-lived plasma cells are responsible for the production of antigen-specific antibodies against pathogens. The initiation of the humoral response requires contact of B cells with their cognate antigen via their B-cell receptor (BCR), most often within secondary lymph nodes (reviewed in [147]). Germinal centres are specialised sites within secondary lymphoid

structures where mature B cells undergo affinity maturation, class switching and proliferation to produce memory B cells during a humoral immune response. Engagement of antigen drives signalling through the BCR initiates the process of B cell activation [148, 149]. Subsequent proliferation for the generation of clonal population of daughter cells occurs either independently or dependently of T follicular helper (Tfh) cells, a subset of $CD4^+$ T cells. T cell dependency is determined by the number of BCR molecules and/or co-receptors engaged by antigen. Antigens that interact with multiple BCRs on the B provoke a T cell-independent proliferation, whereas those with lower valency require further T cell help to proliferate (Reviewed in [150]). In T cell dependent responses, B cell interaction with Tfh occurs at the interface between B and T cell zones within lymph nodes. Such Tfh have already been primed by dendritic cells presenting the same antigen engaged on the BCR, in a process known as linked recognition [151-153]. Expression and engagement of CD40L on Tfh with CD40 expressed on the surface of B cells form an important pathway of T cell help [154]. Additionally, cytokines including IL-4 and IL-21secreted by Tfh are crucially important in promoting B cell proliferation, class switching and differentiation into plasma cells [155, 156]. Following activation, B cells then undergo class switching to change their BCR isotype from the naïve Immunoglobulin (Ig) M and IgD to IgA, IgE and IgG to allow for the production of a broad repertoire of antibodies. IgG is the most abundant in the serum, whereas IgA is the predominant isotype in mucosal secretions (reviewed in [157]).

Mucosal protection of the gut is enhanced by the secretion of IgA antibody by lamina propria-resident plasma cells. Such locally produced IgA are transported into the gut lumen where they coat and regulate commensal and potentially pathogenic bacterial populations (reviewed in [158]). IgA can bind to bacterial cell wall glycans non-

specifically [159] or in a bacterial-specific manner [160], and bacteria that are highly coated with IgA often show the greatest colitogenic potential [161]. As such, B cell responses in the gut are directed to microbial antigens that have the greatest disease potential, demonstrating the host intestinal humoral response is directed against pathogens [161].

1.7.2 T cells

The intestinal tract contains a diverse population of unconventional and classical T cell subsets. Broadly, T cell populations differs dependent on site, with lymphocytes found in the intestinal epithelium, i.e., intraepithelial lymphocytes (IELs), distinct from lamina propria lymphocytes. In contrast to the lamina propria, greater than 90% of IELs of the small intestine are T cells, with 80% expressing CD8 [162]. Within the colon, there are fewer IELs relative to epithelial cells, with a higher proportion of $CD4^+$ T cells [163, 164]. Both IEL and lamina propria T lymphocytes are mostly of an antigen-experienced activated phenotype [165]. In brief, IELs include a wide array of subtypes, including γδ T cells, CD8αα and CD8αβ T cells (reviewed in [166]). Altogether, IELs are at the interface between the innate and adaptive immune response playing important roles in recognition and elimination of infected epithelial cells, as well as aiding repair of the mucosa after inflammatory damage. IEL are outside the scope of this thesis and will not be discussed further.

Intestinal $CD4^+$ T helper cells within GALT play a major role in orchestrating the adaptive immune response of the gut, protecting the host from foreign antigens and dysregulated inflammatory responses. $CD4^+$ T cells include a diverse range of cell subsets with unique cytokine and chemokine profiles that are all present within the healthy gut. The continuous

environmental exposures encountered by the gut, including ingested food antigens, commensal and pathogenic microbes necessitate the existence of a diverse and versatile $CD4^+$ T cell response dependent on the challenge encountered. Communication between responsive $CD4^+$ T cells and foreign antigens, often with help from epithelial cells and antigen-presenting dendritic cells, are central to the maintenance of gut health. Furthermore, there exists an important balance between different T cell subsets, particularly the critical balance between pro-inflammatory effector $CD4^+$ T cells and Tregs. The impairment of either regulatory or inflammatory pathways may result in the development of inflammatory disorders such as IBD, whereby heavy infiltration of $CD4^+$ T cells into the colonic mucosa of such patients is observed (reviewed in [167, 168]). More recently, there is greater understanding of the plasticity of $CD4^+$ T cell subsets, with the ability of lineage differentiated $CD4^+$ T cells to adopt alternate phenotypes driven by innate signals (reviewed in [169]). We discuss below $CD4^+$ T cell development and differentiation to different Th subsets, with a comprehensive review of the phenotype and function of Tregs in the gut.

1.7.2.1 $CD4^+$ T cell development and differentiation

T cells are derived from multipotent lymphoid progenitor stem cells in the bone marrow. Such progenitors migrate from the bone marrow to the thymus where they complete their development into mature naïve T cells equipped with specificity towards a particular antigen. The thymus provides a dedicated and structurally organised environment for the development of T cells. Developing T cells, or thymocytes, enter the thymus and undergo a period of intense proliferation, whilst passing through a series of distinct developmental stages along the T cell lineage differentiation pathway. Both Notch signalling [170] and

IL-7 cytokine production [171] by the thymic stroma is essential for early T cell development. Two important events occur along this pathway: the generation of the α- and β- chains of the T cell receptor (TCR), and the acquisition of the surface CD4 or CD8 receptor (reviewed in [172]. The formation of a diverse TCR repertoire depends on rearrangement of the V, D, and J gene segments, with the recombination activation genes 1 and 2 (*Rag1/2*) essential to this process. Indeed, RAG-1 or 2 enzyme deficient mice do not develop any lymphocytes [173, 174].

Thymic cortical stromal cells are composed of epithelial cells that express both MHC class I and II molecules, and contact between self-peptide-presenting MHC molecules with the developing thymocytes delivers the necessary signal for survival, i.e., positive selection (reviewed in [175]). Thymocytes that express TCRs unable to interact with self MHC molecules die by neglect. Another important process that occurs throughout thymocytes development is the process of negative selection (reviewed in [175]), whereby thymocytes developing TCRs that bind with inappropriately high affinity to self-antigen are deleted. This protective mechanism occurs to prevent the development of autoimmune responses. Negative selection, an example of central tolerance, occurs due to the expression of many tissue-specific proteins by thymic stromal cells, under the control of the autoimmune regulator, or *AIRE* genes. This allows the removal of thymocytes that over-react to self-proteins expressed external to the thymus, such as pancreatic insulin. In the final step of thymic T cell differentiation, mature single $CD4^+$ or $CD8^+$ T cells leave the thymus and migrate through the circulation to take up residence in lymphoid organs and tissue sites. An important thymic $CD4^+$ T cell subset are Tregs (thymic Tregs), and their distinct thymic development is discussed in more detail in section 1.7.2.6. Additionally, it is not possible for all self-proteins to be expressed in the thymus, and as such, a number of

additional peripheral mechanisms, including peripherally induced Tregs also contribute to host tolerance. Their phenotype and development are discussed in section 1.7.2.6.

The activation of naïve T cells by antigen presenting cells requires three key signals in sequence. The first signal involves the binding of a cognate antigen peptide presented on an MHC molecule interacting with its specific TCR receptor (reviewed in [176]). This activation of the T cell is only sustained if followed by a second co-stimulatory survival signal delivered by the same antigen presenting cell (reviewed in [177]). TCR activation without co-stimulatory signals results in anergy [178]. A major co-stimulatory signal involves the interaction of CD28 on T cells with B7 molecules on dendritic cells. Other examples include CD40-CD40L, ICOS-ICOSL and OX40-OX40L (reviewed in [179]). Additionally, a number of co-inhibitory signals also exist that function to restrain and downregulate effector T cell responses, including PD-1, CTLA-4 and LAG3 [180]. Finally, signal three occurs in the form of cytokines primarily provided by macrophages and dendritic cells which critically directs the differentiation of activated T cells into different effector subsets (reviewed in [181]).

Dependent on the antigen and cytokine environment, naïve $CD4^+$ T cells differentiate into a number of effector T cell subsets with unique functions. The main subsets include Th1, Th2, Th17, Tfh, and Tregs. Their functions and cytokine profiles are now reviewed, with an extended focus on Tregs and the key role they play in restraining effector T cell responses to foreign antigens in the gut.

1.7.2.2 Th1 cells

Th1 polarised $CD4^+$ T cells function to control intracellular viruses and bacteria. Such bacteria include mycobacteria that can set up residence within macrophages (reviewed in [182]). Th1 cell induction begins with the secretion of IL-12 and type 1 IFN (IFN- α and IFN-β) by macrophages and dendritic cells upon infection by intracellular pathogens. IL-12 also induces the production of IFN- γ by macrophages and dendritic cells which acts as a positive feedback loop to produce more IL-12. Both IL-12 and IFN- γ are necessary cytokines that induce Th1 differentiation. These cytokines stimulate the JAK-STAT intracellular signalling pathway and result in the activation of signal-transducing activators of transcription (STAT) 1 and 4 that support the activation of T-box transcription factor (*Tbx21*) encoding the T-bet transcription factor characteristic of Th1 cells .

It has been shown that only microbial stimuli that induce Toll-like-receptor (TLR) signalling enable dendritic cells to activate natural killer cells that help in the initiation of the Th1 response [183]. In addition, mice lacking MYD88, the adaptor protein that forms part of the intracellular signalling pathway stimulated by TLRs, do not survive infection by *Toxoplasma gondii*. This parasitic infection is normally kept under control by a strong host Th1 response [184]. Critically, IFN-γ produced exclusively by antigen presenting and natural killer cells act to inhibit activation of the Th2 pathway and prevent Th2 proliferation. Such Th-1 polarised T cells generate abundant amounts of IFN-γ cytokine upon recognition of cognate antigen, with such IFN-γ further driving Th1 differentiation [185, 186].

Evidence exists for Th1 cells driving intestinal inflammation. Clinical studies examining the cytokine profiles in T cell clones generated from the colonic mucosa found high amounts of IFN-γ, but not IL-4 and IL-5 in patients with CD, in comparison to T cell clones originating from patients with non-inframammary bowel conditions [15]. Experimental models confirm these findings, with adoptive transfer of naïve $CD4^+$ $CD45RB^{hi}$ T cells into severe combined immunodeficient (SCID) hosts resulting in a strong Th1 polarised CD4 response [187]. Additionally, administration of an anti IFN-γ monoclonal antibody to host mice after T cell transfer is able to prevent the development of colitis. Similarly, another study demonstrated the critical importance of the canonical Th1 transcription factor, T-bet to promote Th1 mediated colitis. Retroviral transduction of T-bet in naïve $CD4^+$ T cells worsened colitis in SCID mice following adoptive transfer, whereas colitis did not occur upon reconstitution with T-bet deficient T cells [188].

1.7.2.3 Th2 cells

Th2 cells function to protect against parasitic helminths infections and can promote allergic responses. In particular, cytokines such as IL-4 and IL-25 produced by Th2 cells aid B cell class switching to produce IgE antibody to fight parasitic infection, as well as promoting the recruitment of basophils, eosinophils and mast cells [189, 190]. IgE is also the main antibody involved in responses to environmental allergens.

Parasitic helminths induce the production of IL-4 cytokine by basophils and mast cells. IL-4 signalling to antigen stimulated $CD4^+$ T cells activates STAT6, promoting the expression of the canonical Th2 transcription factor GATA-3. In turn, GATA-3 activates many of the cytokines distinct to Th2 function, including IL-4, IL-5 and IL-13, that function to drive the B cell class switching to IgE and promote granule release by basophils and mast cells,

whilst recruiting eosinophils [191]. Furthermore, GATA-3 also promotes its own expression in a positive feedback loop. Studies have shown basophils, eosinophils and mast cells respond to the fungal and helminth parasite polysaccharide chitin, by producing large amounts of IL-4. This is then thought to promote Th2 responses towards allergy and infection [192].

Finally, there exists a complex interplay between Th1 and Th2 cells, with cross-regulation between the two subsets. IL-4 and IL-10 produced by Th2 cells function to inhibit the production of IL-12 by dendritic cells, therefore preventing the development of a Th1 response. In contrast, IFN-γ produced by Th1 cells inhibit Th2 development (reviewed in [193]). This interesting Th1/Th2 paradigm has been studied in the UC and CD subtypes of IBD, with controversy as to whether these distinct IBD subtypes exhibit unique $CD4^+$ T cell differentiation profiles [15, 17, 194-196]. A study systematically examined the immune profiles of $CD4^+$ T cells in the lamina propria of UC and CD clinical intestinal biopsies [197]. The results showed a higher prevalence of IFN-γ or T-bet expressing Th1 skewed cells, with a decrease of Th2 (IL-13 producing or $GATA\text{-}3^+$ $CD4^+$ T cells) in CD compared to UC. Furthermore, unique Th1/Th2 signatures showed correlation with disease activity and response to tumour necrosis factor (TNF) inhibitor therapy.

1.7.2.4 Th17 cells

Th17 cells, first described in 2005 have now been established as a major $CD4^+$ T cell subset in the co-ordination of immune responses, with particularly important functions at barrier sites [198-200]. The main function of Th17 cells is to protect against extracellular bacteria and fungi by inducing neutrophil production and migration to sites of infection.

Th17-polarised cells are generated when IL-6 and transforming growth factor - β (TGFβ) are present in the absence of IL-4 and IL-12. The initial production of IL-21 by T cells acts in an autocrine manner to activate STAT3 that in turn promotes the induction of the signature Th17 transcription factor RORγt. Mice that are deficient in STAT3 and RORγt possess significantly reduced numbers of Th17 cells, indicating the critical role of these transcription factors in maintaining the Th17 phenotype [201, 202]. RORγt is an orphan nuclear hormone receptor that stimulates the production of characteristic Th17 cytokines, including IL-17A, IL-17F, IL-21 and IL-22. Additionally, Th17 cells express the receptor for the IL-23 cytokine, and studies have highlighted IL-23 as dispensable for Th17 differentiation, but critically required for reinforcing Th17 responses and its pathogenic potential [199, 203, 204]. Th17 cells promote inflammation in an indirect manner. Within fibroblasts, keratinocytes or epithelial cells, Th17 cytokines induce the production of chemokines such as CXCL8, CXCL10, CXCL11 and CXCL19 that promote the recruitment of neutrophils to sites of inflammation (reviewed in [205]).

Similar to the cross-regulation between Th1 and Th2 subsets, Th17 are induced by TGFβ and IL-6, but can be inhibited in the presence of IFN-γ or IL-4 and switch to Th1 or Th2 cell development instead. Finally, TGFβ is necessary for the induction of both Th17 and Tregs, with the presence or absence of IL-6 dictating induction of tolerogenic Tregs or pro-inflammatory Th17 cells [206]. While TGF-β is required for Th17 cell differentiation, it also drives the expression of Foxp3, the canonical Treg transcription factor [207, 208]. This reciprocal balance between the two T cell subsets with opposing immune functions plays a major role in governing intestinal homeostasis.

Th17 cells play a critical role in the pathogenesis of intestinal inflammation in murine studies and in genetic and functional studies in humans. Firstly, genome wide association studies (GWAS) have uncovered strong links between IBD and Th17 pathways, with risk alleles in Th17 associated genes, including *CARD9*, *IL12B*, *STAT3*, *RORC*, *IL23R*, *JAK2*, *TYK2*, and *CCR6* [209, 210]. Functional studies have reported increased expression of Th17 cytokines in the intestinal mucosa of active UC and CD patients, including IL-1β, IL-6, IL-17, IL-23, and IL-22 [211-215]. In addition, experimental models have highlighted the critical importance of IL-23 in driving colitis, as demonstrated using mice knock out for the IL-23p19 subunit unique to the IL-23 cytokine [216-218]. Finally, adoptive transfer of Rorγt-deficient T lymphocytes into RAG knock out mice results in an inability to produce Th17 cytokines in the mucosa and a lack of colitis, demonstrating the crucial role of Th17 cells in driving intestinal inflammation [219].

1.7.2.5 T follicular helper cells

Tfh were first identified in the human tonsil, and play a critical role in supporting humoral immunity and aiding B cells to produce antibodies against pathogens. Tfh cells are primarily found in secondary lymphoid organs, such as the spleen and peripheral lymph nodes. Secondary lymphoid organs are organised structures, separated into defined T and B-lymphocyte zones. Tfh cells are located within the B cell follicle, where they are essential in the formation of germinal centres during an immune response. Germinal centres are distinct structures within the B-cell zone that contain Tfh cells, B cells, follicular dendritic cells, macrophages and stroma (reviewed in [155]). Within germinal centres, B cells undergo somatic hypermutation of their B cell receptor genes and class

switch recombination that allow their differentiation into antibody secreting plasma cells and long-lived memory B cells (reviewed in [220]). These have the ability to rapidly produce pathogen-specific antibodies. Mammals express five different antibody isotypes: IgA, IgD, IgE, IgG and IgM (reviewed in [221]). Isotype class switching allows B cells to change its production of antibody from one isotype to another, thus diversifying their antibody repertoire and the ability to respond to a broader range of challenges. Naïve mature B cells that are ready to respond to antigen express both IgD and IgM on their surface. Switching of the constant, but not variable antigen-binding region of the heavy chain allows for changeover to a different isotype such as IgE in Th2 responses, or IgA antibody production required for mucosal protection, without a change in antigen specificity.

Tfh cells provide B cell help through a number of cytokines and cell surface receptors. These include the provision of co-stimulation to B cells through the interaction of the co-stimulatory molecule CD40 with its ligand CD40L on B cells. Cytokine help includes the production of IL-21 and IL-4 which function to maintain B cell survival and induce their proliferation. In addition, both IL-4 and IL-21 are strong inducers of IgG1, the most prevalent class switched antibody [222]. Tfh cells are characteristically defined by the transcription factor B cell lymphoma 6 (BCL6), and the surface markers CXCR5, PD-1 and ICOS. CXCR5 is the receptor for the chemokine CXCL13, produced by stromal cells of the B cell follicle. The first step of Tfh differentiation occurs in the T cell zone of SLOs upon naïve $CD4^+$ T cell recognition of peptide proteins via their T cell receptor presented on MHC II^+ dendritic cells. Dendritic cells provide additional co-stimulatory signals in the form of ICOS-L and IL-6 cytokine, driving commitment of naïve $CD4^+$ T cells to Tfh

lineage. Such developing Tfh cells upregulate the surface receptor CXCR5 and migrate into B cell zones and help in the formation of germinal centres (reviewed in [220]).

Finally, mechanisms are in place to prevent an over-response of germinal centre B cells to pathogen. T follicular regulatory cells (Tfrs) function as negative regulators of the immune B cell response, with the ratio of Tfh to Tfrs a critical determinant of the germinal centre reaction [223-227]. Tfrs express both the Tfh and Treg canonical transcription factors BCL6 and Foxp3, respectively [228, 229]. However, the mechanism of suppression is currently unclear, and it also remains to be established whether Tfr cells achieve its immunoregulatory functions through inhibition of Tfh, similar to the functional role of Tregs, or whether they act directly on activated B cells in the germinal centre.

1.7.2.6 T regulatory cells

Tregs are a critical subset of $CD4^+$ T cells that maintain immunological tolerance and inhibit uncontrolled innate and adaptive immune responses to both self and foreign antigens. As a result, Tregs play a critical role at barrier surfaces, such as the gut, lung and skin, where there exists an interface between the host self and the microbial non-self. Tregs have been shown to be essential in the prevention of inflammatory and auto-immune diseases (reviewed in [230]). Conversely, pro-inflammatory effector T cells are critical in the protection against infections, as well as driving anti-tumour responses. The presence of Tregs at these sites have been shown to correlate with negative outcomes, highlighting the stringent regulation of their induction and function dependent on the immunological context.

Early work showed neonatal thymectomy at day 3 after birth results in the presence of tissue-specific autoimmune antibodies, and subsequent autoimmune damage of various organs, including the ovaries, thyroid and testes [231]. These studies show the existence of both potentially pathogenic self-reactive T cells, as well as a subset of T cells within the thymus that have the ability to suppress such self-reactive T cells and prevent autoimmunity [231, 232]. Furthermore, the evidence that such immuno-tolerant T cells can also suppress effector T cell responses to non-self dietary and/or microbial antigens were revealed in later studies showing transfer of naïve $CD45RB^{high}$ $CD4^{+}$ T cells developed a severe inflammatory wasting disease that was ameliorated by the co-transfer of immune-tolerant antigen-experienced $CD45RB^{low}$ $CD4^{+}$ T cells [233]. Further studies showed this subset of regulatory $CD4^{+}$ T cells faithfully expressed the surface marker IL25 - the IL-2Rα chain, and the canonical transcription factor forkhead box p3 (Foxp3) [234]. It is now clear from numerous depletion or transfer studies, that Tregs play major role in auto-immune and inflammatory disease prevention, including IBD, organ transplantation and allergic responses (reviewed in [235]).

The transcription factor Foxp3 belongs to the fork-head/winged -helix family of transcription factors, and acts as a master regulator of Treg development and function. The *Foxp3* gene was identified in an X-linked recessive mutant mouse strain, Scurfy, whereby male mice die within one month of birth as a result of a systemic autoimmune disease characterised by hyper-responsive $CD4^{+}$ T cells and gross production of pro-inflammatory cytokines [236]. The clinical counterpart of Scurfy mice is the disorder IPEX (immune dysregulation, polyendocrinopathy, enteropathy, X-linked syndrome), whereby a mutation in the human *Foxp3* gene manifests as multiorgan inflammation [237, 238].

Tregs are present in every organ in the body, and normally constitute around 10% of the total CD4 population. However, within the intestinal tract, Tregs make up more than 30% of the colonic tissue, and approximately 20% of the small intestinal lamina propria (reviewed in [239]). Murine studies show the development of intestinal inflammation upon disruption of regulatory T cell pathways, particularly in response to intestinal microbiota [240]. As such, studies have highlighted gut resident Tregs to be a heterogenous population that are distinct from Tregs at other sites that have TCRs directed towards self-antigens. Intestinal Tregs are equipped with a unique set of TCRs specific for intestinal antigens that play a critical role in restraining immune responses against harmless food antigens and the commensal microbiota [241]. This interaction is a two-way conversation as specific members of the microbiota provide in return signals in the form of microbial antigens and immunomodulatory metabolites that influence the development of Tregs.

Treg development

Tregs primarily develop in the thymus during the process of positive and negative selection (thymus-derived/natural Tregs). Similar to conventional T cell development, $CD4^+$ $CD25^+$ Tregs differentiate in the thymus from double-negative $CD4^-$ $CD8^-$ thymocytes following presentation of self-peptide by $MHCII^+$ thymic stromal cells in the presence of co-stimulatory signals. Such signals, including CD28, CD80/86 and CD40 are particularly important, as mice deficient in these signals harbour reduced thymic-derived Tregs with subsequently impaired suppressive capacity [242]. Conventional T cells undergo negative selection due to very strong signals between TCR and MHC:peptide complexes, whereas very low, or a lack of signal results in thymocyte death due to neglect. Positive selection of thymocytes occurs when appropriately weak signals are delivered via

the TCR, permitting survival and ongoing development. Prior studies have suggested thymic-induced Tregs are positively selected based on a signal strength that is somewhere in between negative and positive selection as for conventional T cells (reviewed in [243, 244]). After exiting the thymus, a proportion of Tregs home to the gut where they function to recognise and restrain inappropriate effector responses to intestinal microbial and food antigens (reviewed in [245]). It is therefore likely the intestinal environment in the form of the microbiota further shapes the development of thymic-derived Tregs that promotes their effective function at this site.

Additionally, intestinal tolerance can be further enhanced through the extra-thymic differentiation of naïve $CD4^+$ T cells into $Foxp3^+$ Tregs in the gut (peripherally induced Tregs). Whilst both TCR engagement and IL-2 cytokine are critically required for thymic-derived Treg development, the addition of TGF-β is essential for peripheral Treg induction [77, 246]. The gut, along with other barrier sites, is home to a substantial population of peripherally induced Tregs. Naïve $CD4^+$ $Foxp3^-$ T cells exit the thymus and migrate to the intestines, where encounter with certain commensal microbial and dietary antigens induce the conversion to Tregs. This favourable microbial and/or dietary antigen-associated environment in the gut tissue drives a significantly higher proportion of peripheral Tregs compared to secondary lymphoid organ sites [247]. Furthermore, intestinal associated Treg induction by TGF-β is enhanced by the co-factor retinoic acid, a vitamin A metabolite produced by $CD103^+$ dendritic cells in the gut [76, 248].

To date, no ideal marker exists to reliably differentiate thymic from peripherally-induced Tregs, although the transcription marker Helios, and the surface marker Neuropilin (Nrp-1) have been shown to be preferentially expressed on thymic derived Tregs [249-251]. Furthermore, studies have highlighted distinct roles of thymic versus peripheral Tregs,

with evidence to suggest induced Tregs are an essential regulatory subset by enforcing tolerance through expansion of the regulatory TCR repertoire [252]. Furthermore, three unique non-coding sequences (CNS 1-3) that form regulatory regions of the *Foxp3* gene locus define the size, composition and stability of the Treg pool, with CNS3 and CNS1 specifically relevant for thymic and peripherally-induced Treg development respectively [253, 254]. CNS1-deficient mice develop strong Th2 driven inflammation of the colon and lungs, demonstrating the critical importance of peripherally-induced Tregs in restraining T effector responses at barrier sites [253]. Altogether, it is likely important roles exist for both thymic and induced Tregs in the maintenance of gut homeostasis, however it is currently not clear whether they have overlapping or distinct responsibilities. It may be the case that these two Treg subsets are equipped with different microbial antigen specificities that contributes towards increasing the overall responsiveness of the gut Treg pool to intestinal antigens.

Finally, although Tregs express the canonical transcription factor Foxp3 which is critical to its differentiation and function, they also adapt to their surrounding environment by co-expressing effector T cell-associated transcription factors including Rorγt and GATA-3 to control Th17 and Th2 immune responses respectively. For example, studies have shown gut resident Tregs to co-express Rorγt that plays a critical role in restraining Th1/Th2/Th17 effector responses at mucosal sites [255, 256]. Adoptive co-transfer of congenically marked Foxp3$^+$ Tregs and Rorγt$^+$ T cells along with naïve CD4$^+$ T cells into lymphopenic RAG2- deficient hosts show significant proportions of Foxp3$^+$ Tregs upregulate their Rorγt expression whilst only a minor population of transferred Rorγt$^+$ T cells upregulate their expression of Rorγt$^+$ [257]. This study therefore suggests the majority of Foxp3$^+$ Rorγt$^+$ Tregs originate from Foxp3$^+$ Tregs, and not Rorγt$^+$ Th17 T cells. Such

Rorγt^{+} Foxp3^{+} Tregs are distinct from GATA-3^{+} Foxp3^{+} Tregs which result in a spontaneous inflammatory disorder when deleted [258].

Mechanisms of Treg suppression

Tregs can mediate tolerance through a number of mechanisms, broadly divided into competition for growth factors, local production of inhibitory cytokines and expression of cell surface inhibitory molecules (reviewed in [259]). Tregs require initial activation through TCR stimulation to adopt a suppressor phenotype, which once activated, have the ability to suppress effector responses of many immune cell types, including CD4^{+} and CD8^{+} T cells, dendritic cells, monocytes and natural killer (NK) cells (reviewed in [260]).

Tregs constitutively express the receptor for IL-2, CD25, whereas effector T cells only express CD25 upon TCR stimulation [261, 262]. This temporal difference in CD25 expression equips Tregs with an initial competitive advantage, whilst depriving other effector T cells from utilising this essential growth factor necessary for T cell survival and proliferation. Indeed, in the above studies, Treg mediated competition for IL-2 results in apoptosis of target T cells due to cytokine deficiency. In addition, Tregs are enriched for surface expression of the endonucleases CD39 and CD73 [263, 264]. Upon binding of adenosine to the adenosine A2A receptor, cAMP is increased, resulting in the suppression of proliferation and cytokine production by effector T cells. In these studies, the loss of CD39 or blocking o the A2A receptor ameliorated Treg suppressive function. Interestingly, loss of CD39^{+} Tregs has been associated with the autoimmune condition multiple sclerosis, highlighting the critical role of Tregs in controlling inflammation [265].

Treg secrete a number of highly immunosuppressive cytokines, the main ones being IL-10, TGF-β, and IL-35. Conditional deletion of IL-10 in Foxp3$^+$ Tregs showed that IL-10 production by Tregs is not required for control of systemic autoimmunity, but is critically required for restraining inflammation at mucosal sites such as the gut and lung [266, 267]. Additionally, Treg derived IL-10 is able to control already established colitis and experimental autoimmune encephalitis [268, 269]. Since these seminal studies, IL-10 has been identified as a susceptibility locus in UC [35]. The precise mechanisms of IL-10 mediated suppression is likely to involve numerous mechanisms. One study showed that although IL-10 can suppress a variety of immune cells including dendritic cells, its direct effects on effector/memory T cells is a critical pathway in the prevention of colitis [270]. Indeed, IL-10R signalling in both Tregs and Th17 cells are needed in order to suppress intestinal Th17 pro-inflammatory responses [271, 272], whilst Treg induction of IL-10 is critically required to control IFN-γ transcription during Th1 mediated inflammation [273]. Importantly, IL-10 is now known to not only be produced by Tregs, but also by Foxp3$^-$ T regulatory 1 (Tr1) cells [274], regulatory B cells (reviewed in [275]) and macrophages. Macrophage derived IL-10 has been shown to prevent inflammation through indirect action on Tregs to maintain Foxp3 transcription factor expression [85].

Tregs produce high amounts of both membrane-bound and soluble TGF-β, and mice lacking TGF-β suffer from multi-organ auto-immune damage [276], whilst naïve T cells that can no longer respond to TGF-β escape Treg control [277]. Although dendritic cells in the gut has been shown to produce TGF-β [278], it is the TGF-β1 specifically produced by T cells that control Th1 and Th2 immune responses driving colitis [279].

IL-35, a recently discovered cytokine member of the IL-12 family, has been shown to directly inhibit effector T cell proliferation [280]. IL-35 is a dimeric protein composed of

an IL-12α and an IL-27β chain, encoded by *Il12a* and *Ebi3* respectively. Tregs that are deficient in one of the two chains have reduced suppressor activity in an IBD murine model [280]. Interestingly, the expression of both *Il12a* and *Ebi3* mRNA is upregulated in Treg cells that are actively performing suppressor functions, suggesting cell contact between Tregs and effector cells may be critically necessary for maximal IL-35 secretion. However, in contrast to IL-10 and TGF-β deficiency, these mice did not exhibit spontaneous autoimmune disease.

With regards to contact – dependent mechanisms of suppression, Tregs have the ability to upregulate on their cell surface the expression of a number of key inhibitory molecules. Both dendritic cells and effector T cells can engage with such surface inhibitory molecules. An important suppressive mechanism is the expression of CTLA-4 on the surface of Tregs, which acts to down-regulate and sequester the co-stimulatory molecules CD80 and CD86 on antigen presenting cells [281]. Indeed, mice that were knock out for CTLA-4 or the use of CTLA-4 blocking antibodies resulted in Tregs with reduced suppressor activity, and the development of autoimmune disease [282, 283]. Finally, CTLA-4 binding to CD80/86 can also up-regulate the enzyme indoleamine 2,3-dioxygenase (IDO), which catabolises the essential amino acid tryptophan [284, 285]. This works to limits pro-inflammatory tryptophan, whilst converting it to the immunosuppressive kynurenines [286].

A number of other molecules are present on the surface of Tregs that promote their contact-dependent immunosuppressive function, including GITR, ICOS, PD-1 and OX-40 [287-292]. For example, LAG-3 binds to MHCII molecules with high affinity, preventing dendritic cell maturation and their priming of naïve T cells [288]. The role of LAG-3 was confirmed in experimental models of LAG-3 deficiency or antibody blockade that resulted

in reduced suppressor activity, whilst its overexpression conferred immune-suppressive activity in $CD4^+$ T cells [293]. Finally, studies have also shown surface expression of Nrp-1 on Tregs, but not naïve Th cells, plays a tolerogenic role through the promotion of a longer interaction between the two immune cells, thereby limiting the ability of dendritic cells to initiate an immune response [294].

Tissue versus lymphoid Tregs

Emerging studies highlight Treg immunity varies greatly between tissue and lymphoid sites (reviewed in [295]). It is thought the tissue environment instructs distinct adaptations of Tregs residing at these sites that equips them with the ability to respond to unique conditions not present in lymph nodes. In particular, barrier sites such as the gut present unique challenges to resident Tregs, which have evolved phenotypically and functionally to such environments in order to maintain homeostasis and health. The majority of studies investigating the phenotype of tissue resident Tregs agree in most cases such Tregs are already mature $Foxp3^+$ Tregs when they enter tissue (reviewed in [296]), although questions still remain as to precisely where and when tissue Tregs adopt their unique transcriptional phenotypes. Interestingly, hierarchical clustering of differentially expressed transcripts in Tregs resident in visceral adipose fat, skeletal muscle colon lamina propria and pancreas as compared to lymphoid -associated Tregs highlighted transcript signatures shared by all tissue resident Tregs as well as transcript sets distinct to individual tissues [297]. Emerging data support the notion that distinct populations of Tregs, equipped with tissue-specific phenotypes reside in non-lymphoid tissue and may function to not only restrain inflammatory responses, but also to uphold the distinct physiological functions of the tissue they reside within. Furthermore, questions remain regarding the specific

molecular signals that direct recruitment of Tregs into tissue sites, although it is likely chemokine gradients that are differentially expressed in tissue, but not lymphoid structures play a role. An example includes the tissue specific homing receptor GPR15 that instructs Treg migration into colon lamina propria [298]. Ongoing research therefore aims to establish how Tregs communicate with their tissue environment and uncover the specific ligands or tissue antigens that promote their survival, residency and suppressor functions here, but not within lymphoid sites. We highlight below a number of studies that emphasise the unique phenotype and function of Tregs resident in distinct tissue sites.

Novel single cell RNA sequencing technology of gut tissue has revealed gut resident Tregs display a unique transcriptional profile in comparison to their draining MLN counterparts [299]. In brief, a transcriptional trajectory is observed as Tregs migrate from MLN to colon tissue, emphasising the phenotype and function of Tregs at each of these sites are highly influenced by the environment. Furthermore, tissue-resident Tregs have also been shown to exhibit certain functions that are beneficial to their immediate location. Upon muscle injury, a distinct population of Tregs rapidly migrate and accumulate at this site [297]. Such Tregs play a critical role in restraining the pro-inflammatory myeloid infiltrate and promote muscle repair. These muscle-associated Tregs express the growth factor amphiregulin, and stimulate repair of injured muscle. In addition, during acute infectious lung injury, Tregs in the lung tissue play an important role in promoting repair of damaged lung tissue through the expression of amphiregulin [300]. Critically, such cues driving repair are distinct to their roles in immune suppression of inflammation. Finally, a distinct population of Tregs are found to be present in the visceral adipose tissue (VAT) of normal animals, with both a unique phenotype and transcriptional profile in comparison to Tregs resident in the spleen and lymph nodes [301]. In particular, VAT-associated Tregs are enriched for transcripts encoding the nuclear receptor PPARγ [302]. Ablation of PPARγ

specifically within Tregs results in reduced numbers of Tregs within VAT tissue and a lower expression of Foxp3, showing the critical importance of PPARγ in promoting the accumulation and regulatory phenotype of Tregs within VAT. Furthermore, PPARγ expression within VAT Tregs is critically required for Treg -mediated control of insulin sensitivity.

Treg plasticity

A number of studies have suggested that Tregs might become unstable during periods of intense inflammation and/or infection. Under such conditions, Tregs may adopt a more pro-inflammatory effector T cell phenotype and lose the ability to suppress. Infection with *Toxoplasma gondii* is an example that leads to a Th1 cell polarised immune response resulting in reduced Treg cell numbers through the diminished production of the Treg survival cytokine IL-2 by effector T cells [303]. Furthermore, infection promotes Tregs to acquire pro-inflammatory Th1 T cell properties, including the expression of T-bet and production of IFN-γ. Another setting of physiological stress occurs when Tregs are adoptively transferred into a lymphopenic environment, with approximately 50% losing their expression of Foxp3, whilst administration of its critical survival cytokine IL-2 is able to prevent Foxp3 downregulation. A fraction of such 'ex' Tregs may also retain memory of previous Foxp3 expression and re-acquire suppressive activity upon TCR stimulation [304-307]. These findings highlight Foxp3^{+} Tregs are composed of a heterogenous population of committed and uncommitted subtypes that demonstrate greater plasticity. Further studies are therefore crucial in understanding the critical role of IL-2 availability for the success of Treg therapy in autoimmune/inflammatory disorders.

Outside of a pathogenic environment, using reporter mice to track the induction and downregulation of Foxp3, wild type lymphocyte sufficient mice have been found to harbour approximately 20% ex-Tregs within their $CD4^+$ T cell pool [308]. These ex-Tregs were of a mixed phenotype with heterogenous expression of signature Treg markers, such as CTLA4 and CD103. Finally, in line with a loss of suppressor function, ex-Tregs also produced effector cytokines unique to distinct $CD4^+$ T cell lineages, such as IFN-γ and IL17. Of critical importance, experiments using adoptive transfer of ex-Tregs showed they are pathogenic, and havev the ability to induce islet cell destruction in a similar fashion to effector T cells, and drive autoimmune diabetes [308], and multiple sclerosis in an experimentally induced autoimmune encephalomyelitis model [309].

1.8 Host T cell-microbial cross-talk

Commensal bacteria are known to serve many functions, including digestion of food molecules to promote tissue health, and out-competing pathogenic infections for food and niche space. Of importance, the microbiota educates the local and systemic immune responses and promotes gut health. Several approaches have demonstrated this favourable host-microbial cross-talk, including the immunological defects suffered by germ-free mice (reviewed in [310]), whilst perturbations of the microbiota through antibiotic administration or bacterial strain reconstitution highlight the role of distinct bacterial strains in maintaining gut homeostasis [311-313]. A heterogenous population of T cells have the ability to respond to microbial antigens, including conventional $CD4^+$ and $CD8^+$ T cells, natural killer T cells and mucosal associated invariant T cells (MAITs). The following discussion focuses on the crucial role of the microbiota in promoting the beneficial differentiation of $CD4^+$ T cells at mucosal sites.

Most recently, the ability to track microbiota-specific T cells using TCR transgenic mice models have furthered our understanding of the diverse variety of $CD4^+$ T cell responses that can be directly stimulated by distinct commensals. TCR transgenic mice develop T cells that express TCR of a known antigen specificity, and these models have revealed unique T cell behaviour in response to particular commensal bacteria.

The critical importance of the microbiota in driving host immune responses can be demonstrated by germ free mice that have immature immune system development with reduced $CD4^+$ T cells in the gut, the effect of which can be reversed by colonisation with commensal bacteria (reviewed in [314]). Indeed, the microbiota is critical for both Th17 and Treg cell development, and maintaining balance between these opposing pro- and anti-inflammatory responses [315]. Germ-free mice have very low numbers of Th17 that are normally enriched in the small intestine [316], and fewer Tregs in the colon [317, 318]. However, the Treg number in the small intestines in germ free mice is unchanged, suggesting dietary antigens or developmental control plays an important role in Treg induction at this site [319].

The majority of Th17 cell responses in the intestinal lumen are commensal specific. A landmark study showed colonisation of the murine terminal ileum with a single commensal microbe, segmented filamentous bacteria (SFB) is enough to induce the expansion of Th17 cells that abundantly produce IL-17 and IL-22 in the lamina propria [320]. Indeed, the differences in Th17 abundance between the same mouse strain within different animal facilities is likely explained by the varying presence of SFB [320]. SFB are a group of ileal epithelium-attaching group of gram positive, spore-forming bacteria, that are a genetic relative of the genus *Clostridium* (reviewed in [321]). Indeed, attachment

and adhesion of SFB to intestinal epithelial cells is critical for Th17 cell induction [322]. Specifically, SFB colonisation induces a distinct immune response program in the intestine with increased expression of genes linked to inflammation and anti-microbial defences, including up-regulation of the acute-phase protein serum amyloid A. Finally, SFB has not been identified as a human commensal, however an analogous bacteria, *Bifidobacterium adolescentis* has been identified in human microbiota studies to be closely associated with the gut epithelium and induce a strong Th17 response without any accompanying inflammation [323]. However, *Bifidobacterium adolescentis* stimulates a transcriptional program that is distinct to SFB, indicating in humans, a different mechanism of Th17 induction exists compared to mice.

The function of Th17 cells during health and disease is highly context dependent. Indeed, commensal induced Th17 cells have been reported to have beneficial and harmful effects on the host. On the one hand, colonisation by SFB is thought to compete with pathogenic bacteria *Citrobacter rodentium* for intestinal niche space, and SFB has been shown to promote resistance to *Citrobacter rodentium* [320]. Conversely, commensal reactive Th17 cells have also been reported to drive systemic inflammatory pathologies including arthritis [324] and uveitis [325].

Recently, a TCR transgenic mouse model to the mucin-degrading commensal bacteria *Akkermansia muciniphila (A. muciniphila)* has been developed. *A. muciniphila* is present in humans and associated with favourable outcomes in cancer patients undergoing checkpoint blockade, and the mechanism is likely mediated through a IFN-γ producing Th1 anti-tumour response [326]. Adoptive transfer of *A. muciniphila*-specific naïve T cells into colonised gnotobiotic hosts induced the differentiation of Tfh cells, largely limited to Peyer's patches and MLNs with few detectable cells present in the lamina propria [327].

However, within SPF hosts, there were greater numbers of *A.muciniphila* – specific T cells detected within the lamina propria, with some adopting a Th1 or Th17 pro-inflammatory phenotype. These results highlight the context dependent differentiation of microbial-reactive T cells within different un-inflamed host environments. Greater understanding of the microbial signals that promote distinct T cell fates during conditions may contribute towards the development of more robust anti-cancer immunotherapies.

Available evidence also exists for the microbial induction of Tregs in the gut. Gut resident $Foxp3^+$ Tregs are a discrete population of Tregs distinct from those in other tissues. In particular, unlike Tregs at other sites that have TCRs mainly specific for self-antigens, colonic Tregs harbour TCRs that are reactive to microbial antigens and such Treg populations play a special role in suppressing immune responses to commensal microbes and harmless food antigens (reviewed in [239]). Multiple studies have highlighted the existence of several bacterial strains that provide both direct microbial antigens in addition to metabolites from digestion of food antigens that critically modulate intestinal Treg cell function and survival. Many colonic Tregs are peripherally induced, i.e., they derive from the conversion of $Foxp3^-$ $CD4^+$ naive T cells, and do not express the conventional thymic Treg surface markers Helios and Nrp1 [241]. However, one study did argue towards the existence of thymic-derived Tregs that predominantly mediate tolerance towards intestinal commensals [328]. Nevertheless, multiple studies have shown germ free mice containing an almost exclusive population of thymic-derived $Nrp1^-$ $Helios^-$ $Foxp3^+$ colonic Tregs, with the peripherally induced $Nrp1^-$ $Helios^-$ $Foxp3^+$ population being depleted by antibiotic treatment [255, 256].

A seminal study in 2011 established in addition to thymic education of tolerogenic Tregs to self-antigens, encounter with foreign commensal microbial antigens drives the

generation of an exclusive pool of peripheral Tregs that play an important role in maintaining homeostasis [241]. Such peripherally-educated colonic Tregs, in contrast to their secondary lymph node counterparts, expressed a unique TCR repertoire reactive to antigens derived from commensal bacteria. Of interest, under unfavourable pro-inflammatory conditions, the same commensal-reactive TCRs can induce colitogenic effector cells in a T cell transfer model of colitis. This study was therefore a crucial early demonstration of the presence of a unique population of extra-thymically generated population of Tregs within the colon with TCR specificity to foreign commensal antigens that may be critically important in suppressing effector T cells to maintain tolerance. A particular strength of this study is the use of genetically engineered mice that express a restricted but polyclonal TCR repertoire to permit *in vivo* unbiased profiling and identification of TCRs found in colonic Treg cells. However, this early study did not inform on the process of how commensal bacteria shape the colonic Treg pool.

A later study by the same group addressed this question [329]. Generation of two TCR transgenic lines previously identified to be expressed by microbiota- dependent peripheral colonic Tregs [241] were adoptively transferred into lymphoreplete hosts to study the kinetics of peripheral Treg development in response to the microbiota. Using this experimental model, and in support of our time-course experiment (section 4.2.2), donor TCR tg T cells were locally retained in the draining MLN as soon as 2 days after transfer. Furthermore, Notch2-dependent dendritic cells, but not TGF- b, are critically required for peripheral Treg generation to commensal antigens. Similar to the adoptive transfer model used in our experiments, this technique allows for the real-time *in vivo* tracking of a small physiological population of naïve T cells that have been previously confirmed to be commensal antigen reactive and differentiate into peripherally-induced Tregs within

normal lymphoreplete hosts. However, both studies above involve analysis of Tregs expressing TCRs that are broadly reactive to a number of commensal bacteria, and lacked clarification of how specific bacterial species could drive T effector responses during colitis.

Finally, both the Hsieh and Littman groups have shed light on the pathobiont nature of *Helicobacter spp.*, showing T cell responses to this specific bacterial antigen is context dependent, with the induction of suppressor Tregs during homeostatic conditions, whilst experimental colitis drives an effector T cell response [57, 330]. The Hsieh group used a T cell transfer model of colitis, whereas inflammation was induced by colonisation of *H.hepaticus* in *Il10* $^{-/-}$ mouse hosts in the Littman study. Furthermore, differences exist in the generation of *Helicobacter*-specific TCR transgenic cell lines used to study these responses. The Hsieh group cell line was originally identified through a population of colonic Tregs expressing broadly commensal-reactive TCRs that were later shown *in vitro* to respond with a high degree of specificity to *Helicobacter spp* cultured isolates. The Littman group generated an *H.hepaticus*-specific TCR transgenic cell line by identifying TCR sequences from effector IL-23R^{GFP+} T cells that were antigen-specific to an identified epitope in colitogenic *H.hepticus* infected mice treated with anti-IL10R blockade. As such, the Littman TCRtg model would be distinctively reactive to a particular peptide sequence found on *H.hepaticus*. Additionally, the authors also confirmed TCRtg responses using a MHC class II tetramer loaded with a unique *H.hepaticus* peptide. Such complementary approaches would minimise tracking of T cells reactive to multiple antigens expressed on different bacterial strains.

Taken together, these studies show the presence of a distinct pool of colonic Tregs that are extra-thymically induced by pathobionts with essential roles in suppressing inflammatory responses to non-self antigens. Furthermore, the use of antigen-specific transgenic mouse models have increased our understanding of how the host's response to the same bacterial antigen is context-dependent, with skewing towards a tolerogenic profile during health, whilst an effector T cell response predominates during disease.

With regard to the identity of other bacteria that can induce the expansion of peripherally induced Tregs, several distinct species have been reported. Specifically, the gram positive spore – forming species of Clostridia belonging to clusters IV and XIVa have been shown to promote colonic Treg accumulation [317]. Furthermore, colonisation of host mice with a defined cocktail of Clostridium strains result in upregulation of TGF-β in the colon and intestinal epithelial cells, promoting the accumulation of induced Tregs with strong IL-10 suppressor function. Finally, inoculation of Clostridium in early life promotes resistance to colitis and IgE responses, demonstrating how individual commensal species can impact local inflammatory and systemic antibody responses. Furthermore, commensal *Clostridia* play a role in promoting gut epithelial barrier integrity and the prevention of food allergen sensitisation [331].

Other bacterial strains that have been reported to promote colonic Tregs include *Lactobacillus,* which have been shown to attenuate airway inflammation [332]. The human symbiont Bacteroides fragilis directs the development and increases the suppressor capacity of colonic Tregs through the production of polysaccharide A (PSA) [333]. Bacteroides fragilis was able to protect mice from *H.hepaticus* induced colitis through the

induction of IL-10 producing $CD4^+$ T cells, and this protective mechanism is lost in animals colonised with *Bacteroides fragilis* not expressing PSA [334].

Furthermore, commensal bacteria also conduct vital metabolic processes, and several reports have highlighted metabolite by-products made by the bacterial digestion of food as an additional mechanism of colonic Treg induction. The short chain fatty acid (SCFA) produced by the fermentation of fibre by commensal bacteria include butyrate, propionate and acetate are essential metabolites that promote gut health (reviewed in [335]). Both butyrate and propionate have been shown to promote the differentiation of extrathymic Treg cells [336], and the mechanism includes histone deacetylase (HDAC) inhibition [7]. Critically, this peripherally induced Treg population was capable of ameliorating T cell transfer induced colitis [337].

In sum, bacterial antigens and metabolites produced by commensals facilitate the smooth communication between microbiota and the immune system and this contributes to the delicate balance between health and disease. Recently, a number of clinical therapies have been trailed in an attempt to modulate a dysbiotic microbiome to a more favourable composition. These include the administration of substrates utilised by commensal bacteria to generate beneficial metabolites such as SCFA (prebiotics) and live micro-organisms that engage in favourable interactions with the host (probiotics) (reviewed in [338]). Bifidobacteria and lactobacillus are the most widely commercially available probiotics [339]. Furthermore, the transfer of processed stool from a healthy donor into a host suffering from a disease driven by an 'unhealthy' microbiota (faecal microbiota transfer (FMT)) has seen the greatest success in *Clostridium difficile* infections, with up to 90% cure rate [340]. Clinical trials of FMT in IBD have shown some promise although currently evidence is lacking to support its routine use [341]. Of particular importance, a

number of risks are associated with FMT, including the transmission of pathogenic bacterial strains, including *Escherichia coli*, and the theoretical risk of transfer of disease-causing microbial signatures from donor to host.

1.9 Aims of the thesis

There has been much interest in the role of gut tissue-associated lymphoid tissue in mucosal immune responses. Tregs are a key player in mediating tolerance in the gut, and studies have reported the presence of Tregs within such lymphoid structures. However, it is currently unclear how Tregs function here distinct to the surrounding lamina propria tissue to promote intestinal health. One potential mechanism involves the alarmin IL-33 expressed in lymphoid structures, and known to mediate essential reparative functions during inflammation through interactions with its receptor ST2 present on a subset of gut resident Tregs. Additionally, such lymphoid structures have also been reported as local sites of immune induction and may support the differentiation of naïve T cell into Tregs. At barrier sites, common antigens presented to T cells include microbial peptides derived from the gut microbiota.

We therefore aim to understand the cellular interactions within gut associated lymphoid structures that are critically required to maintain Treg function and support intestinal homeostasis.

The specific aims of this thesis are:

1. To characterise the tissue-associated lymphoid structures of the murine gut.
2. To explore the spatial relationship between IL-33 cytokine and $ST2^+$ Tregs within lymphoid structures during health and disease.
3. To determine what role cellular interactions within tissue-associated lymphoid structures play in promoting the activation and function of microbe-reactive T cells.

Chapter 2. Materials and Methods

2.1 Mice

C57BL/6J (B6), B6.Foxp3^{GFP} , B6Rag1$^{-/-}$, B6.dsRedhCD2, B6.Foxp3^{hCD2}IL-10^{GFP} [342, 343] and B6.Nur77^{GFP} mice were bred and maintained under specific pathogen-free (SPF) conditions in an accredited animal facility at the University of Oxford. Lta^{tm1Dch} mice were purchased from Jackson Laboratories. HH7-2tg TCR transgenic mice were provided by Dan R. Littman (New York). HH7-2tg mice were crossed in-house to B6.dsRedhCD2 and either B6.Foxp3^{hCD2} IL-10^{GFP} or B6.Nur77^{GFP} mice to generate HH7-2tgDsredIL-10^{GFP} or HH7-2tgDsred Nur77^{GFP} respectively. HH7-2tg mice were crossed to B6Rag1$^{-/-}$ to generate HH7-2tgRag1$^{-/-}$ mice.

Mice were free of *Helicobacter spp*. and other known intestinal pathogens. Mice used for experiments were age and sex-matched and between 6 to 12 weeks old. Animals were randomly assigned to experimental groups, and cages contained mice of all different experimental groups. All experiments were conducted in accordance with the UK Scientific Procedures Act of 1986, and by persons holding a personal license, working under a project license authorised by the UK Home Office.

2.2 *In vivo* experiments

2.2.1 *Helicobacter hepaticus*/anti-IL10R induction of colitis

H. hepaticus NCI-Frederick isolate 1A (strain 51449) was cultured on blood agar plates containing 7.5% laked horse blood (Thermo Scientific supplemented with Skirrow Campylobacter antibiotic (Oxoid) under microaerophilic conditions with agitation at 37oC for 48 hours. Bacteria was subsequently transferred to liquid culture of Trypton soya broth (Oxoid) supplemented with 10% fetal calf serum (Sigma Aldrich) and Skirrow Campylobacter antibiotic in a vented Erlenmeyer Flask (Corning). This culture was allowed to grow under microaerophilic conditions at 37^{o}C in a shaking incubator. Optimal bacteria growth was assessed by optical density (OD) using a Biophotometer (Eppendorf) read at 600nm.

For oral gavage, bacterial culture was centrifuged at 3500rpm for 20 minutes and mice were infected using a 22G curved needle on day 0 and 1 with 1x10^{8} colony-forming units (cfu)- equal to 1OD. For colitis experiments, mice were also injected with 1mg anti-IL10R blocking antibody (clone 1B1.2, produced in house) via intraperitoneal injection weekly starting on day 0. Mice were sacrificed at peak of colon inflammation on 14 days after first *H.hepaticus* colonisation.

2.2.2 Dextran sulphate sodium induction of colitis

Dextran sulphate sodium (MP Biomedicals UK) was added to drinking water at a concentration of 2.7 %. This was given from day 1 of the experiment, refreshed on day 3,

and switched to normal drinking water on day 5. The mice were monitored daily for weight loss and clinical signs of colitis. Mice were culled once they reached 20% weight loss limit, with a maximum duration of 9 days from the start of DSS administration.

2.2.3 Lymph node lymphocyte egress blocking experiment

Recipient mice were infected with *H.hepaticus* on day 0 and 1, with adoptive transfer of HH7-2tg on day 7. Subsequently, recipient mice were treated every 24 hours with 1mg/kg of the sphingosine-1-phosphate antagonist, Fingolimod (FTY720, Sigma Aldrich) by intraperitoneal injection on day 8, 9 and 10 post intravenous HH7-2tg cell injection. Mice were sacrificed 11 days after the first dose of *H.hepaticus* gavage.

2.3 Cell isolation

2.3.1 Isolation of leukocytes from blood

Murine blood was collected from the tail vein into a tube containing 300ul of 0.5M EDTA, and red blood cells subsequently lysed with 500ul if ACK lysis buffer for 3minutes at room temperature. Cells were washed, centrifuged and resuspended in PBS/0.1% BSA/5mM EDTA, and stained with surface antibody for flow cytometry analysis.

2.3.2 Isolation of leucocytes from spleens and mesenteric lymph nodes

Spleens and mesenteric lymph nodes were harvested from mice after sacrifice. Organs were mechanically disrupted through a 70μm strainer, washed in PBS/0.1% BSA/5mM

EDTA (Sigma-Aldrich) and centrifuged at 1500rpm for 5 minutes. Splenic cells were additionally incubated with 1ml ACK lysis buffer for 3 minutes at room temperature to lyse red blood cells, followed by washing in PBS/0.1%
BSA/5mM EDTA. Single cell leukocyte spleen and lymph node suspensions were resuspended in an appropriate volume of PBS/0.1% BSA/5mM EDTA, stained with antibody ready for flow cytometry analysis.

2.3.3 Isolation of leukocytes from the colon, caecum, caecal patch and organised lymphoid structures

Colon and caecum tissue were harvested from mice after sacrifice, opened, rinsed in PBS/0.1%BSA/0.5mM EDTA and washed in RPMI (Sigma Aldrich)/10% FCS/5mM EDTA at 37^{o}C with agitation for 25 mins each to remove epithelial cells. Tissues were transferred to RPMI/10%FCS/15mM Hepes (Sigma Aldrich) for 10 minutes to neutralise EDTA activity. Caecal patches and OLS were identified under x40 brightfield microscopy and removed using a scalpel and a 16G needle respectively.

The remaining colon and caecum tissue, OLS and caecal patches were digested for 40 minutes at 37^{o}C with agitation in RPMI/10%FCS15mM Hepes with 100U/ml collagenase VIII (Sigma Aldrich) and 20mg/ml DNase I (Sigma Aldrich). Cells were filtered through a 70µm strainer to remove undigested tissue, and the digest was terminated by the addition of ice-cold RPMI/10%FCS/5mM EDTA. Digested cells were pelleted by centrifugation at 1500rpm for 5 minutes. A 30/40/70% Percoll (GE Healthcare) density gradient was used to enrich and isolate leucocytes from epithelial and stromal cells. Digested cells were

resuspended in the 30% gradient layer, on top of the 40% and 70% layers, centrifuged for 20 minutes at 1800rpm without brake. Leukocytes recovered at the interface of the 40/70% Percoll gradient were washed and resuspended in PBS/0.1% BSA/5mM EDTA ready for plating.

2.4 Flow cytometry and cell sorting

2.4.1 PMA/Ionomycin re-stimulation of cells for intracellular cytokine staining

Single cell suspensions isolated from caecum, colon, OLS and caecal patch tissues were plated into 96 well round bottom plates (Corning) in complete RPMI-1640-medium (Sigma) supplemented with 10% FCS, 2mM L glutamine (Life Technologies), 0.05mM 2mercaptoethanol (Life technologies), 100U/ml each of penicillin and streptomycin (Sigma-Aldrich). To this, 0.1µM phorbol 12-myristate 13-acetate (PMA) and 1µm ionomycin together with 10µg/ml brefeldin A (Sigma-Aldrich) were added and cells were incubated for 3 hours 45 mins at 37ºC, washed and ready for further processing for flow cytometry analysis.

2.4.2 Cell surface staining

All surface stains and washing were performed in PBS/0.1% BSA/5mM EDTA, with centrifugations at 1500rpm for 5 mins. Mouse cells were surface stained with a

combination of the following monoclonal antibodies, which were purchased from Biolegend, eBioscience and Invitrogen: CD4 (RM4-5), TCRβ (H57-957), CD45.1 (A20), CD45.2 (104), CD11c (N418), CD11b (M1/70), anti-human CD2 (TS1/8), CXCR5 (L138D7), PD-1 (J43), IgD (11-26c.2a), CD19 (6D5), ST2 (101001B), with dead cells excluded using efluor-780 fixable viability dye. Cells were incubated with surface antibodies in a 96 V-bottom plate for 20minutes at 4°C in the dark followed by two washes. The anti-ST2 antibody used was biotinylated, and therefore cells were stained with streptavidin conjugated to a fluorophore for an additional 15 minutes at 4°C in the dark before washing. Samples were acquired on the FACS Fortessa and FACS LSRII flow cytometers (Becton Dickinson) using FACSDiva software (BD Biosciences). Absolute cell numbers were calculated by adding 10^3 CountBright beads (Life Technologies) to each sample before acquisition on a flow cytometer. Data was analysed using FlowJo (Tree Star, Inc).

2.4.3 Intracellular staining

Cells were firstly stained with surface antibodies as described above. For intracellular staining of transcription factors Foxp3 (FJK-16s), Rorγt (Q31-378), GATA-3 (TWAJ), T-bet (4B10), Helios (22F6), Ki-67 (SolA15) and cytokines TNFα (MP6-XT22), IL-10 (JESS-16E3), IFN-γ (XMG1.2), IL-17A (TC11-18H10.1), cells were fixed and permeabilised using Foxp3/Transcription Factor Staining Buffer Set (eBioscience) following the manufacturer's instructions. Cells were acquired and analysed on the flow cytometer as before.

2.4.4 Sorting and adoptive transfer of HH7-2tg cells

Recipient mice were infected with *H.hepaticus* by oral gavage 3 to 7 days prior to adoptive transfer of donor HH7-2tg T cells. Donor HH7-2tg mice spleens were harvested after sacrifice and mechanically dissociated through a sterile 70µm filter. 500µl of ACK lysis buffer was used to lyse splenic red cells, with subsequent labelling with surface antibodies: CD3 (145-2C11), CD25 (eBio3c7), CD11b (M1/70), CD11c (N418), B220 (RA3-6B2), CD62L (MEL-14), TCRVb6 (RR4-7), CD44 (IM7), CD45 (30-F11), CD4 (RM4-5). Dead cells were excluded using efluor-780 fixable viability dye (eBioscience). Naïve HH7-2tg T cells were sorted as single, live $CD45^{+}CD3^{+}CD4^{+}CD25^{-}CD44^{lo}CD62L^{hi}Vb6^{+}$(HH7-2tg) on Aria II (BD Bioscience) sorter. Sorted HH7-2tg T cells were resuspended in sterile PBS and intravenously injected into *H.hepaticus* colonised recipient mice via the tail vein. 2000 and 50,000 naïve donor HH7-2tg T cells were injected for flow cytometric analysis and live imaging respectively.

2.5 *In vitro* co-culture

Bone marrow cells were extracted from WT mouse tibias and femurs after sacrifice. Cell were cultured for 7 days in RPMI (Sigma) supplemented with 1% Pen-Strep antibiotics (Sigma), 10% FCS (Life Technologies), 1% Glutamax (Invitrogen) and 20ng/ml murine GM-CSF (Peprotech). The medium was topped up after 3 days with media and GM-CSF. At day 7, bone marrow derived dendritic cell morphology was checked using a brightfield microscope and plated in round bottom 96 well plates at a density of $1x10^4$ cells/well overnight at 37°C. The following day, 1mg/ml *H.hepaticus* peptide (Genscript) was added for one hour incubation, after which $1x10^5$ sorted naïve HH7-2tg$Nur77^{GFP}$ T cells were

added to the wells in RPMI/10% FCS/1% Glutamax/1% pen-strep and 50mM b-mercaptoethanol (Life Technologies). Anti-mouse I-A/I-E antibody was added at 4, 12, 24, 48, 72 and 96 hours after plating HH7-2tg Nur77^{GFP} T cells to block further antigen stimulation. At the appropriate time points, cells were washed, stained with surface antibody and the Nur77^{GFP} MFI was acquired on FACS Fortessa flow cytometer.

2.6 Imaging of *ex vivo* and *in vivo* tissue

2.6.1 Immunofluorescent ex vivo tissue imaging

Caecum and colon tissue were harvested after sacrifice, rolled tightly into 'swiss rolls' and embedded into OCT compound (Tissue-Tek) to preserve architecture. A cryostat (Leica) was used to cut 7mm sections onto Superfrost Plus Micro Slides (VWR) and stored at -20^{o}C. For immunofluorescent labelling, slides were thawed at room temperature, washed in PBS to remove residual OCT and fixed with 3.7% formalin (Merck) for 3 minutes. Second fixation was performed using cold Fix-perm buffer for a further 5 minutes (Foxp3/Transcription staining buffer set, eBioscience). Non-specific staining was blocked using 10% donkey serum (Sigma-Aldrich) and 1% Fc block (eBioscience) in permeabilisation buffer (Foxp3/Transcription factor staining buffer set, eBioscience). Primary antibody staining was performed in 10% rabbit/donkey serum in permeabilization buffer overnight at 4oC. Following overnight incubation, slides were washed extensively in PBS to remove residual unstained antibody, and secondary antibodies were applied for 1 hour in blocking serum. Slides were washed again in PBS, mounted with Prolong Gold Antifade mountant with DAPI stain (ThermoFisher Scientific) and imaged on an Olympus BX51 microscope. Whole colon 'swiss roll' images were collected at x20 magnification

on a Zeiss LSM 780 confocal microscope. We obtained 20 x 20 tiled images with a pixel size of 0.83μm, and 4 Z-stacks per tile.

Acquired immunofluorescent images were processed and analysed using Imaris 9 (Bitplane, UK). Fluorescently marked cells of interest were identified using the Surface Creation Wizard in Imaris. The distance transformation function was used to determine distances between cells of interest. Fluorescence intensity of each marker and x, y, position coordinate statistics were exported into Excel FlowJo 10.3 (Tree Star) for further analysis to determine clustering.

All primary and secondary antibodies used for immunofluorescent labelling are listed below.

Primary antibodies

B220 (RA3-6B20), host species rat

CD4 (RM4-5), host species rat

MHC Class II (M5/114.15.2), host species rat

Purified Rorγt (AFKJS-9), host species rat

Purified Foxp3 (1054C), host species rabbit

Purified IL-33 (AF3626), host species goat

Secondary antibodies

Donkey anti rat – AF488

Donkey anti-goat – AF647

Donkey anti rabbit – AF555

2.6.2 Two-photon microscopy

Gut caecum imaging was performed as described in Pearson and Thornton et al [344]. mice were anaesthetised with isoflurane, the caecum exposed and immobilised with a suctioning imaging window. Images were collected using a 20x water dipping lens and the spectral detector of a Zeiss 880 multiphoton microscope (Carl Zeiss, Germany). Images were linearly unmixed using the Zen software (Carl Zeiss) to separate autofluorescence, collagen, EGFP, Dsred and Texas-red dextran based on single colour controls.

2.6.3 Blood vessel labelling

Mice were anaesthetised and injected intravenously via tail vein with 25mg of 70kDa Texas-Red labelled dextran (Life Technologies) immediately prior to imaging as above.

2.6.4 *In vivo* Image analysis and histo-cytometry

All intravital microscopy images were analysed using Imaris 9 (Bitplane, UK). Following unmixing, autofluorescence was subtracted from Dsred and GFP channels. Positively staining GFP and Dsred cells were marked using the Surface Creation Wizard in Imaris, and their co-expression and location within LP and lymphoid aggregate micro-niches was recorded. Finally, Dsred and GFP fluorescent intensities within tissue micro-niches were quantified using Histo-cytometry [345]. Briefly, surfaces marking positively staining GFP

and Dsred cells were created as before. Statistics for each channel and location was exported into Excel (Microsoft) and the mean fluorescent intensity was plotted in Flowjo (Treestar, Inc).

Intravital movies were drift corrected based on mucus or collagen signal. Images were smoothed using a Gaussian filter for display.

2.7 Statistical analysis

Statistical analysis was performed using Prism 8 (GraphPad). The t- test was used to compare two unpaired samples. For more than two groups, the ordinary one-way ANOVA was used. Differences were considered statistically significant when $p \leq 0.05$. Significance is indicated by the following: * $p \leq 0.05$,** $p \leq 0.01$,***$p \leq 0.001$,****$p \leq 0.0001$. Technical replicates are from the same sample, processed and analysed on the same day. Biological replicates are from independent experiments.

Chapter 3. Solitary Isolated lymphoid tissue as a regulatory T cell niche

3.1 Introduction

The gut – associated lymphoid tissue (GALT) forms the largest collection of lymphoid tissue in the body, and along with the intestinal epithelial barrier, plays a critical role in controlling the balance between tolerance and immune response to foreign antigens, including ingested food and the microbiota (reviewed in [346]). GALT is comprised of both macroscopic and microscopic structures. The macroscopic structures include the draining mesenteric lymph nodes, Peyer's patches and caecal patch. The microscopic structures include the solitary isolated lymphoid tissue (SILTs) [102]. The MLNs have traditionally been identified as the main site for co-ordinating the adaptive immune response and the opposing tolerogenic versus inflammatory responses necessary to manage beneficial and harmful bacteria respectively has recently been shown to involve compartmentalised drainage of anatomically segregated gut sections to functionally separate lymph nodes [347].

Tregs are an essential $CD4^+$ T cell subset that plays a major role in maintaining immunological tolerance through the restraint of inappropriate T effector responses to self and commensal antigens. Single cell RNA-sequencing of transcriptional differences between MLN and colon tissue-resident Tregs provide clues as to how intestinal Tregs adapt to their local gut environment. As Tregs transition from lymph node to non-lymphoid gut tissue, they downregulate lymph node-related genes (*Lef1, Tcf7, Sell*), whilst

tissue associated genes are upregulated (*Nfil3, Ccr8, Cxcr6, Cd44 and Il10*) [299]. This idea of lymph node versus tissue compartmentalisation can also be applied to the tissue microenvironment itself. Here, an additional specialised network of tissue-embedded lymphoid structures, collectively known as SILTs, which include cryptopatches, isolated lymphoid follicles and tertiary lymphoid structures, are present [102, 348]. It is possible but currently unconfirmed whether signals within SILTs could contribute positively to adaptation of intestinal Tregs to their tissue environment.

Intestinal SILTs are composed of a heterogenous population of stromal, innate and adaptive immune cells. Whether SILTs contribute to Treg function in the gut, and the signalling pathways within SILTs that promote Treg survival and proliferation during health and disease is not known. It is well established the cytokine IL-2 signals through the high affinity IL-2Rα chain (CD25) on Tregs, and this is critically required for sustaining the Treg pool at a size vital to maintain homeostasis [349]. More recently, signalling of the alarmin cytokine IL-33 to Tregs bearing the IL-33 receptor, ST2, has also been shown to be an important pathway involved in the function of mucosal-associated Tregs [350]. This is of particular interest as the Powrie group has determined through two-photon microscopy using steady state IL-33^{citrine} reporter mice, the expression of the alarmin IL-33 is non-uniform across the length of the colon: IL-33 expression is clustered within small lymphoid aggregates of the proximal and mid colons, whilst epithelial cells expressed IL-33 in the distal colon [Chomka, unpublished data]. Such aggregates likely represent intestinal SILTs, and further characterisation confirmed CD45$^-$ Epcam$^-$ PDGFRα$^+$ stromal cells to be the source of IL-33 production. Therefore, one possible mechanism of how SILTs contribute to the intestinal immune response is by supporting local IL-33 signalling to ST2$^+$ immune cells.

However, controversy exists as to whether IL-33 plays a protective or pathogenic role in the intestine. Both IL-33 and its receptor has been found to be increased in the inflamed mucosa of IBD patients in comparison to health controls [138-141]. However, in murine models, IL-33 and ST2-deficient mice do not develop spontaneous abnormalities under homeostatic conditions, highlighting a critical role of IL-33 when hosts are challenged with an inflammatory insult [351-354]. Studies of the effect of IL-33 fall into two broad categories: IL-33 has been shown to either promote immune dysregulation and drive pro-inflammatory adaptive immune responses, or it can function to promote epithelial proliferation and regeneration of gut barrier function. In support of the first hypothesis, DSS induced colitis in IL-33 KO [355] and ST2 KO [142, 146] mice revealed less severe pathology compared to wild-type controls. In contrast, studies using different models of colitis, including TNBS [145] and oxazolone-induced colitis [144] showed IL-33 to be protective and function to ameliorate tissue injury. An interesting concept put forward is IL-33 may have dual roles depending on its site of action, with IL-33 driving pro-inflammatory responses on lamina propria immune cells, but promote healing and repair when acting on gut epithelial cells [356]. Whether the spatial distribution of IL-33 expression within epithelial cells versus SILTs observed in distinct colon regions of IL-$33^{citrine}$ mouse support the dichotomous roles of IL-33 remains unknown.

Available evidence so far suggests IL-33 may play dual, and often opposing roles in the immune response. However, despite abundant clinical and murine data exploring the expression and effects of IL-33 in inflammatory conditions, functional studies to understand the mechanisms of the IL-33 pathway in the maintenance of homeostasis is still lacking. Recently, IL-33 has been identified to play an essential role in promoting tissue resident $ST2^{+}$ Tregs that result in beneficial effects on the host. For example, IL-33 plays

an essential role in the maintenance and development of visceral adipose tissue (VAT) - resident $ST2^+$ Tregs that prevents inflammation, insulin resistance and type 2 diabetes [357-359]. Within the gut, our group has shown the enrichment of $ST2^+$ Tregs within barrier sites of the gut, lung and skin, with the EGF receptor ligand, amphiregulin that is known to play important roles in tissue repair, specifically upregulated in $ST2^+$ Tregs [Chomka, unpublished data]. Furthermore, IL-33 signalling to intestinal $ST2^+$ Tregs promotes its regulatory function and ability to restrain intestinal inflammation [360].

Altogether, colonic SILTs may form local sites of the intestinal adaptive immune response that functions to promote Treg tolerance and maintain gut health. IL-33 has been shown to be abundantly expressed within SILTs, and the IL-33/Treg signalling pathway could be one important process occurring in SILTs that promote homeostasis and/or repair during intestinal inflammation. Similar to lymph nodes, larger SILTs have been shown to exhibit structural organisation (reviewed in [361]). It is therefore possible IL-33 signals to $ST2^+$ Tregs that inhabit unique niches found in close proximity to IL-33 expressing cells. Although cytokines can permeate a tissue and influence a large population of cells, a recent study explored the role of the local microenvironment in eliciting the function of cytokines in distinct cell subsets [362]. That study highlighted the importance of contact-dependent $CD8^+$ T cell to $CD8^+$ T cell interactions to drive maximal IFN-γ signalling during bacterial infection. We therefore hypothesise IL-33 signals to $ST2^+$ Tregs within SILTs to promote their expansion and tolerogenic potential, and this pathway is enhanced by the positioning of $ST2^+$ Tregs within distinct SILT compartments that are spatially near to IL-33 expressing cells. To explore this, we will use flow cytometry combined with confocal microscopy and quantitative imaging analysis to perform a detailed investigation

of IL-33/ST2^{+} Treg pathway compartmentalisation in SILTs throughout the colon in health and disease.

The main objectives of this chapter are:

1. To define the distribution and composition of SILTs in the steady state colon.

2. To explore the spatial compartmentalisation of IL-33-producing cells and ST2^{+} Tregs within SILTs under homeostatic and inflammatory conditions.

3.2 Results

3.2.1 ST2$^+$ Foxp3$^+$ Tregs are unevenly distributed across the lower GI tract

To assess whether there were differences in ST2$^+$ Treg distribution along the length of the caecum and colon, we performed flow cytometry analysis of leukocytes within distinct regions: caecum excluding the caecal patch, caecal patch alone, proximal, mid and distal colon (Fig 3.1a). Tregs are infrequently found in MLN, and therefore these acted as a negative control.

Firstly, we found Tregs to be non-uniformly distributed throughout the caecum and colon, with the highest percentage of Foxp3$^+$ Tregs of total CD4$^+$ T cells located in the caecum and proximal colon, and a gradual declining population moving into the mid and distal parts of the colon (Fig. 3.1b).

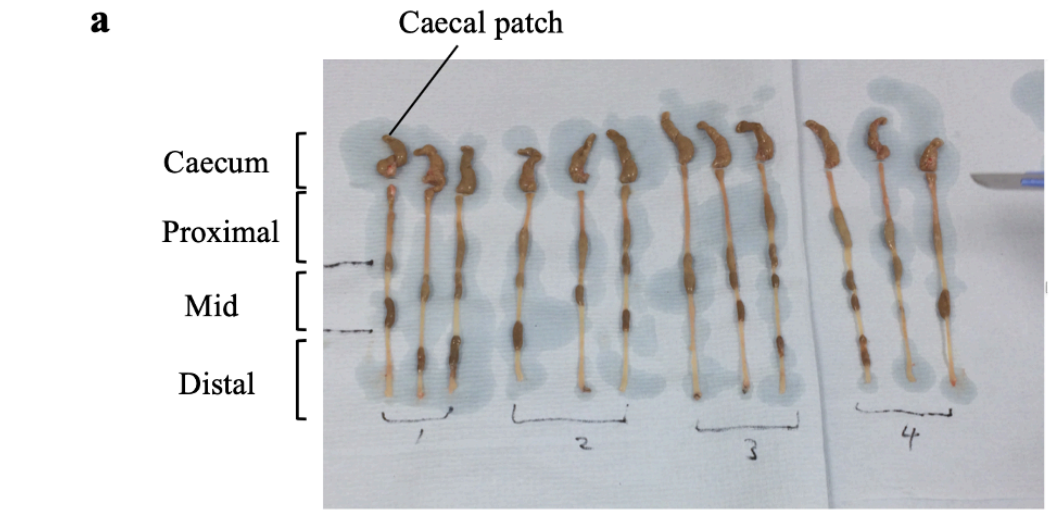
Similarly, there was differential expression of GATA-3$^+$ Tregs, with few in the MLN and caecal patch, higher frequency in the caecum and proximal colon (~30-40%), and again less in the mid and distal parts of the colon (Fig. 3.1c). In line with the lab's previous finding of ST2 receptor restricted to GATA-3$^+$ Tregs, we observed ST2 mirroring that of GATA-3 expression on Tregs (Fig. 3.1d).

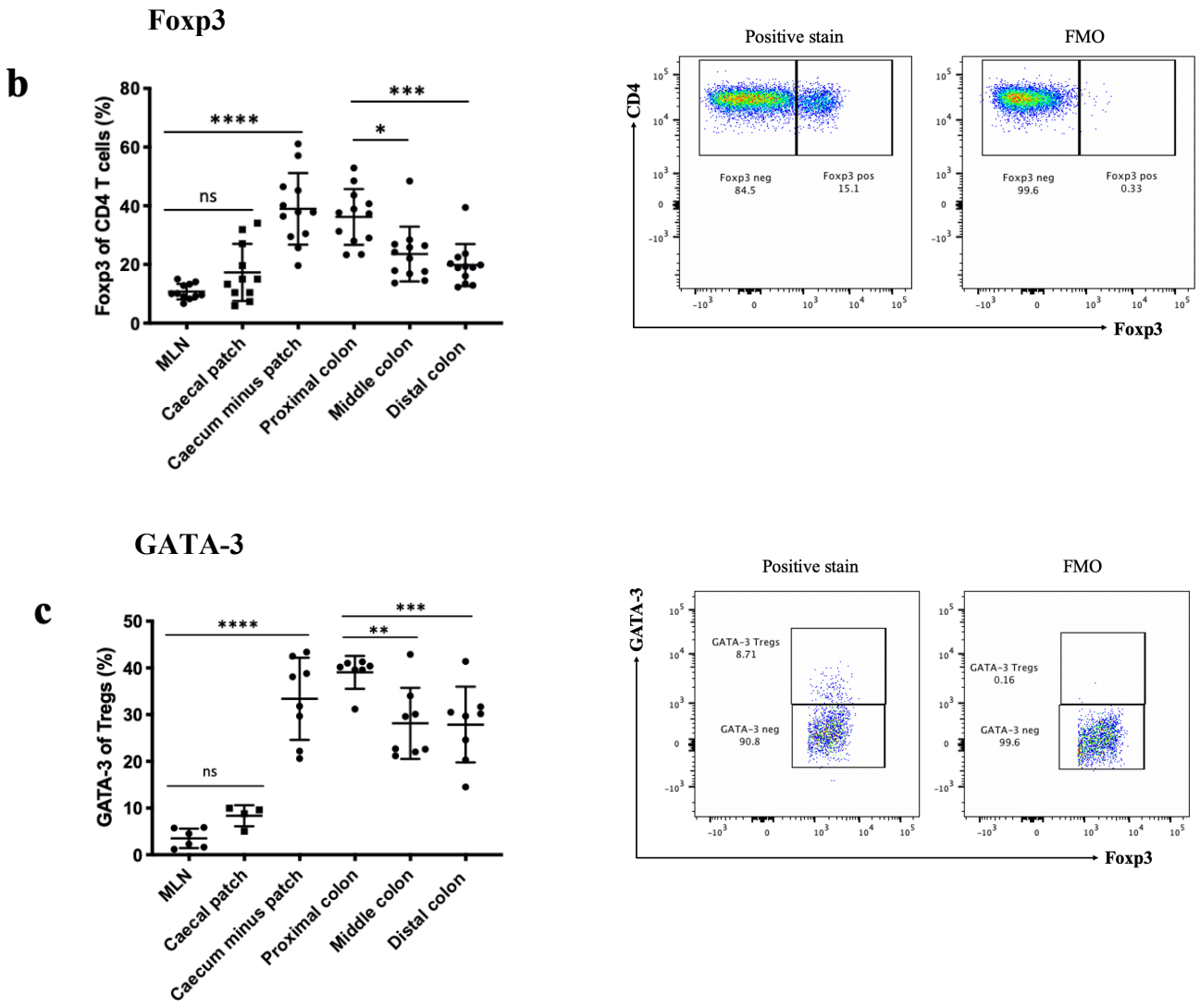
GATA-3$^+$ ST2$^+$ Tregs are thought to be thymically derived, and we used the marker Helios to identify Tregs of thymic origin [249]. Somewhat surprisingly, in contrast to the distribution of GATA-3$^+$ Tregs, the frequency of Helios$^+$ Tregs was largely uniformly distributed throughout the caecum and colon, at approximately 50% of total Tregs (Fig.

3.1e). Indeed, the reliability of Helios, along with the only other maker of thymic Tregs, Neuropilin-1, has been questioned in recent years [363-365]. Finally, Rorγt^{+} Tregs were primarily found in the caecum, caecal patch and proximal colon, with the lowest frequency in the distal colon (Fig. 3.1f).

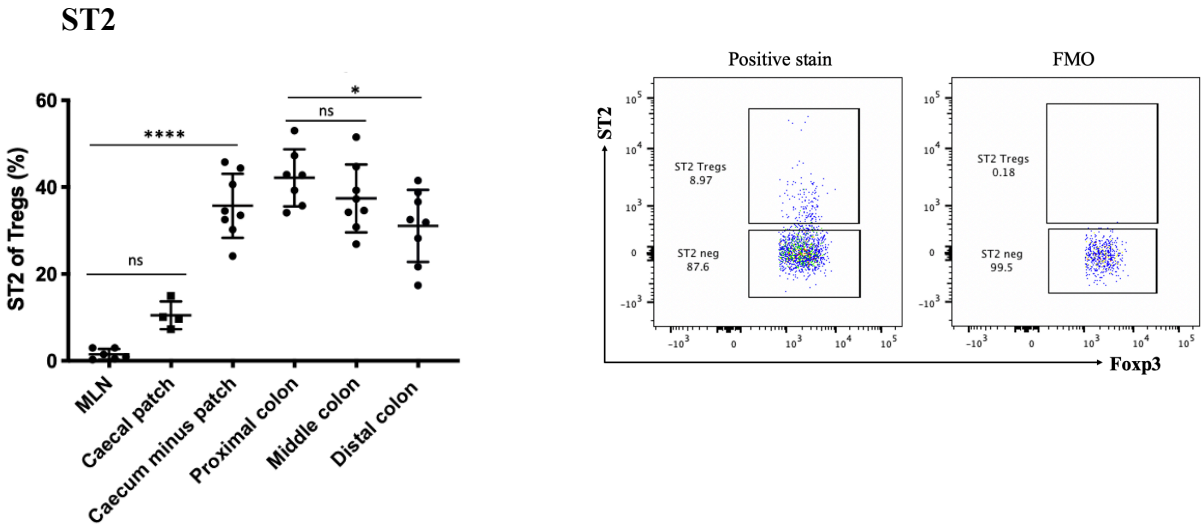
In summary, we show the frequency of ST2^{+} Tregs is unevenly distributed within the lower intestinal tract. There are many factors that may contribute to this variability, including variable expression of IL-33 [Chomka, unpublished] and/or differences in the microbial load across the length of the colon.

However, it is not possible to infer from the existing data whether the relationship between ST2^{+} Tregs and IL-33 and/or microbial diversity and burden is simply correlative or whether there is a strong causative effect between these factors.

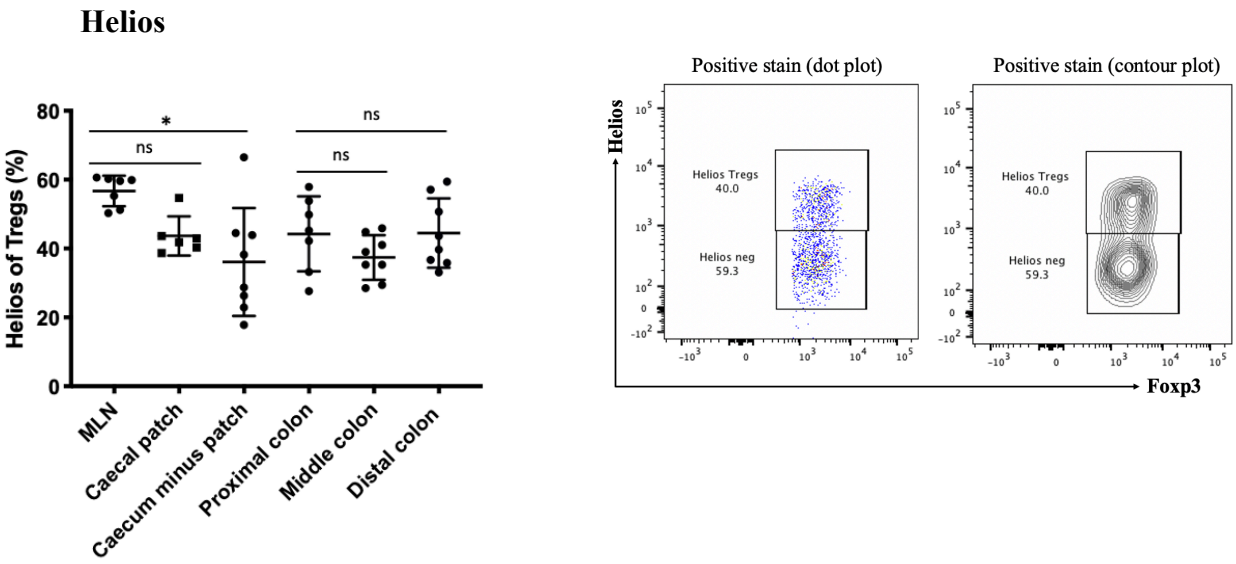

a
Caecal patch
Caecum
Proximal
Mid
Distal
1
2
3
4


Foxp3
b
Foxp3 of CD4 T cells (%)
****
***
*
ns
MLN
Caecal patch
Caecum minus patch
Proximal colon
Middle colon
Distal colon
Positive stain
FMO
CD4
Foxp3 neg
84.5
Foxp3 pos
15.1
Foxp3 neg
99.6
Foxp3 pos
0.33
Foxp3
GATA-3
c
GATA-3 of Tregs (%)
****
***
**
ns
GATA-3
GATA-3 Tregs
8.71
GATA-3 neg
90.8
GATA-3 Tregs
0.16
GATA-3 neg
99.6

d


ST2
ST2 of Tregs (%)
60
40
20
0
****
ns
*
ns
MLN
Caecal patch
Caecum minus patch
Proximal colon
Middle colon
Distal colon
Positive stain
FMO
ST2
ST2 Tregs
8.97
ST2 neg
87.6
ST2 Tregs
0.18
ST2 neg
99.5
Foxp3

e


Helios
Helios of Tregs (%)
80
60
40
20
0
*
ns
ns
ns
MLN
Caecal patch
Caecum minus patch
Proximal colon
Middle colon
Distal colon
Positive stain (dot plot)
Positive stain (contour plot)
Helios
Helios Tregs
40.0
Helios neg
59.3
Helios Tregs
40.0
Helios neg
59.3
Foxp3

f

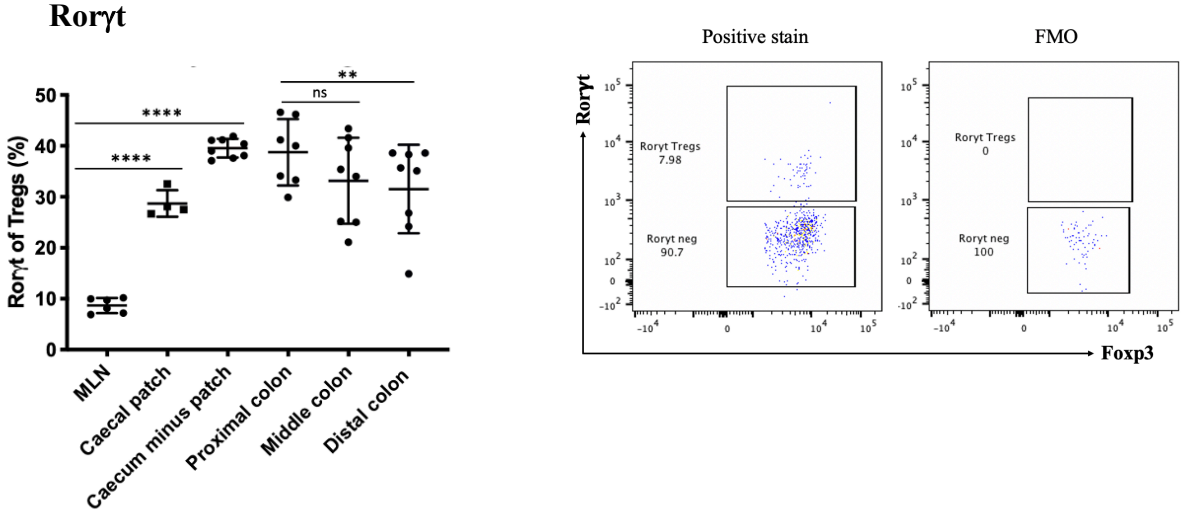

Rorγt
Rorγt of Tregs (%)
50
40
30
20
10
0
****
****
**
ns
MLN
Caecal patch
Caecum minus patch
Proximal colon
Middle colon
Distal colon
Positive stain
FMO
Rorγt
Rorγt Tregs
7.98
Rorγt neg
90.7
Rorγt Tregs
0
Rorγt neg
100
Foxp3

Figure 3.1 The distribution of Foxp3$^+$ Tregs is non-uniform across the lower gastrointestinal tract.

WT C57BL/6 mice were sacrificed at steady state. The caecum and colon tissue were divided into distinct anatomical regions and the frequency of Tregs and Treg subsets were analysed at the indicated sites.

- **a.** Anatomical segregation of caecal patch, caecum minus patch, proximal, mid and distal colon sections for flow cytometry analysis from wild type C57BL/6 mice. Each section is pooled from three mice in order to increase cell numbers.
- **b.** Frequency of Foxp3$^+$ Tregs among total CD4 T cells by flow cytometry at each anatomical location and representative flow cytometry plots of positive Foxp3 staining and FMO
- **c.** Frequency of GATA-3$^+$ of total Foxp3$^+$ T regs by flow cytometry at each anatomical location and representative flow cytometry plots of positive GATA-3 staining and FMO.
- **d.** Frequency of ST2$^+$ of total Foxp3$^+$ Tregs by flow cytometry at each anatomical location and representative flow cytometry plots of positive ST2 staining and FMO
- **e.** Frequency of Helios$^+$ of total Foxp3$^+$ Tregs by flow cytometry at each anatomical location and representative flow cytometry dot and contour plot of positive Helios staining (no FMO available).
- **f.** Frequency of Rorγt$^+$ of total Foxp3$^+$ Tregs by flow cytometry at each anatomical location and representative flow cytometry plots of positive Rorγt staining and FMO.

Each point represents a single mouse (pooled from 3 mice tissues) and bars represent mean ± SEM.

Data represents pooled results from three independent experiments (n = 4 each).

Statistical significance was determined using an ordinary one-way ANOVA with a Tukey's multiple comparisons test. Differences were considered statistically significant when $p \leq 0.05$. Significance is indicated as follows: * $p \leq 0.05$, ** $p \leq 0.01$, ***$p \leq 0.001$, ****$p \leq 0.0001$.

3.2.2 The gut is associated with a diverse range of lymphoid structures

Previous work had shown IL-33-producing cells are present in SILTs located within the proximal and mid colon [Chomka, unpublished data]. We therefore wondered whether the differences in $ST2^+$ Tregs frequency seen could be explained by varying characteristics of SILTs that may be located in distinct regions of the intestinal tract.

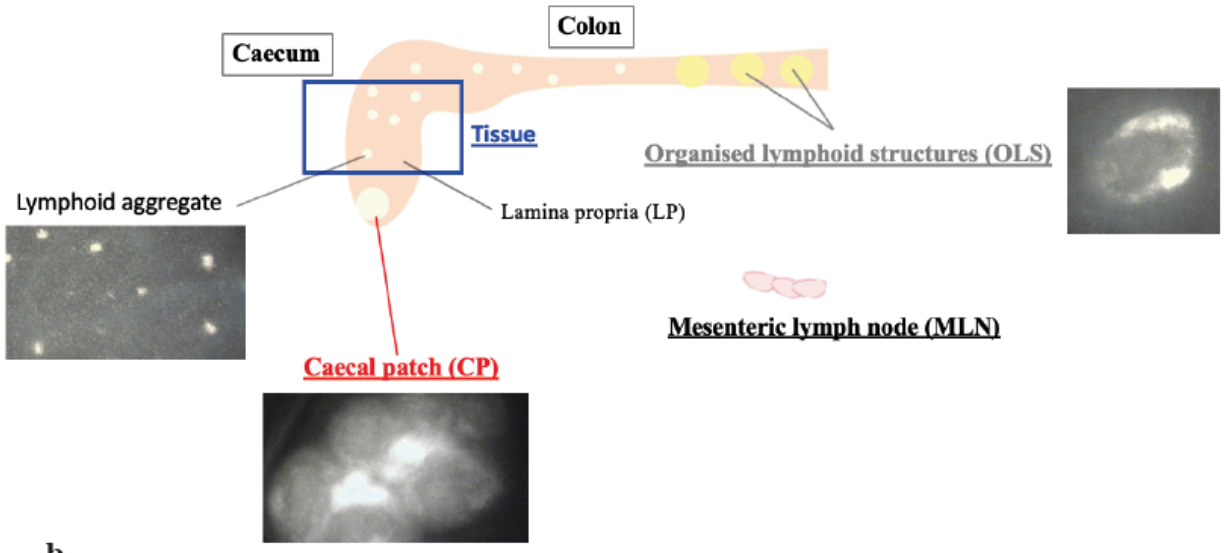
We firstly set out to define the SILTs associated with the steady state murine gut using the hCD2-DsRed T cells reporter mouse. We identified the gut secondary lymphoid organs to include the draining MLNs positioned within the mesentery, the caecal patch located at the tip of the caecum, and the distal colon-associated organised lymphoid structures (OLS), that contain tertiary lymphoid structures (TLS) (Fig 3.2a). In contrast to the MLN, the caecal patch is a tissue-associated SLO that is multi-follicular in structure. Steady state mice were found to approximately contain between one to three OLS in the distal colon. In addition, the proximal colon and caecum lamina propria contains hundreds of smaller lymphoid aggregates. Both the caecal patch and OLS are visible with the naked eye, although small lymphoid aggregates require at least x40 magnification on a brightfield microscope using a reporter mouse.

We next characterised the organisation and cellular composition of the above gut-associated lymphoid structures using immunofluorescent staining of surface markers for CD4, B220, MHCII and the DNA label DAPI. We found the caecal patch and OLS structures exhibited organisation, with a large central $B220^+$ B cell zone surrounded by a thin rim of $CD4^+$ T cells (Fig 3.2b and c). However, although B and T lymphocytes were present within the smaller lymphoid structures, these were not architecturally organised into distinct zones (Fig 3.2d). Finally, MHC II expression was abundant and found

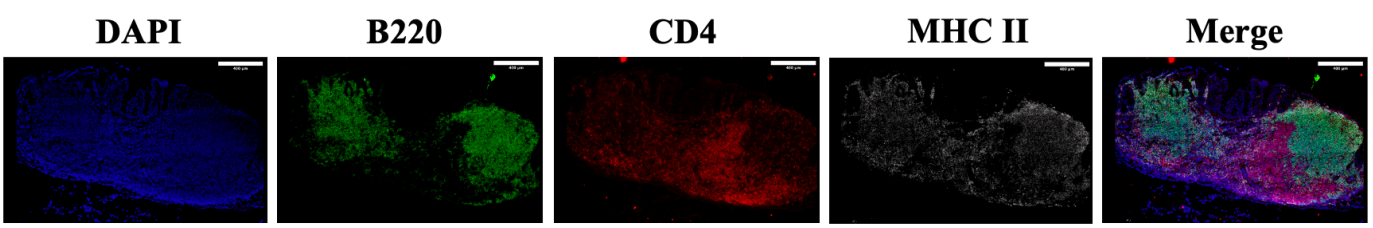
throughout OLS, caecal patch and small lymphoid aggregate structures in steady state mice (Fig 3.2b-d). MHC II expression will be found on antigen presenting cells, including dendritic cells, macrophages and B cells. Surprisingly, within the caecal patch, the expression of MHC II is present throughout this lymphoid structure, but fluorescence appears less 'bright', suggesting less protein expression on a per cell basis, compared to OLS and lymphoid aggregates (Fig 3.2b). One possibility could be the predominance of MHC I expression on antigen presenting cells within the caecal patch.

In summary, we show the caecum and colon of non-inflamed mice to contain SILTs of various sizes, located in different regions, and containing a mixture of immune cell subtypes. Such variation in SILT composition may contribute to the distinct Treg distribution seen across the intestinal tract.

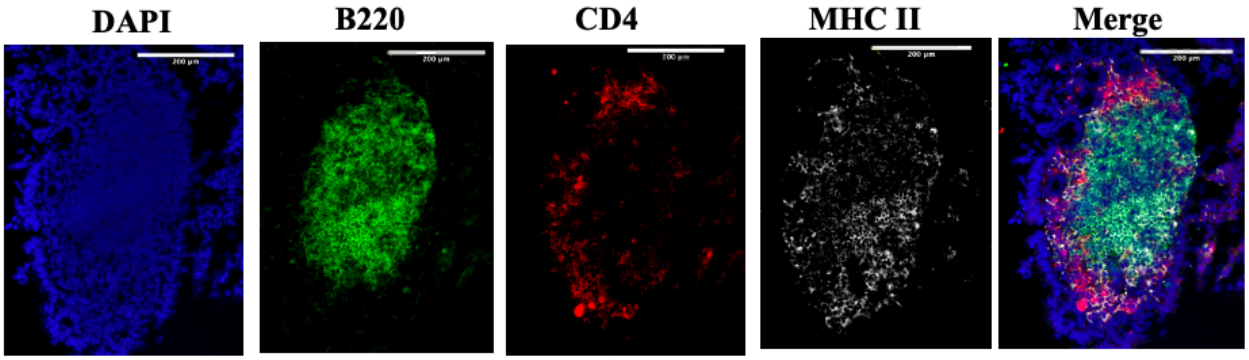
a.



b. Caecal patch



c. Organised lymphoid structure



d. lymphoid aggregates

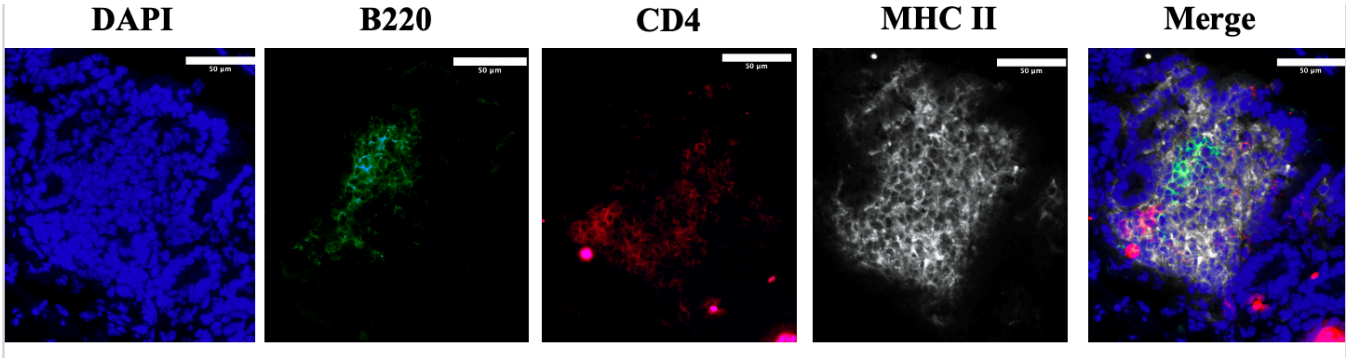


Figure 3.2 SILTs are heterogenous in size and cellular composition

Gut associated lymphoid structures were identified in WT hCD2-DsRed at steady state using brightfield microscopy. Immunofluorescent staining of colon swiss rolls was performed to identify SILTs.

DAPI in blue, B220 in green, CD4 in red and MHCII in white.

- **a.** Schematic of spatial positioning of tissue and lymphoid sites in the murine caecum and colon, with representative images of caecal patch, OLS and lymphoid aggregates in hCD2-DsRed WT mouse
- **b.** Representative images of immunofluorescence staining of DAPI, B220, CD4 and MHCII in the caecal patch.
- **c.** Representative images of immunofluorescence staining of DAPI, B220, CD4 and MHCII in the OLS.
- **d.** Representative images of immunofluorescence staining of DAPI, B220, CD4 and MHCII in the lymphoid aggregates.

Original magnification 4X in (b), 10X in (c), and 40X in (d). Scale bar: 400μm in (b), 200μm in (c), 50μm in (d).

Images are representative of two independent experiments (n = 2 mice each)

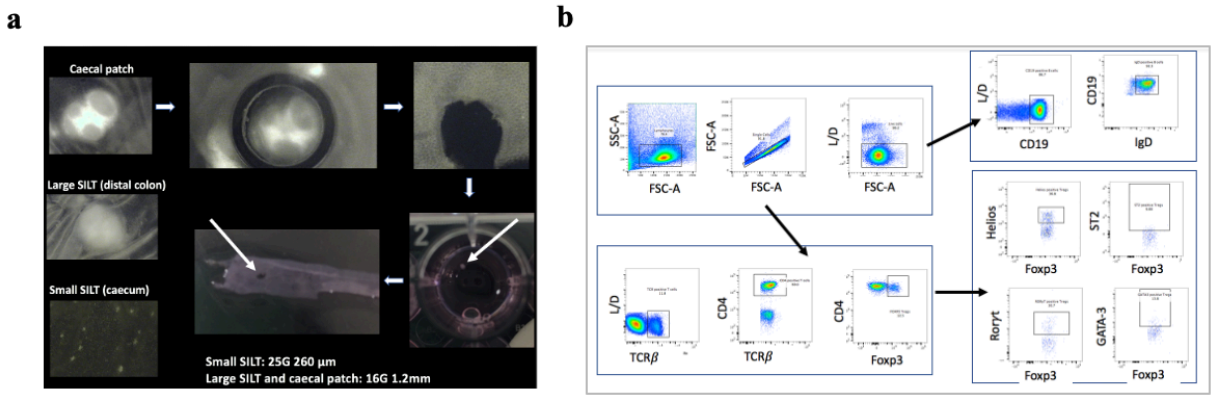
3.2.3 SILT composition varies between young and old mice

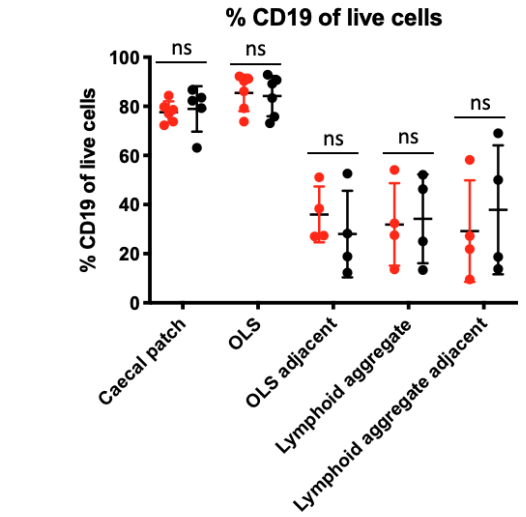
We next asked how the immune composition within SILTs is distinct from surrounding lamina propria tissue. We established a novel technique to isolate in steady state C57BL/6 mice the caecal patch and SILTs from the lamina propria and compared these to adjacent tissue of the corresponding size by flow cytometry (Fig. 3.3a and b). The canonical transcription factors associated with Th2 and Th17 cells, GATA-3 and Rorγt respectively, have been shown to be co-expressed with Foxp3 in Tregs and represent different developmental states [255, 256, 258, 366]. GATA-3$^+$ Tregs are largely Helios$^+$ and thymus-derived, whilst Rorγt$^+$ Tregs can be induced peripherally following stimulation by microbial antigens in the gut [255, 258, 367]. Mice are weaned from the mother's milk to solid food at around 3 weeks postpartum, and previous data confirm a decrease in the frequency of GATA-3$^+$ Tregs, with a concomitant expansion of Rorγt$^+$ Tregs at weaning [Chomka, unpublished data]. Weaning mice likely experience shifts in their intestinal microbiota in response to solid food antigens and their associated microbial contaminants. We therefore additionally asked whether the previously shown differential expression of Rorγt$^+$ and GATA-3$^+$ Tregs in mice pre- and post-weaning is due to an effect within or outside the SILTs. We compared immune make up of SILTs and adjacent tissue in both young (approximately 4 weeks old) and old mice (3 months old). The caecal patch and OLS were visually identified under brightfield microscopy (10X magnification) and manually dissected from the surrounding caecum and colon tissue respectively using a 16 gauge (1.2mm) needle attached to a syringe containing 1ml of RPMI/10%FCS/15mM Hepes. Lymphoid aggregates were isolated from the surrounding tissue using a 25 gauge (260μm) needle under 40X magnification. The adjacent lamina propria tissue for both OLS and lymphoid aggregates were isolated using a 16 gauge needle (Fig 3.3a). All SILTs and adjacent tissues were digested and processed for flow cytometry analysis as detailed in

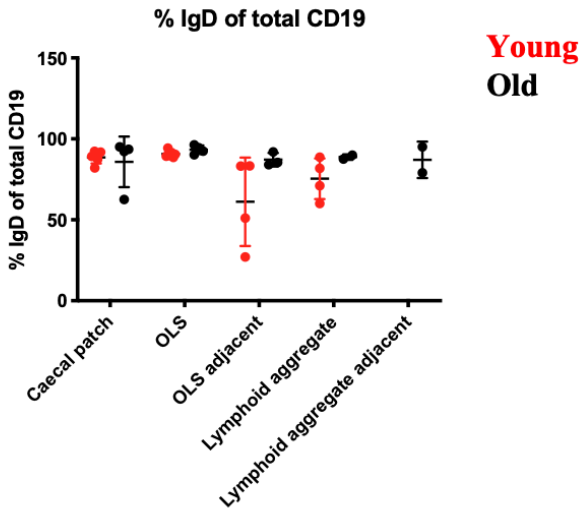
2.3.3 in Materials and Methods. The flow cytometry gating strategy is shown in Fig 3.3b. Due to limited Treg cell numbers digested from small lymphoid aggregates, meaningful analysis of GATA-3^{+} and Rorγt^{+} Tregs frequencies is only possible from caecal patches and OLS.

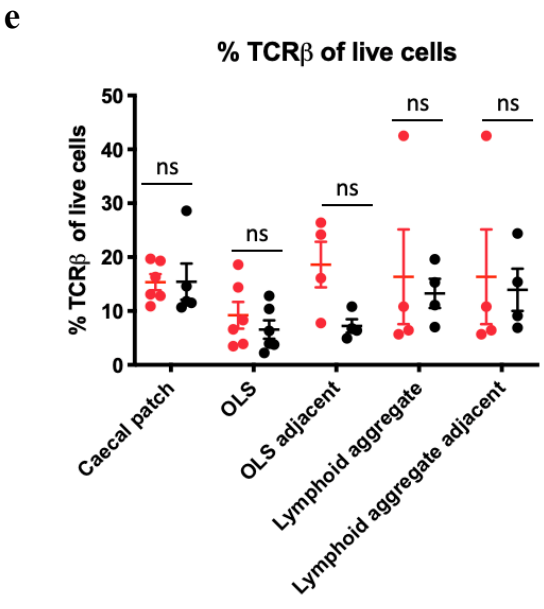
In keeping with our previous results on the general architecture of SILTs, we found a difference in the proportion of CD19^{+} B cells within OLS versus lymphoid aggregates, with B cells comprising the majority of lymphocytes in OLS. (Fig. 3.3c). Within these steady state mice, almost all B cells are IgD positive, i.e., naïve (Fig. 3.3d).
We observed comparable numbers of TCRβ^{+} T cells (approximately 10-30% of total live lymphocytes) within OLS and lymphoid aggregates and their corresponding adjacent tissue of both young and old mice (Fig. 3.3e). Finally, we found increased frequency of GATA-3^{+} Helios^{+} Tregs within the caecal patch and OLS of younger mice (Fig. 3.3f and g). This confirms the lab's previous data showing higher frequency of GATA-3^{+} Tregs in whole colon digest of younger mice, and further suggest these shifts in the ratio of GATA-3: Rorγt is due to changes within the SILTs themselves.

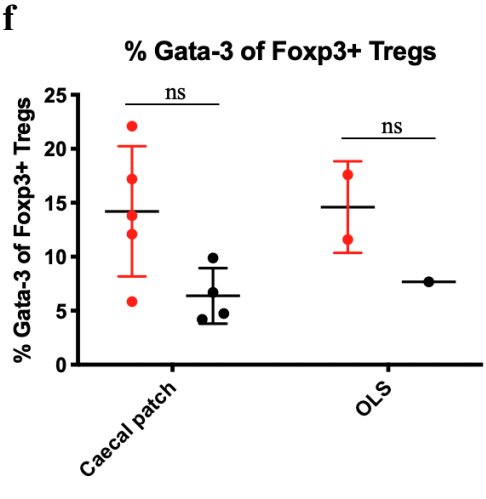
Altogether, we establish a novel approach of isolating SILTs from the surrounding tissue. Furthermore, we utilise FACS analysis as a technique to complement immunofluorescent imaging in the study of immune cells within SILTs.


a
Caecal patch
Large SILT (distal colon)
Small SILT (caecum)
Small SILT: 25G 260 µm
Large SILT and caecal patch: 16G 1.2mm
b
SSC-A
FSC-A
L/D
CD19
IgD
CD4
TCRβ
Foxp3
Helios
ST2
Roryt
GATA-3


c
% CD19 of live cells
% CD19 of live cells
ns
Caecal patch
OLS
OLS adjacent
Lymphoid aggregate
Lymphoid aggregate adjacent


d
% IgD of total CD19
% IgD of total CD19
Young
Old
Caecal patch
OLS
OLS adjacent
Lymphoid aggregate
Lymphoid aggregate adjacent


e
% TCRβ of live cells
% TCRβ of live cells
ns
Caecal patch
OLS
OLS adjacent
Lymphoid aggregate
Lymphoid aggregate adjacent


f
% Gata-3 of Foxp3+ Tregs
% Gata-3 of Foxp3+ Tregs
ns
Caecal patch
OLS

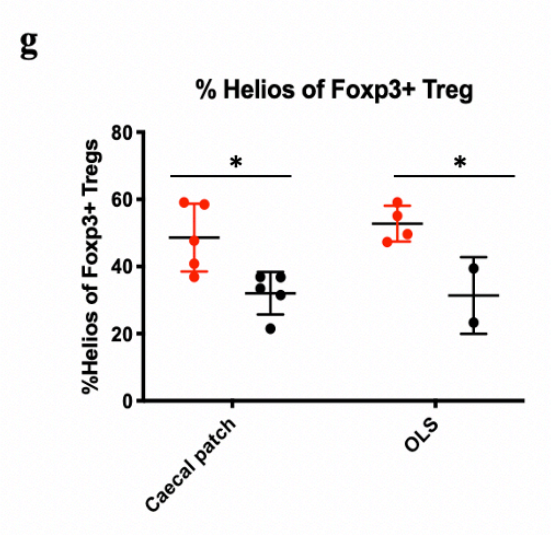


Figure 3.3 Young mice contain a higher proportion of Helios$^+$ GATA-3$^+$ Tregs within caecal patch and OLS

Young (4 weeks old, red) and old (3 months old, black) WT C57BL/6 mice were sacrificed at steady state and colons harvested for the isolation of SILTs and adjacent lamina propria. The phenotypes of B and T cells, and Tregs were analysed by flow cytometry at each of the indicated sites.

a. The step-by-step technique of SILT isolation from the surrounding lamina propria using specific gauge needles.
b. Flow cytometry gating strategy of digested SILT tissue to characterise Treg phenotypes
c. Frequency of CD19$^+$ B cells of live cells at each anatomical site
d. Frequency of IgD$^+$ of CD19$^+$ B cells at each anatomical site
e. Frequency of TCRβ$^+$ of live cells at each anatomical site
f. Frequency of GATA-3$^+$ of Foxp3$^+$ Tregs in the caecal patch and OLS
g. Frequency of Helios$^+$ of Foxp3$^+$ Tregs in the caecal patch and OLS

Each point represents a single mouse and bars represent mean ± SEM.

Data represents results from a single experiment representative of 3 independent experiments (n = 5 for old mice, n = 6 for young mice).

Statistical significance was determined using an ordinary two-way ANOVA with a Sidak's multiple comparisons test. Differences were considered statistically significant when $p \leq 0.05$. Significance is indicated as follows: * $p \leq 0.05$, ** $p \leq 0.01$, ***$p \leq 0.001$, ****$p \leq 0.0001$.

3.2.4 OLS form germinal centres during Hh/anti-IL10R colitis

Finally, having observed a significant population of naïve B cells within OLS in section 3.2.2, we further characterised these B cells and wondered whether they were able to form germinal centres with the development of IgA^+ plasma cells. We therefore performed immunofluorescent staining of OLS and lymphoid aggregates using the markers IgD to detect naïve B cells, and BCL-6 to mark activated germinal centre B cells.

Secondary lymphoid organs, such as Peyer's patches of un-inflamed mice are known to be an important source of germinal centre B cells [368]. We found caecal patches to also contain $BCL6^+$ germinal centres at steady state (Fig 3.4a).

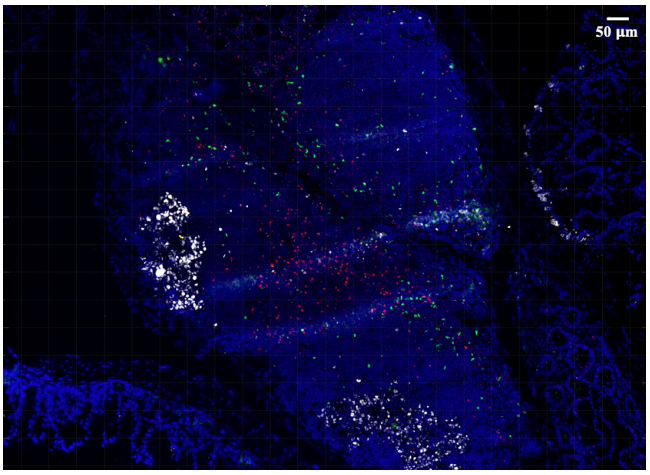
However, in un-infected steady state mice, the vast majority of $B220^+$ B cells in both OLS and lymphoid aggregates were naïve, and no germinal centres were observed (Fig 3.4b). We then hypothesised that upon inflammation (using both the DSS and H.h/anti-IL10R colitis models), OLS and lymphoid aggregates would develop germinal centres with a strong IgA response. Interestingly, in H.h./anti-IL10R colitis, germinal centre B cells developed in OLS but not lymphoid aggregates, indicating the more mature nature of these lymphoid structures (Fig 3.4c).

We used 2% DSS in drinking water to ensure mice only needed to be culled after at least 7 days to allow time for the formation of germinal centres. At this concentration of DSS, mice were culled between 9 and 10 days after the start of DSS. Within the DSS colitis model, we did not observe the formation of germinal centres in either the lymphoid aggregates or OLS (Fig 3.4d).

In conclusion, B cells within OLS and lymphoid aggregates, unlike the caecal patch and Peyer's patch, do not form germinal centres at steady state. H.h/anti-IL10R, but not DSS colitis induces the formation of germinal centres only in OLS, but not in lymphoid aggregates. This suggests the B cell response could be directed to a specific bacterial antigen, such as *H.hepaticus,* administered to the mice at high concentration. Additionally, it highlights a functional distinction between large OLS and small lymphoid aggregate SILTs.

a

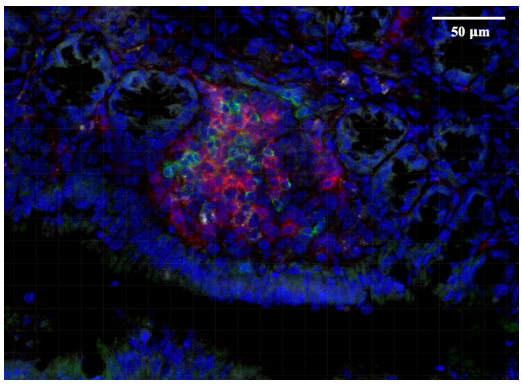
Un-infected caecal patch



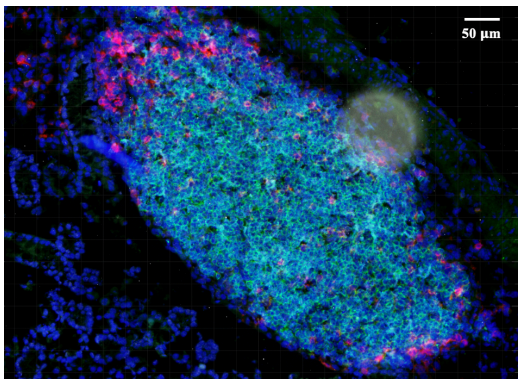
DAPI BCL6 Rorγt Foxp3

b

Un-infected lymphoid aggregate



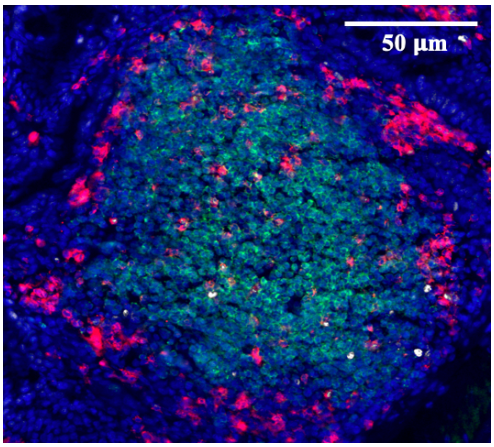
Un-infected OLS



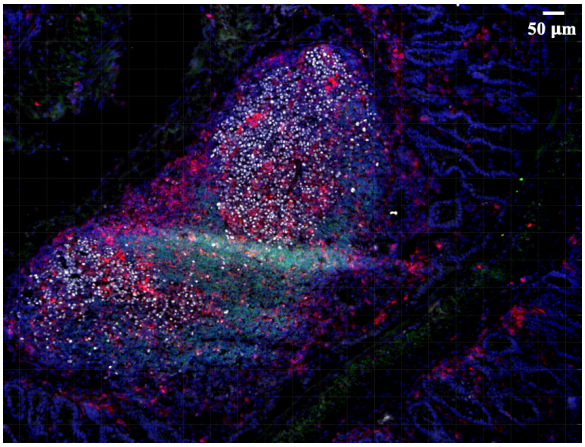
DAPI IgD CD4 BCL6

c

Hh/anti-IL10R lymphoid aggregate



Hh/anti-IL10R OLS



DAPI IgD CD4 BCL6

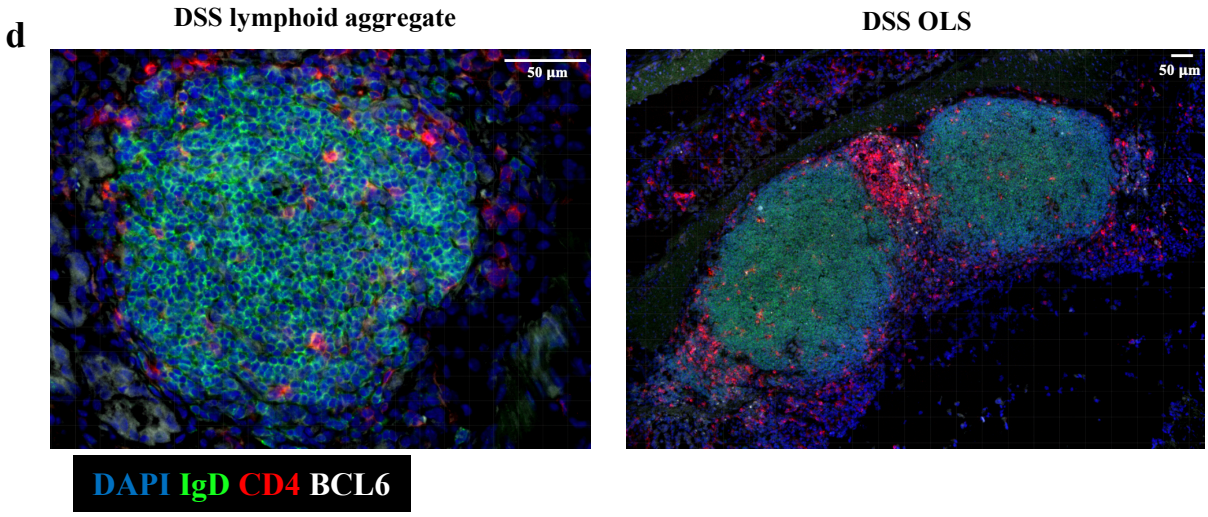


Figure 3.4 Germinal centres form in OLS, but not lymphoid aggregates during H.h/anti-IL10R colitis

WT C57BL/6 mice were sacrificed at steady state, and at the peak of inflammation in Hh/anti-IL10R (14 days) and DSS (9 to 10 days) colitis. Caecum and colons were rolled into swiss rolls and stained for immunofluorescent imaging. Germinal centre formation was assessed in the caecal patch, OLS and lymphoid aggregates by brightfield microscopy.

DAPI in blue, IgD in green, CD4 in red and BCL6 in white

a. Representative image of immunofluorescence staining of BCL6 germinal centre in caecal patch of un-infected steady state mice

b. Representative images of immunofluorescence staining of BCL6 germinal centres in lymphoid aggregate and OLS of un-infected steady state mice

c. Representative images of immunofluorescence staining of BCL6 germinal centres in lymphoid aggregate and OLS of Hh/anti-IL10R colitis mice

d. Representative images of immunofluorescence staining of BCL6 germinal centres in lymphoid aggregate and OLS of DSS colitis mice

Original magnification 10X for caecal patch and OLS, and 40X for lymphoid aggregate. Scale bar: 50 µm (a-d). Each staining was performed in n = 4 mice in steady state, n = 4 mice in DSS colitis and n = 5 mice in Hh/antiIL-10R colitis.

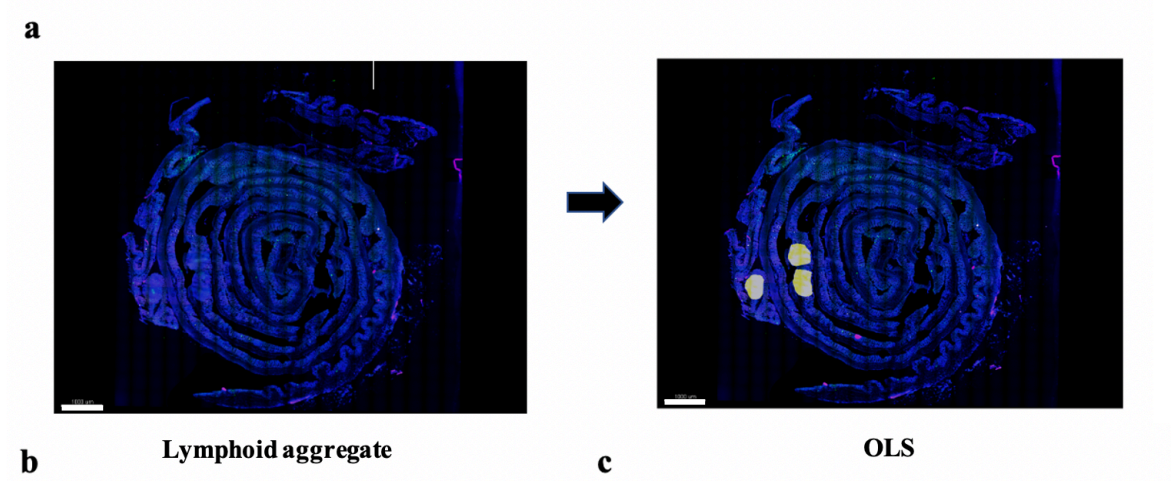
3.2.5 OLS contain IL-33$^+$ cells in close proximity to Treg subsets

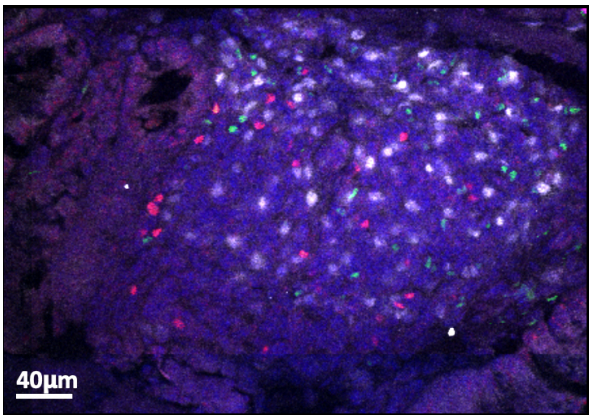
IL-33 is an alarmin with up-regulated expression in the gut during cell damage. Our group has previously shown the primary source of IL-33 in the proximal and mid colon was concentrated in SILTs, whilst epithelial cells predominantly expressed IL-33 in the distal colon [Chomka, unpublished]. Furthermore, our lab showed the IL-33 receptor, ST2, to be predominantly expressed on GATA$^+$ Treg subset [360]. Therefore, to further explore the spatial relationship between IL-33-producing cells and ST2$^+$/GATA-3$^+$ Tregs within SILTs, we performed immunofluorescent staining of fresh frozen OCT sections of steady state mouse colons. To study the complete colon lamina propria, colons were rolled into tight 'swiss rolls' with distal colons located centrally. OLS were identified and visually separated from the rest of the colon tissue (Fig. 3.5a).

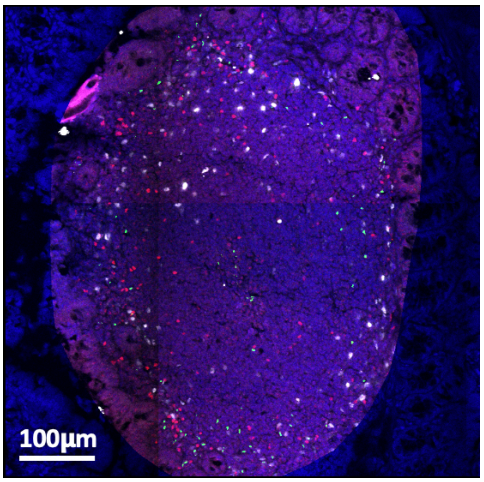
Immunofluorescent staining was firstly used to identify IL-33$^+$ and Foxp3$^+$ cells within lymphoid aggregates and OLS. Addition of a third stain, Rorγt, allowed for identification of Tregs co-expressing Rorγt and Foxp3. Unfortunately, due to technical difficulties we were not able to successfully optimise GATA-3 transcriptional factor and ST2 surface staining within lymphoid tissue, and therefore for this experiment, Foxp3$^+$ Rorγt$^-$ Tregs are a heterogeneous population of Tregs, which include those expressing GATA-3$^+$. Immunofluorescent staining of lymphoid aggregates revealed IL-33-producing cells along with Tregs in no particular pattern of spatial distribution (Fig 3.5b). However, within OLS, IL-33-producing cells are located around the perimeter, in close proximity to Tregs within the T cell zone (Fig 3.5c).

Altogether, these results show the presence of numerous OLS within the steady state mouse colon that can be identified by the tight clustering of immune cells.

Immunofluorescent staining reveals Rorγt^{+} and Rorγt^{-} Treg cells, which are found to be close to IL-33-producing cells situated within the inner perimeter of OLS.







Rorγt Foxp3 IL33 DAPI

Figure 3.5 IL-33$^+$ cells are located spatially close to Tregs within the inner perimeter of OLS

WT C57BL/6 mice were sacrificed at steady state and colons rolled into swiss rolls and stained for immunofluorescent imaging. OLS and lymphoid aggregates were imaged by confocal microscopy.

DAPI in blue, Rorγt in green, Foxp3 in red and IL-33 in white

a. Representative image of whole mouse colon swiss rolls with DAPI nuclear staining, and surface application using Imaris to define OLS structures
b. Representative images of immunofluorescence staining of IL-33, Rorγt, Foxp3 and DAPI staining of lymphoid aggregate (40X)
c. Representative images of immunofluorescence staining of IL-33, Rorγt, Foxp3 and DAPI staining of OLS (10X)

Images were acquired using a confocal microscope at 20X magnification, 20x20 tiles with a pixel size of 0.83µm, and 4 Z-stacks per tile. Scale bar 1000µm (a), 40µm (b), 100µm (c)

Each colon swiss roll was stained and imaged in n = 8 mice in steady state.

3.2.6 Compartmentalisation of Rorγt$^+$ Tregs in OLS during steady state and colitis

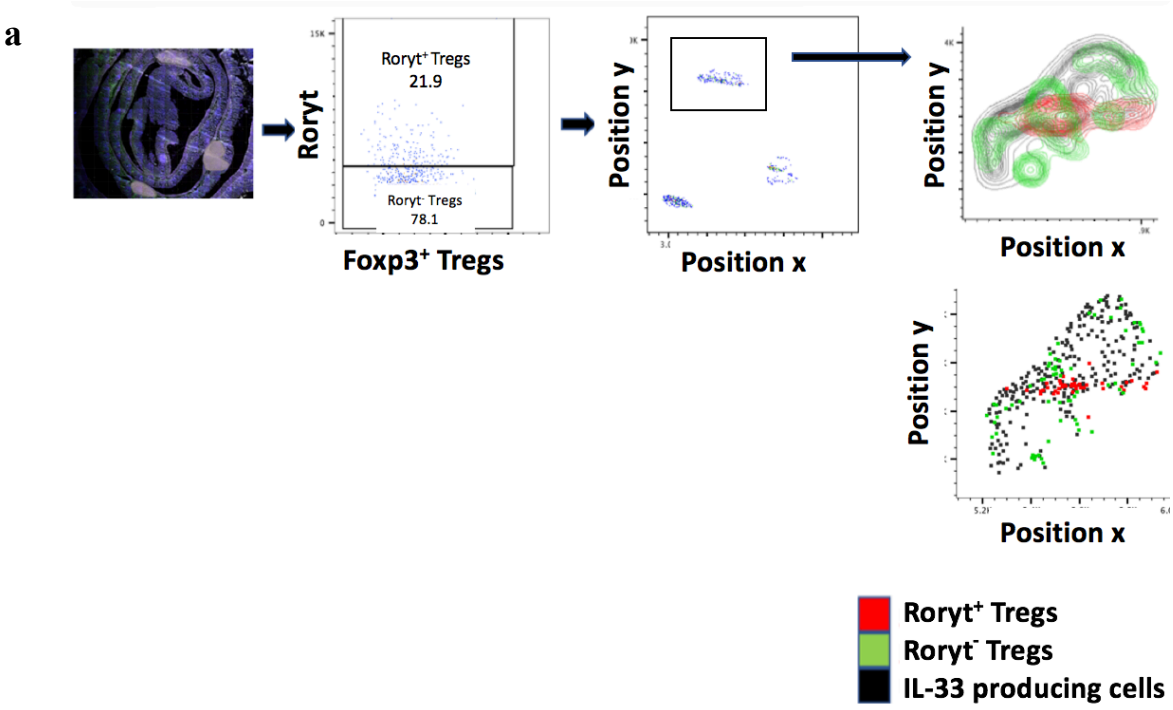
Our immunofluorescent imaging data show Tregs spatially close to IL-33-producing cells within OLS. Combined with Rorγt staining, it is possible to distinguish Rorγt$^+$ and Rorγt$^-$ Treg subsets and their relationship to IL-33. In order to spatially visualise and quantify phenotypically distinct cell populations obtained by tiled confocal microscopy of tissue sections, we used the technique of 'histo-cytometry' as detailed in a previous study investigating dendritic cell subsets within lymph nodes [345]. We performed histo-cytometry across a number of mice in different conditions of steady state, Hh/anti-IL10R and DSS colitis by exporting the staining intensity (representing protein expression) and x,y, location co-ordinates of Rorγt, Foxp3 and IL-33 immunofluorescent staining using Imaris (Bitplane) image analysis software. We then constructed dot plots and cell density contour plots in FlowJo v10.3 (Treestar) software (Fig 3.6a).

In both steady state and inflammation, the contour plots confirmed firstly IL-33-producing cells to be primarily located around the perimeter of OLS (Fig. 3.6b). Rorγt$^-$ Tregs are commonly found where IL-33$^+$ cells are present, mostly surrounding the outer region of the lymphoid structures, although they can be more central. This close association between the two cell types is preserved in the steady state and in colitis.

Furthermore, Rorγt$^+$ Tregs clustered in certain areas within OLS. In both steady state and H.h/anti-IL10R colitis, most Rorγt$^+$ Tregs are located towards the outer zones (Fig 3.6b). However, in DSS, we see some Rorγt$^+$ Tregs positioned more centrally and further from

IL-33^{+} cells, whilst others remain within the outer areas. As these are static confocal images, it is unclear whether differences in Rorγt positioning under different conditions are due to active movements of cells or whether they represent different Rorγt populations. *In vivo* live imaging to track cellular movements within lymphoid aggregates could be used to answer this question.

Altogether, our results show differences between Rorγt^{+} Tregs positioning in homeostasis, DSS and H.h./anti-IL-10R colitis- the cause may be linked to distinct microbial disruptions between the colitis models, severity of inflammation and/or location of disease.


a
Roryt
Roryt+ Tregs
21.9
Roryt- Tregs
78.1
Foxp3+ Tregs
Position y
Position x
Position y
Position x
Position y
Position x
Roryt+ Tregs
Roryt- Tregs
IL-33 producing cells

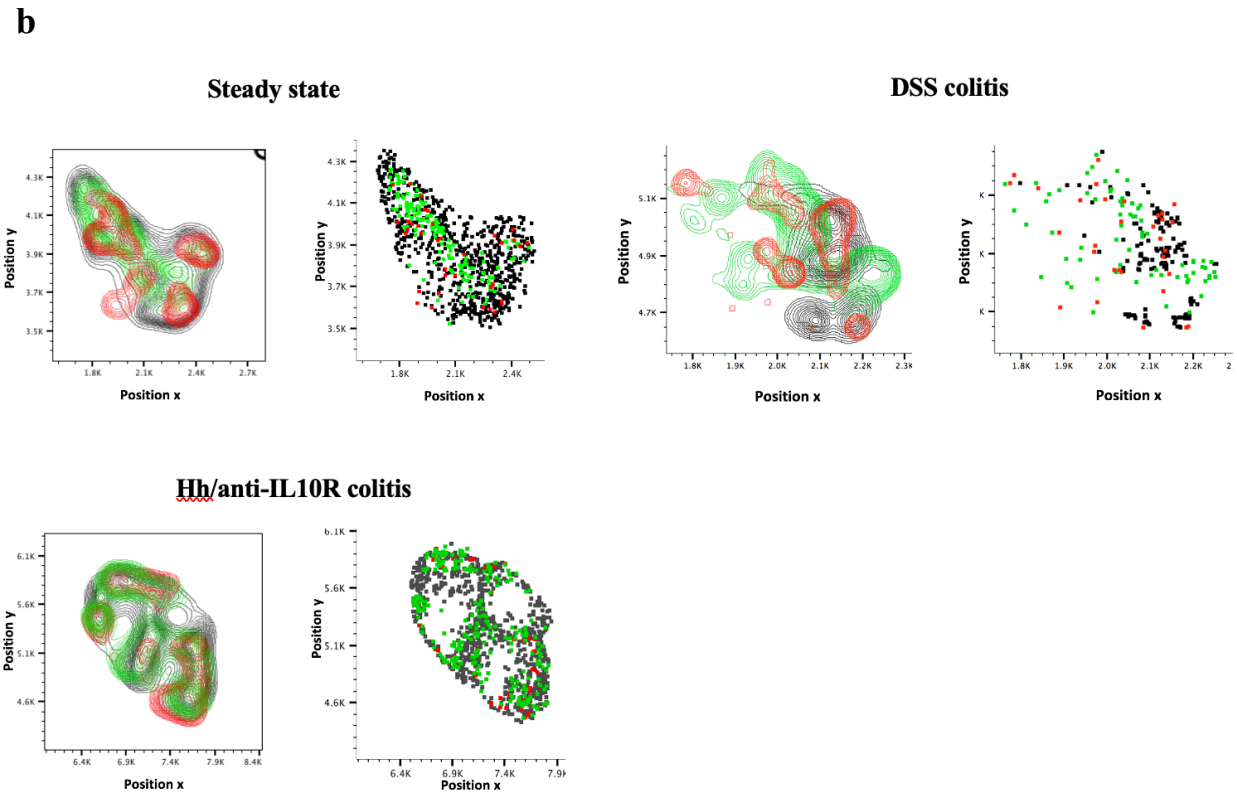

b
Steady state
DSS colitis
Hh/anti-IL10R colitis
Position y
Position x

Figure 3.6 Rorγt^{+} and Rorγt^{-} Tregs occupy distinct niches in OLS during steady state and colitis

Histo-cytometry analysis was performed on immunofluorescent stained colon swiss rolls of WT C57BL/6 mice at steady state, H.h/anti-IL10R and DSS colitis. Spatial compartmentalisation of cell subsets was represented visually.

Rorγt^{+} Tregs in red, Rorγt^{-} Tregs in green, IL-33^{+} cells in black

a. Foxp3^{+} Tregs were gated on Rorγt expression, and their relative locations overlaid with the location of IL-33-producing cells. Protein expression and spatial data were then visualised as pseudocolour or contour plots in Flowjo (Treestar).

b. Visual representation of dot and contour plots of Rorγt^{+}, Rorγt^{-} and IL-33^{+} cells in OLS of steady state, DSS and Hh/anti-IL10R colitis mice.

Confocal microscopy at 20X magnification, 20x20 tile scan, with a pixel size of 0.83µm, and 4 Z-stacks per tile.

Each colon swiss roll was stained and imaged in n = 8 mice in steady state, n = 4 mice in DSS colitis, and n = 6 mice in Hh/anti-IL10R colitis.

3.2.7 Colitis drives changes in the spatial compartmentalisation of Treg subsets relative to IL-33$^+$ cells in OLS

The IL-33 receptor ST2 is expressed on GATA-3$^+$ Tregs [360]. We therefore hypothesised that Rorγt$^-$ Tregs would be located closest in terms of distance to IL-33-producing cells within lymphoid tissue. We measured distances of Rorγt$^+$ and Rorγt$^-$ Treg subsets to the nearest IL-33-producing cell in both lymphoid aggregates and OLS in steady state mice by using the distance transformation tool in Imaris (Bitplane). Somewhat surprisingly, our results in both lymphoid aggregates and OLS showed the opposite to be true: Rorγt$^-$ Tregs were in fact located further from IL-33$^+$ cells than Rorγt$^+$ Tregs (mean of 14.9µm compared to 39.1µm in lymphoid aggregates, and 23.5µm versus 37.1µm in OLS). We found non-Tregs to be at a comparable distance as Rorγt$^+$ Tregs to IL-33$^+$ cells (Fig. 3.7a).

Altogether, these data show there is indeed spatial segregation of Rorγt$^+$ and Rorγt$^-$ Tregs within lymphoid aggregates and OLS during homeostasis relative to IL-33-producing cells. However, Rorγt$^-$ Tregs that include the GATA-3$^+$ Treg subset are not located closer to IL-33-producing cells, which suggests either close contact is not necessary for effective function of cytokine and receptor, or the effect of IL-33 cytokine on ST2$^+$ Tregs is not critically needed under steady state conditions. Additionally, the Rorγt$^-$ subset includes a large and heterogenous population of Tregs, of which the GATA-3$^+$ Tregs likely forms a small proportion. It is therefore not possible with the current available immunofluorescent markers to be certain of the positioning of GATA-3$^+$ Tregs within the Rorγt$^-$ subset.

We next hypothesised inflammation itself would induce changes in cell movement or recruitment within lymphoid tissue, with Rorγt$^-$ Tregs located closer to IL-33-producing cells in order to maximise the reparative function of IL-33 cytokine signalling in GATA-3$^+$ Tregs. We assessed the effects of inflammation, using both acute (DSS) and chronic (H.h/anti-IL10R) colitis models. Additionally, As Hh/anti-ILR drives inflammation predominately in the caecum and proximal colon tissue where lymphoid aggregates are located, whereas DSS colitis is mainly within the distal colon at the site of OLS, using both models therefore allowed us to study cellular interactions within these distinct lymphoid organs at the peak of inflammation.

The results showed a distinction between DSS and Hh/anti-IL-10R colitis. In DSS colitis, there was no significant difference between the distances of Rorγt$^-$ and Rorγt$^+$ Treg subsets to the closest IL-33-producing cell in lymphoid aggregates, OLS or both combined (mean distance 37.9μm versus 39μm) (Fig 3.7b). Interestingly, in Hh/anti-IL-10R colitis, Rorγt$^+$ and Rorγt$^-$ Tregs were located at a similar distance to the nearest IL-33$^+$ cell within lymphoid aggregates (23.7μm versus 21.7μm). In OLS, the pattern of Treg subset localisation was similar to steady state, with Rorγt$^-$ Tregs located surprisingly further from IL-33$^+$ cells (40.6μm versus 22.9μm) (Fig 3.7c).

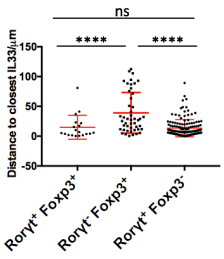
In conclusion, we demonstrate spatial segregation of Rorγt$^+$ and Rorγt$^-$ Tregs within lymphoid aggregates and OLS in steady state, with changes observed in two models of colitis. Whether these changes in positioning represent movement of cells or their recruitment to proliferate at new sites is currently unclear. Nevertheless, we believe Tregs within lymphoid structures are poised to respond to inflammation at specific tissue sites,

and their positioning is likely to play a key role in tissue damage control and repair. Although we did not directly observe a closer distance between Rorγt$^-$ Tregs and IL-33-producing cells within lymphoid tissue, it does not exclude an interaction between IL-33 ligand and the ST2 receptor on GATA-3$^+$ Tregs. It is possible that IL-33 can exert its effects in a more far-reaching manner, with its reparative functions occurring indirectly at distant sites.

a.

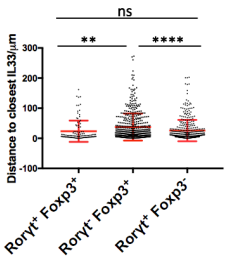
Steady state

Lymphoid aggregates



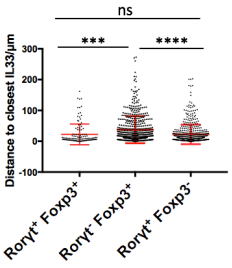
Rorγt⁺ Foxp3⁺ 14.9 µm
Rorγt⁻ Foxp3⁺ 39.1 µm
Rorγt⁺ Foxp3⁻ 13.4 µm

OLS



Rorγt⁺ Foxp3⁺ 23.5 µm
Rorγt⁻ Foxp3⁺ 37.3 µm
Rorγt⁺ Foxp3⁻ 25.7 µm

Combined

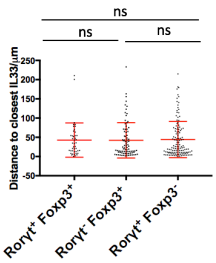


Rorγt⁺ Foxp3⁺ 22.1 µm
Rorγt⁻ Foxp3⁺ 37.5 µm
Rorγt⁺ Foxp3⁻ 22.3 µm

b.

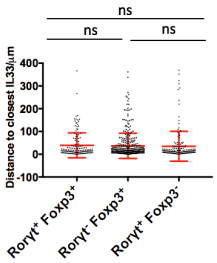
DSS colitis

Lymphoid aggregates



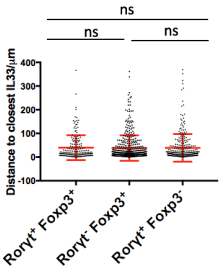
Rorγt⁺ Foxp3⁺ 42.7µm
Rorγt⁻ Foxp3⁺ 42.2 µm
Rorγt⁺ Foxp3⁻ 44.3 µm

OLS



Rorγt⁺ Foxp3⁺ 39.1 µm
Rorγt⁻ Foxp3⁺ 37.0 µm
Rorγt⁺ Foxp3⁻ 34.9 µm

Combined

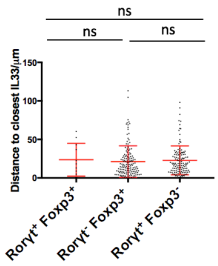


Rorγt⁺ Foxp3⁺ 39.0 µm
Rorγt⁻ Foxp3⁺ 37.9 µm
Rorγt⁺ Foxp3⁻ 38.9 µm

c.

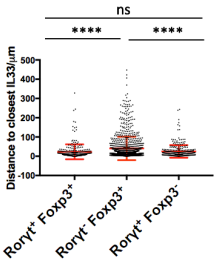
Hh/anti-IL10R colitis

Lymphoid aggregates



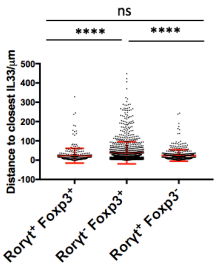
Rorγt⁺ Foxp3⁺ 23.7 µm
Rorγt⁻ Foxp3⁺ 21.2 µm
Rorγt⁺ Foxp3⁻ 22.8 µm

OLS



Rorγt⁺ Foxp3⁺ 22.9 µm
Rorγt⁻ Foxp3⁺ 40.6 µm
Rorγt⁺ Foxp3⁻ 24.9 µm

Combined



Rorγt⁺ Foxp3⁺ 22 µm
Rorγt⁻ Foxp3⁺ 38.0 µm
Rorγt⁺ Foxp3⁻ 24 µm

Figure 3.7 Rorγt$^-$ Tregs are not located spatially closer to IL-33$^+$ cells during steady state or H.h/anti-IL10R colitis

WT C57BL/6 mice were sacrificed at steady state, and at the peak of inflammation in Hh/anti-IL10R (14 days) and DSS (9 to 10 days) colitis. Colons were harvested and rolled into swiss rolls and stained for Rorγt$^+$, Rorγt$^-$ and IL-33 for immunofluorescent imaging by confocal microscopy. The distance transformation tool in Imaris (Bitplane) was used to measure distances between Rorγt$^+$ and Rorγt$^-$ Tregs and the nearest IL-33$^+$ cell in OLS.

Distance of Rorγt$^+$ and Rorγt$^-$ Tregs to nearest IL-33$^+$ cell within lymphoid aggregates, OLS and both combined in

- **a.** Steady state
- **b.** DSS colitis
- **c.** Hh/anti-IL10R colitis

Each colon swiss roll was stained and imaged in n = 8 mice in steady state, n = 4 mice in DSS colitis, and n = 6 mice in Hh/anti-IL10R colitis. Mean distance of each cell subset to the nearest IL-33$^+$ cell within lymphoid aggregates, OLS and both combined stated in the box below each graph.

Statistical significance was determined using an ordinary one-way ANOVA with a Tukey's multiple comparisons test. Differences were considered statistically significant when $p \leq 0.05$. Significance is indicated as follows: * $p \leq 0.05$, ** $p \leq 0.01$, ***$p \leq 0.001$, ****$p \leq 0.0001$.

3.3 Discussion

It is currently not known whether intestinal SILTs contribute to Treg adaptation in the gut. In particular, it is unclear where these lymphoid structures are located in the tissue, and the factors that influence their function in distinct gut microenvironments. Recently, work in our group and others have highlighted IL-33/Treg signalling as an important regulatory pathway that maintains intestinal homeostasis and promotes repair of inflamed tissue. We therefore wondered whether IL-33 signalling specifically within SILTs to Tregs contributes to this regulatory pathway. Using a combination of flow cytometry and confocal microscopy, we firstly characterised the spatial distribution and cellular composition of intestinal SILTs. Next, using histo-cytometry we analysed the spatial relationship between IL-33 expressing cells and Tregs bearing its receptor, ST2, within SILTs in health and disease. The detailed study of cellular interactions within SILTs is both novel and challenging, particularly designing a workflow that allows imaging data to be quantified in a reproducible manner.

We firstly identified SILTs to be located at distinct sites within the steady state WT C57BL/6 mice caecum and colon. The size and complexity of SILTs were largely dependent on their location: small lymphoid aggregates were found in the caecum and proximal colon, whilst large, more structurally organised OLS are in the distal colon. The small lymphoid aggregates we identified likely include both cryptopatches and isolated lymphoid follicles (ILF), as well as intermediates that fall in between the two (reviewed in [102]). The OLS identified in the distal colon of steady mice are likely to include tertiary lymphoid structures, that are larger than ILFs, but maintain similar structural composition and complexity. Previously, systematic analysis of tissue-associated lymphoid structures

have focussed on only small intestinal SILTs of the murine or human small intestine, or the presence of SILTs without further information of their spatial distribution across distinct colon regions [348, 369-373]. Our data therefore offers a novel and comprehensive overview of the differential location of distinct SILT structures across the whole length of the colon. It is currently unclear what drives this regional discrimination of small lymphoid aggregates versus larger OLS. However, a number of studies have highlighted the dynamic nature of SILTs, with gut inflammation driving the expansion of tertiary lymphoid structures [374]. Furthermore, the gut microbiota has also been shown to influence SILT identity [369], with one study demonstrating bacterial peptidoglycans driving the transformation of cryptopatches into ILFs [375]. As the microbiota of the gut varies longitudinally with the bacterial content increasing distally from the ileum to the colon [376], it is possible differences in the microbial burden influence the regional compartmentalisation of SILTs we have identified.

Finally, we identified hundreds of small lymphoid aggregates in the steady state caecum and proximal colon, likely indicating they play an important role in intestinal immunity. They were first described in 1996 as ‘tiny clusters’ of aggregating lymphocytes situated below intestinal crypts [372]. To date, cryptopatches have not been identified in humans [375]. However, the majority of human biopsies are taken from the colon, where most cryptopatches have likely already undergone conversion to isolated lymphoid follicles due to interactions with the gut microbiota [375]. Isolated lymphoid follicles are the next most complex SILT, and have been described in both the small and large intestine of mice, and humans [348, 377, 378]. Amongst the small lymphoid aggregates we identified in the caecum and proximal colon, some variation exists with regards to their size. Although not formally studied, these differences could be the result of variable microbial diversity

within distinct caecum/proximal colon niches where such lymphoid aggregates reside. Indeed cryptopatches and isolated lymphoid follicles are known to exist on a continuum, with both structures often exhibiting shared characteristics [379]. Challenges have arisen in separating, for example, a mature cryptopatch from an immature ILF. A comprehensive study of tissue-associated lymphoid structures in WT, un-infected mice agree with this notion, and show that tissue associated lymphoid structures do not fall neatly into distinct categories, with some small lymphoid aggregates displaying characteristic traits of both cryptopatches and ILFs [379]. Our results confirm this, with both cryptopatches and less mature ILFs included within our definition of lymphoid aggregates. However, whilst a strict segregation of cryptopatches and ILFs may not exist, our data makes the more important distinction of a clear separation between lymphoid structure and the surrounding lamina propria tissue in terms of cellular composition. We further study the role of small lymphoid aggregates in modulating the T cell response to pathobionts in chapters 4 and 5.

Despite a number of studies characterising the cellular composition of intestinal SILTs in the literature (reviewed in [380]), less is known about how cells interact and signal to each other within SILTs. Combining flow cytometry with histo-cytometry for visualising and quantifying multiple cell populations directly within tissue sections [345], we firstly observed IL-33 producing cells and $CD4^+$ T cells to inhabit similar niches within the outer zones of OLS. Furthermore, we found $Ror\gamma t^+$ and $Ror\gamma t^-$ Treg subsets were spatially segregated under steady state conditions. Next, using $Ror\gamma t^-$ Tregs as a surrogate marker to include the GATA-3^+ $ST2^+$ Treg subset, we speculated an essential need for IL-33 to be spatially close to $ST2^+$ Tregs for optimal cytokine function [360]. Surprisingly, we did not detect a spatial closeness of IL-33 producing cells with the $ST2^+$ Treg subset in OLS in

both homeostatic or inflammatory conditions. Nevertheless, we have developed a novel and reproducible pipeline to quantitively assess the spatial relationship between a cytokine and Treg signalling pathway within a distinct lymphoid structure embedded in the gut tissue.

A number of reasons may explain why IL-33 producing cell are not spatially closer to Rorγt$^-$ Tregs in SILTs. Firstly, we use Rorγt$^-$ Tregs as an indirect measure of ST2$^+$ Tregs. If such ST2$^+$ Tregs represent a small proportion of the total Rorγt$^-$ Tregs, the effect of ST2$^+$ Tregs may be 'drowned out' by other non ST2$^-$ Rorγt$^-$ Tregs. Additionally, as IL-33 can be secreted as an extracellular cytokine, and its effects may therefore be far-reaching, this may reduce the need for physical closeness between it and its ST2 receptor expressing cell. Additionally, the soluble ST2 receptor (sST2) functions as a decoy, mopping up any free IL-33, and if present within SILTs, may disrupt the IL-33/ST2$^+$ Treg signalling pathway. Furthermore, as IL-33 is known to be a potent inducer of the Th2 immune response [381], using a Th2-focussed murine model of colitis such as oxazolone that mimics human UC [46] may highlight the potential alarmin functions of IL-33 signalling in OLS during colitis. The ST2 receptor is expressed on many immune cells aside from Tregs, including Th1, Th2, CD8 and ILC2s (reviewed in [382]). It is possible some or all such cells may be present within OLS, and signalling of IL-33 to these other immune-modulating cells may play a critical role in either driving or preventing inflammatory responses.

The IL-33/Treg signalling pathway may still be critically important for maintaining homeostasis in response to an inflammatory insult, but it may occur through IL-33 produced by epithelial and/or stromal cells outside of SILTs in the surrounding lamina propria tissue. Further work would involve comparing IL-33/ST2$^+$ Treg spatial

relationships within and outside of OLS. Finally, a knock-in/knock-out IL-33^{citrine} reporter strain is also available whereby mice are deficient in IL-33, but report where IL-33 expression would be present. Such mice could be used to interrogate whether IL-33 signalling is critically required and directly influences the spatial positioning of ST2^{+} Tregs within SILTs. Finally, as controversy exists on the role of IL-33 in intestinal inflammation, crossing the IL-33^{citrine} reporter to lymphotoxin-α deficient mice [383] that are devoid of all lymphoid structures could further our understanding of the critical importance of IL-33/Treg signalling within SILTs.

Altogether, studies to define the precise role of IL-33 signalling to ST2^{+} Tregs within tissue micro-compartments could prove useful in the maintenance of homeostasis not only of the gut, but at other immunological barrier sites. A study examining the function of lung-resident Tregs during influenza virus infection highlighted a role for IL-33 in driving Treg mediated tissue repair through expression of the epidermal growth factor amphiregulin [384]. Furthermore, a disease-ameliorating role for IL-33/Treg signalling may also be in operation in the skin. Exogenous IL-33 administration in an allogeneic skin transplant drives expansion of skin Tregs and promotes conversion of Foxp3^{-} CD4 T cells into Tregs *in vivo,* resulting in longer survival of the transplanted tissue [385]. Altogether, available evidence suggests IL-33 signalling to Tregs, particularly in tissue is an important regulator of inflammatory pathology, and our data indicates IL-33 production in SILTs could form one local site that contributes to this reparative signalling pathway.

Chapter 4. The role of the tissue in modulating the T cell response to pathobionts

4.1 Introduction

Gut homeostasis is maintained through orchestration of specialised and diverse populations of cells interacting with one another. This network of cells includes the single layer of epithelial cells in contact with the gut luminal microbial community, the supporting stromal cells within the lamina propria, as well as dedicated tissue-orientated population of both innate and adaptive immune cells. In chapter 3, we identified SILTs of various sizes and maturity that are confined to distinct regions of the steady state gut, with the caecum and proximal colon containing hundreds of small, architecturally disorganised lymphoid aggregates, whilst the distal colon contained a few structurally mature organised lymphoid structures (OLS). Of interest, MHC II^+ antigen presenting cells and CD4 T cells were present in close proximity in both lymphoid aggregates and OLS, suggesting the potential for the activation of T cells at these sites.

Despite their extensive characterisation in the literature, controversy still exists with regards to the function and contribution of SILTs to tissue immunity. It is well documented that inflammatory processes in the gut induce the formation of SILTs, in both murine models such as DSS colitis and human disease, including UC and CD [106, 107, 374, 386-388]. Nevertheless, it is still unclear whether this expanded lymphoid network function to exacerbate or ameliorate inflammatory pathology, and how they differ in function from the scattered immune cells of the lamina propria. Several studies have shown ILFs to act in a tolerogenic manner by controlling intestinal immune responses to

microbiota through the generation of IgA^+ plasma cells and Tregs [389, 390]. Blocking of ILF formation with LTβR-IgG treatment resulted in a 10-fold increase of commensal bacteria [375]. With regards to infectious pathogens, studies have shown ILFs can provide an important micro-environment needed for the induction of an effective host response against harmful enteric bacteria. ILFs harbour specific commensal bacteria that induce the production of IL-10 by dendritic cells and IL-22 by ILC3s, limiting the pro-inflammatory Th17 response, contributing to a tissue specific protection against lethal intestinal damage [391]. Furthermore, IL-22 production by LTi regulated the organisation and maintenance of ILFs in the colon, a process critical during host defence against *Citrobacter rodentium* infection [392]. Finally, chronic inflammation in tissue caused by inflammatory response, infection and malignancy [393], induce the genesis of TLS. They are defined as a highly organised cluster of immune cells with regional segregation, active germinal centres and mature follicular dendritic cell networks similar to secondary lymphoid organs. TLS are often found local to lymphatic vessels, and distinguished by the development of high endothelial venules (HEV) (reviewed in [394]). A number of studies have revealed TLS to be pathogenic in rheumatoid synovitis [395], lupus nephritis [396], thyroiditis [397], multiple sclerosis [398] and pulmonary complications in rheumatoid arthritis [399]. Conversely, TLS have also been shown to be clinically favourable in certain disease pathologies, particularly malignant processes, including lung cancer [400, 401] and prostate cancer [402]. Of further interest, the ability of TLS to modulate the local immune response was recently highlighted in studies showing enrichment of B cells in TLS within the tumour microenvironment associated with favourable response to checkpoint therapy [403-405]. It is therefore likely the role of TLS is context dependent, with its opposing roles potentially explained by tissue-and/or disease specific factors.

The host immune system has adapted to mutually exist with the microbiota in a symbiotic manner, with the bacterial community positively supporting gut tissue health. An example of this mutual beneficial relationship comes from the study of germ-free mice which are devoid of all microbial organisms. Such mice have under-developed lymphoid systems and defective immune responses to some pathogens [406]. Specific defects include reduced numbers of IgA-secreting plasma cells, smaller Peyer's patches, and diminished T cell numbers, particularly affecting the CD4+ T cell subset of the lamina propria [407-409]. Similar to antibiotic treated mice, germ-free mice are more susceptible to a variety of pathogens, particularly in the intestinal tract, including vancomycin-resistant enterococcus, salmonella and *Clostridium difficile* [410-412], in addition to respiratory tract bacterial pneumonia [413, 414], and systemic *Escherichia coli* infections [415]. Infection by the pathobiont *H.hepaticus* is an informative model system for studying the importance of Tregs at barrier sites, and can be used to demonstrate why some hosts are tolerant to colonisation by pathobionts, whilst others succumb to inflammation. Tolerance to *H.hepaticus* in WT specific pathogen free (SPF) C57BL/6 mice is now known to occur through the production of IL-10 cytokine. This is a key regulatory cytokine produced by Tregs which is lost in IL-10 deficient mice that subsequently develop a spontaneous enterocolitis [267]. Maintenance of homeostasis in the gut is therefore reliant on a delicate balance between regulatory and effector T cells, with the pro-inflammatory cytokine IL-23 known to tip this balance towards colitis through the inhibition of Treg induction [22, 216, 416]. However, how *H.hepaticus* promotes the induction of Tregs to maintain homeostasis within lymph node, tissue and SILT sites is currently unknown. The use of TCR transgenic mouse models have also furthered our understanding of how pathobionts such as *H.hepaticus* induce pathogenic T cells in some susceptible hosts, but are tolerated in healthy individuals. Using the novel *H.hepaticus* TCR transgenic mouse model,

colonisation of wild-type mice with *H.hepaticus* was shown to promote the differentiation of Rorγt^{+} (i.e., peripherally-induced) Foxp3^{+} T regulatory cells (Tregs) in the colon lamina propria that restrain a pro-inflammatory Th17 cells. Furthermore, this Treg response towards *H.hepaticus* has been shown to be dependent on the transcription factor c-MAF [57]. In that study, the Treg response to *H.hepaticus* colonisation was investigated within the whole colon tissue without distinguishing the lamina propria versus SILT micro-environments. It therefore remains unknown how the tissue and SILTs contribute to the fate of *H.hepaticus* reactive T cells to promote tolerance.

Altogether, these studies highlight the critical role of *H.hepaticus*-reactive Tregs in maintaining homeostasis in the gut towards pathobionts. However, it is not known if T cells receive TCR signalling and subsequently differentiate into cytokine-producing effector T cells in response to pathobionts solely in the MLN, or whether the gut tissue and its associated SILT lymphoid compartments play a role. In this chapter we aim to investigate whether the colon tissue affects the antigen-specific T cell response to *H.hepaticus* in a unique manner as compared to the compartmentalised lymphoid structures. We will track the phenotype, priming, activation and function of *H.hepaticus* -reactive T cells within the tissue and the organised SILT structures. We hypothesise tissue derived signals contribute to the development and maintenance of Tregs, with interactions in SILTs playing an important role in the response towards pathobionts.

4.2 Results

4.2.1 Validation of the antigen specificity of HH7-2tg T cells to *H.hepaticus*

We previously characterised the diverse range of lymphoid structures in the murine gut which include MLN, caecal patch in the caecum, small lymphoid aggregates in the proximal colon and caecum and OLS in the distal colon in section 3.2.2. We therefore aimed to define the behaviour of naïve *H.hepaticus* specific T cells (HH7-2tg) upon adoptive transfer into *H.hepaticus*-colonised un-inflamed wild type hosts at these distinct tissue versus lymphoid compartments. Due to the difficulty in separating the lamina propria from the hundreds of small lymphoid aggregates, in the following results we refer to the 'tissue' as the composite of the lamina propria (LP) and the small lymphoid aggregates.

TCR transgenic mouse models are a valuable immunological tool to study antigen-specific responses, for example to bacterial antigen, as the majority of T cells developing in such mice express TCR of a known specificity. However, mice containing artificially high numbers of T cells that are only reactive to one antigen are not physiologically relevant, and therefore adoptive transfer of a limited number of TCR transgenic T cells into syngeneic non-TCR transgenic recipient hosts is a common experimental approach to obtain a smaller, but detectable population for tracking *in vivo*. However, whereas expression of the β-chain transgene normally results in complete allelic exclusion of the endogenous β-chain, expression of the α-chain transgene frequently results in incomplete suppression of the endogenous α-chain gene [417]. Therefore, TCR transgenic mice may need to be crossed onto a RAG-1 or RAG-2 deficient background to prevent V(D)J rearrangement and ensure the development of a single population of monoclonal T cells.

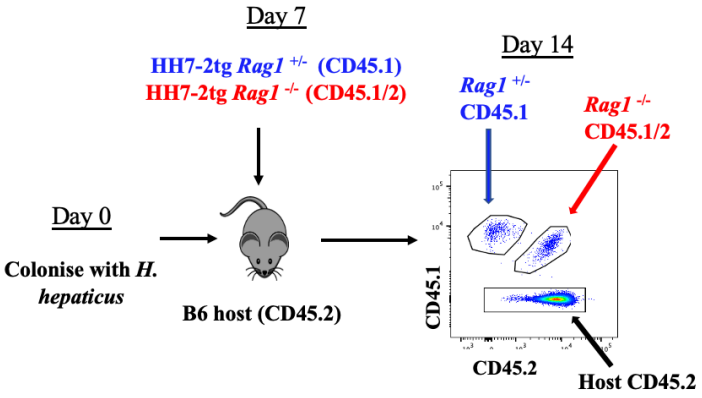
This was demonstrated in a study using T cells from a TCR transgenic mice reactive to CBir1 flagellin expressing *Clostridia* on a WT background were in fact responsive to other intestinal bacteria, including *H.hepaticus* due to the expression of re-arranged endogenously non-transgenic TCRα chains [418].

To validate the antigen specificity of *H.hepaticus*-reactive T cells in our experimental model, we performed co-transfer of naïve HH7-2tg on a $Rag^{-/-}$ and $Rag^{+/-}$ background into *H.hepaticus*-infected WT mice (Fig 4.1a). Naïve HH7-2tg T cells were sorted from splenocytes as $CD45^{+}$ $CD3^{+}$ $CD4^{+}$ $CD44^{-}$ $CD62L^{+}$ $CD25^{-}$ $V\beta6^{+}$. Comparing the two different transferred populations using the congenic CD45.1 and CD45.1/2 surface markers allowed us to verify the antigen specificity of HH7-2tg and exclude the possibility of rearrangement of the endogenous TCRα in cells that express the RAG enzyme. Reassuringly, we did not detect any differences in the frequency of HH7-2tg on a $Rag^{-/-}$ versus $Rag^{+/-}$ background of total CD4 T cells within different tissue and lymphoid sites, suggesting similar accumulation at these locations (Fig 4.1b and c). Furthermore, characterisation of Treg versus non-Treg differentiation of the two transferred HH7-2tg cell populations do not show any significant differences at each of the indicated sites, suggesting the same response of HH7-2tg to H.hepaticus on both a $Rag^{-/-}$ and $Rag^{+/-}$ background (Fig 4.1 d and e). Finally, HH7-2tg T cells were not detectable 14 days after adoptive transfer into hosts that were not colonised with *H.hepaticus*, indicating their failure to survive in the absence of their cognate bacterial antigen (Fig 4.1f). This confirms the need for TCR stimulation for T cell expansion *in vivo*.

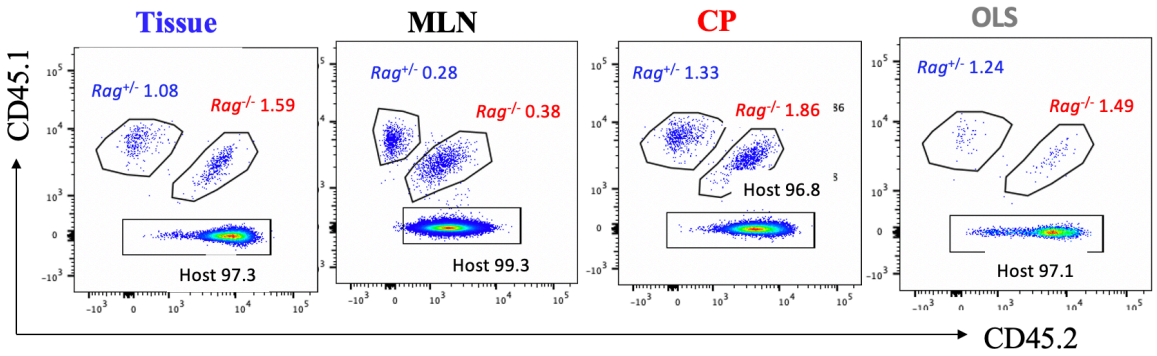
In summary, our results show that naïve T cells from HH7-2tg on a $Rag^{+/-}$ and $Rag^{-/-}$ background showed identical differentiation patterns in response to *H.hepaticus*, indicating

endogenous re-arrangement of the non-transgene TCRα chain unlikely in HH7-2tg mice on a *Rag*$^{+/-}$ background. As such, this provided reassurance that future experiments could be undertaken using donor T cells from HH7-2tg mice on a WT background. Further confirmation of this comes from adoptive transfer of HH7-2tg T cells into *H.hepaticus* un-colonised hosts, illustrating the antigen specific nature of these T cells towards their cognate antigen, and may suggest continued need for TCR stimulation for T cell survival.

a

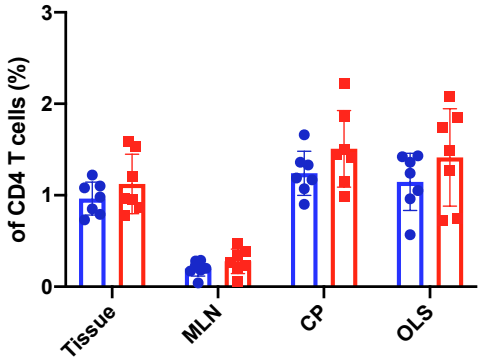


b

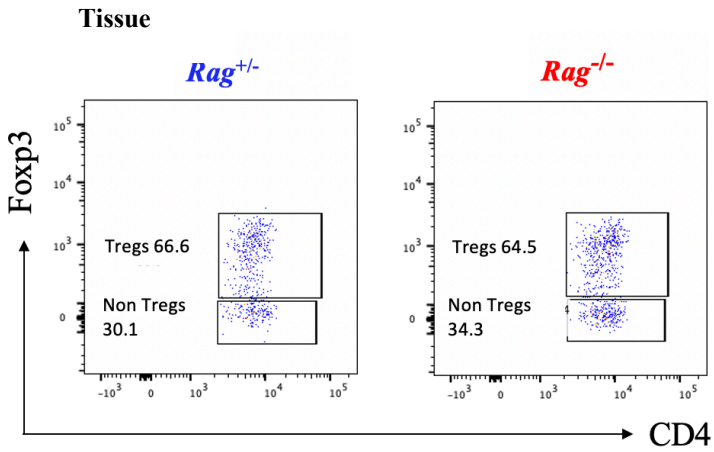


c

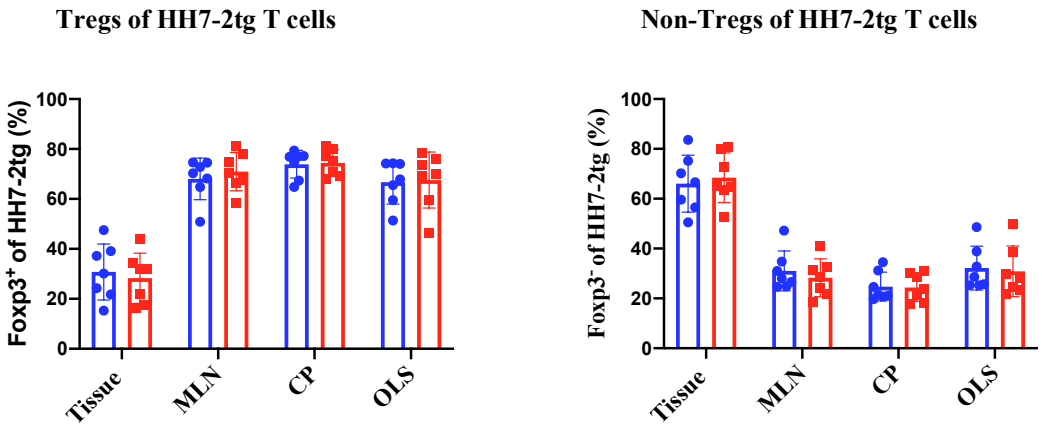
Frequency of HH7-2tgRag$^{+/-}$ and HH7-2tgRag$^{-/-}$ of total CD4 T cells



d


Tissue
Rag+/-
Rag-/-
Foxp3
Tregs 66.6
Non Tregs
30.1
Tregs 64.5
Non Tregs
34.3
CD4

e


Tregs of HH7-2tg T cells
Non-Tregs of HH7-2tg T cells
Foxp3+ of HH7-2tg (%)
Foxp3- of HH7-2tg (%)
Tissue
MLN
CP
OLS

f

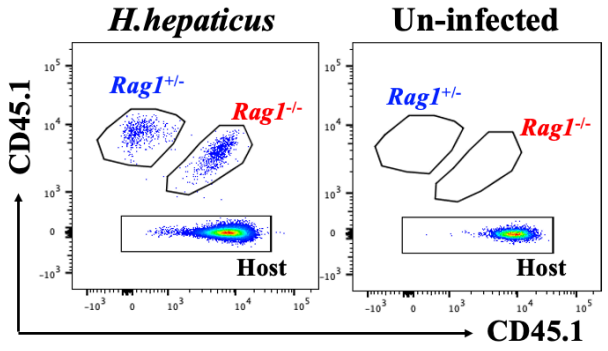

H.hepaticus
Un-infected
Rag1+/-
Rag1-/-
Host
CD45.1
CD45.1

Figure 4.1 Adoptive transfer of HH7-2tg on a *Rag*$^{-/-}$ and *Rag*$^{+/-}$ background confirm identical differentiation profiles

Sorted naive T cells from HH7-2tg mice on a *Rag*$^{-/-}$ (red) and *Rag*$^{+/-}$ (blue) were co-transferred into *H.hepaticus* colonised C57BL/6 mice. Mice were sacrificed at 14 days post cell transfer and HH7-2tg T cell phenotypes were processed for flow cytometry analysis at the indicated sites.

a. Experimental scheme for co-transfer of HH7-2tgRag$^{+/-}$ and HH7-2tgRag$^{-/-}$ naive T cells into *H.hepaticus*-colonised WT hosts.
b. Representative flow cytometry plots of HH7-2tgRag$^{+/-}$ (CD45.1), HH7-2tgRag$^{-/-}$ (CD45.1/2) and host (CD45.2) at the indicated sites at 14 days post cell transfer.
c. The frequency of HH7-2tgRag$^{+/-}$ and HH7-2tgRag$^{-/-}$ of total CD4^{+} T cells at each site.
d. Representative flow cytometry plots of Treg versus non-Treg differentiation of total HH7-2tgRag$^{+/-}$ and HH7-2tgRag$^{-/-}$ CD4 T cells in the tissue.
e. Frequency of Tregs and non-Tregs of total HH7-2tgRag$^{+/-}$ and HH7-2tgRag$^{-/-}$ CD4 T cells at the indicated sites.
f. Representative flow cytometry of HH7-2tg Rag$^{+/-}$ and HH7-2tg Rag$^{-/-}$ of total CD4^{+} T cells in un-infected and *H.hepaticus*-colonised hosts.

Each point represents a single mouse and bars represent mean ± SEM

Data represents results from a single experiment (n = 5 mice in the un-infected group, n = 7 in the *H.hepaticus* colonised group).

Statistical significance was determined using a two-tailed unpaired t test. Differences were considered statistically significant when $p \leq 0.05$. Significance is indicated as follows : * $p \leq 0.05$,** $p \leq 0.01$,***$p \leq 0.001$,****$p \leq 0.0001$.

4.2.2 HH7-2tg are present in SLOs prior to localising to gut tissue

Recently, the fate of *H.hepaticus*-reactive T cells (HH7-2tg) has been tracked in vivo [419], and the results showed differentiation of HH7-2tg into peripherally-induced Tregs in the colon of wild type (WT) mice. However, that study did not distinguish between the tissue and the OLS. We therefore sought to understand the natural history of *H.hepaticus*-reactive T cells in the context of their spatial compartmentalisation. We performed a time-course experiment to study the fate of HH7-2tg T cell differentiation in distinct tissue versus lymphoid sites (MLN, caecal patch and OLS) by charting donor HH7-2tg T cells in these different compartments at defined days post adoptive transfer.

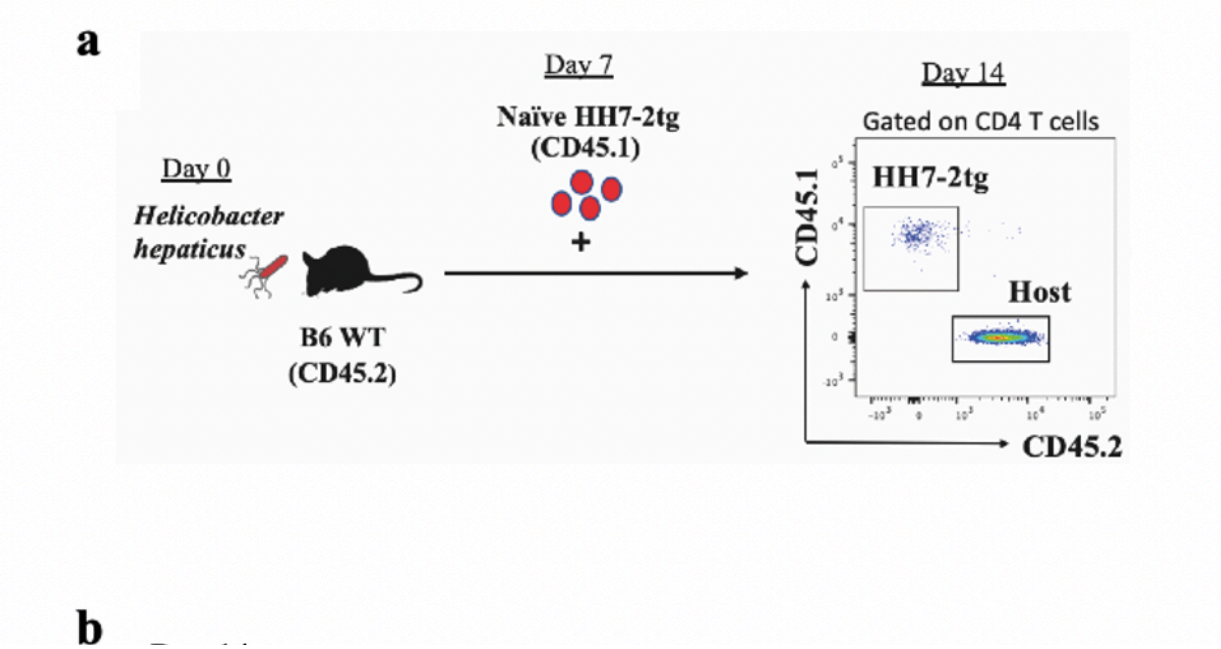
Naïve sorted T cells from HH7-2tg mice on a CD45.1 background were adoptively transferred by intravenous injection into *H.hepaticus*-colonised CD45.2 WT host mice (Fig 4.2a). We firstly examined the differentiation of transferred HH7-2tg T cells at various time points post transfer, starting at 24 hours, and subsequently at day 3, 7, 10 and 14. We picked these time points to comprehensively examine the location of transferred T cells from soon after transfer to maximal *H.hepaticus* colonisation. We hypothesised naïve T cells would rapidly accumulate in secondary lymph nodes within the first 3 days following intravenous tail vein injection, undergo rapid proliferation before localising in tissue approximately 1 week later.

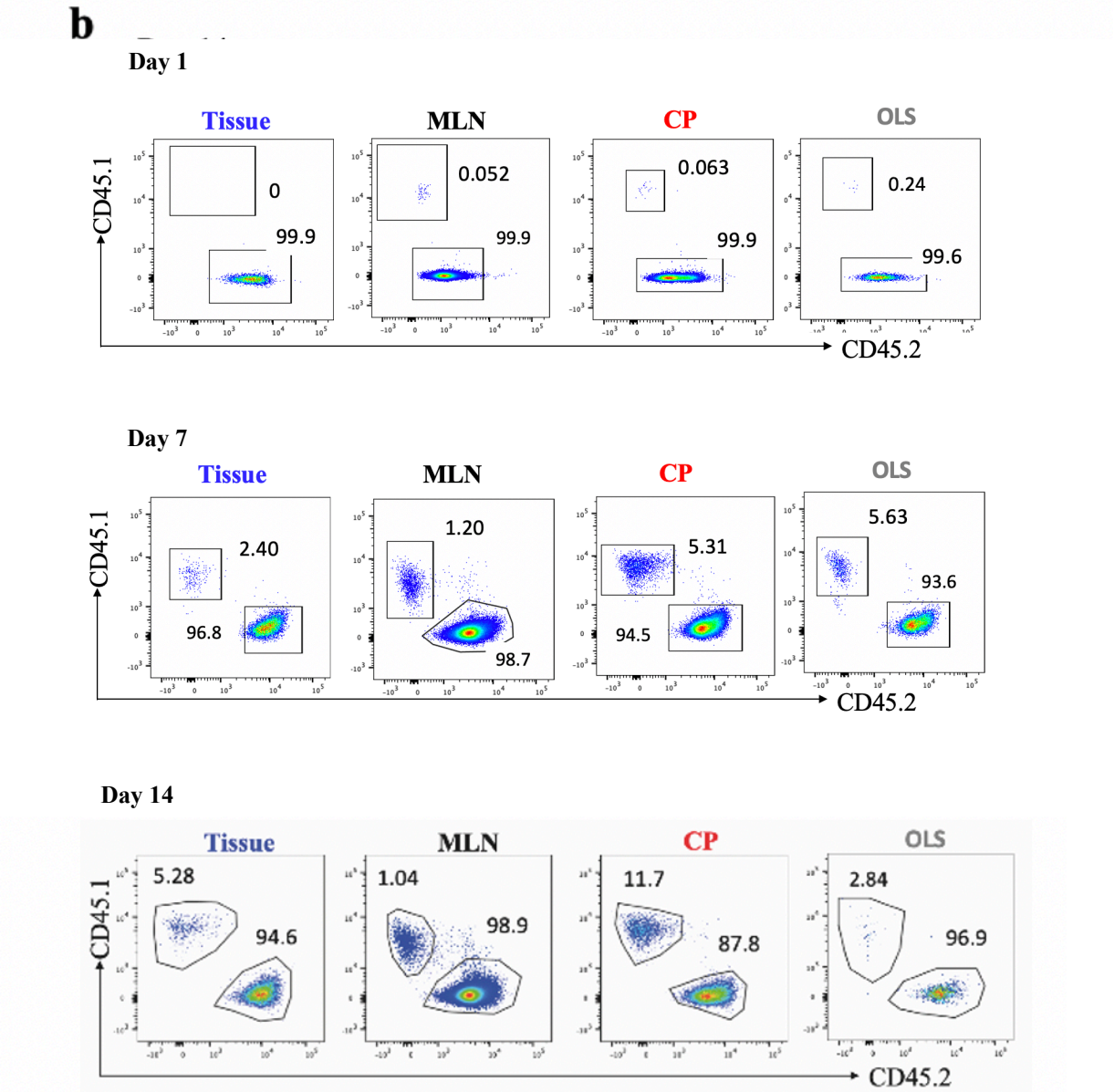
We found accumulation of HH7-2tg T cells as early as 24 hours following transfer to MLN, caecal patch and OLS (Fig 4.2b and c). HH7-2tg T cells steadily increased over the course of the time points examined, with a peak of HH7-2tg among $CD4^+$ T cells at day 10 post transfer. This proportion was highest at day 10 within the caecal patch (present at between 7 to 15% of total $CD4^+$ T cells), followed by the OLS (ranging between 3% to

6%). By day 14, the proportion of HH7-2tg T cells is lower compared to day 10, and this may reflect the host's own T cell response starting to 'catch up' (Fig 4.2c). It is also interesting to note that the frequency of HH7-2tg T cells of total CD4 T cells was approximately 10 fold higher in the caecal patch compared to the MLN at day 14, suggesting the possibility of rapid proliferation at this gut-associated secondary lymphoid organ (Fig 4.2b).

In contrast, within the tissue, HH7-2tg T cells were not detectable at 24 hours post adoptive transfer, and with very few present at day 3 (Fig 4.2b and c). However, HH7-2tg T cells were reliably detected by day 7 post transfer, after which point the dynamics are similar to the SLOs, with peak at day 10, wherein they make up approximately 4-6% of total $CD4^+$ T cells. The HH7-2tg T cell response in the tissue also declines by day 14 (Fig. 4.2c).

Overall, the results indicate accumulation of *H.hepaticus*-reactive T cells in gut tissue approximately 7 days after detection within MLN, caecal patch and OLS. In all tissue and secondary lymphoid sites, the proportion of HH7-2tg of total $CD4^+$ T cells reaches a peak at 10 days post adoptive transfer.


a
Day 7
Naïve HH7-2tg
(CD45.1)
+
Day 14
Gated on CD4 T cells
Day 0
Helicobacter
hepaticus
B6 WT
(CD45.2)
HH7-2tg
Host
CD45.1
CD45.2


b
Day 1
Tissue
MLN
CP
OLS
0
99.9
0.052
99.9
0.063
99.9
0.24
99.6
CD45.1
CD45.2
Day 7
Tissue
MLN
CP
OLS
2.40
96.8
1.20
98.7
5.31
94.5
5.63
93.6
CD45.1
CD45.2
Day 14
Tissue
MLN
CP
OLS
5.28
94.6
1.04
98.9
11.7
87.8
2.84
96.9
CD45.1
CD45.2

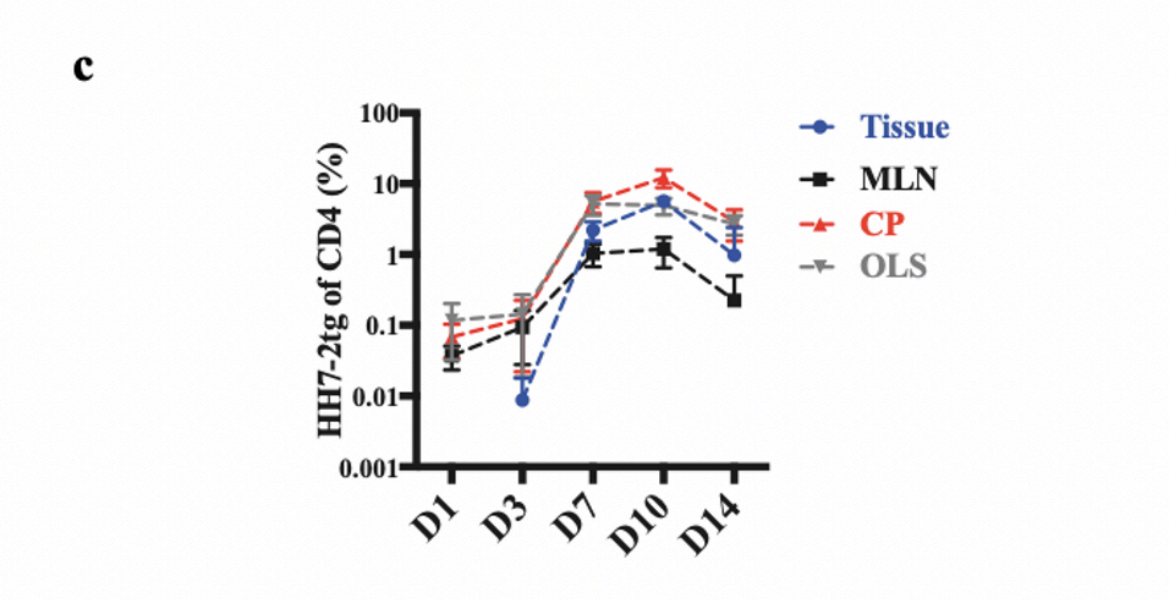


Figure 4.2 HH7-2tg T cells accumulate in lymphoid organs within 24 hours, but not in tissue until 7 days post transfer.

Sorted naïve HH7-2tg T cells were adoptively transferred into *H.hepaticus* colonised WT C57BL/6 hosts. Mice were sacrificed at the indicated timepoints post cell transfer, and tissues were analysed for the presence of HH7-2tg T cells by flow cytometry at the indicated sites.

a. Experimental set-up of transfer of naive CD45.1 HH7-2tg T cells into *H.hepaticus*-colonised WT hosts.
b. Representative flow cytometry plots at day 1,7 and 14 post cell transfer of donor HH7-2tg among total $CD4^+$ T cells at the indicated sites.
c. Frequency of donor HH7-2tg among total $CD4^+$ T cells at indicated time points after adoptive transfer. HH7-2tg T cells were not detected at 24 hours post transfer in the tissue.

Each point represents the mean ± SEM of 4 mice.

Data represents results of a single experiment (n = 4).

4.2.3 HH7-2tg adopt a Treg phenotype within tissue sites

We next studied the fate of transferred naïve HH7-2tg T cells within tissue versus MLN, caecal patch and OLS sites at 14 days post adoptive transfer into *H.hepaticus*-colonised hosts.

14 days following cell transfer, naïve transferred HH7-2tg T cells differentiated into Foxp3$^+$ Tregs, although this was most enriched within tissue sites (approximately 60% of HH7-2tg T cells in tissue, compared to approximately 30% in MLN, and 20% in caecal patch) (Fig 4.3a and b). In addition, the majority of Tregs expressed the transcription factor Rorγt, indicating they are peripherally induced in response to *H.hepaticus* (Fig 4.3c).

A previous study by Xu et al showed a similar HH7-2tg differentiation phenotype and proportion among CD4$^+$ T cells in the colon, but their result studied gut tissue inclusive of OLS [57]. Our data therefore emphasises the distinctive role of the tissue in supporting Treg induction. In addition, HH7-2tg T cells enter the gut tissue as differentiated Tregs on day 7 post adoptive transfer (Fig 4.3d). This indicates the majority of priming of naïve HH7-2tg has occurs in secondary lymphoid structures, but some priming may to Tregs may still occur subsequently in the tissue.

Altogether, our results suggest pathobiont-reactive HH7-2tg T cells are first primed in MLN, casecal patch and OLS sites. Upon activation by *H.hepaticus* antigen, differentiation to a peripherally-induced Foxp3$^+$ Treg occurs within such secondary lymphoid sites, before migrating to tissue. Critically, our data show an enrichment of HH7-2tg Tregs within the tissue compared to secondary lymphoid sites.

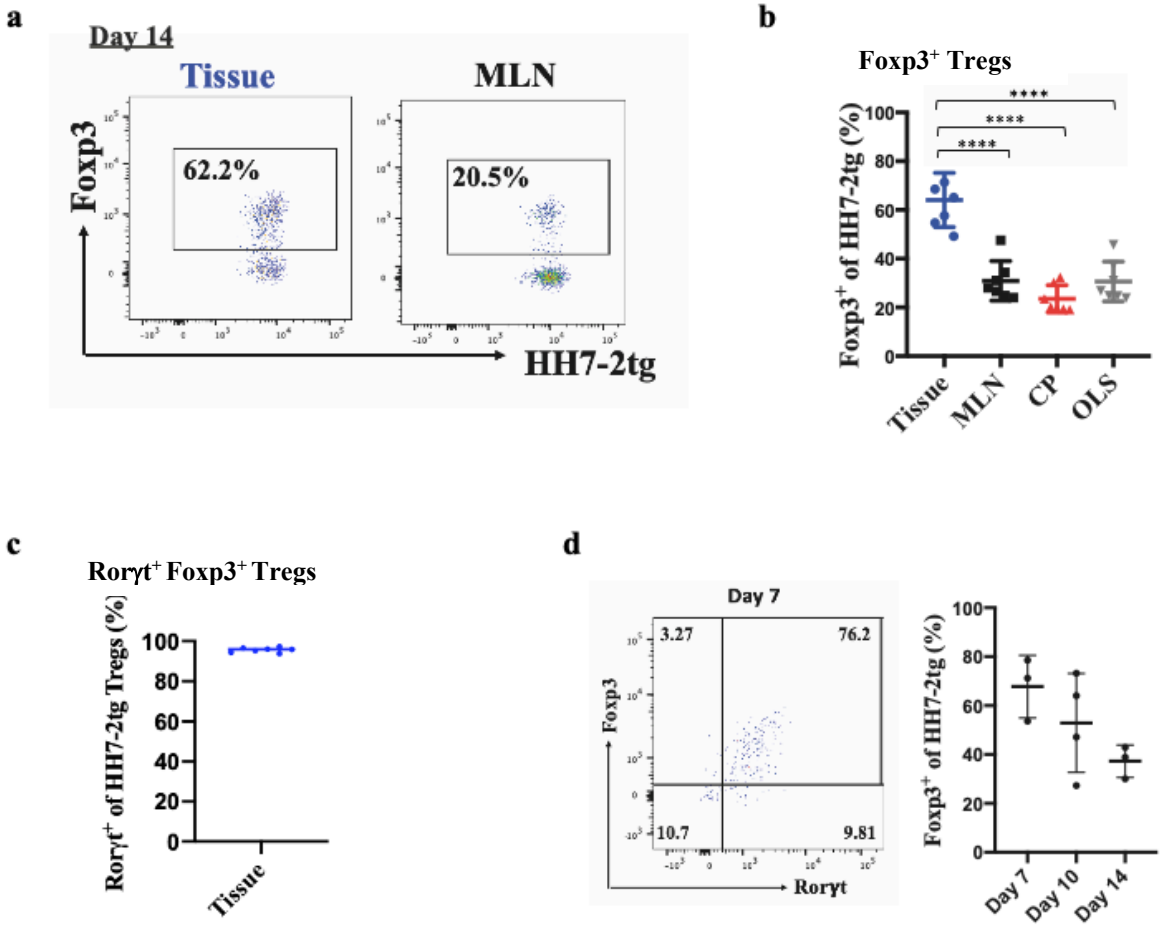

a
Day 14
Tissue
MLN
Foxp3
62.2%
20.5%
HH7-2tg
b
Foxp3+ Tregs
Foxp3+ of HH7-2tg (%)
****
****
****
Tissue
MLN
CP
OLS
c
Rorγt+ Foxp3+ Tregs
Rorγt+ of HH7-2tg Tregs (%)
Tissue
d
Day 7
Foxp3
3.27
76.2
10.7
9.81
Roryt
Foxp3+ of HH7-2tg (%)
Day 7
Day 10
Day 14

Figure 4.3 *H.hepaticus*-specific naïve T cells differentiate into peripherally-induced Tregs, with enrichment within tissue sites

Sorted naive HH7-2tg T cells were adoptively transferred into *H.hepaticus* colonised WT C57BL/6 hosts. Mice were sacrificed at 14 days post cell transfer and HH7-2tg Treg differentiation analysed by flow cytometry at the indicated sites.

a. Representative flow cytometry plot of $Foxp3^+$ of donor T cells at 14 days post cell transfer at the indicated sites.
b. Frequency of $Foxp3^+$ of total donor T cells at 14 days post cell transfer at the indicated sites.
c. Frequency of $Ror\gamma t^+$ of total HH7-2tg Tregs in the tissue at 14 days post donor T cell transfer.
d. Representative flow cytometry plot and frequency of $Foxp3^+$ among donor HH7-2tg in the tissue at the indicated time points after adoptive transfer.

Each point represents a single mouse and bars represent mean ± SEM

(a-c) Data represents results from a single experiment representative of more than two independent experiments (n = 7 mice).

(d) Data represents results from a single experiment (n =4)

Statistical significance was determined using an ordinary one-way ANOVA with a Tukey's multiple comparisons test. Differences were considered statistically significant when $p \leq 0.05$. Significance is indicated as follows: * $p \leq 0.05$,** $p \leq 0.01$,***$p \leq 0.001$,****$p \leq 0.0001$.

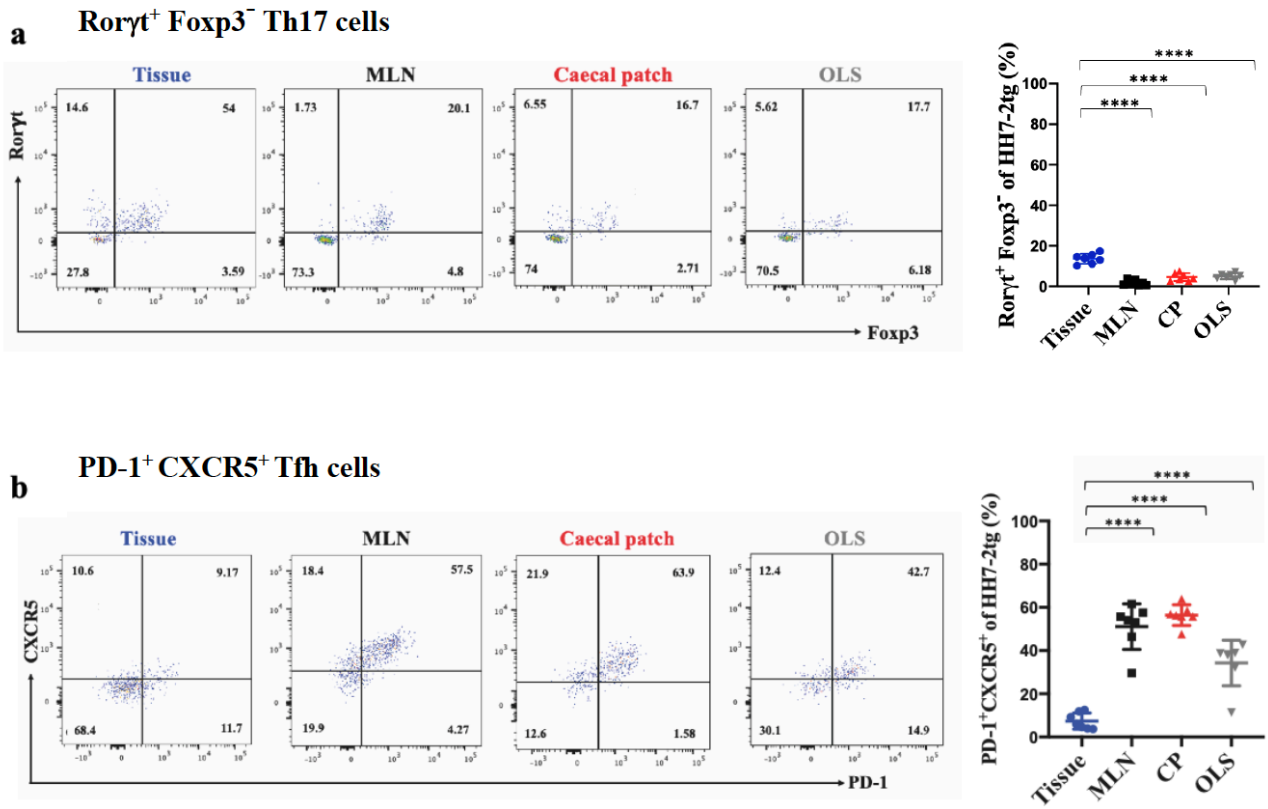
4.2.4 HH7-2tg adopt a T follicular helper cell phenotype at SLO sites

In contrast to tissue sites, within MLN, caecal patch and OLS sites, only 20% to 40% of HH7-2tg differentiated into Tregs. We next investigated the phenotype of these non-Treg cells within these sites. Xu et al had shown HH7-2tg differentiate into a pro-inflammatory Rorγt^{+} Th17 phenotype within IL-10$^{-/-}$ hosts. However, within WT hosts, very few HH7-2tg differentiate into Rorγt^{+} Th17 cells in both tissue and secondary lymphoid sites (Fig 4.4a). Instead, naïve HH7-2tg T cells differentiate into a CXCR5^{+} PD-1^{+} Tfh phenotype in secondary lymphoid structures, but not tissue locations, with approximately 60% adopting a Tfh phenotype in MLN and caecal patch sites, versus only 10% in tissue) (Fig 4.4b). Tfh cells are a specialised CD4^{+} T cell subset that provide essential help for germinal centre formation, affinity maturation of B cells and the development of antibodies and memory B cells within lymphoid tissue (reviewed in [155]).

We had previously observed OLS to contain a large, central B220^{+} B cell zones at steady state that have the ability to form IgD^{-} BCL6^{+} germinal centres upon *H.hepaticus*/anti-IL10R colitis (section 3.2.4). We therefore next wondered if germinal centres could form in *H.hepaticus* colonisation alone, without the induction of H.h/anti-IL10R colitis in OLS. To this end, we performed immunofluorescent staining on colon swiss rolls from *H.hepaticus*-colonised mice to detect the presence of BCL6^{+} IgD^{-} germinal centres with BLC6 marking germinal centre activated B cells, and IgD identifying naïve B cells. Immunofluorescent staining was performed 14 days after colonisation of *H.hepaticus* to allow time for the formation of germinal centres. Indeed we observed the formation of germinal centres in OLS, but not small lymphoid aggregates (Fig 4.4c). These results

correlate with the flow cytometry data showing induction of *H.hepaticus* specific Tfh cells in the OLS, but not in the tissue where lymphoid aggregates are sited.

Altogether, our results show HH7-2tg mainly differentiate into Tregs within tissue sites, whilst adopting a Tfh phenotype within MLN, caecal patch and OLS sites. Tfh differentiation in secondary lymphoid structures likely induces the formation of germinal centres in response to *H.hepaticus*, suggesting Tfh cells provide help towards the B cell and immunoglobulin response against pathobionts. Overall, this process highlights the importance of the compartmentalisation of tissue versus lymphoid sites in determining T cell fate, and indicates there is a division of labour between these locations in supporting Treg versus Tfh phenotypes. Further work would include studying the specific cues that drive these differing T cell phenotypes from naïve T cells with identical TCR and primed within roughly the same time frame. It is likely dendritic cells, together with distinctive cytokine profiles located at these distinct tissue and lymphoid sites provide unique signalling cues that promote Treg versus Tfh differentiation.



c. *H.hepaticus*

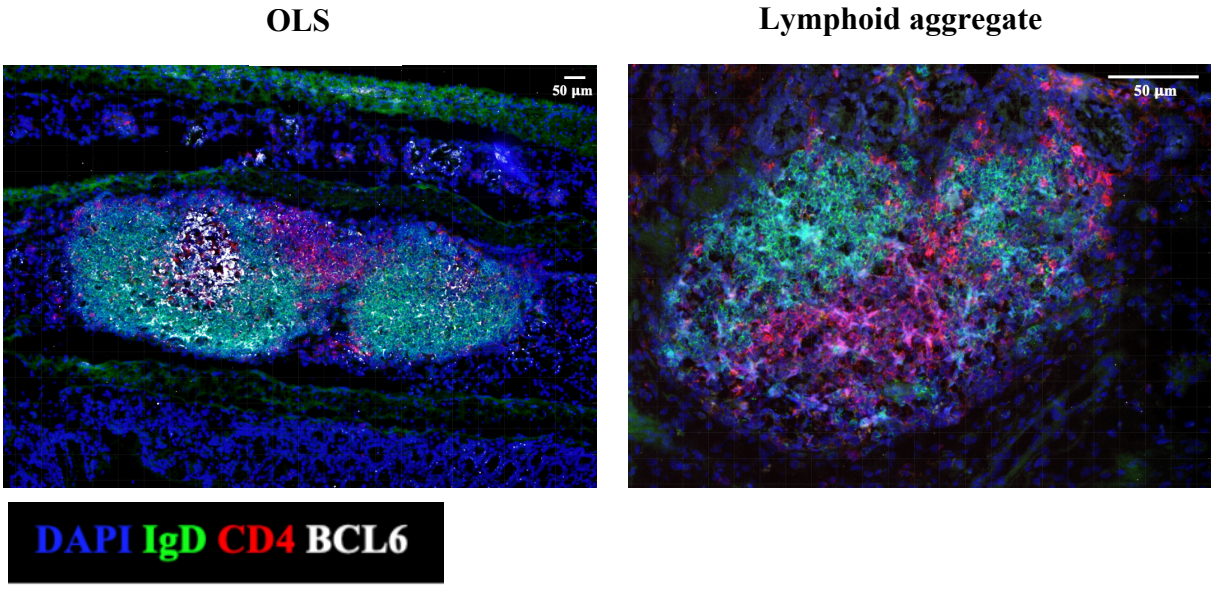


Fig 4.4 HH7-2tg differentiate into Tfh cells in secondary lymphoid structures

Sorted naive HH7-2tg T cells were adoptively transferred into *H.hepaticus* colonised WT C57BL/6 hosts. Mice were sacrificed at 14 days and flow cytometry was performed on the indicated sites to analyse HH7-2tg Th17 and Tfh differentiation. Immunofluorescent staining was also performed on colon swiss rolls to analyse germinal centre formation in lymphoid aggregates and SILTs.

IgD in green, CD4 in red, BCL6 in white, DAPI in blue

a. Representative flow cytometry plot at day 14 and frequency of Rorγt^{+} and Foxp3^{+} expression of HH7-2tg in tissue and secondary lymphoid structures.
b. Representative flow cytometry plots at day 14 and frequency of PD-1^{+}CXCR5^{+} Tfh expression of HH7-2tg in tissue and secondary lymphoid structures.
c. Representative immunofluorescent images of BCL6^{+} IgD^{-} germinal centre staining in OLS and lymphoid aggregates of *H.hepaticus* colonised hosts.

(a-b) Each point represents a single mouse and bars represents mean ± SEM.

Data represents a single experiment representative of two independent experiments (n = 7).

Statistical significance was determined using an ordinary one-way ANOVA with a Tukey's multiple comparisons test. Differences were considered statistically significant when $p \leq 0.05$. Significance is indicated as follows: * $p \leq 0.05$,** $p \leq 0.01$,***$p \leq 0.001$,****$p \leq 0.0001$.

(c) Original magnification 10X for OLS, and 40X for lymphoid aggregate. Scale bar 50 μm. Each staining was performed in n = 6 mice.

4.2.5 The tissue is the site of strongest HH7-2tg TCR stimulation

Having observed an enrichment of HH7-2tg Tregs within tissue, we next wanted to investigate how the tissue supports Treg phenotype and function. A previous study highlighted the role of continued TCR signalling in lymph node resident differentiated Tregs as a critical mechanism that maintains Treg suppressor function [420]. We therefore hypothesised the gut tissue may provide TCR signals to tissue-resident Tregs that permits their tolerogenic role towards microbial antigens.

The ability to distinguish genuine antigen stimulated T cells from general stimulation secondary to an inflammatory milieu is challenging *in vivo*. Previously, CD69 has been used as a marker of T cell activation, but this is upregulated in response to a general inflammatory stimuli. CD69 is also a marker of tissue resident memory cells (reviewed in [421]). Nur77 is an early gene that is rapidly upregulated upon TCR signalling, and the creation of the Nur77^{GFP} transgenic reporter mouse allows for the faithful reporting of TCR stimulation [422]. Furthermore, the level of GFP expression accurately reflects the strength of TCR stimulation [423]. We therefore aimed to determine firstly whether the gut tissue can provide TCR signals to differentiated Tregs that may maintain their suppressor function, and secondly, the strength of this TCR signal in comparison to secondary lymphoid sites.

To address this, we crossed the HH7-2tg to Nur77^{GFP} mice (HH7-2tgNur77^{GFP}) to study TCR stimulation within *H.hepaticus* specific T cells in tissue versus MLN, caecal patch and OLS sites. We studied the Nur77^{GFP} signal at 8 days post cell transfer as we wanted to investigate how the tissue could support Tregs soon after they enter the colon. Despite earlier data indicating priming of HH7-2g within secondary lymphoid sites, interestingly,

the highest HH7-2tg Nur77^{GFP} mean fluorescent intensity (MFI) signal was observed in the tissue, and not in the MLN, caecal patch or OLS (Fig 4.5a). This indicates the strongest HH7-2tg TCR signal occurs in the tissue.

The half-life of GFP has previously been shown to be long [423], and it is therefore possible that the Nur77^{GFP} signal detected in the tissue could in fact be due to recently migrated HH7-2tg that received TCR stimulation in the MLN. Therefore, in order to characterise the Nur77^{GFP} signalling dynamics in donor HH7-2tgNur77^{GFP} cells, we performed an *in vitro* co-culture of bone marrow-derived dendritic cells (BMDC) loaded with *H.hepaticus* peptide and naïve HH7-2tgNur77^{GFP} T cells. We blocked BMDC – T cell interactions using anti-MHCII 24 hours after contact, and subsequently studied GFP signal decay using flow cytometry.

The GFP signal reached a maximal MFI at 24 hours post BMDC-T cell interaction, and returned to baseline at 72 hours following TCR stimulation (Fig 4.5b). Thus, in order to analyse TCR dynamics *in vivo,* adoptive transfer of HH7-2tgNur77^{GFP} naïve T cells was performed as before into WT hosts. On day 8, approximately 24 hours after first entry into the gut, the sphingosine 1-phosphate receptor agonist FTY720 was injected daily into host mice in order to block further HH7-2tgNur77^{GFP} T cell egress from MLNs. FTY720 is a first-in-class immunomodulatory drug which when phosphorylated by sphingosine kinase *in vivo,* results in the internalisation and degradation of S1P receptors that are normally highly expressed on lymphocytes exiting lymph nodes. Studies have also shown FTY720 to primarily inhibit naïve and central memory CD4^{+} T cells from entering the circulation [424]. Daily injections of FTY720 for 72 hours (3 days) ensured any GFP signalling from TCR stimulation in the MLN would decline back to baseline. Analysis of gut tissue at 72

hours post first FTY720 injection, i.e., at 11 days post initial cell transfer, would ensure only tissue-induced GFP signalling would be detected (Fig 4.5c).

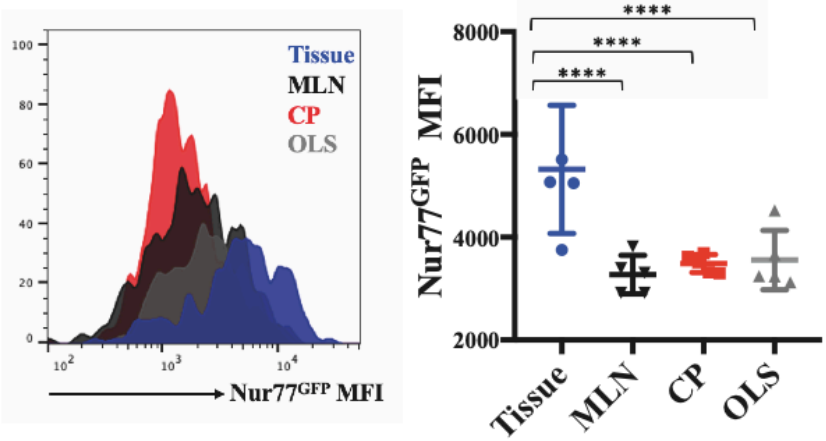
We confirmed the effect of FTY720 by analysing the proportion of TCRβ^+ of total CD45 leukocytes in the peripheral circulation as a measure of lymphocyte retention within lymph nodes. We found an approximate four-fold reduction in T cells in the peripheral blood of FTY720 treated mice, indicating a significant reduction in T cell egress from lymph nodes (Fig 4.5d). Interestingly, the absolute number of HH7-2tg T cells in the tissue was comparable between FTY720-treated and controls, alluding to the possibility of rapid tissue proliferation of donor T cells in FTY720- treated hosts (Fig 4.5e).

Analysis of donor HH7-2tgNur77^{GFP} T cells at 11 days post adoptive transfer revealed the tissue again induced the strongest Nur77^{GFP} signal compared to secondary lymphoid sites, and this was on par with control mice, suggesting cellular interactions locally within the tissue environment can provide strong TCR stimulation (Fig 4.5f and g).

Altogether, our results show interactions within the gut tissue stimulates the strongest TCR signals to HH7-2tg Tregs. Furthermore, such stimulation may induce their ongoing proliferation, as shown by the inability of FTY720 to affect T cell numbers in the gut.

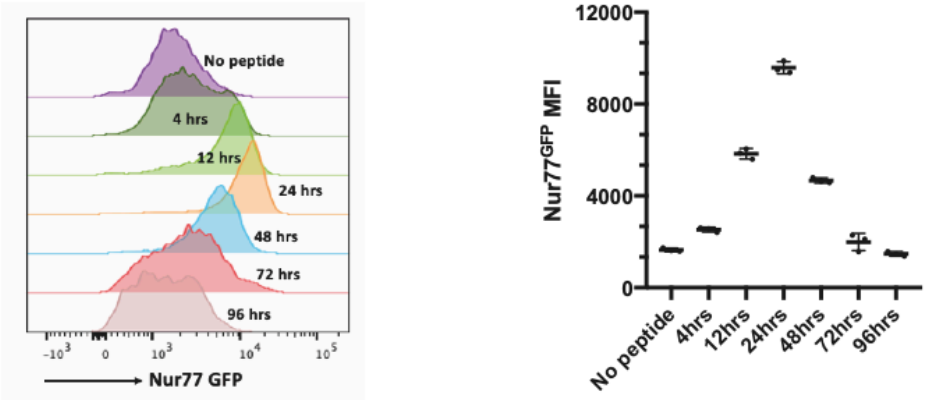
a

Day 8 Nur77^{GFP} MFI

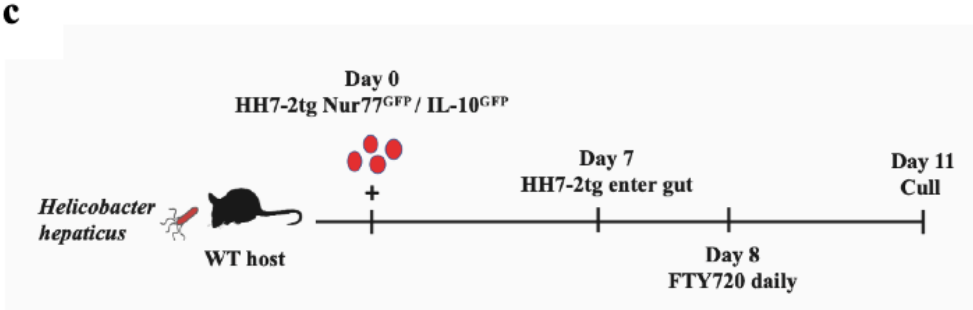


b

Co-culture of BMDC and HH7-2tgNur77^{GFP}



c



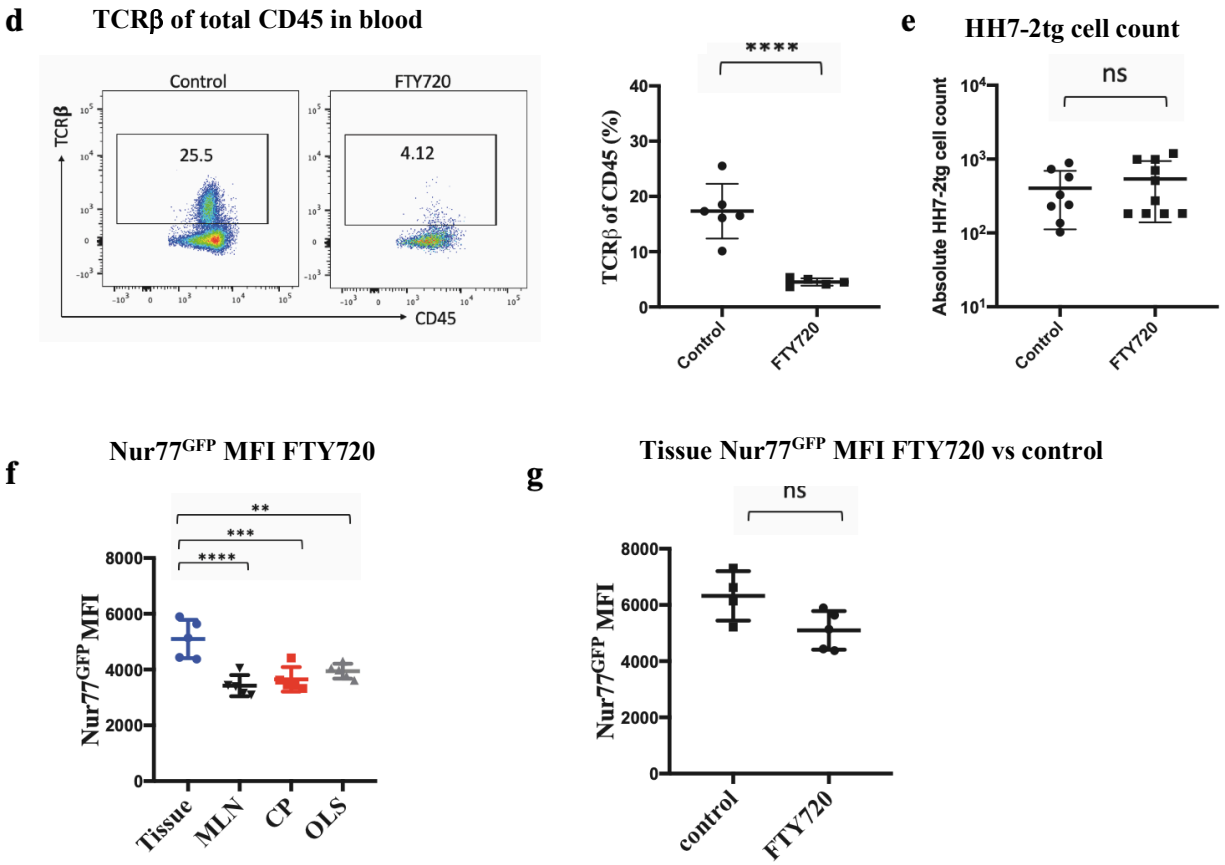


Figure 4.5 The tissue is the site of strongest TCR stimulation by HH7-2tg T cells

Sorted naïve HH7-2tgNur77^{GFP} T cells were adoptively transferred into *H.hepaticus*-colonised C57BL/6 hosts. Mice were sacrificed at 8 days post cell transfer and the Nur77^{GFP} MFI representing strength of TCR stimulation was analysed in donor HH7-2tg T cells at the indicated sites (a).

H.hepaticus peptide-loaded BMDCs were co-cultures with sorted naïve HH7-2tgNur77^{GFP} T cells and the Nur77^{GFP} MFI was analysed by flow cytometry at the indicated time points (b).

Sorted naïve donor HH7-2tg Nur77^{GFP} T cells were adoptively transferred into *H.hepaticus*-colonised WT C57BL/6 hosts. FTY720 was administered by i/p injection daily for 3 days starting from day 8 post cell transfer. Mice were sacrificed at day 11 post cell transfer and the efficiency of lymphocyte egress blockade was analysed (d and e). The Nur77^{GFP} MFI representing strength of TCR stimulation in donor HH7-2tg T cells was analysed by flow cytometry at each of the indicated sites and compared to non-FTY720 treated mice (control) (f and g).

a. Representative histogram overlay and GFP MFI of donor HH7-2tgNur77^{GFP} at indicated sites 8 days post adoptive transfer.

b. Representative histogram overlay and quantification of MFI of HH7-2tgNur77^{GFP} T cells co-cultured with *H.hepticus*-fed BMDCs at the indicated time points.

c. Experimental set-up of transfer of donor HH7-2tg Nur77^{GFP} T cells into FTY720-treated mice.

d. Representative flow cytometry plots and quantification of TCRβ of total CD45 cells in peripheral blood of control and FTY720 treated mice.

e. Absolute HH7-2tg cell numbers in tissue of control and FTY720 treated mice.

f. Nur77^{GFP} MFI of donor HH7-2tgNur77^{GFP} in FTY720 treated host mice at indicated sites.

g. Nur77^{GFP} MFI of donor HH7-2tgNur77^{GFP} in tissue in FTY720 treated and control mice.

Each point represents a single mouse, and bars represents mean ± SEM.
(a) Data represents results from a single experiment representative of two independent experiments (n= 5)
(b) Data represents results from a single experiment (n =3)
(d) Data represents results from a single experiment representative of two independent experiments (n = 7 for control group, n=7 for FTY720-treated group)
(e) Data represents results from a single experiment representative of two independent experiments (n=7 for control group, n=7 for FTY720-treated group)
(f-g) Data represents results from a single experiment representative of three independent experiments (n = 4 in the control group, n =5 in the FTY720-treated group.

Statistical significance was determined using an ordinary one-way ANOVA with a Tukey's multiple comparisons test (a and f), and a two-tailed unpaired t test (d,e and g). Differences were considered statistically significant when $p \leq 0.05$. Significance is indicated as follows: * $p \leq 0.05$,** $p \leq 0.01$,***$p \leq 0.001$,****$p \leq 0.0001$.

4.2.6 Interactions within tissue promote the highest production of IL-10 by HH7-2tg

Cytokine secretion by T cells plays a key role in shaping adaptive immune responses. The IL-10 cytokine produced by Tregs at barrier sites is critical in maintaining tolerance through a number of mechanisms. These include inhibition of MHCII and co-stimulatory molecule B7-1 and B7-2 expression on macrophages, limiting the production of pro-inflammatory cytokines such as IL-1α, IL-6 and TNF-α, as well as acting directly on T effector cells to limit their proliferation [425-427]. Having observed tissue associated antigen presenting cells distinctively inducing strong TCR signals within Tregs, we next wondered whether such TCR stimulation could promote their suppressor function at this site.

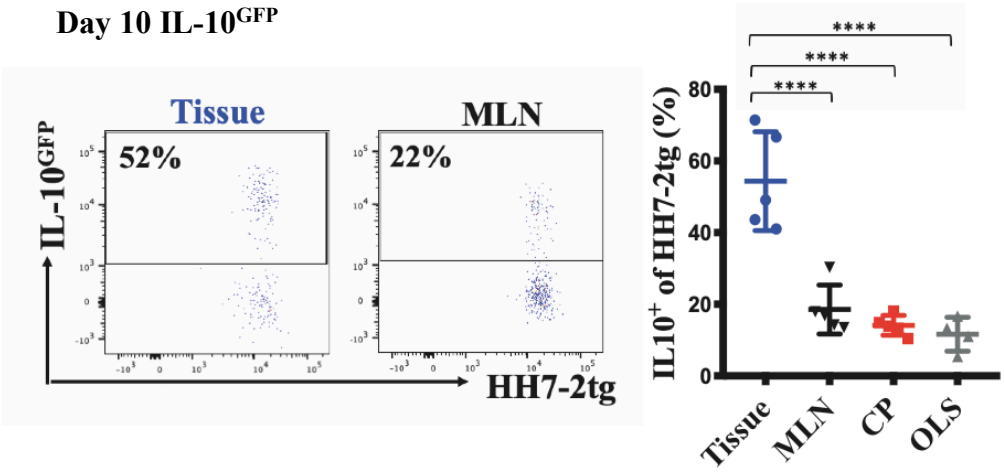
Thus, to study the spatial compartmentalisation of IL-10 production by HH7-2tg Tregs within tissue versus lymphoid sites, we next crossed HH7-2tg to the B6.Foxp3^{hCD2} IL-10^{GFP} reporter mice (HH7-2tgIL-10^{GFP}), and adoptively transferred naïve T cells into *H.hepaticus*-colonised WT hosts as before. We observed once again the tissue, and not the secondary lymphoid sites, to be the location with the highest proportion of IL-10 expressing HH7-2tg T cells (Fig 4.6a). As the tissue was also the site of the strongest TCR interaction, this suggests TCR signalling to HH7-2tg in the tissue may be important in maintaining Treg suppressor function to *H.hepaticus* via the production of large amounts of IL-10 cytokine.

Furthermore, blocking of lymphocyte egress using FTY720 as previously described in section 4.2.5 once again showed the MFI of HH7-2tg IL-10^{GFP} remained the highest in the

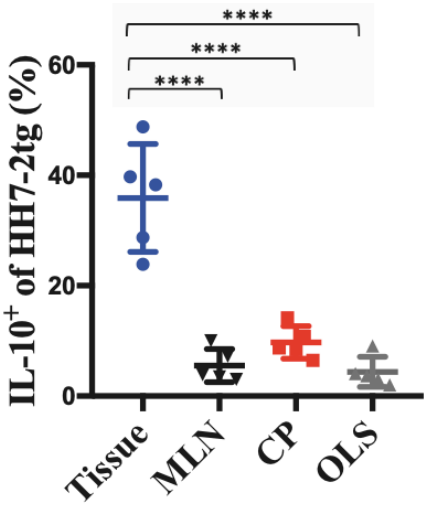
tissue compared to other secondary lymphoid sites (Fig 4.6b). The IL-10^{GFP} MFI was also comparable between FTY720 treated and untreated controls (Fig 4.6c), indicating the tissue provides cues that drive TCR stimulation to HH7-2tg on a par with those T cells migrating first through secondary lymphoid structures.

In conclusion, interactions within the distinct tissue environment provides key signals that promote TCR engagement and likely subsequent IL-10 production by HH7-2tg in response to *H.hepaticus* pathobiont. However, it is unclear whether such tissue cues promoting regulatory IL-10 production are only possible following initial priming in secondary lymphoid structures.

a


Day 10 IL-10GFP
Tissue
MLN
52%
22%
IL-10GFP
HH7-2tg
IL10+ of HH7-2tg (%)
****
****
****
Tissue
MLN
CP
OLS

b


IL-10GFP FTY720
IL-10+ of HH7-2tg (%)
****
****
****
Tissue
MLN
CP
OLS

c

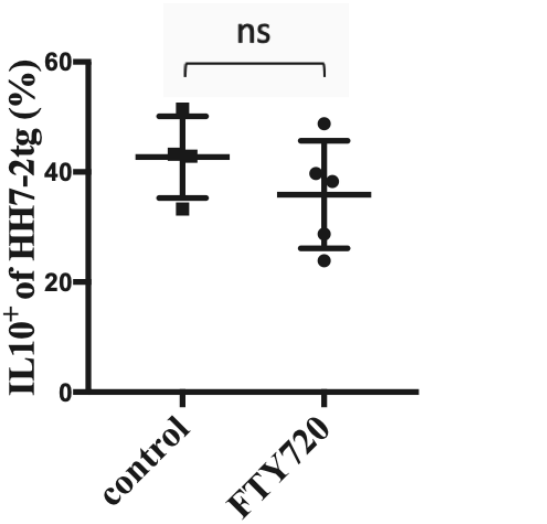

Tissue IL-10GFP FTY720 vs control
IL10+ of HH7-2tg (%)
ns
control
FTY720

Figure 4.6 The tissue is the site of the highest proportion of IL-10 production by HH7-2tg T cells

Sorted naïve HH7-2tgIL-10^{GFP} T cells were adoptively transferred into *H.hepaticus*-colonised C57BL/6 hosts. Mice were sacrificed at 8 days post cell transfer and the IL-10^{GFP} representing the amount of IL-10 production on a per cell basis in donor HH7-2tg T cells was analysed by flow cytometry at the indicated sites (a).

Sorted naïve donor HH7-2tg IL-10^{GFP} T cells were adoptively transferred into *H.hepaticus*-colonised WT C57BL/6 hosts. FTY720 was administered by i/p injection daily for 3 days starting from day 8 post cell transfer. Mice were sacrificed at day 11 post cell transfer and the IL-10GFP representing the amount of IL-10 production on a per cell basis in donor HH7-2tg T cells was analysed by flow cytometry at each of the indicated sites and compared to non-FTY720 treated mice (control) (b and c).

a. Representative flow cytometry plot and frequency of IL-10^{+} among donor HH7-2tgIL-10^{GFP} cells 10 days post cell transfer at the indicated sites.

b. Frequency of IL-10^{GFP} among donor HH7-2tgIL-10^{GFP} at indicated sites in FTY720 treated host mice.

c. Frequency of IL-10^{GFP} among donor HH7-2tgIL-10^{GFP} in tissue in FTY720 treated and control mice.

Each point represents a single mouse, and bars represent mean ± SEM.

(a-b) Data represents results from a single experiment representative of two independent experiments (n = 5)

(c-d) Data represents results from a single experiment representative of two independent experiments (n = 4 in control group, n = 5 in FTY720-treated group).

Statistical significance was determined using an ordinary one-way ANOVA with a Tukey's multiple comparisons test (a -b), and a two-tailed unpaired t test (c). Differences were considered statistically significant when $p \leq 0.05$. Significance is indicated as follows: * $p \leq 0.05$,** $p \leq 0.01$,***$p \leq 0.001$,****$p \leq 0.0001$.

4.2.7 MLNs are critical for Treg differentiation

Having observed a tissue-specific signal that stimulates TCR and IL-10 production in HH7-2tg T cells migrating from lymph node into tissue, we next wondered whether these local cellular interactions could occur independently of prior MLN priming.

Mice deficient in lymphotoxin-α (Lta^{tm1Dch}), an inflammatory mediator that plays crucial roles in lymphoid organ development, are devoid of all morphologically detectable lymph nodes, including MLNs and Peyer's patches, but undergo normal thymus development [428]. In addition, previous work studying un-inflamed Lta^{tm1Dch} mice reported a lack of all tissue-associated lymphoid aggregates (cryptopatches and ILFs) of all sizes in the small intestine [379, 429]. We were therefore interested to study the fate of adoptively transferred naïve HH7-2tg T cells in the gut tissue of Lta^{tm1Dch} hosts in order to verify whether draining lymph nodes are strictly necessary for the induction of Treg suppressor function.

We crossed HH7-2tg to B6.$Foxp3^{hCD2}$ IL-10^{GFP} to generate a *H.hepaticus*-specific double reporter whereby $Foxp3^{+}$ Tregs can be identified using the surface marker hCD2 without the need to fix and permeabilise the cells that would otherwise destroy the IL-10^{GFP} signal. Naïve splenic T cells from these mice were subsequently adoptively transferred into *H.hepaticus*-colonised Lta^{tm1Dch} host mice. Mice were sacrificed 11 days after cell transfer, at which point we confirmed the lack of MLNs, and also observed a total lack of caecal patch and OLS (data not shown). As Lta^{tm1Dch} mice used were not fluorescent reporters, we were unable to confirm whether such mice still retained small lymphoid aggregates within gut tissue. Furthermore, despite the lack of secondary lymphoid structures, the mice did not appear to have any macroscopic signs of inflammation in the caecum or colon.

Despite T cells acquiring gut homing receptors in lymph nodes to facilitate their migration into tissue, we were surprised to find HH7-2g T cells were still able to migrate into gut tissue despite the lack of MLNs (Fig 4.7a). This implies the imprinting of gut homing receptors does not solely occur within secondary lymph nodes. However, whilst transferred HH7-2tg T cells were able to migrate into gut tissue, they no longer differentiated into $Foxp3^{+}$ Tregs (Fig 4.7d). However, HH7-2tg T cells within Lta^{tm1Dch} hosts retained the ability to produce IL-10, albeit at a lower frequency compared to control mice (Fig 4.7b). There seems to be a shift of labour with IL-10 predominantly by non-Tregs (Fig 4.7c). IL-10 production by such non-Treg HH7-2tg cells in Lta^{tm1Dch} hosts likely prevents spontaneous colitis occurring in these mice.

Overall, the above data suggests that MLNs are crucial for Treg induction in response to *H.hepaticus,* but the tissue itself is an independent site for the induction of IL-10 production.

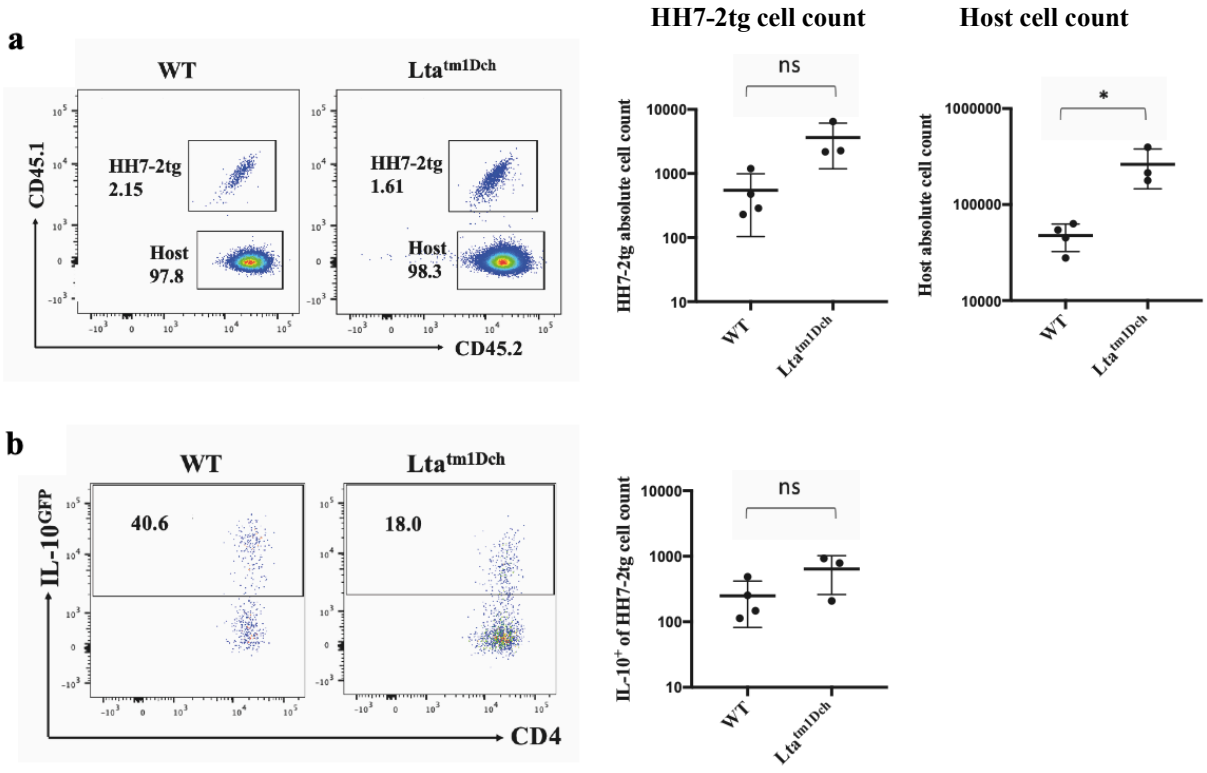

a
WT
Lta tm1Dch
CD45.1
CD45.2
HH7-2tg 2.15
Host 97.8
HH7-2tg 1.61
Host 98.3
HH7-2tg cell count
ns
HH7-2tg absolute cell count
Host cell count
*
Host absolute cell count
b
IL-10GFP
CD4
40.6
18.0
IL-10+ of HH7-2tg cell count
c
IL-10+ of HH7-2tg Tregs
***
IL-10+ of HH7-2tg Tregs (%)
IL-10+ of HH7-2tg T cells
IL-10+ of HH7-2tg (%)
d
Foxp3+ of HH7-2tg
hCD2 (Foxp3)
25.1
0.27
Foxp3+ of HH7-2tg (%)

Figure 4.7 MLN are critical for Treg differentiation but not IL-10 production by HH7-2tg

Sorted naive HH7-2tg T cells were adoptively transferred into *H.hepaticus* colonised WT C57BL/6 and Lta^{tm1Dch} hosts. Mice were sacrificed at 11 days post cell transfer and the fate of HH7-2tg T cells was analysed by flow cytometry in the gut tissue.

- **a.** Representative flow cytometry plot of HH7-2tg in tissue of WT and Lta^{tm1Dch} hosts, and donor HH7-2tg and host absolute cell counts.
- **b.** Representative flow cytometry plot and absolute cell count of IL-10^{+} within HH7-2tg T cells in tissue.
- **c.** Proportion of IL-10^{+} among HH7-2tg Tregs and total HH7-2tg in tissue of WT and Lta^{tm1Dch} hosts.
- **d.** Representative flow cytometry plot and proportion of Foxp3 expression among HH7-2tg in tissue of WT and Lta^{tm1Dch} hosts.

Each point represents a single mouse and bars represents mean ± SEM.

Data represents results from a single experiment (n = 4 in the WT group, n = 3 in the Lta^{tm1Dch} group). Statistical significance was determined using a two-tailed unpaired t test. Differences were considered statistically significant when $p \leq 0.05$. Significance is indicated as following: * $p \leq 0.05$,** $p \leq 0.01$,***$p \leq 0.001$,****$p \leq 0.0001$.

4.3 Discussion

In chapter 3, we characterised the distribution and cellular composition of SILTs in the steady state mouse caecum and colon. Existing literature suggests SILTs may act as local tissue sites of adaptive immunity. Intestinal colonisation of wild type C57BL/6 mice by the pathobiont *H.hepaticus* induces tolerance however it is currently unclear where this regulatory response occurs within the gut. We hypothesised signals within SILTs play a major contributory role to the activation and maintenance of Treg phenotype and function in response to *H.hepaticus*. We studied this by tracking the differentiation of antigen specific HH7-2tg T cells to *H.hepaticus* within different intestinal tissue and lymphoid compartments.

We show firstly HH7-2tg T cells adapt to tissue and lymphoid environments in unique ways, and secondly, interactions in the MLN are critical in priming Tregs in response to *H.hepaticus.* We discuss these two main findings in detail below.

HH7-2tg predominately adopt a Treg phenotype in the tissue versus Tfh in secondary lymphoid structures (MLN, caecal patch and OLS). These different differentiation profiles occur despite TCR stimulation of HH7-2tg by the same antigen peptide, demonstrating cell extrinsic cues may act to promote this division of labour. Both Tregs and the adaptive humoral immune response play important yet distinct roles in reinforcing intestinal homeostasis and this spatial compartmentalisation may occur as an adaptation of HH7-2tg to their environment. IgA antibodies are very abundant at the steady state mucosal surface, with 80% of gut-resident plasma cells producing IgA [430]. Whilst IgA has been known for some time to coat certain commensal bacteria [431-433], IgG has recently been reported to target pathogenic gram-negative bacterial antigen, such as *Escherichia coli* and

Salmonella [434]. In line with an enriched HH7-2tg Tfh phenotype in secondary lymphoid structures, we show the formation of germinal centres in caecal patch (present in steady state) and OLS in mice colonised with *H.hepaticus*. Small lymphoid aggregates do not form germinal centres in either steady state or during *H.hepaticus* colonisation, demonstrating their structural and functional immaturity as compared to OLS.

The functional relevance and mechanisms of *H.hepaticus* coating by IgA and/or IgG is currently under investigation, and results from our data suggests *H.hepaticus*– specific Tfh cells may provide help to B cells within MLN, caecal patch and OLS germinal centres for the production of a protective Ig response against a pathobiont. Further work would aim to clarify this antigen specific Tfh and IgA/IgG relationship in the context of *H.hepaticus* colonisation. Measuring *H.hepaticus* – specific coating in an unbiased manner using IgA-SEQ [161] in the HH7-2tg adoptive transfer hosts would confirm a gut associated IgA or IgG humoral response to *H.hepaticus* in this model. Furthermore, studying the B cell response within OLS in terms of plasma cell markers such as CD38 and CD138, and Ig markers (IgD, IgA, IgG) will provide a further understanding of the adaptive humoral response within SILTs during *H.hepaticus* colonisation. To investigate how the B cell response to *H.hepaticus* may contribute to the maintenance of gut homeostasis, Bcl6 knock out mice that fail to develop germinal centres [435] can be used interrogate the effects of IgA/IgG coating of H.hepaticus. Of greater interest, the lymphotoxin system is critically required for lymphoid development, with lymph nodes developing *in utero* whilst SILTs form postnatally in response to microbial stimuli (reviewed in [436]). As such, blocking of this pathway using the lymphotoxin-beta receptor-immunoglobulin (LTbetaR-Ig) fusion protein ([437] and reviewed in [438]) in Bcl6 knock out mice soon after birth can be used

to study the relative contributions of germinal centre formation and the humoral response in MLN and Peyer's patches versus SILTs.

In stark contrast to lymphoid structures, interactions in the tissue drive a strong differentiation of HH7-2tg towards peripherally-induced Rorγt^{+} Tregs. Evidence suggests the microbiota plays a major role in shaping the intestinal Treg pool. Tregs isolated from SPF mice exhibiting enhanced suppressor functions than those derived from germ free mice, and earlier work showing *H.hepaticus* promoting tolerogenic Treg function [56]. However, it still remains undefined what signals specifically operate within tissue, but not lymphoid sites that drive tissue-associated Treg differentiation in response to a pathobiont. Additional studies to characterise tissue-specific cytokine signals, such as IL-2 and TGFβ [439], or specialised CD103^{+} dendritic cell subsets [76] that promote Treg differentiation would be informative. The immunosuppressive IL-10 cytokine is an important effector molecule produced by Tregs to enhance intestinal homeostasis in response to the microbiota, with IL-10$^{-/-}$ mice particularly susceptible to inflammation driven by *H.hepaticus* [53]. Numerous studies have confirmed the critical importance of microbial antigens from both commensal, pathobiont and pathogenic sources triggering IL-10 production (reviewed in [440]), and a previous study using an IL-10^{GFP} reporter mouse found IL-10 expression to be inducible by anti-CD3 and strongly expressed by CD4^{+} T cells of the colon lamina propria [441]. However, it is not known from that study where precisely IL-10 production occurs in the context of the separate tissue versus SILT compartments. Our data indicates IL-10 expression by HH7-2tg T cells in response to *H.hepaticus* is most abundant in the tissue, and not within the caecal patch and OLS sites. IL-10 is known to act on a range of both myeloid and lymphoid cells types, including macrophages, dendritic cells, neutrophils and B and T cells (reviewed in [442]).

Importantly, intestinal macrophages that failed to sense IL-10 due to an IL-10R signalling defect resulted in the development of a spontaneous ulcerative colitis like gut inflammation [443]. This study therefore highlights the critical role of IL-10 signalling into intestinal macrophages as a regulatory pathway maintaining gut homeostasis. Our data may link into this earlier finding, and suggest IL-10 signalling in particular to tissue-resident macrophages may be a vital pathway that prevents inflammation in response to a pathobiont. Finally, whereas Tregs represent a continually present population in the gut, the pathways that promote IL-10 production are still under investigation. IL-27 signalling can induce IL-10 expression in CD4 T cells by upregulating c-Maf and IL-21 which acts as a growth factor for IL-10^+ T cells [444, 445]. Comparing the expression of IL-27 within different tissue and SILT niches would provide further information of the signalling cues that drive IL-10 production in certain compartments.

Lymphatic trafficking of lymphocytes and dendritic cells to the main draining lymph of the gut, the mesenteric lymph nodes, has traditionally been viewed as the central process for co-ordinating the intestinal adaptive immune response to foreign antigens. Earlier studies have highlighted tolerance to foreign ingested food antigens is induced almost exclusively in the MLN, occurring after the migration of food peptide-loaded dendritic cells from the gut mucosa [446]. Furthermore, a study showed a critical link between dendritic cells that traffic from the gut epithelium and Peyer's patches to the mesenteric lymph nodes that promote T cell tolerance to foreign ingested antigens [447]. In mice lacking mesenteric lymph nodes, oral tolerance failed to be induced [448]. With regard to the microbiota, live commensal bacteria are highly immunogenic and healthy individuals

have adapted to develop locally tolerant responses in the gut, whilst remaining readily responsive to any systemic invasion by such microbes. Mesenteric lymph nodes have been shown to be a key player in this immune segregation, acting as a 'firewall' to restrict distal travel of microbe-laden dendritic cells penetrating the thoracic duct and entering the circulation to induce systemic tolerance [449]. It is therefore clear dendritic cells in the MLN play a major role in priming Tregs, although it remains to be established whether antigen presenting cells in the tissue, and indeed in the tissue-associated SILTs can also contribute to Treg priming and activation. Data from our time-course experiment show accumulation of transferred HH7-2tg T cells at secondary lymphoid structures one week prior to their expansion within tissue sites, however whether T cells home to the MLN before the gut tissue remains unknown. Photoactivation marking with subsequent tracking and detection of MLN HH7-2tg T cells in the gut tissue would definitively show homing of T cells to the gut tissue and/or SILTs following initial transit through the MLN. Analysis of HH7-2tg T cells soon after they enter the gut showed 60% had already differentiated into Tregs, suggesting priming in MLNs if these T cells had previously migrated from there. However, it does not exclude the possibility that further priming can occur through interactions with antigen presenting cells in the lamina propria tissue and/or SILTs to maintain the enriched Treg pool in the gut tissue. Although the Nur77^{GFP} reporter mouse is a useful tool to distinguish antigen stimulated TCR signalling from general activation in response to an inflammatory milieu [422], it does not provide information on whether the TCR stimulation results in priming of naïve T cells or the continued TCR signalling into already primed Tregs. Therefore our data showing the highest Nur77^{GFP} MFI in the tissue compared to MLN only indicates the strength of TCR signalling is highest in tissue, but does not inform us of where priming occurs. Finally, we were surprised to detect HH7-2tg within gut tissue of Lta^{tm1Dch} hosts as homing of effector T

cells to the gut occurs via $\alpha_4\beta_7$ and CCR9 homing receptors, the expression of which is normally upregulated within MLNs (reviewed in [450]). The presence of HH7-2tg in gut tissue of Lta^{tm1Dch} mice, albeit at a lower frequency of total CD4 T cells compared to WT hosts (2.15% versus 1.16%) indicate the upregulation of $\alpha_4\beta_7$ and CCR9 expression can occur outside of MLN, possibly within small lymphoid aggregates if present in Lta^{tm1Dch} hosts.

The study of HH7-2tg T cell behaviour in Lta^{tm1Dch} hosts shown in this chapter is preliminary data that needs to be confirmed and further characterised in future experiments. In particular, the finding that T cells in Lta^{tm1Dch} hosts do not differentiate into Tregs, but maintains expression of IL-10 by non-Treg HH7-2tg T cells at approximately a third of the level produced by HH7-2tg transferred into wild type hosts is of interest. Seminal studies in the early 1990's showed mice fully deficient in IL-10 ($IL10^{-/-}$) developed a spontaneous inflammation of the colon [40]. Such inflammatory responses within $IL10^{-/-}$ hosts were characterised by a Th1 cytokine profile [53, 54], with recent studies confirming the integral role of IL-10 cytokine using WT mice treated with an anti-IL10 receptor antibody (anti-IL-10R) developing a colitis driven by IFN-γ and IL-17 cytokines [22]. Furthermore, IL-10 secretion by Tregs is particularly important in regulating immune responses to antigen at barrier sites, with knock out of IL-10 in $Foxp3^{+}$ Tregs ($IL\text{-}10^{fl/fl}$ × Foxp3-cre) developing spontaneous enterocolitis [266]. It is therefore clear some IL-10 production is needed at barrier sites to maintain homeostasis, although it is unknown exactly how much is enough to restrain effector Th1/Th17 responses. Whether the 20% of HH7-2tg T cell production of IL-10 in Lta^{tm1Dch} hosts versus 60% in WT hosts represents adequate regulatory function will be assessed in future studies through histological scoring of colitis at sacrifice, and a more detailed study of the activation and

proliferation potential of effector T cells including their expression of CD62L, CD44 and Ki-67. Overall, it is possible distinct dendritic cell signals operate within MLN but not tissue sites, that prime the induction of Tregs, whereas shared signals are present in both MLN and tissue that induce the expression of IL-10. Single cell sequencing of dendritic cell subsets within these different lymphoid versus tissue compartments may further our knowledge in the compartmentalised adaptation of T cell immunity.

Furthermore, despite confirming the lack of MLN, caecal patch and OLS in Lta^{tm1Dch} hosts by visual inspection, it is still unclear whether such colons contain the small microscopic lymphoid aggregates. Although two studies reported a lack of cryptopatches and ILFs in steady state Lta^{tm1Dch} hosts, SILTs are known to be induced by the presence of bacterial antigens [103, 375], and it therefore remains unestablished whether *H.hepaticus* colonisation in our study induces the formation of lymphoid aggregates within Lta^{tm1Dch} hosts. Future experiments would therefore be to cross the Lta^{tm1Dch} to the dsRedhCD2 T cell reporter [451] to enable visual confirmation of either the presence or absence of small lymphoid aggregates under brightfield microscopy. If present, lymphoid aggregates in this setting may support local TCR signaling and the production of a limited level of IL-10 by HH7-2tg non-Tregs. The presence of lymphoid aggregates in this experiment would also indicate secondary lymphoid structures such as MLN are critically required for priming Tregs, and this role cannot be redirected to SILTs. Although clear structural differences exist between lymph nodes and SILTs, it remains undefined whether SILTs can prime Tregs and if and how this differs to priming in lymph nodes. Blocking of the lymphotoxin system using the lymphotoxin-beta receptor-immunoglobulin (LTbetaR-Ig) fusion protein soon after birth in Lta^{tm1Dch} and wild type hosts could be used to study the effects of HH7-2tg Tregs priming in hosts with exclusive deficiency in secondary lymph nodes or SILTs.

Finally, as Lta^{tm1Dch} lack all MLN, caecal patches and OLS, it is not possible to ascertain the contributory role of these separate secondary lymphoid structures for the priming of Tregs. We showed caecal patches and OLS to exhibit strong structural organisation with abundant $MHCII^{+}$ cells and distinct B and T cell zones similar to lymph nodes, suggesting they may have the ability to prime naïve T cells in place of MLN. Characterising the presence of organisation of the vasculature, in particular the high endothelial venule (HEV) network, and lymphatic draining of OLS and caecal patches that facilitate entry and exit of antigen presenting cells and T cells for priming in lymph nodes (reviewed in [452, 453]) would provide further evidence of their capabilities to support dendritic cell-T cell interactions.

Altogether, Tregs and their production of IL-10 forms a critical regulatory mechanism for the maintenance of gut homeostasis in response to pathobionts. Our data highlight the tissue as a distinct structure supporting this pathway and we explore in chapter 5 the interactions within the tissue micro-niches that may promote Treg activation and function.

Chapter 5. The role of lymphoid aggregates in modulating the T cell response to pathobionts

5.1 Introduction

Our results in chapter 4 highlighted a distinct spatial compartmentalisation segregating the unique *H.hepaticus*-reactive T cell responses occurring in the secondary lymphoid structures and the tissue of the gut. We identified in chapter 3 the presence of hundreds of small lymphoid aggregates present within the caecum and proximal colon lamina propria, which coincidently form the two major sites of *H.hepaticus* colonisation. The data prompts further study of the *in situ* tissue micro-environments, namely the small lymphoid aggregates and lamina propria tissue to understand how these micro-niches in the gut govern Treg activation and function.

Such small lymphoid aggregates likely include a spectrum of cryptopatches and less mature ILF. Lymphoid tissue inducer (LTi) cells play a central role in gut -associated lymphoid tissue development. They were originally identified in secondary lymph nodes, with secondary lymphoid structures known to form in the sterile environment of the foetus [94]. Following birth, the gut is colonised by billions of commensal bacteria, coinciding with the clustering of hundreds of lymphoid -tissue inducer (LTi) cells between the crypts of the lamina propria. This process initiates the formation of cytptopatches, which are found in their thousands in the murine gut (reviewed in [454]). They contain dendritic cells, common lymphoid progenitor cells (Lin^{-} $cKit^{+}$ $IL\text{-}7Ra^{+}$) and LTi-like cells [380]. Of

interest, cryptopatches are found in both RAG-deficient competent hosts, indicating the genetically determined innate functions of LTi cells [455]. Although extensively described in the murine intestine, cryptopatches have not been found in humans, although clusters of CCR6 positive LTi cells and cyptopatch-like aggregates have been identified in the human gut [456].

In contrast, ILFs have been extensively described in both murine and human small and large intestine [348], and are mainly composed of B cells, surrounded by dendritic cells, LTi/LTi-like cells and few T cells [100, 457]. ILF containing B cells preferentially class switch to IgA producing plasma cells, required to target commensal and pathogenic intestinal bacteria to maintain gut health [458]. ILFs are induced to form by the intestinal microbiota, and regress upon antibiotic administration [103, 375, 459]. Although ILFs can be detected throughout the intestine, immature ILFs with few B cells were more frequently found in the proximal colon where the bacterial diversity was low, whereas mature ILFs with a more organised B-cell follicle were most prominent in the distal colon, which is home to a more diverse community of commensals [460]. Furthermore, colonisation of germ-free mice with commensal bacteria leads to a shift in the spectrum of SILTs, with skewing of cryptopatches towards more mature ILFs [103]. Altogether, cryptopatches and ILFs exist on a spectrum, with a shift towards ILF formation driven by distinct members of commensal bacteria. Their abundant presence in the steady state gut indicates they likely play a critical role in intestinal immune responses, although their exact role is currently undefined. It is likely they collectively function within tissue to influence T cell adaptive immune responses to gut commensals.

Supporting evidence for the ability of SILTs to participate in the processing and presentation of microbial antigen is derived from a number of structures found to be associated with ILFs: M cells that transport bacterial antigens from the lumen, and a subepithelial dome that contains $CD11c^+$ DCs [348, 377, 461]. Furthermore, studies show both ILFs and TLSs to harbour $CD11c^+$ dendritic cells in close proximity to B/T lymphocytes, indicating a potential role for local antigen presentation at these sites [462]. Finally, ILFs in humans have been shown to be sites of regional immunity in the gut, with distinct B and T cell zones, associated MAdCAM-1^+ HEVs and a surrounding network of lymphatics allowing the entry and exit of immune cells [377]. These ILFs act as colonic foci for germinal centre priming of B cells, and support the production of IgA [377]. Altogether, it is likely that tissue-associated lymphoid structures play a role in the adaptive immune response to commensal microbes. However, it is currently unclear how this local initiation of the immune response is compartmentalised in the tissue. It is possible the T cell responses display spatial distinction between lymphoid aggregates and lamina propria in a similar manner to Treg adaptation between MLN and gut tissue. Additionally, the compartmentalised tissue versus lymphoid behaviour of T cells in a microbe-reactive manner has not been studied to date.

In this chapter, we aim to understand how lymphoid aggregates support the education of *H.hepaticus*-reactive T cells. We aim to use novel *in vivo* live imaging techniques to interrogate how cellular interactions within lymphoid aggregates differ to those present in the surrounding lamina propria tissue, and what effect this has on T cell receptor stimulation and IL-10 production by *H.hepaticus*-reactive T cells. We hypothesise lymphoid aggregates contribute to the adaptive immune response by providing signals to

tissue resident microbe-reactive T cells that promote their activation and regulatory function.

5.2 Results

5.2.1 Experimental set up of two photon in vivo live imaging

The tissue has been shown to be an important site of independent TCR stimulation and IL-10 production by pathobiont-reactive T cells. We therefore wanted to determine where specifically these cellular interactions occur in the context of lamina propria tissue versus small lymphoid aggregate microenvironments. Due to the high number of $MHCII^{+}$ antigen presenting cells (to include dendritic cells, macrophages and B cells) within lymphoid aggregates, we hypothesised most recently TCR-stimulated $Nur77^{+}$ donor HH7-2tg cells in the gut tissue would be positioned within lymphoid aggregates where they are able to interact with antigen presenting cells. However, antigen presenting cells are also present in the lamina propria, albeit at a much lower density as they are scattered throughout the gut tissue.

To this end, we bred HH7-2tg$Nur77^{GFP}$ to hCD2-DsRed mice (HH7-2tg^{Dsred} $Nur77^{GFP}$). Sorted naive splenic T cells were adoptively transferred from these mice into *H.hepaticus*-colonised WT $Foxp3^{GFP}$ hosts as before, and live imaging was performed at 7 to 8 days post cell transfer (Fig 5.1a). During *in vivo* live imaging, host lymphoid aggregates containing Tregs are labelled as green clusters, whilst transferred HH7-2tg T cells appear red, with co-expression of green $Nur77^{GFP}$ fluorescence upon TCR engagement (Fig 5.1b).

We adapted a previously published multi-photon live imaging technique [463] to study the contribution of tissue intrinsic lymphoid structures in T cell activation and function. *In vivo* live imaging of colon tissue is a novel and challenging technique, particularly when applied to gut tissue [344]. The attainment of reproducible images and time-lapse videos in

the gut is especially challenging due to several factors: peristalsis and breathing movement artefacts during acquisition, light scattering due to overlying collagen and muscle layers, and autofluorescence of macrophages, mucus and faeces.

We optimised and performed *in vivo* live imaging of the caecum tissue as this represents an easily accessible region of gut tissue that encompasses a spectrum of tissue and lymphoid sub-types: caecal patch, lamina propria (LP) tissue and numerous small lymphoid aggregates.

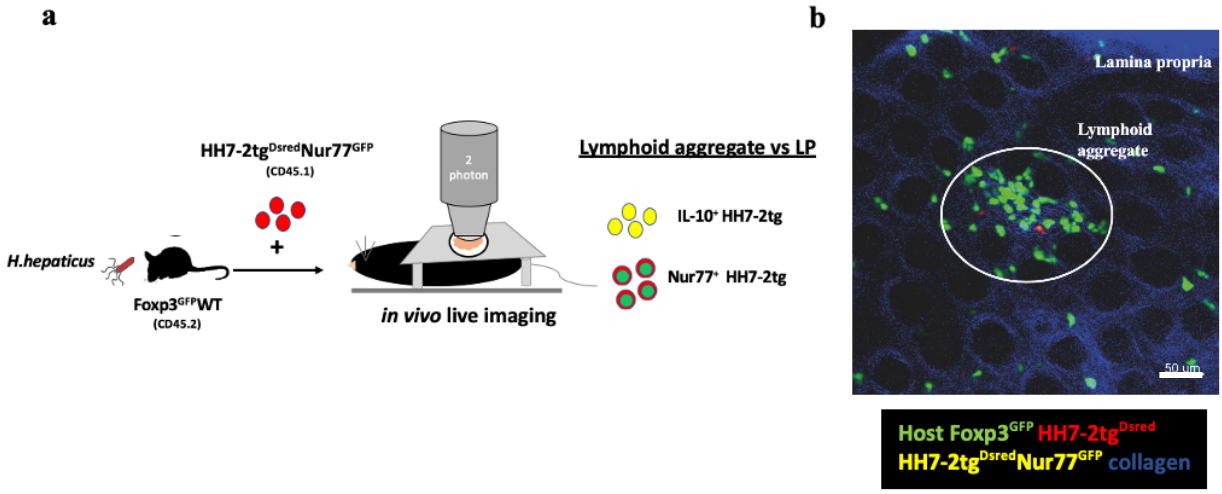


Figure 5.1 Experimental set up of two photon *in vivo* live imaging of caecal lymphoid aggregates

Sorted naive HH7-2tg^{Dsred} Nur77^{GFP} T cells were adoptive transferred into *H.hepaticus*-colonised WT C57BL/6 Foxp3^{GFP} hosts and two–photon *in vivo* live imaging was performed on caecal patch, caecum lamina propria and small lymphoid aggregates at 8 days post cell transfer.

Transferred donor HH7-2tg^{Dsred} T cells appear red, host Foxp3^{GFP} appear green, TCR stimulated donor HH7-2tg^{Dsred} T cells co-express green and red.

a. Experimental set up of two photon *in vivo* live imaging of transfer of naive CD45.1 HH7-2tg T cells into *H.hepaticus*-colonised WT Foxp3^{GFP} hosts.
b. Representative two-photon live imaging view of tissue associated lymphoid aggregate (circled) and surrounding lamina propria.

Original magnification 20X. Scale bar 50µm. Host Foxp3^{GFP} in green, HH7-2tg^{Dsred} in red, HH7-2tg^{Dsred}Nur77^{GFP} in yellow, collagen in blue.

5.2.2 TCR stimulated pathobiont-reactive T cells are evenly distributed within local tissue micro-niches

We aimed to understand where *H.hepaticus*-reactive T cells are positioned and receive TCR stimulation in the context of the separate micro-niches of the caecal patch, lamina propria tissue and the lymphoid aggregates using *in vivo* live imaging of the caecum tissue.

We firstly examined HH7-2tg TCR stimulation within the caecal patch to study how T cell activation at this tissue- associated secondary lymphoid site differs to that of the lamina propria tissue. We found few donor HH7-2tg T cells were Nur77^{GFP} positive within the caecal patch at 8 days post infection (Fig 5.2a). This confirms the previous result obtained by flow cytometry showing few Nur77^{GFP} positive donor T cells in the caecal patch (Fig 4.5a). This indicates few TCR stimulation events at the time of imaging in the caecal patch despite abundant *H.hepaticus* colonisation here [464]. It is likely T cells are being stimulated here, but it may have occurred at a timepoint before *in vivo* imaging.

Within the tissue, Nur77^{GFP} positive donor HH7-2tg T cells were present in lymphoid aggregates as hypothesised (Fig 5.2c). To our surprise however, Nur77^{GFP} positive HH7-2tg T cells were also located within the lamina propria and spatially distant from lymphoid aggregates (Fig 5.2b). This suggests likely interactions between HH7-2tg T cells and lamina propria-resident antigen presenting cells, or rapid migration of HH7-2tg out of lymphoid aggregates after receiving TCR stimulation.

Comprehensive imaging of numerous lymphoid aggregates and lamina propria tissue of 6 mice over two independent experiments allowed quantification of the proportion of

Nur77^{GFP} positive among total HH7-2tg donor T cells within these separate tissue micro-niches. Overall, TCR-engaged donor HH7-2tg cells were evenly distributed between lymphoid aggregates and lamina propria (Fig 5.2d).

Finally, we used *in vivo* live imaging to track the movement of such Nur77^{GFP} positive HH7-2tg T cells within gut tissue. We found TCR-engaged *H.hepaticus* -specific T cells to be highly motile, moving throughout lymphoid aggregates and lamina propria. This suggests activated T cells may have wide-ranging effects throughout the tissue (Video 1)

In conclusion, we reveal that contrary to our initial hypothesis, recent TCR-engaged *H.hepaticus*-specific T cells are present throughout the gut tissue, within both small lymphoid aggregates and the lamina propria tissue. However, they are continuously motile throughout the tissue, indicating they could be TCR activated in one location, before migrating to another.

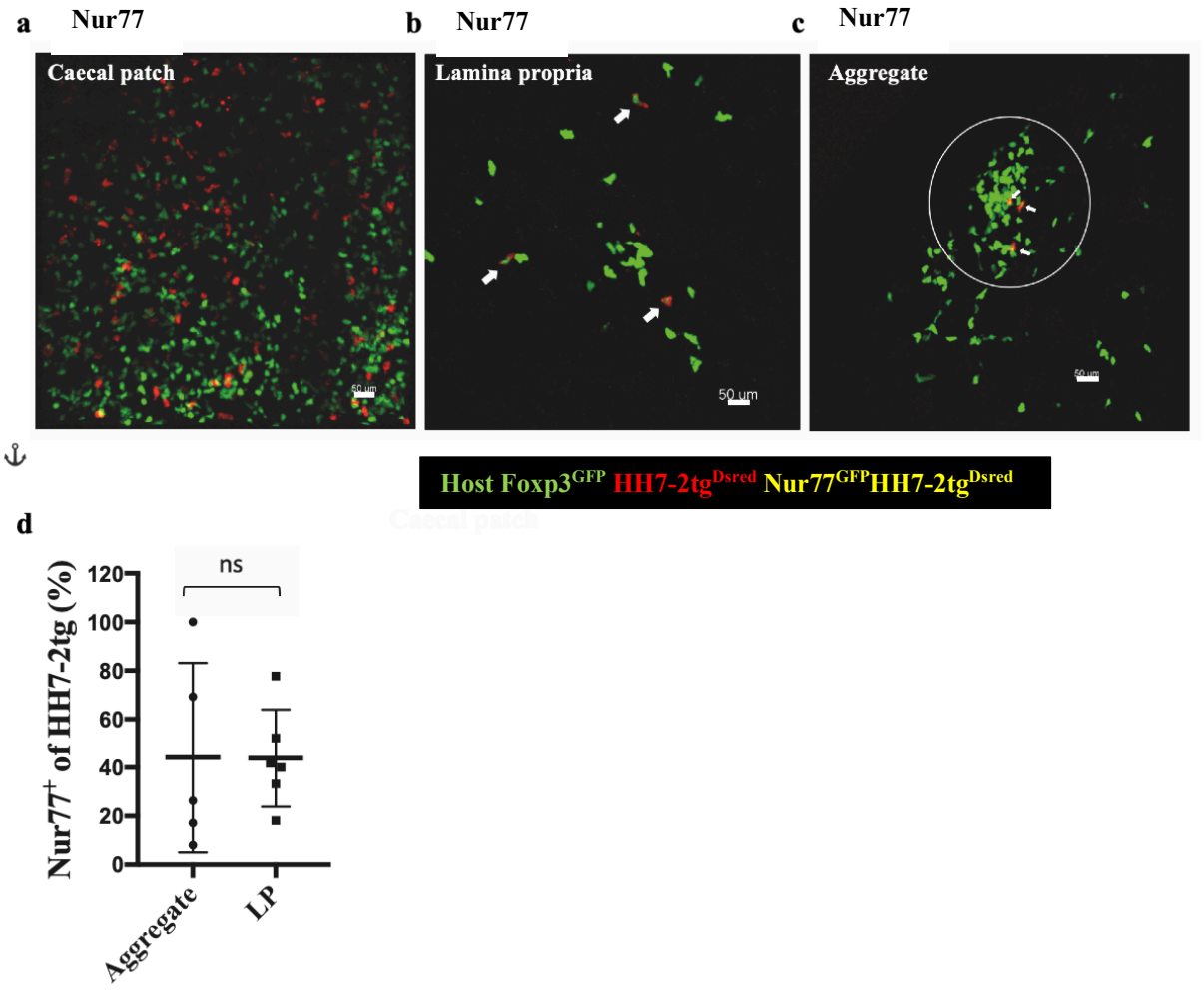

a
Nur77
Caecal patch
b
Nur77
Lamina propria
50 um
c
Nur77
Aggregate
50 um
Host Foxp3GFP HH7-2tgDsred Nur77GFPHH7-2tgDsred
d
ns
Nur77+ of HH7-2tg (%)
120
100
80
60
40
20
0
Aggregate
LP

Figure 5.2 Recent TCR-stimulated HH7-2tg T cells are present throughout lamina propria tissue and lymphoid aggregate micro-niches

Sorted naive HH7-2tg^{Dsred} Nur77^{GFP} T cells were adoptive transferred into *H.hepaticus*-colonised WT C57BL/6 Foxp3^{GFP} hosts and two–photon *in vivo* live imaging was performed to study the presence of Nur77^{GFP} positive TCR stimulation in HH7-2tg T cells within caecal patch, caecum lamina propria and small lymphoid aggregates at 8 days post cell transfer.

Transferred donor HH7-2tg^{Dsred} T cells appear red, host Foxp3^{GFP} appear green, and TCR stimulated donor HH7-2tg^{Dsred} T cells co-express red and green.

a. Representative image of donor HH7-2tg^{Dsred} Nur77^{GFP} cells in the caecal patch.
b. Representative image of donor HH7-2tg^{Dsred} Nur77^{GFP} cells in lamina propria (Nur77^{GFP} positive indicated by white arrowheads).
c. Representative image of donor HH7-2tg^{Dsred} Nur77^{GFP} cells in lymphoid aggregates (Nur77^{GFP} positive indicated by white arrowheads).
d. Frequency of Nur77^{GFP} positive of HH7-2tg within lymphoid aggregates and lamina propria.

Original magnification 20X. Scale bar 50μm. Host Foxp3^{GFP} in green, HH7-2tg^{Dsred} in red, HH7-2tg^{Dsred}Nur77^{GFP} in yellow.

Images are representative of 4 independent experiments (each n = 3).

Each point represents pooled data from a single mouse (each mouse with an average of 6 to 10 images taken of lamina propria/lymphoid aggregate areas). Statistical significance was determined using an unpaired two-tailed t test (d). Differences were considered statistically significant when $p \leq 0.05$. Significance is indicated as follows: * $p \leq 0.05$,** $p \leq 0.01$,***$p \leq 0.001$,****$p \leq 0.0001$.

5.2.3 TCR-stimulated pathobiont-reactive T cells exhibit uniform TCR signal strength between tissue micro-niches.

We show even distribution of Nur77^{GFP} positive T cells within lymphoid aggregates and lamina propria. However, it is still possible differences exist between Nur77^{GFP} positive cells in terms of their TCR signalling strength, as reflected by the GFP MFI. We hypothesise TCR signalling strength is higher for HH7-2tg T cells within lymphoid aggregates due to the higher density of antigen presenting cells here resulting in more chance of frequent TCR stimulation.

Histo-cytometry is an analytical microscopy technique that allows for both spatial visualisation and fluorescent intensity quantification of cell populations of interest directly within the tissue [345]. We used this method to quantify the intensity of GFP fluorescence MFI in Nur77^{GFP} positive HH7-2tg T cells within lymphoid aggregates and lamina propria. However, this analysis is limited by the varying depth of tissue imaged, with HH7-2tg cells deeper within tissue emitting a relatively lower GFP MFI compared to the same GFP signal emitted by cells closer to the tissue surface due to light scattering. As such, the GFP MFI is displayed relative to the Dsred MFI of each HH7-2tg T cell, as the Dsred MFI should be of similar intensity for every T cell and therefore gives an indication of the depth of tissue analysed. Surprisingly, we detected no significant difference between the MFI of Nur77^{GFP} as a readout of the strength of TCR signalling between HH7-2gg T cells within lymphoid aggregate and the lamina propria tissue (Fig 5.3a and b). However, there is a small population of GFP^{high} signal within lymphoid aggregates, which could suggest recent TCR activation of a small number of cells within lymphoid aggregates.

Altogether, these results indicate TCR-engaged *H.hepaticus*-specific T cells are distributed throughout the tissue micro-niches and receive TCR signalling of equal strength. It is likely they receive TCR stimulation from antigen presenting cells, such as dendritic cells, although there remains the possibility different subsets of dendritic cells activate HH7-2tg T cells in different tissue micro-compartments.

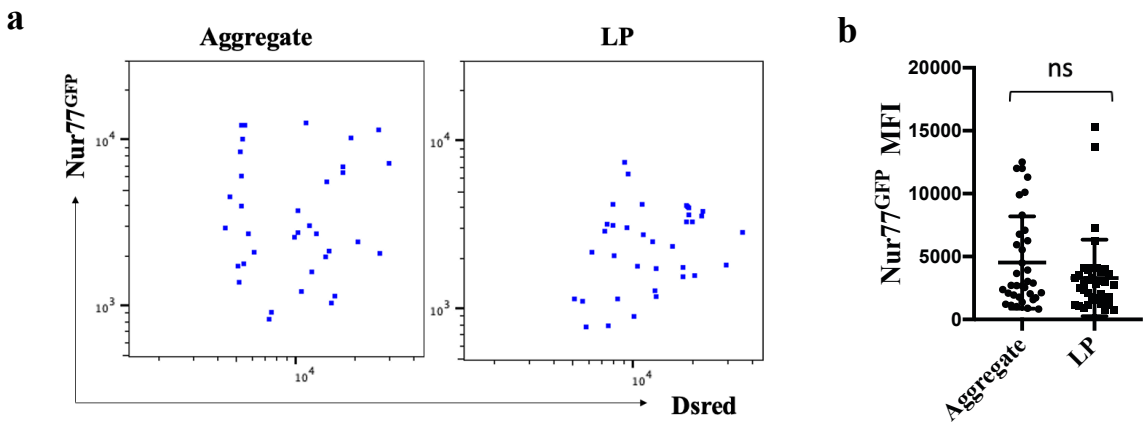


Figure 5.3 Strength of HH7-2tg TCR signal is comparable between lamina propria tissue and lymphoid aggregates

Sorted naive HH7-2tg^{Dsred} Nur77^{GFP} T cells were adoptive transferred into *H.hepaticus*-colonised WT C57BL/6 Foxp3^{GFP} hosts and two–photon *in vivo* live imaging was performed at 8 days post cell transfer to study the GFP MFI of Nur77^{GFP} positive HH7-2tg T cells in caecum lamina propria and lymphoid aggregate micro-niches. Histo-cytometry was used to quantify the strength of TCR stimulation.

a. Histo-cytometry plot of GFP MFI of Nur77^{GFP} positive HH7-2tg T cells in lymphoid aggregates and lamina propria

b. Quantification of GFP MFI of Nur77^{GFP} positive HH7-2tg cells in lymphoid aggregates and lamina propria

Each point represents a single donor HH7-2tg^{Dsred} cell pooled from 4 independent experiments (n = 3 mice each).

Statistical significance was determined using an unpaired two-tailed t test (b). Differences were considered statistically significant when $p \leq 0.05$. Significance is indicated as follows: * $p \leq 0.05$, ** $p \leq 0.01$, ***$p \leq 0.001$, ****$p \leq 0.0001$.

5.2.4 FTY720 treatment does not alter the spatial compartmentalisation of Nur77^{GFP+} HH7-2tg T cells

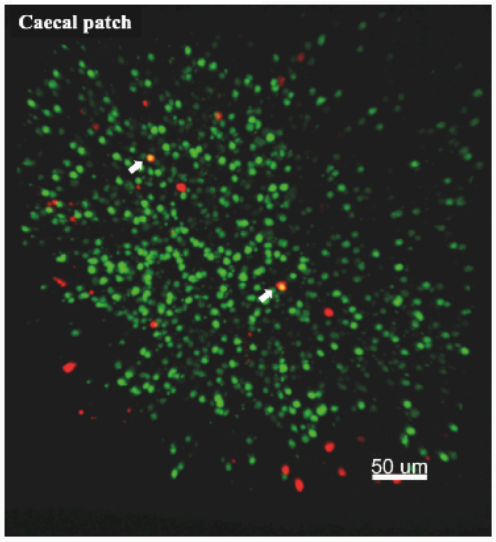
Using FTY720 treated hosts, we previously observed cellular interactions within the tissue induce TCR stimulation and IL-10 production by HH7-2tg T cells (Fig 4.5f and 4.6b). We next asked whether these tissue-specific signals affected the spatial distribution of TCR-engaged donor T cells.

To address this, we adoptively transferred naïve sorted HH7-2tg^{Dsred} Nur77^{GFP} cells as before into *H.hepaticus* colonised hosts. As previously detailed in chapter 4, blocking of lymphocyte egress with daily FTY720 injections was started at day 8 post transfer for 3 days, with *in vivo* live imaging performed at 11 days following cell transfer. Imaging at this timepoint again showed equal distribution of Nur77^{GFP}-positive TCR stimulated HH7-2tg cells within both the lamina propria tissue and lymphoid aggregates, with only a few Nur77^{GFP} positive T cells in the caecal patch (Fig 5.4a-c). These results therefore emphasise the presence of local signals that can drive spatial localisation of pathobiont-reactive T cells. Additionally, within the tissue, FTY720 treatment failed to block lymphocyte egress from lymphoid aggregates. This suggests lymphocytes trafficking out of such lymphoid aggregates are not governed by the S1P gradient controlling lymph node exit.

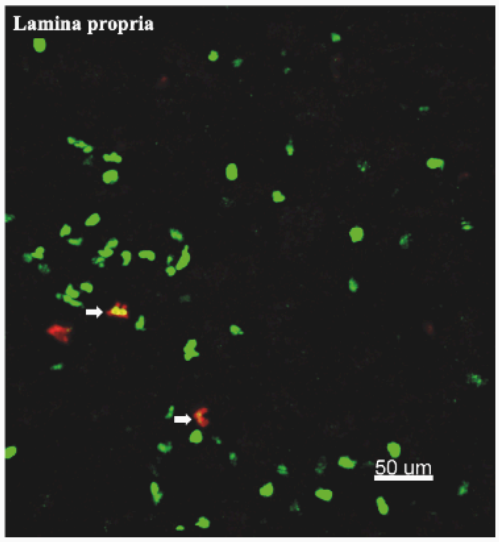
In conclusion, the interactions in the tissue itself can control the spatial compartmentalisation of pathobiont-reactive T cells. Furthermore, lymphocyte exit from tissue-embedded lymphoid aggregates may be independent of the S1P gradient.

Nur77 FTY720

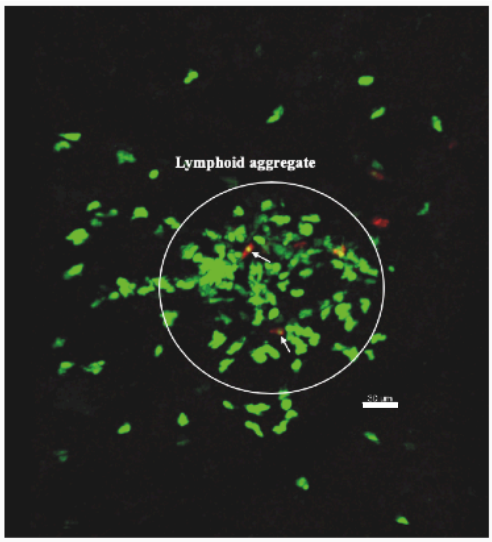
a.



b.



c.



Host Foxp3^{GFP} HH7-2tg^{Dsred} Nur77^{GFP}HH7-2tg^{Dsred}

Figure 5.4 Local tissue-derived signals dictate TCR signalling in HH7-2tg T cells

Sorted naive HH7-2tg^{Dsred} Nur77^{GFP} T cells were adoptive transferred into *H.hepaticus*-colonised WT C57BL/6 Foxp3^{GFP} hosts. Daily i/p FTY720 injections was administered for 3 days starting on day 8 post cell transfer, and two photon *in vivo* live imaging was performed on day 11 post cell transfer to study the presence of Nur77^{GPF} positive TCR stimulated donor HH7-2tg T cells in the caecal patch, lamina propria and lymphoid aggregates.

Transferred donor HH7-2tg^{Dsred} T cells appear red, host Foxp3^{GFP} appear green, TCR stimulated donor HH7-2tg^{Dsred} T cells co-express red and green.

a. Representative image of HH7-2tg^{Dsred} Nur77^{GFP} donor T cells in caecal patch of WT host mice
b. Representative image of HH7-2tg^{Dsred} Nur77^{GFP} donor T cells in the lamina propria of WT host mice
c. Representative image of HH7-2tg^{Dsred} Nur77^{GFP} donor T cells in the lymphoid aggregate of WT host mice

Original magnification 20X. Scale bar 50μm (a-b), 30μm (c). Host Foxp3^{GFP} in green, HH7-2tg^{Dsred} in red, HH7-2tg^{Dsred}Nur77^{GFP} in yellow.

Images are representative of 2 independent experiments (each n = 3).

5.2.5 IL-10^{+} HH7-2tg cells are predominantly positioned in the lamina propria, away from lymphoid aggregates

Having observed equal distribution of TCR-engaged HH7-2tg within tissue micro-niches, we next asked whether IL-10 cytokine production followed a similar distribution pattern. We hypothesised IL-10 production occurs locally in lymphoid aggregates following TCR engagement, as these lymphoid sites would be an optimal location for Tregs to influence other lymphocytes and innate immune cells, such as macrophages.

We therefore bred HH7-2tgIL-10^{GFP} to hCD2-DsRed mice (HH7-2tg^{Dsred} IL-10^{GFP}), and adoptively transferred sorted naïve splenic cells into *H.hepaticus*-colonised Foxp3^{GFP} hosts. As previous, host lymphoid aggregates appear as green clusters, transferred HH7-2tg donor T cells are red, with co-expression of green fluorescence (giving the appearance of a yellow hue) upon IL-10 expression.

In vivo live imaging 8 days post cell transfer confirmed minimal IL-10^{GFP} positive T cells in the caecal patch as previously shown by flow cytometry (Fig 5.5a and Fig 4.6a). Surprisingly, imaging of the tissue showed production of IL-10 by HH7-2tg T cells was highly restricted to the lamina propria, spatially separated from lymphoid aggregates, which had minimal IL-10 expression (Fig 5.5b and c). Quantification of the data as before using 6 mice across 2 independent experiments confirm approximately 70% of HH7-2tg T cells positioned in the lamina propria express IL-10, versus less than 20% in the lymphoid aggregates (Fig 5.5d). Furthermore, *in vivo* live imaging to track the movement of such IL-10^{GFP} positive HH7-2tg T cells within the lamina propria show them to be highly motile

(Video 2). This suggests HH7-2tg T cells are acting to restrain innate and adaptive effector immune responses to *H.hepaticus* within the tissue environment.

Lastly, in spite of a much lower proportion of IL-10^{GFP} positive HH7-2tg T cells within lymphoid aggregates compared to lamina propria, we use histo-cytometry as before to show there is no difference in the GPF MFI between these two compartments (Fig 5.5e). This indicates equal expression of IL-10 protein on a per cell basis at these two sites. Interestingly, there are a number of GFP^{high} HH7-2tg T cells within the lamina propria, suggesting a population of T cells that express higher amounts of IL-10 that are not present in the lymphoid aggregates. However, as previously, the caveat remains that the depth of HH7-2tg T cells imaged within the tissue affects the true GFP MFI, with light scattering within deeper tissue regions masking the true brightness of the GFP signal emitted.

Taken together, our results show that T cells respond to bacterial intestinal infection by expressing IL-10 predominantly within the lamina propria tissue. These IL-10 producers are also motile throughout the lamina propria, potentially contributing to a wider spatial area of intestinal tolerance.

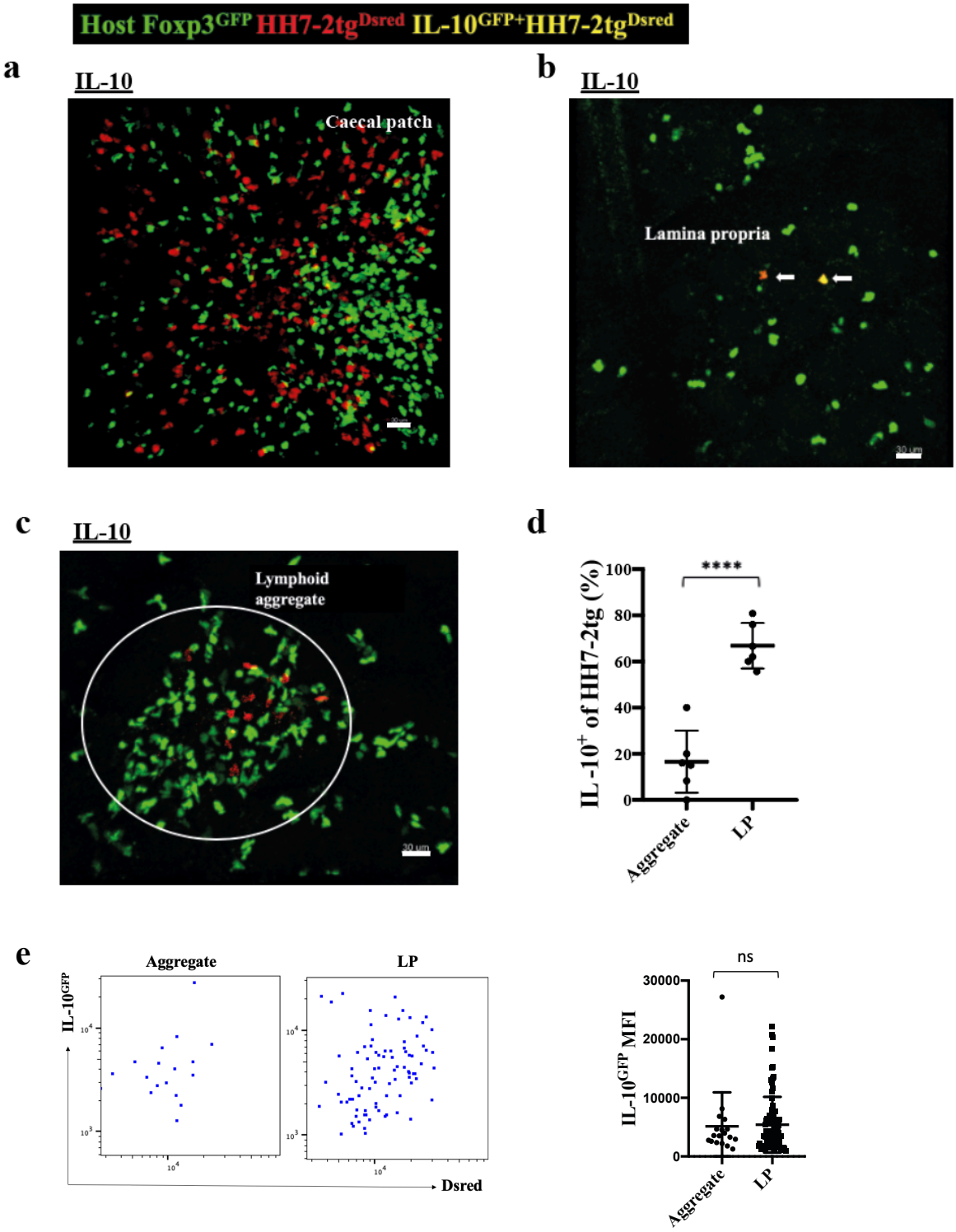

Host Foxp3GFP HH7-2tgDsred IL-10GFP+HH7-2tgDsred
a
IL-10
Caecal patch
b
IL-10
Lamina propria
c
IL-10
Lymphoid aggregate
d
IL-10+ of HH7-2tg (%)
****
Aggregate
LP
e
Aggregate
LP
IL-10GFP
Dsred
ns
IL-10GFP MFI
Aggregate
LP

Figure 5.5 IL-10 producing HH7-2tg cells are predominantly located in the lamina propria tissue, away from lymphoid aggregates

Sorted naive HH7-2tg^{Dsred} IL-10^{GFP} T cells were adoptive transferred into *H.hepaticus*- colonised WT C57BL/6 Foxp3^{GFP} hosts. Two-photon *in vivo* live imaging was performed at 8 days post cell transfer to study the proportion of IL-10^{GFP} positive HH7-2tg T cells in the caecal patch, lamina propria and lymphoid aggregates. Histo-cytometry was used to quantitatively study the IL-10^{GFP} MFI as in the lamina propria and lymphoid aggregates as a read-out of amount of IL-10 production.

Transferred donor HH7-2tg^{Dsred} T cells appear red, host Foxp3^{GFP} appear green, and IL-10 producing donor HH7-2tg^{Dsred} T cells appear yellow.

a. Representative image of donor HH7-2tg^{Dsred} Nur77^{GFP} cells in caecal patch.
b. Representative image of donor HH7-2tg^{Dsred} Nur77^{GFP} cells in lamina propria (IL-10^{GFP} positive indicated by white arrowheads.
c. Representative image of donor HH7-2tg^{Dsred} Nur77^{GFP} cells in lymphoid aggregate (IL-10^{GFP} positive indicated by white arrowheads).
d. Frequency of IL-10^{GFP} positive of HH7-2tg within lymphoid aggregates and lamina propria (each dot represents one mouse).
e. Histo-cytometry plot and quantification of GFP MFI of IL-10^{GFP} positive HH7-2tg cells in lymphoid aggregates and lamina propria.

Original magnification 20X. Scale bar 30μm (a-c). Host Foxp3^{GFP} in green, HH7-2tg^{Dsred} in red, HH7-2tg^{Dsred}IL-10^{GFP} in yellow.

(a-c) Images are representative of 4 independent experiments (each n = 3).

(d) Each point represents pooled data from a single mouse (each mouse with an average of 6 to 10 images taken of lamina propria/lymphoid aggregate areas).

(e) Each point represents a single donor HH7-2tg^{Dsred} cell pooled form 4 independent experiments (n = 3 mice each).

Statistical significance was determined using an unpaired two-tail t test (d and e). Differences were considered statistically significant when $p \leq 0.05$. Significance is indicated as follows: * $p \leq 0.05$, ** $p \leq 0.01$, ***$p \leq 0.001$, ****$p \leq 0.0001$.

5.3 Discussion

In chapter 4 we showed HH7-2tg T cells adapt to the tissue compartment differently to how they behave phenotypically and functionally in secondary lymphoid structures with regards to the acquisition of TCR signalling and IL-10 effector functions. Where precisely this microbe-specific T cell response occurs in the tissue is currently unknown. We showed in chapter 3 the presence of hundreds of small lymphoid aggregates embedded within this tissue compartment, and next hypothesised, similar to the role of secondary lymphoid structures, signalling within tissue-associated lymphoid aggregates contribute to the regional T cell immune response to *H.hepaticus*. Adapting a previously published two-photon live imaging technique [344, 463], we interrogate the *in vivo* behaviour of adoptively transferred HH7-2tg T cells in the tissue micro-compartments.

We show firstly, recent TCR-engaged pathobiont-reactive T cells are present throughout the gut tissue, within both small lymphoid aggregates and the lamina propria tissue, and secondly, IL-10 producing HH7-2tg are predominantly located in the tissue, and not in lymphoid aggregates. We discuss these two main findings in further detail below.

For both findings, we faced particular technical challenges concerning the use of two-photon live imaging. The real-time study and tracking of cellular behaviour *in vivo* within live organisms is a novel imaging technique, and so far, most studies have been performed within lymph nodes [465]. *In vivo* live imaging of tissue is a particularly challenging, especially when applied to gut tissue. The Powrie group have previously optimised *in vivo* live imaging to study the behaviour of innate lymphoid cells within cryptopatches during colitis [344]. The attainment of reproducible images and time-lapse videos in the gut is technically complex due to several factors: peristalsis and breathing movement artefacts of

the mouse during acquisition, light scattering due to overlying collagen and muscle layers, and autofluorescence of macrophages, mucus and faeces. Several solutions can be applied to improve the accuracy of imaging, including correcting for drift and movement artifacts, and using a spectral detector to more accurately identify true fluorophore emission from autofluorescence. In addition, imaging was performed on at least 3 individual mice, and each experiment was repeated in most cases on 4 separate occasions to minimise bias. Furthermore, histo-cytometry to analyse Nur77^{GFP} and IL-10^{GFP} MFI is a useful tool to quantify the TCR signalling strength and level of IL-10 expression by HH7-2tg T cells within different tissue micro-niches. However, the GFP MFI acquired from real-time 3D imaging data is influenced by the depth of tissue imaged - a lower MFI will be recorded for a T cell expressing the same GFP MFI if it is present deeper in the tissue. To correct for this, we represented the GFP MFI data relative to the MFI of Dsred which should be expressed at the same MFI within all HH7-2tg T cells present at the same tissue depth.

Our immunofluorescent static imaging in chapter 3 had identified a high density of MHCII^{+} antigen presenting cells within small lymphoid aggregates. The theory that cryptopatches may play a role in T cell activation is supported by a study showing the antigen-specific priming of T cell responses within tissue-associated lymphoid tissue following the recruitment and proliferation of ovalbumin- specific T cells locally in bronchus-associated lymphoid tissue (BALT) in response to ovalbumin-pulsed DCs administered intratracheally [466]. We thus hypothesised HH7-2tg T cells would acquire TCR signals, and of the highest strength, almost exclusively within lymphoid aggregates. We were therefore surprised to find Nur77GFP^{+} HH7-2tg T cells present in both the lymphoid aggregates and lamina propria, with no difference in TCR signal strength

between the two micro-niches. Two factors may account for this. Firstly, as shown in chapter 4, it takes up to 72 hours for Nur77 GFP fluorescence to decay, and secondly, time-lapse movies show Nur77GFP^{+} T cells to be highly motile throughout the tissue, possibly in an attempt to actively pursue nearby dendritic cells presenting their cognate antigen. These caveats therefore make it impossible to say for certain the precise location of acquisition of TCR signalling – it may be HH7-2tg T cells receive TCR signal in one defined location, for example, in lymphoid aggregates, before rapidly exiting into the lamina propria tissue. In order to clarify whether interactions in lymphoid aggregates are critically required to maintain TCR signalling of HH7-2tg, further work would include blocking their formation using the lymphotoxin-beta receptor-immunoglobulin (LTbetaR-Ig) fusion protein postnatally to study the effects on Nur77^{GFP} presence and distribution in tissue. Finally, it had been shown previously that continuous TCR signalling within already differentiated Tregs, although expendable for maintenance of their Treg phenotype, is critically essential to promote a transcriptional program necessary for their immunosuppressive functions [420]. It was unclear where such continued TCR signalling occurs. Our results show that regardless of whether HH7-2tg T cells receive TCR signalling, either within the lamina propria or lymphoid aggregates, additional TCR stimulation in the gut tissue as a whole is likely critically important for the maintenance of tolerance to pathobionts. Nevertheless, as previously discussed in chapter 4, the detection of Nur77^{GFP} positive cells is a read-out of TCR signal strength, and does not provide information on whether such TCR signals represent priming or maintained activation.

Interestingly, we also show FTY720 treatment failed to block the egress of lymphocytes from lymphoid aggregates, suggesting lymphocyte exit here may not be governed by the

same S1P gradient that controls lymphocyte trafficking within lymph nodes. Studies have highlighted the presence of high endothelial venules (HEVs) supporting colonic patches and tertiary lymphoid organs [361, 467], however the vascular and lymphatic network facilitating the entry and exit of lymphocytes in smaller SILTs such as cryptopatches and ILFs remains unknown. Understanding of the signalling pathway that induces pathobiont-reactive T cell entry and exit into lymphoid aggregates would help the design of SILT targeted therapies to, for example, induce the exit of Tregs into the lamina propria tissue to promote tolerance in response to pathobionts. Further work would therefore involve using imaging to map the presence and distribution of the lymphatic drainage and HEV system supporting the adaptive immune response of lymphoid aggregates. Additionally, studying the local homing receptors present on T cells that promote their migration towards lymphoid aggregates, as well as the selectins and vascular addressins on HEV endothelial cells that drive their entry into lymphoid aggregates would shed light on how pathobiont reactive T cells enter and exit SILTs. Such studies will also inform on how the adaptive T cell immune response to the same pathobiont may be different in lymph nodes compared to SILTs.

Early work has demonstrated infection by *H.hepaticus* induces the production of IL-10 by polyclonal Tregs - essential for the suppression of inflammatory T effectors cells that would otherwise cause colitis [53, 267]. However, it is not currently defined where microbe-reactive Tregs produce IL-10 in the setting of lymphoid aggregates versus the lamina propria tissue micro-niches. As small lymphoid aggregates are enriched for effector T and B lymphocytes in comparison to the surrounding lamina propria, we therefore hypothesised the majority of IL-10 producing HH7-2tg T cells would be found within such

lymphoid aggregates in order to exert maximal regulatory function on T effector cells. To our surprise, we found the expression of IL-10 by HH7-2tg to be highly compartmentalised, and largely confined to the lamina propria niche, away from lymphoid aggregates. Additionally, time-lapse videos tracking HH7-2tg T cells in real time confirm IL-10 producing HH7-2tg cells to be highly motile throughout the lamina propria tissue. It is likely their active movement contributes to the far-reaching tissue regulatory function throughout the tissue compartment. An study investigating the production of IL-10 by antigen-specific Tregs showed IL-10 to be predominately produced in the tissue, and not the draining lymph node [468]. Our data builds on this earlier work and identifies a particular tissue micro-niche that drives the production of IL-10 in response to a microbial antigen.

It is not clear why HH7-2tg T cells that have recently received TCR stimulation are present throughout both the lymphoid aggregates and lamina propria micro-niches, but IL-10 production is primarily limited to the lamina propria. Whether there are inhibitory signals present that inhibit IL-10 production in the lymphoid aggregates or whether IL-10 inducing pathways exist in the lamina propria tissue is currently unknown. Due to the donor HH7-2tg^{Dsred} reporter marking all T cells, it is not possible to ascertain the Th phenotype of the IL-10 producing cells, although we had previously shown approximately 60% of HH7-2tg T cells in the tissue differentiate into Tregs in response to *H.hepaticus*. It is therefore likely the majority of IL-10 producing HH7-2tg are Tregs. However, we also show that of the 40% HH7-2tg T cells that did not adopt a Treg phenotype in the tissue, approximately 20% were primed to a Rorγt^{+} Foxp3^{-} Th17 effector phenotype. It is possible therefore that the HH7-2tg T cells that did not express IL-10 in the lymphoid aggregates could be producing Th17 related cytokines, such as IL-17. Further work would involve

crossing the HH7-2tgDsred to an IL-17A YFP reporter mouse [469] in order to verify the compartmentalised expression of *H.hepaticus*-specific IL-17. The balance between IL-17 versus IL-10 production within different tissue micro-niches may act as a critical control of host immune response to a pathobiont and determine whether homeostasis is maintained. If spatial compartmentalisation of IL-10 versus IL-17 expression exists, this will also inform on the design of targeted therapies that may work to specifically block pro-inflammatory cytokine signals from lymphoid aggregates, whilst preserving tolerogenic IL-10 expression in the lamina propria. We showed in chapter 4 a division of labour between lymphoid and tissue compartments with regards to the differentiation of Tfh versus Treg cells respectively. As such, a similar compartmentalisation could exist in the tissue itself, with Tregs primed in the lamina propria, whilst HH7-2tg T cells adopt a Tfh fate in the lymphoid aggregates. Adoptive transfer of donor cells derived from breeding of HH7-2tg^{Dsred} to Tfh [470] and Treg [471] reporter mice would clarify the differentiation fates within lymphoid aggregate and lamina propria micro-niches.

We next aim to investigate the cellular interactions and signals driving these site-specific differences in HH7-2tg T cell phenotype and function. Enrichment of signals critical for the induction of Tregs and their production of IL-10, such as IL-2 [472], IL-27 [444] and IL-21 [445], may be present within the lamina propria, but deficient in the lymphoid aggregates. Of further interest, we hypothesise distinct subsets of antigen priming cells are resident within lymphoid aggregates and lamina propria niches that present the same *H.hepaticus* peptide, but provide distinct differentiation signals to naïve and/or previously activated T cells. Dendritic cells are the most potent type of antigen presenting cells, with the CD103^{+} tolerogenic dendritic cell subset playing an important role in tolerance to commensal bacteria by inducing Tregs through the production of TGF-β and retinoic acid

[76]. We believe dendritic cells in the lamina propria are likely more tolerogenic in their phenotype or transcriptional profile as compared to those in lymphoid aggregates. We plan to study this using adoptive transfer of naïve HH7-2tg cells into *H.hepaticus* colonised photo-activatable mouse hosts. Such transgenic mice express photoactivatable GFP within all tissues, allowing for the conditional *in situ* labelling of cells within a defined micro-anatomical tissue region upon photo-conversion with light of a particular wavelength [465]. Photo-activation of a defined region around transferred HH7-2tg T cells within lymphoid aggregates with little IL-10 expression as compared to areas around HH7-2tg with high IL-10 expression in the lamina propria should capture antigen presenting cells that may provide distinct signals to differentiating T cells. Subsequent single cell RNA-seq of these spatially distinct antigen presenting cells will be used to investigate transcriptional differences in order to further understand which cues are critical in promoting regulatory IL-10 expression in order to maintain homeostasis in response to colonising pathobionts. We plan to use an unbiased 10x sequencing approach that allows us to investigate both stromal and cellular differences at these locations as the antigen presenting cell in question include a wide range of cell types, and may be of either haematopoietic or non-haematopoietic origin. It is important to note that as HH7-2tg T cells are in constant motion, it is not possible to define the exact cellular interaction and location where they meet their cognate antigen. However, a promising recent study did identify receptor-ligand interactions between dendritic cells and $CD4^+$ T cells in live mice using sortase labelling across immune synapses (LIPSTIC) allowing for the study of dynamic cell-cell interactions *in vivo* [473].

The production of IL-10 in the gut in response to the pathobiont *H.hepaticus* has been shown to be critically important in the maintenance of intestinal homeostasis. Our results

confirm the tissue as the main site of IL-10 production, but of greater significance, we show the tissue is not a structurally homogenous structure. Further studies investigating the influence of cellular interactions and signalling pathways that promote distinct immunological functions within the tissue micro-niches is warranted.

Chapter 6. General discussion

Intestinal health is maintained by a specialised network of innate and adaptive immune cells interacting with one another. Tregs have a key role in the maintenance of homeostasis at barrier sites by restraining inappropriate immune responses to food and microbial-derived antigens. As such, Tregs are pivotal in preventing the development of chronic autoimmune and inflammatory pathologies such as coeliac disease, food allergies and inflammatory bowel disease. Studies have highlighted the existence of a spectrum of lamina propria tissue-associated lymphoid structures, or SILTs, that range from small and immature cryptopatches, to more mature isolated lymphoid follicles and the most developed tertiary lymphoid structures [361]. Recent evidence suggests these microscopic lymphoid structures, similar to the draining mesenteric lymph nodes, could also be sites of antigen presentation, shaping the adaptive immune response locally. The gut is a unique barrier site that contains hundreds of SILTs under steady state conditions, however little is known about how such microscopic lymphoid structures may contribute to the priming of Tregs by microbial antigens to maintain homeostasis. The experiments performed in this thesis were therefore designed to gain a greater understanding of how cellular interactions specifically within SILTs promote the induction and function of intestinal Tregs under both inflammatory and steady state conditions.

Controversy exists surrounding the purpose of SILTs, although studies demonstrate the expansion of SILTs during a strong inflammatory response secondary to intestinal bacterial infection [474]. It is currently unclear whether SILTs function to restore homeostasis following an inflammatory insult, or act as tissue site specific reservoirs for local microbial antigen presentation and priming of effector T cells. A recently discovered

population of lymphocytes that exclusively occupy tissue, termed tissue resident memory T (Trm) cells, have been shown to act as a rapid line of defence eliminating pathogens re-encountered at barrier surfaces. Available evidence suggest they do not re-circulate and remain phenotypically and functionally distinct from their central and effector memory T cell counterparts [475]. An area of active research involves understanding the mechanisms that sustain Trm cells within tissue, and importantly, the local signalling cues promoting their survival, phenotype and function here. Concerning tissue resident Tregs, continued signalling via the TCR has been shown to be a critically important mechanism that maintains Treg suppressor function within secondary lymphoid structures [420]. However, little is known about whether Treg TCR priming occurs at other sites, including within SILTs or in the lamina propria itself, and what consequences this has on Treg function.

We identified the steady state murine colon to contain a heterogenous population of SILTs with classification largely dependent on spatial location. Such SILTs contain a heterogenous population of immune cells, with stromal cells producing the alarmin IL-33 in close spatial proximity to Tregs, suggesting one possible mechanism that may promote tolerance to microbial antigens and repair of damaged tissue.
The experimental data obtained investigating the spatial relationship between an alarmin and Tregs in SILTs using different models of inflammation suggests one potential pathway that could contribute to the tolerance of commensal bacteria.

Additionally, a number of studies have reported the presence of M cells within isolated lymphoid follicles that can transport bacteria from the lumen that are subsequently processed and presented by $CD11c^{+}$ dendritic cells [348, 377]. These provide evidence for the local induction of T cells by microbial peptides within SILTs. In line with this, we

observed the presence of MHC II^+ antigen presenting cells in close contact with T cells and Tregs within SILTs. However, we currently understand little about how lymphoid structures operate to educate T cell differentiation and function in a microbial antigen-specific manner. As intestinal Tregs provide continued surveillance and down-regulation of inappropriate immune responses to microbial antigen even during steady state conditions, we performed adoptive transfer of *H.hepaticus*-specific T cells into wild type mice colonised with *H.hepaticus,* but without the blockade of regulatory IL-10 cytokine. This experimental model allows for the study of Treg function to maintain homeostasis during steady state in response to colonisation by specific pathobionts. *H.hepaticus* is a well-studied model system to understand how the host immune system can engage with a specific commensal bacteria to drive both pro-inflammatory and tolerogenic responses [50]. In particular, it has furthered our knowledge of how Tregs can directly suppress inflammatory responses to intestinal microbiota. Historically, the critical initial steps of T cell induction in response to *H.hepaticus* microbial antigen is challenging to study *in vivo*, but the recently developed *H.hepaticus* TCR transgenic mouse models allow for the detection and tracking of rare populations of antigen-specific T cells. Using this model, we show mesenteric lymph nodes to be critical in Treg induction, but not IL-10 production. Furthermore, microbe-reactive T cells receive additional TCR signals within the tissue. Our data provides insight into this process, supporting SILTs as regional immune sites of T cell priming and confirms the complexity of the tissue and its local micro-environments which play unique roles in supporting tolerance towards pathobionts with signalling in distinct micro-niches driving IL-10 production.

Altogether, these findings provide an exciting and novel perspective to the distinct roles played by lymphoid versus tissue sites at barrier surfaces to promote tolerance to

commensals. The recently developed single-cell RNA sequencing technology has reported transcriptional differences between lymph node and gut tissue associated Tregs [299]. Our results agree unique differences exist at these sites, whilst providing further understanding of the functional relevance of this division of labour that contributes to gut health in the face of potential microbial pathogens. We introduce further insight into the traditionally held view of T cell trafficking and priming within lymph nodes, and show mesenteric lymph nodes are critically important for the induction of microbe-reactive Tregs, but production of regulatory IL-10 by non-Treg $CD4^+$ T cells can still occur following tissue-induced signalling. Further work would investigate using experimental models of colitis whether tissue-induced IL-10 production is adequate to control inflammation induced by pathobionts, without the need for mesenteric lymph nodes and the induction of Tregs. In the last decade, numerous pre- and clinical studies have focussed on investigating the feasibility of Treg-based cellular therapies as a treatment strategy in place of immunosuppressive drugs for autoimmune disease, GVHD and transplant rejection [476]. Such therapies have been met with some success, but challenges remain, including concerns regarding product purity as Tregs have no uniquely identifying surface markers and achieving adequate numbers following ex-vivo expansion. Our findings potentially offer a new avenue for immunosuppressive therapy development and could shift the focus more to exploiting tissue – induced IL-10 expression as a tolerogenic mechanism to inflammatory or autoimmune pathologies driven by microbial dysbiosis.

In summary, we have identified the tissue and its SILT micro-niches to play distinct roles in supporting commensal-reactive T cells through TCR stimulation and functional IL-10 production. Such SILTs exist in its various forms at a number of other barrier sites including the lung and skin where an interface is present between the host and the resident

microbiota. In the skin, the immune pathways that promote Tregs are less well understood compared to the gut and despite a high microbial burden, the predominant Treg population resident in the skin are GATA-3^{+} thymic rather than Rorγt^{+} peripherally induced Tregs [367, 477-479]. Whether regional specialisation of the immune system occurs in the skin, and how skin associated lymphoid tissue can influence resident thymic Treg phenotype and function is currently unclear. Furthermore, SILTs are inducible, formed during certain conditions such as cancer, inflammatory and autoimmune diseases. Interestingly, a dysregulated microbiome, often dominated by certain bacterial species, may contribute to the pathogenesis of many of these disorders. More recently, evidence suggests the intestinal microbiota can influence the efficacy of systemic immunotherapy, and a number of clinical trials are underway [480-482]. Additionally, Tregs have been shown in numerous studies to suppress anti-cancer immune surveillance and responses [483]. How the host immune system participates in promoting the microbial effects of immunotherapy is unknown, but it is likely tissue-resident commensal-reactive Tregs are involved, with interactions in SILTs playing a contributary role in driving their suppressor functions.

References

1. Maloy, K.J. and F. Powrie, *Intestinal homeostasis and its breakdown in inflammatory bowel disease.* Nature, 2011. **474**(7351): p. 298-306.
2. Gill, S.R., et al., *Metagenomic analysis of the human distal gut microbiome.* Science, 2006. **312**(5778): p. 1355-9.
3. Ley, R.E., et al., *Evolution of mammals and their gut microbes.* Science, 2008. **320**(5883): p. 1647-51.
4. Proctor, L.M., *The Human Microbiome Project in 2011 and beyond.* Cell Host Microbe, 2011. **10**(4): p. 287-91.
5. Round, J.L. and S.K. Mazmanian, *The gut microbiota shapes intestinal immune responses during health and disease.* Nature reviews. Immunology, 2009. **9**(5): p. 313-323.
6. Tappenden, K.A. and A.S. Deutsch, *The physiological relevance of the intestinal microbiota--contributions to human health.* J Am Coll Nutr, 2007. **26**(6): p. 679s-83s.
7. Arpaia, N., et al., *Metabolites produced by commensal bacteria promote peripheral regulatory T-cell generation.* Nature, 2013. **504**(7480): p. 451-5.
8. Turnbaugh, P.J., et al., *An obesity-associated gut microbiome with increased capacity for energy harvest.* Nature, 2006. **444**(7122): p. 1027-31.
9. Wen, L., et al., *Innate immunity and intestinal microbiota in the development of Type 1 diabetes.* Nature, 2008. **455**(7216): p. 1109-13.
10. Larson, D., R.A. Kyle, and S.V. Rajkumar, *Prevalence and Monitoring of Oligosecretory Myeloma.* New England Journal of Medicine, 2012. **367**(6): p. 580-581.
11. Pasvol, T.J., et al., *Incidence and prevalence of inflammatory bowel disease in UK primary care: a population-based cohort study.* BMJ Open, 2020. **10**(7): p. e036584.
12. Hendrickson, B.A., R. Gokhale, and J.H. Cho, *Clinical aspects and pathophysiology of inflammatory bowel disease.* Clin Microbiol Rev, 2002. **15**(1): p. 79-94.
13. Abraham, C. and J.H. Cho, *Inflammatory Bowel Disease.* New England Journal of Medicine, 2009. **361**(21): p. 2066-2078.
14. de Souza, H.S.P. and C. Fiocchi, *Immunopathogenesis of IBD: current state of the art.* Nature Reviews Gastroenterology & Hepatology, 2016. **13**(1): p. 13-27.
15. Parronchi, P., et al., *Type 1 T-helper cell predominance and interleukin-12 expression in the gut of patients with Crohn's disease.* The American journal of pathology, 1997. **150**(3): p. 823-832.
16. Inoue, S., et al., *Characterization of cytokine expression in the rectal mucosa of ulcerative colitis: correlation with disease activity.* Am J Gastroenterol, 1999. **94**(9): p. 2441-6.
17. Heller, F., et al., *Interleukin-13 is the key effector Th2 cytokine in ulcerative colitis that affects epithelial tight junctions, apoptosis, and cell restitution.* Gastroenterology, 2005. **129**(2): p. 550-64.
18. Fujino, S., et al., *Increased expression of interleukin 17 in inflammatory bowel disease.* Gut, 2003. **52**(1): p. 65-70.

19. Nielsen, O.H., et al., *Upregulation of Interleukin-12 and -17 in Active Inflammatory Bowel Disease.* Scandinavian Journal of Gastroenterology, 2003. **38**(2): p. 180-185.
20. Andoh, A., et al., *Interleukin-22, a member of the IL-10 subfamily, induces inflammatory responses in colonic subepithelial myofibroblasts.* Gastroenterology, 2005. **129**(3): p. 969-84.
21. Hue, S., et al., *Interleukin-23 drives innate and T cell-mediated intestinal inflammation.* J Exp Med, 2006. **203**(11): p. 2473-83.
22. Kullberg, M.C., et al., *IL-23 plays a key role in Helicobacter hepaticus–induced T cell–dependent colitis.* The Journal of Experimental Medicine, 2006. **203**(11): p. 2485-2494.
23. Powrie, F., et al., *Regulatory interactions between CD45RBhigh and CD45RBlow CD4+ T cells are important for the balance between protective and pathogenic cell-mediated immunity.* J Exp Med, 1994. **179**(2): p. 589-600.
24. Boden, E.K. and S.B. Snapper, *Regulatory T cells in inflammatory bowel disease.* Curr Opin Gastroenterol, 2008. **24**(6): p. 733-41.
25. Hedin, C.R., et al., *Altered intestinal microbiota and blood T cell phenotype are shared by patients with Crohn's disease and their unaffected siblings.* Gut, 2014. **63**(10): p. 1578-86.
26. Mondot, S., et al., *Highlighting new phylogenetic specificities of Crohn's disease microbiota.* Inflamm Bowel Dis, 2011. **17**(1): p. 185-92.
27. Frank, D.N., et al., *Molecular-phylogenetic characterization of microbial community imbalances in human inflammatory bowel diseases.* Proceedings of the National Academy of Sciences of the United States of America, 2007. **104**(34): p. 13780-13785.
28. Strober, W., I.J. Fuss, and R.S. Blumberg, *The immunology of mucosal models of inflammation.* Annu Rev Immunol, 2002. **20**: p. 495-549.
29. Sellon, R.K., et al., *Resident enteric bacteria are necessary for development of spontaneous colitis and immune system activation in interleukin-10-deficient mice.* Infection and immunity, 1998. **66**(11): p. 5224-5231.
30. Garrett, W.S., et al., *Enterobacteriaceae act in concert with the gut microbiota to induce spontaneous and maternally transmitted colitis.* Cell Host Microbe, 2010. **8**(3): p. 292-300.
31. Elinav, E., et al., *NLRP6 inflammasome regulates colonic microbial ecology and risk for colitis.* Cell, 2011. **145**(5): p. 745-57.
32. Brant, S.R., *Update on the heritability of inflammatory bowel disease: The importance of twin studies.* Inflammatory Bowel Diseases, 2011. **17**(1): p. 1-5.
33. Duerr, R.H., et al., *A genome-wide association study identifies IL23R as an inflammatory bowel disease gene.* Science (New York, N.Y.), 2006. **314**(5804): p. 1461-1463.
34. Van Limbergen, J., D.C. Wilson, and J. Satsangi, *The genetics of Crohn's disease.* Annu Rev Genomics Hum Genet, 2009. **10**: p. 89-116.
35. Glocker, E.O., et al., *Inflammatory bowel disease and mutations affecting the interleukin-10 receptor.* N Engl J Med, 2009. **361**(21): p. 2033-45.
36. Targan, S.R., et al., *A Short-Term Study of Chimeric Monoclonal Antibody cA2 to Tumor Necrosis Factor α for Crohn's Disease.* New England Journal of Medicine, 1997. **337**(15): p. 1029-1036.
37. Peyrin-Biroulet, L., *Anti-TNF therapy in inflammatory bowel diseases: A huge review.* Minerva gastroenterologica e dietologica, 2010. **56**: p. 233-43.

38. Lord, J.D., *Promises and paradoxes of regulatory T cells in inflammatory bowel disease.* World J Gastroenterol, 2015. **21**(40): p. 11236-45.
39. Salas, A. and J. Panés, *Regulatory T cells for treatment of Crohn's disease.* Nature Reviews Gastroenterology & Hepatology, 2015. **12**(6): p. 315-316.
40. Kuhn, R., et al., *Interleukin-10-deficient mice develop chronic enterocolitis.* Cell, 1993. **75**(2): p. 263-74.
41. Spencer, S.D., et al., *The orphan receptor CRF2-4 is an essential subunit of the interleukin 10 receptor.* J Exp Med, 1998. **187**(4): p. 571-8.
42. Mombaerts, P., et al., *Spontaneous development of inflammatory bowel disease in T cell receptor mutant mice.* Cell, 1993. **75**(2): p. 274-82.
43. Watanabe, M., et al., *Interleukin 7 transgenic mice develop chronic colitis with decreased interleukin 7 protein accumulation in the colonic mucosa.* J Exp Med, 1998. **187**(3): p. 389-402.
44. Okayasu, I., et al., *A novel method in the induction of reliable experimental acute and chronic ulcerative colitis in mice.* Gastroenterology, 1990. **98**(3): p. 694-702.
45. Qiu, B.S., et al., *The role of CD4+ lymphocytes in the susceptibility of mice to stress-induced reactivation of experimental colitis.* Nat Med, 1999. **5**(10): p. 1178-82.
46. Heller, F., et al., *Oxazolone Colitis, a Th2 Colitis Model Resembling Ulcerative Colitis, Is Mediated by IL-13-Producing NK-T Cells.* Immunity, 2002. **17**(5): p. 629-638.
47. Morrissey, P.J., et al., *CD4+ T cells that express high levels of CD45RB induce wasting disease when transferred into congenic severe combined immunodeficient mice. Disease development is prevented by cotransfer of purified CD4+ T cells.* J Exp Med, 1993. **178**(1): p. 237-44.
48. Powrie, F., et al., *Phenotypically distinct subsets of CD4+ T cells induce or protect from chronic intestinal inflammation in C. B-17 scid mice.* Int Immunol, 1993. **5**(11): p. 1461-71.
49. Koroleva, E.P., et al., *Citrobacter rodentium-induced colitis: A robust model to study mucosal immune responses in the gut.* J Immunol Methods, 2015. **421**: p. 61-72.
50. Fox, J.G., et al., *Helicobacter hepaticus infection in mice: models for understanding lower bowel inflammation and cancer.* Mucosal Immunol, 2011. **4**(1): p. 22-30.
51. Ward, J.M., et al., *Chronic active hepatitis in mice caused by Helicobacter hepaticus.* Am J Pathol, 1994. **145**(4): p. 959-68.
52. Fox, J.G., et al., *Helicobacter hepaticus sp. nov., a microaerophilic bacterium isolated from livers and intestinal mucosal scrapings from mice.* J Clin Microbiol, 1994. **32**(5): p. 1238-45.
53. Kullberg, M.C., et al., *Helicobacter hepaticus Triggers Colitis in Specific-Pathogen-Free Interleukin-10 (IL-10)-Deficient Mice through an IL-12- and Gamma Interferon-Dependent Mechanism.* Infection and Immunity, 1998. **66**(11): p. 5157-5166.
54. Kullberg, M.C., et al., *Helicobacter hepaticus-induced colitis in interleukin-10-deficient mice: cytokine requirements for the induction and maintenance of intestinal inflammation.* Infect Immun, 2001. **69**(7): p. 4232-41.
55. Arnold, I.C., et al., *CD11c(+) monocyte/macrophages promote chronic Helicobacter hepaticus-induced intestinal inflammation through the production of IL-23.* Mucosal Immunol, 2016. **9**(2): p. 352-63.

56. Kullberg, M.C., et al., *Bacteria-triggered CD4(+) T Regulatory Cells Suppress Helicobacter hepaticus–induced Colitis.* The Journal of Experimental Medicine, 2002. **196**(4): p. 505-515.
57. Xu, M., et al., *c-Maf-dependent regulatory T cells mediate immunological tolerance to intestinal microbiota.* bioRxiv, 2017.
58. Perše, M. and A. Cerar, *Dextran Sodium Sulphate Colitis Mouse Model: Traps and Tricks.* Journal of Biomedicine and Biotechnology, 2012. **2012**: p. 13.
59. Wirtz, S., et al., *Chemically induced mouse models of intestinal inflammation.* Nat Protoc, 2007. **2**(3): p. 541-6.
60. Poritz, L.S., et al., *Loss of the tight junction protein ZO-1 in dextran sulfate sodium induced colitis.* J Surg Res, 2007. **140**(1): p. 12-9.
61. Kim, J.J., et al., *Investigating intestinal inflammation in DSS-induced model of IBD.* J Vis Exp, 2012(60).
62. Perše, M. and A. Cerar, *Dextran sodium sulphate colitis mouse model: traps and tricks.* J Biomed Biotechnol, 2012. **2012**: p. 718617.
63. Kiesler, P., I.J. Fuss, and W. Strober, *Experimental Models of Inflammatory Bowel Diseases.* Cell Mol Gastroenterol Hepatol, 2015. **1**(2): p. 154-170.
64. De Fazio, L., et al., *Longitudinal analysis of inflammation and microbiota dynamics in a model of mild chronic dextran sulfate sodium-induced colitis in mice.* World J Gastroenterol, 2014. **20**(8): p. 2051-61.
65. Randhawa, P.K., et al., *A review on chemical-induced inflammatory bowel disease models in rodents.* Korean J Physiol Pharmacol, 2014. **18**(4): p. 279-88.
66. Nagalingam, N.A., J.Y. Kao, and V.B. Young, *Microbial ecology of the murine gut associated with the development of dextran sodium sulfate-induced colitis.* Inflamm Bowel Dis, 2011. **17**(4): p. 917-26.
67. Deplancke, B., et al., *Gastrointestinal and microbial responses to sulfate-supplemented drinking water in mice.* Exp Biol Med (Maywood), 2003. **228**(4): p. 424-33.
68. Håkansson, Å., et al., *Immunological alteration and changes of gut microbiota after dextran sulfate sodium (DSS) administration in mice.* Clin Exp Med, 2015. **15**(1): p. 107-20.
69. Amarante-Mendes, G.P., et al., *Pattern Recognition Receptors and the Host Cell Death Molecular Machinery.* Frontiers in Immunology, 2018. **9**(2379).
70. Shouval, D.S., et al., *Interleukin-10 receptor signaling in innate immune cells regulates mucosal immune tolerance and anti-inflammatory macrophage function.* Immunity, 2014. **40**(5): p. 706-719.
71. Girard-Madoux, M.J.H., et al., *IL-10 control of CD11c+ myeloid cells is essential to maintain immune homeostasis in the small and large intestine.* Oncotarget, 2016. **7**(22): p. 32015-32030.
72. Mora, J.R., et al., *Selective imprinting of gut-homing T cells by Peyer's patch dendritic cells.* Nature, 2003. **424**(6944): p. 88-93.
73. Bogunovic, M., et al., *Origin of the lamina propria dendritic cell network.* Immunity, 2009. **31**(3): p. 513-25.
74. Varol, C., et al., *Intestinal lamina propria dendritic cell subsets have different origin and functions.* Immunity, 2009. **31**(3): p. 502-12.
75. Agace, W.W. and E.K. Persson, *How vitamin A metabolizing dendritic cells are generated in the gut mucosa.* Trends Immunol, 2012. **33**(1): p. 42-8.
76. Coombes, J.L., et al., *A functionally specialized population of mucosal CD103+ DCs induces Foxp3+ regulatory T cells via a TGF-beta and retinoic acid-dependent mechanism.* J Exp Med, 2007. **204**(8): p. 1757-64.

77. Sun, C.-M., et al., *Small intestine lamina propria dendritic cells promote de novo generation of Foxp3 T reg cells via retinoic acid.* Journal of Experimental Medicine, 2007. **204**(8): p. 1775-1785.
78. Chen, W., et al., *The indoleamine 2,3-dioxygenase pathway is essential for human plasmacytoid dendritic cell-induced adaptive T regulatory cell generation.* Journal of immunology (Baltimore, Md. : 1950), 2008. **181**(8): p. 5396-5404.
79. Cerovic, V., et al., *Intestinal macrophages and dendritic cells: what's the difference?* Trends Immunol, 2014. **35**(6): p. 270-7.
80. Schulz, O., et al., *Intestinal CD103+, but not CX3CR1+, antigen sampling cells migrate in lymph and serve classical dendritic cell functions.* J Exp Med, 2009. **206**(13): p. 3101-14.
81. Bain, C.C., et al., *Resident and pro-inflammatory macrophages in the colon represent alternative context-dependent fates of the same Ly6Chi monocyte precursors.* Mucosal immunology, 2013. **6**(3): p. 498-510.
82. Platt, A.M., et al., *An Independent Subset of TLR Expressing CCR2-Dependent Macrophages Promotes Colonic Inflammation.* The Journal of Immunology, 2010. **184**(12): p. 6843-6854.
83. Ueda, Y., et al., *Commensal microbiota induce LPS hyporesponsiveness in colonic macrophages via the production of IL-10.* Int Immunol, 2010. **22**(12): p. 953-62.
84. Rivollier, A., et al., *Inflammation switches the differentiation program of Ly6Chi monocytes from antiinflammatory macrophages to inflammatory dendritic cells in the colon.* The Journal of experimental medicine, 2012. **209**(1): p. 139-155.
85. Murai, M., et al., *Interleukin 10 acts on regulatory T cells to maintain expression of the transcription factor Foxp3 and suppressive function in mice with colitis.* Nat Immunol, 2009. **10**(11): p. 1178-84.
86. Hadis, U., et al., *Intestinal tolerance requires gut homing and expansion of FoxP3+ regulatory T cells in the lamina propria.* Immunity, 2011. **34**(2): p. 237-46.
87. Kang, B., et al., *Commensal microbiota drive the functional diversification of colon macrophages.* Mucosal Immunology, 2020. **13**(2): p. 216-229.
88. Eberl, G., et al., *Innate lymphoid cells: A new paradigm in immunology.* Science, 2015. **348**(6237): p. aaa6566.
89. Spits, H., et al., *Innate lymphoid cells — a proposal for uniform nomenclature.* Nature Reviews Immunology, 2013. **13**(2): p. 145-149.
90. Zhou, W. and G.F. Sonnenberg, *Activation and Suppression of Group 3 Innate Lymphoid Cells in the Gut.* Trends in Immunology, 2020.
91. Sonnenberg, G.F., et al., *Innate Lymphoid Cells Promote Anatomical Containment of Lymphoid-Resident Commensal Bacteria.* Science, 2012. **336**(6086): p. 1321-1325.
92. Hepworth, M.R., et al., *Innate lymphoid cells regulate CD4+ T-cell responses to intestinal commensal bacteria.* Nature, 2013. **498**(7452): p. 113-117.
93. Sonnenberg, G.F., et al., *CD4+ Lymphoid Tissue-Inducer Cells Promote Innate Immunity in the Gut.* Immunity, 2011. **34**(1): p. 122-134.
94. Mebius, R.E., P. Rennert, and I.L. Weissman, *Developing Lymph Nodes Collect CD4+CD3− LTβ+ Cells That Can Differentiate to APC, NK Cells, and Follicular Cells but Not T or B Cells.* Immunity, 1997. **7**(4): p. 493-504.
95. van de Pavert, S.A. and R.E. Mebius, *New insights into the development of lymphoid tissues.* Nat Rev Immunol, 2010. **10**(9): p. 664-74.

96. Cupedo, T., et al., *Human fetal lymphoid tissue–inducer cells are interleukin 17–producing precursors to RORC+ CD127+ natural killer–like cells.* Nature Immunology, 2009. **10**(1): p. 66-74.
97. Cupedo, T., *Human lymph node development: An inflammatory interaction.* Immunology Letters, 2011. **138**(1): p. 4-6.
98. Eberl, G. and D.R. Littman, *The role of the nuclear hormone receptor RORgammat in the development of lymph nodes and Peyer's patches.* Immunol Rev, 2003. **195**: p. 81-90.
99. Neyt, K., et al., *Tertiary lymphoid organs in infection and autoimmunity.* Trends Immunol, 2012. **33**(6): p. 297-305.
100. Tsuji, M., et al., *Requirement for Lymphoid Tissue-Inducer Cells in Isolated Follicle Formation and T Cell-Independent Immunoglobulin A Generation in the Gut.* Immunity, 2008. **29**(2): p. 261-271.
101. Forchielli, M.L. and W. Walker, *The role of gut-associated lymphoid tissues and mucosal defence.* The British journal of nutrition, 2005. **93 Suppl 1**: p. S41-8.
102. Mowat, A.M. and W.W. Agace, *Regional specialization within the intestinal immune system.* Nat Rev Immunol, 2014. **14**(10): p. 667-85.
103. Pabst, O., et al., *Adaptation of solitary intestinal lymphoid tissue in response to microbiota and chemokine receptor CCR7 signaling.* J Immunol, 2006. **177**(10): p. 6824-32.
104. Spahn, T.W., et al., *Induction of colitis in mice deficient of Peyer's patches and mesenteric lymph nodes is associated with increased disease severity and formation of colonic lymphoid patches.* Am J Pathol, 2002. **161**(6): p. 2273-82.
105. McNamee, E.N., et al., *Ectopic lymphoid tissue alters the chemokine gradient, increases lymphocyte retention and exacerbates murine ileitis.* Gut, 2013. **62**(1): p. 53-62.
106. Kaiserling, E., *Newly-formed lymph nodes in the submucosa in chronic inflammatory bowel disease.* Lymphology, 2001. **34**(1): p. 22-9.
107. Carlsen, H.S., et al., *B cell attracting chemokine 1 (CXCL13) and its receptor CXCR5 are expressed in normal and aberrant gut associated lymphoid tissue.* Gut, 2002. **51**(3): p. 364-371.
108. Makiyama, K., M.K. Bennett, and D.P. Jewell, *Endoscopic appearances of the rectal mucosa of patients with Crohn's disease visualised with a magnifying colonoscope.* Gut, 1984. **25**(4): p. 337-40.
109. Liew, F.Y., J.-P. Girard, and H.R. Turnquist, *Interleukin-33 in health and disease.* Nature Reviews Immunology, 2016. **16**(11): p. 676-689.
110. Schmitz, J., et al., *IL-33, an interleukin-1-like cytokine that signals via the IL-1 receptor-related protein ST2 and induces T helper type 2-associated cytokines.* Immunity, 2005. **23**(5): p. 479-90.
111. Xu, D., et al., *Selective expression of a stable cell surface molecule on type 2 but not type 1 helper T cells.* The Journal of experimental medicine, 1998. **187**(5): p. 787-794.
112. Löhning, M., et al., *T1/ST2 is preferentially expressed on murine Th2 cells, independent of interleukin 4, interleukin 5, and interleukin 10, and important for Th2 effector function.* Proceedings of the National Academy of Sciences of the United States of America, 1998. **95**(12): p. 6930-6935.
113. Gajardo Carrasco, T., et al., *Alarmin' Immunologists: IL-33 as a Putative Target for Modulating T Cell-Dependent Responses.* Frontiers in immunology, 2015. **6**: p. 232-232.

114. Hayakawa, H., et al., *Soluble ST2 Blocks Interleukin-33 Signaling in Allergic Airway Inflammation.* Journal of Biological Chemistry, 2007. **282**(36): p. 26369-26380.
115. Lingel, A., et al., *Structure of IL-33 and its interaction with the ST2 and IL-1RAcP receptors--insight into heterotrimeric IL-1 signaling complexes.* Structure (London, England : 1993), 2009. **17**(10): p. 1398-1410.
116. Cayrol, C. and J.P. Girard, *Interleukin-33 (IL-33): A nuclear cytokine from the IL-1 family.* Immunol Rev, 2018. **281**(1): p. 154-168.
117. Baekkevold, E.S., et al., *Molecular characterization of NF-HEV, a nuclear factor preferentially expressed in human high endothelial venules.* Am J Pathol, 2003. **163**(1): p. 69-79.
118. Carriere, V., et al., *IL-33, the IL-1-like cytokine ligand for ST2 receptor, is a chromatin-associated nuclear factor in vivo.* Proceedings of the National Academy of Sciences of the United States of America, 2007. **104**(1): p. 282-287.
119. Ali, S., et al., *The dual function cytokine IL-33 interacts with the transcription factor NF-κB to dampen NF-κB-stimulated gene transcription.* J Immunol, 2011. **187**(4): p. 1609-16.
120. Choi, Y.-S., et al., *Nuclear IL-33 is a transcriptional regulator of NF-κB p65 and induces endothelial cell activation.* Biochemical and Biophysical Research Communications, 2012. **421**(2): p. 305-311.
121. Bessa, J., et al., *Altered subcellular localization of IL-33 leads to non-resolving lethal inflammation.* J Autoimmun, 2014. **55**: p. 33-41.
122. Cayrol, C. and J.-P. Girard, *The IL-1-like cytokine IL-33 is inactivated after maturation by caspase-1.* Proceedings of the National Academy of Sciences of the United States of America, 2009. **106**(22): p. 9021-9026.
123. Lüthi, A.U., et al., *Suppression of Interleukin-33 Bioactivity through Proteolysis by Apoptotic Caspases.* Immunity, 2009. **31**(1): p. 84-98.
124. Talabot-Ayer, D., et al., *Interleukin-33 is biologically active independently of caspase-1 cleavage.* The Journal of biological chemistry, 2009. **284**(29): p. 19420-19426.
125. Lefrançais, E., et al., *Central domain of IL-33 is cleaved by mast cell proteases for potent activation of group-2 innate lymphoid cells.* Proc Natl Acad Sci U S A, 2014. **111**(43): p. 15502-7.
126. Lefrançais, E., et al., *IL-33 is processed into mature bioactive forms by neutrophil elastase and cathepsin G.* Proc Natl Acad Sci U S A, 2012. **109**(5): p. 1673-8.
127. Chen, W.-Y., et al., *Myocardial pressure overload induces systemic inflammation through endothelial cell IL-33.* Proceedings of the National Academy of Sciences of the United States of America, 2015. **112**(23): p. 7249-7254.
128. Kakkar, R., et al., *Interleukin 33 as a mechanically responsive cytokine secreted by living cells.* The Journal of biological chemistry, 2012. **287**(9): p. 6941-6948.
129. Cohen, E.S., et al., *Oxidation of the alarmin IL-33 regulates ST2-dependent inflammation.* Nat Commun, 2015. **6**: p. 8327.
130. Garlanda, C., et al., *Decoys and Regulatory "Receptors" of the IL-1/Toll-Like Receptor Superfamily.* Frontiers in Immunology, 2013. **4**(180).
131. Miller, A.M., *Role of IL-33 in inflammation and disease.* Journal of inflammation (London, England), 2011. **8**(1): p. 22-22.
132. Moffatt, M.F., et al., *A large-scale, consortium-based genomewide association study of asthma.* N Engl J Med, 2010. **363**(13): p. 1211-1221.

133. Coyle, A.J., et al., *Crucial role of the interleukin 1 receptor family member T1/ST2 in T helper cell type 2-mediated lung mucosal immune responses.* J Exp Med, 1999. **190**(7): p. 895-902.
134. Kondo, Y., et al., *Administration of IL-33 induces airway hyperresponsiveness and goblet cell hyperplasia in the lungs in the absence of adaptive immune system.* International immunology, 2008. **20**: p. 791-800.
135. Kurowska-Stolarska, M., et al., *IL-33 induces antigen-specific IL-5+ T cells and promotes allergic-induced airway inflammation independent of IL-4.* J Immunol, 2008. **181**(7): p. 4780-90.
136. Leung, B.P., et al., *A Novel Therapy of Murine Collagen-Induced Arthritis with Soluble T1/ST2.* The Journal of Immunology, 2004. **173**(1): p. 145-150.
137. Sanada, S., et al., *IL-33 and ST2 comprise a critical biomechanically induced and cardioprotective signaling system.* J Clin Invest, 2007. **117**(6): p. 1538-49.
138. Beltran, C.J., et al., *Characterization of the novel ST2/IL-33 system in patients with inflammatory bowel disease.* Inflamm Bowel Dis, 2010. **16**(7): p. 1097-107.
139. Kobori, A., et al., *Interleukin-33 expression is specifically enhanced in inflamed mucosa of ulcerative colitis.* J Gastroenterol, 2010. **45**(10): p. 999-1007.
140. Pastorelli, L., et al., *Epithelial-derived IL-33 and its receptor ST2 are dysregulated in ulcerative colitis and in experimental Th1/Th2 driven enteritis.* Proc Natl Acad Sci U S A, 2010. **107**(17): p. 8017-22.
141. Seidelin, J.B., et al., *IL-33 is upregulated in colonocytes of ulcerative colitis.* Immunol Lett, 2010. **128**(1): p. 80-5.
142. Pushparaj, P.N., et al., *Interleukin-33 exacerbates acute colitis via interleukin-4 in mice.* Immunology, 2013. **140**(1): p. 70-7.
143. Monticelli, L.A., et al., *IL-33 promotes an innate immune pathway of intestinal tissue protection dependent on amphiregulin-EGFR interactions.* Proc Natl Acad Sci U S A, 2015. **112**(34): p. 10762-7.
144. Waddell, A., et al., *IL-33 Signaling Protects from Murine Oxazolone Colitis by Supporting Intestinal Epithelial Function.* Inflamm Bowel Dis, 2015. **21**(12): p. 2737-46.
145. Duan, L., et al., *Interleukin-33 ameliorates experimental colitis through promoting Th2/Foxp3(+) regulatory T-cell responses in mice.* Mol Med, 2012. **18**: p. 753-61.
146. Sedhom, M.A., et al., *Neutralisation of the interleukin-33/ST2 pathway ameliorates experimental colitis through enhancement of mucosal healing in mice.* Gut, 2013. **62**(12): p. 1714-23.
147. Cyster, J.G. and C.D.C. Allen, *B Cell Responses: Cell Interaction Dynamics and Decisions.* Cell, 2019. **177**(3): p. 524-540.
148. Yang, J. and M. Reth, *Receptor Dissociation and B-Cell Activation.* Current topics in microbiology and immunology, 2015. **393**.
149. Liu, W., H. Wang, and C. Xu, *Antigen Receptor Nanoclusters: Small Units with Big Functions.* Trends in Immunology, 2016. **37**(10): p. 680-689.
150. Zubler, R.H., *Naive and memory B cells in T-cell-dependent and T-independent responses.* Springer Seminars in Immunopathology, 2001. **23**(4): p. 405-419.
151. Hong, S., et al., *B Cells Are the Dominant Antigen-Presenting Cells that Activate Naive CD4+ T Cells upon Immunization with a Virus-Derived Nanoparticle Antigen.* Immunity, 2018. **49**(4): p. 695-708.e4.
152. Allen, C.D.C., T. Okada, and J.G. Cyster, *Germinal-Center Organization and Cellular Dynamics.* Immunity, 2007. **27**(2): p. 190-202.

153. Qi, H., W. Kastenmüller, and R.N. Germain, *Spatiotemporal Basis of Innate and Adaptive Immunity in Secondary Lymphoid Tissue.* Annual Review of Cell and Developmental Biology, 2014. **30**(1): p. 141-167.
154. Ise, W., et al., *T Follicular Helper Cell-Germinal Center B Cell Interaction Strength Regulates Entry into Plasma Cell or Recycling Germinal Center Cell Fate.* Immunity, 2018. **48**(4): p. 702-715.e4.
155. Crotty, S., *T follicular helper cell differentiation, function, and roles in disease.* Immunity, 2014. **41**(4): p. 529-542.
156. Vinuesa, C.G., et al., *Follicular Helper T Cells.* Annual Review of Immunology, 2016. **34**(1): p. 335-368.
157. Schroeder, H.W., Jr. and L. Cavacini, *Structure and function of immunoglobulins.* The Journal of allergy and clinical immunology, 2010. **125**(2 Suppl 2): p. S41-S52.
158. Brandtzaeg, P., et al., *The B-cell system of human mucosae and exocrine glands.* Immunological Reviews, 1999. **171**(1): p. 45-87.
159. Mestecky, J. and M.W. Russell, *Specific antibody activity, glycan heterogeneity and polyreactivity contribute to the protective activity of S-IgA at mucosal surfaces.* Immunology letters, 2009. **124**(2): p. 57-62.
160. Hapfelmeier, S., et al., *Reversible microbial colonization of germ-free mice reveals the dynamics of IgA immune responses.* Science, 2010. **328**(5986): p. 1705-9.
161. Palm, N.W., et al., *Immunoglobulin A coating identifies colitogenic bacteria in inflammatory bowel disease.* Cell, 2014. **158**(5): p. 1000-1010.
162. Guy-Grand, D., et al., *Two gut intraepithelial CD8+ lymphocyte populations with different T cell receptors: a role for the gut epithelium in T cell differentiation.* J Exp Med, 1991. **173**(2): p. 471-81.
163. Beagley, K.W., et al., *Differences in intraepithelial lymphocyte T cell subsets isolated from murine small versus large intestine.* J Immunol, 1995. **154**(11): p. 5611-9.
164. van Wijk, F. and H. Cheroutre, *Intestinal T cells: facing the mucosal immune dilemma with synergy and diversity.* Seminars in immunology, 2009. **21**(3): p. 130-138.
165. Cheroutre, H., *Starting at the beginning: new perspectives on the biology of mucosal T cells.* Annu Rev Immunol, 2004. **22**: p. 217-46.
166. Cheroutre, H., F. Lambolez, and D. Mucida, *The light and dark sides of intestinal intraepithelial lymphocytes.* Nature Reviews Immunology, 2011. **11**(7): p. 445-456.
167. Maynard, C.L. and C.T. Weaver, *Intestinal effector T cells in health and disease.* Immunity, 2009. **31**(3): p. 389-400.
168. Kaser, A., S. Zeissig, and R.S. Blumberg, *Inflammatory Bowel Disease.* Annual Review of Immunology, 2010. **28**(1): p. 573-621.
169. Caza, T. and S. Landas, *Functional and Phenotypic Plasticity of CD4(+) T Cell Subsets.* BioMed research international, 2015. **2015**: p. 521957-521957.
170. García-León, M.J., et al., *Dynamic regulation of NOTCH1 activation and Notch ligand expression in human thymus development.* Development, 2018. **145**(16): p. dev165597.
171. Tani-ichi, S., et al., *Interleukin-7 receptor controls development and maturation of late stages of thymocyte subpopulations.* Proceedings of the National Academy of Sciences, 2013. **110**(2): p. 612-617.
172. Germain, R.N., *T-cell development and the CD4–CD8 lineage decision.* Nature Reviews Immunology, 2002. **2**(5): p. 309-322.

173. Mombaerts, P., et al., *RAG-1-deficient mice have no mature B and T lymphocytes.* Cell, 1992. **68**(5): p. 869-77.
174. Shinkai, Y., et al., *Restoration of T cell development in RAG-2-deficient mice by functional TCR transgenes.* Science, 1993. **259**(5096): p. 822-5.
175. Klein, L., et al., *Positive and negative selection of the T cell repertoire: what thymocytes see (and don't see).* Nature Reviews Immunology, 2014. **14**(6): p. 377-391.
176. Lanzavecchia, A., G. Iezzi, and A. Viola, *From TCR engagement to T cell activation: a kinetic view of T cell behavior.* Cell, 1999. **96**(1): p. 1-4.
177. Smith-Garvin, J.E., G.A. Koretzky, and M.S. Jordan, *T cell activation.* Annu Rev Immunol, 2009. **27**: p. 591-619.
178. Appleman, L.J. and V.A. Boussiotis, *T cell anergy and costimulation.* Immunological Reviews, 2003. **192**(1): p. 161-180.
179. Chen, L. and D.B. Flies, *Molecular mechanisms of T cell co-stimulation and co-inhibition.* Nature Reviews Immunology, 2013. **13**(4): p. 227-242.
180. Attanasio, J. and E.J. Wherry, *Costimulatory and Coinhibitory Receptor Pathways in Infectious Disease.* Immunity, 2016. **44**(5): p. 1052-1068.
181. Curtsinger, J.M. and M.F. Mescher, *Inflammatory cytokines as a third signal for T cell activation.* Current opinion in immunology, 2010. **22**(3): p. 333-340.
182. Kaiko, G.E., et al., *Immunological decision-making: how does the immune system decide to mount a helper T-cell response?* Immunology, 2008. **123**(3): p. 326-338.
183. Zanoni, I., et al., *TLR-dependent activation stimuli associated with Th1 responses confer NK cell stimulatory capacity to mouse dendritic cells.* J Immunol, 2005. **175**(1): p. 286-92.
184. LaRosa, D.F., et al., *T cell expression of MyD88 is required for resistance to Toxoplasma gondii.* Proceedings of the National Academy of Sciences of the United States of America, 2008. **105**(10): p. 3855-3860.
185. Macatonia, S.E., et al., *Dendritic cells and macrophages are required for Th1 development of CD4+ T cells from αβ TCR transgenic mice: IL-12 substitution for macrophages to stimulate IFN-γ production is IFN-γ-dependent.* International Immunology, 1993. **5**(9): p. 1119-1128.
186. Seder, R.A., et al., *Interleukin 12 acts directly on CD4+ T cells to enhance priming for interferon gamma production and diminishes interleukin 4 inhibition of such priming.* Proceedings of the National Academy of Sciences, 1993. **90**(21): p. 10188-10192.
187. Powrie, F., et al., *Inhibition of Thl responses prevents inflammatory bowel disease in scid mice reconstituted with CD45RBhi CD4+ T cells.* Immunity, 1994. **1**(7): p. 553-562.
188. Neurath, M.F., et al., *The transcription factor T-bet regulates mucosal T cell activation in experimental colitis and Crohn's disease.* The Journal of experimental medicine, 2002. **195**(9): p. 1129-1143.
189. Luckheeram, R.V., et al., *CD4$^+$T cells: differentiation and functions.* Clin Dev Immunol, 2012. **2012**: p. 925135.
190. Fort, M.M., et al., *IL-25 induces IL-4, IL-5, and IL-13 and Th2-associated pathologies in vivo.* Immunity, 2001. **15**(6): p. 985-95.
191. Bonecchi, R., et al., *Differential expression of chemokine receptors and chemotactic responsiveness of type 1 T helper cells (Th1s) and Th2s.* J Exp Med, 1998. **187**(1): p. 129-34.
192. Reese, T.A., et al., *Chitin induces accumulation in tissue of innate immune cells associated with allergy.* Nature, 2007. **447**(7140): p. 92-96.

193. Evans, C.M. and R.G. Jenner, *Transcription factor interplay in T helper cell differentiation.* Briefings in functional genomics, 2013. **12**(6): p. 499-511.
194. Ohtani, K., et al., *Increased mucosal expression of GATA-3 and STAT-4 in pediatric ulcerative colitis.* Pediatr Int, 2010. **52**(4): p. 584-9.
195. Kakazu, T., et al., *Type 1 T-helper cell predominance in granulomas of Crohn's disease.* Am J Gastroenterol, 1999. **94**(8): p. 2149-55.
196. Camoglio, L., et al., *Altered Expression of Interferon-γ and Interleukin-4 in Inflammatory Bowel Disease.* Inflammatory Bowel Diseases, 1998. **4**(4): p. 285-290.
197. Li, J., et al., *Profiles of Lamina Propria T Helper Cell Subsets Discriminate Between Ulcerative Colitis and Crohn's Disease.* Inflamm Bowel Dis, 2016. **22**(8): p. 1779-92.
198. Harrington, L.E., et al., *Interleukin 17–producing CD4+ effector T cells develop via a lineage distinct from the T helper type 1 and 2 lineages.* Nature Immunology, 2005. **6**(11): p. 1123-1132.
199. Langrish, C.L., et al., *IL-23 drives a pathogenic T cell population that induces autoimmune inflammation.* The Journal of experimental medicine, 2005. **201**(2): p. 233-240.
200. Park, H., et al., *A distinct lineage of CD4 T cells regulates tissue inflammation by producing interleukin 17.* Nature Immunology, 2005. **6**(11): p. 1133-1141.
201. Ivanov, II, et al., *The orphan nuclear receptor RORgammat directs the differentiation program of proinflammatory IL-17+ T helper cells.* Cell, 2006. **126**(6): p. 1121-33.
202. Harris, T.J., et al., *Cutting edge: An in vivo requirement for STAT3 signaling in TH17 development and TH17-dependent autoimmunity.* J Immunol, 2007. **179**(7): p. 4313-7.
203. Ghoreschi, K., et al., *Generation of pathogenic T(H)17 cells in the absence of TGF-β signalling.* Nature, 2010. **467**(7318): p. 967-971.
204. McGeachy, M.J., et al., *The interleukin 23 receptor is essential for the terminal differentiation of interleukin 17-producing effector T helper cells in vivo.* Nat Immunol, 2009. **10**(3): p. 314-24.
205. Martinez, G.J., et al., *Regulation and function of proinflammatory TH17 cells.* Annals of the New York Academy of Sciences, 2008. **1143**: p. 188-211.
206. Zhang, S., *The role of transforming growth factor β in T helper 17 differentiation.* Immunology, 2018. **155**(1): p. 24-35.
207. Bettelli, E., et al., *Reciprocal developmental pathways for the generation of pathogenic effector TH17 and regulatory T cells.* Nature, 2006. **441**(7090): p. 235-8.
208. Mangan, P.R., et al., *Transforming growth factor-β induces development of the TH17 lineage.* Nature, 2006. **441**(7090): p. 231-234.
209. Jostins, L., et al., *Host-microbe interactions have shaped the genetic architecture of inflammatory bowel disease.* Nature, 2012. **491**(7422): p. 119-24.
210. Huang, H., et al., *Fine-mapping inflammatory bowel disease loci to single-variant resolution.* Nature, 2017. **547**(7662): p. 173-178.
211. Leal, R.F., et al., *Identification of inflammatory mediators in patients with Crohn's disease unresponsive to anti-TNFα therapy.* Gut, 2015. **64**(2): p. 233-42.
212. Arijs, I., et al., *Mucosal gene signatures to predict response to infliximab in patients with ulcerative colitis.* Gut, 2009. **58**(12): p. 1612-9.

213. Rismo, R., et al., *Normalization of mucosal cytokine gene expression levels predicts long-term remission after discontinuation of anti-TNF therapy in Crohn's disease.* Scand J Gastroenterol, 2013. **48**(3): p. 311-9.
214. Kobayashi, T., et al., *IL23 differentially regulates the Th1/Th17 balance in ulcerative colitis and Crohn's disease.* Gut, 2008. **57**(12): p. 1682-9.
215. Rovedatti, L., et al., *Differential regulation of interleukin 17 and interferon gamma production in inflammatory bowel disease.* Gut, 2009. **58**(12): p. 1629-36.
216. Hue , S., et al., *Interleukin-23 drives innate and T cell–mediated intestinal inflammation.* Journal of Experimental Medicine, 2006. **203**(11): p. 2473-2483.
217. Uhlig, H.H., et al., *Differential activity of IL-12 and IL-23 in mucosal and systemic innate immune pathology.* Immunity, 2006. **25**(2): p. 309-18.
218. Ahern, P.P., et al., *Interleukin-23 drives intestinal inflammation through direct activity on T cells.* Immunity, 2010. **33**(2): p. 279-88.
219. Leppkes, M., et al., *RORgamma-expressing Th17 cells induce murine chronic intestinal inflammation via redundant effects of IL-17A and IL-17F.* Gastroenterology, 2009. **136**(1): p. 257-67.
220. De Silva, N.S. and U. Klein, *Dynamics of B cells in germinal centres.* Nature reviews. Immunology, 2015. **15**(3): p. 137-148.
221. Stavnezer, J. and C.E. Schrader, *IgH chain class switch recombination: mechanism and regulation.* Journal of immunology (Baltimore, Md. : 1950), 2014. **193**(11): p. 5370-5378.
222. Avery, D.T., et al., *IL-21-induced isotype switching to IgG and IgA by human naive B cells is differentially regulated by IL-4.* J Immunol, 2008. **181**(3): p. 1767-79.
223. Fonseca, V.R., et al., *Human blood T(fr) cells are indicators of ongoing humoral activity not fully licensed with suppressive function.* Sci Immunol, 2017. **2**(14).
224. Fonseca, V.R., et al., *The Ratio of Blood T Follicular Regulatory Cells to T Follicular Helper Cells Marks Ectopic Lymphoid Structure Formation While Activated Follicular Helper T Cells Indicate Disease Activity in Primary Sjögren's Syndrome.* Arthritis Rheumatol, 2018. **70**(5): p. 774-784.
225. Romão, V.C., et al., *T Follicular Regulatory Cells Are Decreased in Patients With Established Treated Rheumatoid Arthritis With Active Disease: Comment on the Article by Liu et al.* Arthritis Rheumatol, 2018. **70**(11): p. 1893-1895.
226. Dhaeze, T., et al., *Circulating Follicular Regulatory T Cells Are Defective in Multiple Sclerosis.* J Immunol, 2015. **195**(3): p. 832-40.
227. Liu, C., et al., *Increased Circulating Follicular Treg Cells Are Associated With Lower Levels of Autoantibodies in Patients With Rheumatoid Arthritis in Stable Remission.* Arthritis Rheumatol, 2018. **70**(5): p. 711-721.
228. Chung, Y., et al., *Follicular regulatory T cells expressing Foxp3 and Bcl-6 suppress germinal center reactions.* Nature Medicine, 2011. **17**(8): p. 983-988.
229. Linterman, M.A., et al., *Foxp3+ follicular regulatory T cells control the germinal center response.* Nature Medicine, 2011. **17**: p. 975.
230. Dominguez-Villar, M. and D.A. Hafler, *Regulatory T cells in autoimmune disease.* Nature Immunology, 2018. **19**(7): p. 665-673.
231. Sakaguchi, S., T. Takahashi, and Y. Nishizuka, *Study on cellular events in postthymectomy autoimmune oophoritis in mice. I. Requirement of Lyt-1 effector cells for oocytes damage after adoptive transfer.* J Exp Med, 1982. **156**(6): p. 1565-76.

232. Asano, M., et al., *Autoimmune disease as a consequence of developmental abnormality of a T cell subpopulation.* The Journal of experimental medicine, 1996. **184**(2): p. 387-396.
233. Powrie, F. and D. Mason, *OX-22high CD4+ T cells induce wasting disease with multiple organ pathology: prevention by the OX-22low subset.* J Exp Med, 1990. **172**(6): p. 1701-8.
234. Sakaguchi, S., et al., *Immunologic self-tolerance maintained by activated T cells expressing IL-2 receptor alpha-chains (CD25). Breakdown of a single mechanism of self-tolerance causes various autoimmune diseases.* J Immunol, 1995. **155**(3): p. 1151-64.
235. Sakaguchi, S., et al., *Regulatory T cells and immune tolerance.* Cell, 2008. **133**(5): p. 775-87.
236. Brunkow, M.E., et al., *Disruption of a new forkhead/winged-helix protein, scurfin, results in the fatal lymphoproliferative disorder of the scurfy mouse.* Nature Genetics, 2001. **27**(1): p. 68-73.
237. Bennett, C.L., et al., *The immune dysregulation, polyendocrinopathy, enteropathy, X-linked syndrome (IPEX) is caused by mutations of FOXP3.* Nature Genetics, 2001. **27**(1): p. 20-21.
238. Wildin, R.S., et al., *X-linked neonatal diabetes mellitus, enteropathy and endocrinopathy syndrome is the human equivalent of mouse scurfy.* Nat Genet, 2001. **27**(1): p. 18-20.
239. Tanoue, T., K. Atarashi, and K. Honda, *Development and maintenance of intestinal regulatory T cells.* Nat Rev Immunol, 2016. **16**(5): p. 295-309.
240. Izcue, A., J.L. Coombes, and F. Powrie, *Regulatory Lymphocytes and Intestinal Inflammation.* Annual Review of Immunology, 2009. **27**(1): p. 313-338.
241. Lathrop, S.K., et al., *Peripheral education of the immune system by colonic commensal microbiota.* Nature, 2011. **478**(7368): p. 250-254.
242. Paust, S., et al., *Engagement of B7 on effector T cells by regulatory T cells prevents autoimmune disease.* Proc Natl Acad Sci U S A, 2004. **101**(28): p. 10398-403.
243. Hogquist, K.A., T.A. Baldwin, and S.C. Jameson, *Central tolerance: learning self-control in the thymus.* Nat Rev Immunol, 2005. **5**(10): p. 772-82.
244. Kronenberg, M. and A. Rudensky, *Regulation of immunity by self-reactive T cells.* Nature, 2005. **435**(7042): p. 598-604.
245. Barnes, M.J. and F. Powrie, *Regulatory T Cells Reinforce Intestinal Homeostasis.* Immunity, 2009. **31**(3): p. 401-411.
246. Li, M.O., S. Sanjabi, and R.A. Flavell, *Transforming growth factor-beta controls development, homeostasis, and tolerance of T cells by regulatory T cell-dependent and -independent mechanisms.* Immunity, 2006. **25**(3): p. 455-71.
247. Atarashi, K., et al., *Treg induction by a rationally selected mixture of Clostridia strains from the human microbiota.* Nature, 2013. **500**(7461): p. 232-6.
248. Benson, M.J., et al., *All-trans retinoic acid mediates enhanced T reg cell growth, differentiation, and gut homing in the face of high levels of co-stimulation.* J Exp Med, 2007. **204**(8): p. 1765-74.
249. Thornton, A.M., et al., *Expression of Helios, an Ikaros transcription factor family member, differentiates thymic-derived from peripherally induced Foxp3+ T regulatory cells.* J Immunol, 2010. **184**(7): p. 3433-41.
250. Yadav, M., et al., *Neuropilin-1 distinguishes natural and inducible regulatory T cells among regulatory T cell subsets in vivo.* J Exp Med, 2012. **209**(10): p. 1713-22, s1-19.

251. Weiss, J.M., et al., *Neuropilin 1 is expressed on thymus-derived natural regulatory T cells, but not mucosa-generated induced Foxp3+ T reg cells.* J Exp Med, 2012. **209**(10): p. 1723-42, s1.
252. Haribhai, D., et al., *A requisite role for induced regulatory T cells in tolerance based on expanding antigen receptor diversity.* Immunity, 2011. **35**(1): p. 109-122.
253. Zheng, Y., et al., *Role of conserved non-coding DNA elements in the Foxp3 gene in regulatory T-cell fate.* Nature, 2010. **463**(7282): p. 808-812.
254. Campbell, C., et al., *Extrathymically Generated Regulatory T Cells Establish a Niche for Intestinal Border-Dwelling Bacteria and Affect Physiologic Metabolite Balance.* Immunity, 2018. **48**(6): p. 1245-1257.e9.
255. Ohnmacht, C., et al., *MUCOSAL IMMUNOLOGY. The microbiota regulates type 2 immunity through RORgammat(+) T cells.* Science, 2015. **349**(6251): p. 989-93.
256. Sefik, E., et al., *Individual intestinal symbionts induce a distinct population of RORγ⁺ regulatory T cells.* Science, 2015. **349**(6251): p. 993-997.
257. Yang, B.H., et al., *Foxp3(+) T cells expressing RORgammat represent a stable regulatory T-cell effector lineage with enhanced suppressive capacity during intestinal inflammation.* Mucosal Immunol, 2016. **9**(2): p. 444-57.
258. Wang, Y., Maureen A. Su, and Yisong Y. Wan, *An Essential Role of the Transcription Factor GATA-3 for the Function of Regulatory T Cells.* Immunity. **35**(3): p. 337-348.
259. Shevach, E.M., *Mechanisms of foxp3+ T regulatory cell-mediated suppression.* Immunity, 2009. **30**(5): p. 636-45.
260. Schmidt, A., N. Oberle, and P.H. Krammer, *Molecular mechanisms of treg-mediated T cell suppression.* Frontiers in immunology, 2012. **3**: p. 51-51.
261. de la Rosa, M., et al., *Interleukin-2 is essential for CD4+CD25+ regulatory T cell function.* Eur J Immunol, 2004. **34**(9): p. 2480-8.
262. Barthlott, T., et al., *CD25+ CD4+ T cells compete with naive CD4+ T cells for IL-2 and exploit it for the induction of IL-10 production.* Int Immunol, 2005. **17**(3): p. 279-88.
263. Kobie, J.J., et al., *T regulatory and primed uncommitted CD4 T cells express CD73, which suppresses effector CD4 T cells by converting 5'-adenosine monophosphate to adenosine.* J Immunol, 2006. **177**(10): p. 6780-6.
264. Deaglio, S., et al., *Adenosine generation catalyzed by CD39 and CD73 expressed on regulatory T cells mediates immune suppression.* J Exp Med, 2007. **204**(6): p. 1257-65.
265. Borsellino, G., et al., *Expression of ectonucleotidase CD39 by Foxp3+ Treg cells: hydrolysis of extracellular ATP and immune suppression.* Blood, 2007. **110**(4): p. 1225-32.
266. Rubtsov, Y.P., et al., *Regulatory T cell-derived interleukin-10 limits inflammation at environmental interfaces.* Immunity, 2008. **28**(4): p. 546-58.
267. Asseman, C., et al., *An Essential Role for Interleukin 10 in the Function of Regulatory T Cells That Inhibit Intestinal Inflammation.* Journal of Experimental Medicine, 1999. **190**(7): p. 995-1004.
268. Uhlig, H.H., et al., *Characterization of Foxp3+CD4+CD25+ and IL-10-secreting CD4+CD25+ T cells during cure of colitis.* J Immunol, 2006. **177**(9): p. 5852-60.
269. McGeachy, M.J., L.A. Stephens, and S.M. Anderton, *Natural recovery and protection from autoimmune encephalomyelitis: contribution of CD4+CD25+ regulatory cells within the central nervous system.* J Immunol, 2005. **175**(5): p. 3025-32.

270. Kamanaka, M., et al., *Memory/effector (CD45RB(lo)) CD4 T cells are controlled directly by IL-10 and cause IL-22-dependent intestinal pathology.* J Exp Med, 2011. **208**(5): p. 1027-40.
271. Huber, S., et al., *Th17 cells express interleukin-10 receptor and are controlled by Foxp3(-) and Foxp3+ regulatory CD4+ T cells in an interleukin-10-dependent manner.* Immunity, 2011. **34**(4): p. 554-65.
272. Chaudhry, A., et al., *Interleukin-10 signaling in regulatory T cells is required for suppression of Th17 cell-mediated inflammation.* Immunity, 2011. **34**(4): p. 566-78.
273. Sojka, D.K. and D.J. Fowell, *Regulatory T cells inhibit acute IFN-γ synthesis without blocking T-helper cell type 1 (Th1) differentiation via a compartmentalized requirement for IL-10.* Proc Natl Acad Sci U S A, 2011. **108**(45): p. 18336-41.
274. Roncarolo, M.G., et al., *Interleukin-10-secreting type 1 regulatory T cells in rodents and humans.* Immunol Rev, 2006. **212**: p. 28-50.
275. Mauri, C. and M.R. Ehrenstein, *The 'short' history of regulatory B cells.* Trends Immunol, 2008. **29**(1): p. 34-40.
276. Kulkarni, A.B. and S. Karlsson, *Transforming growth factor-beta 1 knockout mice. A mutation in one cytokine gene causes a dramatic inflammatory disease.* The American journal of pathology, 1993. **143**(1): p. 3-9.
277. Fahlén, L., et al., *T cells that cannot respond to TGF-beta escape control by CD4(+)CD25(+) regulatory T cells.* J Exp Med, 2005. **201**(5): p. 737-46.
278. Travis, M.A., et al., *Loss of integrin alpha(v)beta8 on dendritic cells causes autoimmunity and colitis in mice.* Nature, 2007. **449**(7160): p. 361-5.
279. Li, M.O., Y.Y. Wan, and R.A. Flavell, *T cell-produced transforming growth factor-beta1 controls T cell tolerance and regulates Th1- and Th17-cell differentiation.* Immunity, 2007. **26**(5): p. 579-91.
280. Collison, L.W., et al., *The inhibitory cytokine IL-35 contributes to regulatory T-cell function.* Nature, 2007. **450**(7169): p. 566-9.
281. Cederbom, L., H. Hall, and F. Ivars, *CD4+CD25+ regulatory T cells down-regulate co-stimulatory molecules on antigen-presenting cells.* European Journal of Immunology, 2000. **30**(6): p. 1538-1543.
282. Read, S., V. Malmström, and F. Powrie, *Cytotoxic T lymphocyte-associated antigen 4 plays an essential role in the function of CD25(+)CD4(+) regulatory cells that control intestinal inflammation.* J Exp Med, 2000. **192**(2): p. 295-302.
283. Wing, K., et al., *CTLA-4 control over Foxp3+ regulatory T cell function.* Science, 2008. **322**(5899): p. 271-5.
284. Grohmann, U., et al., *CTLA-4-Ig regulates tryptophan catabolism in vivo.* Nat Immunol, 2002. **3**(11): p. 1097-101.
285. Munn, D.H., et al., *Inhibition of T cell proliferation by macrophage tryptophan catabolism.* The Journal of experimental medicine, 1999. **189**(9): p. 1363-1372.
286. Belladonna, M.L., et al., *Immunosuppression via tryptophan catabolism: the role of kynurenine pathway enzymes.* Transplantation, 2007. **84**(1 Suppl): p. S17-20.
287. Griseri, T., et al., *OX40 is required for regulatory T cell-mediated control of colitis.* J Exp Med, 2010. **207**(4): p. 699-709.
288. Liang, B., et al., *Regulatory T Cells Inhibit Dendritic Cells by Lymphocyte Activation Gene-3 Engagement of MHC Class II.* The Journal of Immunology, 2008. **180**(9): p. 5916-5926.
289. Totsuka, T., et al., *Regulation of murine chronic colitis by CD4+CD25- programmed death-1+ T cells.* Eur J Immunol, 2005. **35**(6): p. 1773-85.

290. Herman, A.E., et al., *CD4+CD25+ T regulatory cells dependent on ICOS promote regulation of effector cells in the prediabetic lesion.* The Journal of experimental medicine, 2004. **199**(11): p. 1479-1489.
291. Shimizu, J., et al., *Stimulation of CD25(+)CD4(+) regulatory T cells through GITR breaks immunological self-tolerance.* Nat Immunol, 2002. **3**(2): p. 135-42.
292. McHugh, R.S., et al., *CD4(+)CD25(+) immunoregulatory T cells: gene expression analysis reveals a functional role for the glucocorticoid-induced TNF receptor.* Immunity, 2002. **16**(2): p. 311-23.
293. Huang, C.-T., et al., *Role of LAG-3 in Regulatory T Cells.* Immunity, 2004. **21**(4): p. 503-513.
294. Sarris, M., et al., *Neuropilin-1 Expression on Regulatory T Cells Enhances Their Interactions with Dendritic Cells during Antigen Recognition.* Immunity, 2008. **28**(3): p. 402-413.
295. Whibley, N., A. Tucci, and F. Powrie, *Regulatory T cell adaptation in the intestine and skin.* Nat Immunol, 2019. **20**(4): p. 386-396.
296. Panduro, M., C. Benoist, and D. Mathis, *Tissue Tregs.* Annual Review of Immunology, 2016. **34**(1): p. 609-633.
297. Burzyn, D., et al., *A special population of regulatory T cells potentiates muscle repair.* Cell, 2013. **155**(6): p. 1282-95.
298. Kim, S.V., et al., *GPR15-Mediated Homing Controls Immune Homeostasis in the Large Intestine Mucosa.* Science, 2013. **340**(6139): p. 1456-1459.
299. Miragaia, R.J., et al., *Single-Cell Transcriptomics of Regulatory T Cells Reveals Trajectories of Tissue Adaptation.* Immunity, 2019. **50**(2): p. 493-504.e7.
300. Arpaia, N., et al., *A Distinct Function of Regulatory T Cells in Tissue Protection.* Cell, 2015. **162**(5): p. 1078-89.
301. Feuerer, M., et al., *Lean, but not obese, fat is enriched for a unique population of regulatory T cells that affect metabolic parameters.* Nature Medicine, 2009. **15**(8): p. 930-939.
302. Cipolletta, D., et al., *PPAR-γ is a major driver of the accumulation and phenotype of adipose tissue Treg cells.* Nature, 2012. **486**(7404): p. 549-553.
303. Oldenhove, G., et al., *Decrease of Foxp3+ Treg cell number and acquisition of effector cell phenotype during lethal infection.* Immunity, 2009. **31**(5): p. 772-86.
304. Duarte, J.H., et al., *Natural Treg cells spontaneously differentiate into pathogenic helper cells in lymphopenic conditions.* Eur J Immunol, 2009. **39**(4): p. 948-55.
305. Komatsu, N., et al., *Heterogeneity of natural Foxp3+ T cells: a committed regulatory T-cell lineage and an uncommitted minor population retaining plasticity.* Proc Natl Acad Sci U S A, 2009. **106**(6): p. 1903-8.
306. Yurchenko, E., et al., *Inflammation-Driven Reprogramming of CD4+Foxp3+ Regulatory T Cells into Pathogenic Th1/Th17 T Effectors Is Abrogated by mTOR Inhibition in vivo.* PLOS ONE, 2012. **7**(4): p. e35572.
307. Miyao, T., et al., *Plasticity of Foxp3(+) T cells reflects promiscuous Foxp3 expression in conventional T cells but not reprogramming of regulatory T cells.* Immunity, 2012. **36**(2): p. 262-75.
308. Zhou, X., et al., *Instability of the transcription factor Foxp3 leads to the generation of pathogenic memory T cells in vivo.* Nat Immunol, 2009. **10**(9): p. 1000-7.
309. Bailey-Bucktrout, S.L., et al., *Self-antigen-driven activation induces instability of regulatory T cells during an inflammatory autoimmune response.* Immunity, 2013. **39**(5): p. 949-62.

310. Smith, K., K.D. McCoy, and A.J. Macpherson, *Use of axenic animals in studying the adaptation of mammals to their commensal intestinal microbiota.* Semin Immunol, 2007. **19**(2): p. 59-69.
311. Sekirov, I., et al., *Antibiotic-induced perturbations of the intestinal microbiota alter host susceptibility to enteric infection.* Infect Immun, 2008. **76**(10): p. 4726-36.
312. Hill, D.A., et al., *Metagenomic analyses reveal antibiotic-induced temporal and spatial changes in intestinal microbiota with associated alterations in immune cell homeostasis.* Mucosal Immunol, 2010. **3**(2): p. 148-58.
313. Rakoff-Nahoum, S., et al., *Recognition of commensal microflora by toll-like receptors is required for intestinal homeostasis.* Cell, 2004. **118**(2): p. 229-41.
314. Macpherson, A.J. and N.L. Harris, *Interactions between commensal intestinal bacteria and the immune system.* Nature Reviews Immunology, 2004. **4**(6): p. 478-485.
315. Geuking, M.B., et al., *Intestinal bacterial colonization induces mutualistic regulatory T cell responses.* Immunity, 2011. **34**(5): p. 794-806.
316. Ivanov, I.I., et al., *Specific Microbiota Direct the Differentiation of IL-17-Producing T-Helper Cells in the Mucosa of the Small Intestine.* Cell Host & Microbe, 2008. **4**(4): p. 337-349.
317. Atarashi, K., et al., *Induction of colonic regulatory T cells by indigenous Clostridium species.* Science, 2011. **331**(6015): p. 337-41.
318. Min, B., et al., *Gut flora antigens are not important in the maintenance of regulatory T cell heterogeneity and homeostasis.* Eur J Immunol, 2007. **37**(7): p. 1916-23.
319. Kim, K.S., et al., *Dietary antigens limit mucosal immunity by inducing regulatory T cells in the small intestine.* Science, 2016. **351**(6275): p. 858-63.
320. Ivanov, I.I., et al., *Induction of intestinal Th17 cells by segmented filamentous bacteria.* Cell, 2009. **139**(3): p. 485-498.
321. Hedblom, G.A., et al., *Segmented Filamentous Bacteria – Metabolism Meets Immunity.* Frontiers in Microbiology, 2018. **9**(1991).
322. Atarashi, K., et al., *Th17 Cell Induction by Adhesion of Microbes to Intestinal Epithelial Cells.* Cell, 2015. **163**(2): p. 367-380.
323. Tan, T.G., et al., *Identifying species of symbiont bacteria from the human gut that, alone, can induce intestinal Th17 cells in mice.* Proceedings of the National Academy of Sciences, 2016. **113**(50): p. E8141-E8150.
324. Wu, H.-J., et al., *Gut-residing segmented filamentous bacteria drive autoimmune arthritis via T helper 17 cells.* Immunity, 2010. **32**(6): p. 815-827.
325. Horai, R., et al., *Microbiota-Dependent Activation of an Autoreactive T Cell Receptor Provokes Autoimmunity in an Immunologically Privileged Site.* Immunity, 2015. **43**(2): p. 343-53.
326. Routy, B., et al., *Gut microbiome influences efficacy of PD-1–based immunotherapy against epithelial tumors.* Science, 2018. **359**(6371): p. 91-97.
327. Ansaldo, E., et al., *Akkermansia muciniphila induces intestinal adaptive immune responses during homeostasis.* Science, 2019. **364**(6446): p. 1179-1184.
328. Cebula, A., et al., *Thymus-derived regulatory T cells contribute to tolerance to commensal microbiota.* Nature, 2013. **497**(7448): p. 258-262.
329. Nutsch, K., et al., *Rapid and Efficient Generation of Regulatory T Cells to Commensal Antigens in the Periphery.* Cell Rep, 2016. **17**(1): p. 206-220.

330. Chai, J.N., et al., *Helicobacter species are potent drivers of colonic T cell responses in homeostasis and inflammation.* Science Immunology, 2017. **2**(13).
331. Stefka, A.T., et al., *Commensal bacteria protect against food allergen sensitization.* Proc Natl Acad Sci U S A, 2014. **111**(36): p. 13145-50.
332. Karimi, K., et al., *Lactobacillus reuteri-induced regulatory T cells protect against an allergic airway response in mice.* Am J Respir Crit Care Med, 2009. **179**(3): p. 186-93.
333. Round, J.L. and S.K. Mazmanian, *Inducible Foxp3+ regulatory T-cell development by a commensal bacterium of the intestinal microbiota.* Proc Natl Acad Sci U S A, 2010. **107**(27): p. 12204-9.
334. Mazmanian, S.K., J.L. Round, and D.L. Kasper, *A microbial symbiosis factor prevents intestinal inflammatory disease.* Nature, 2008. **453**(7195): p. 620-5.
335. den Besten, G., et al., *The role of short-chain fatty acids in the interplay between diet, gut microbiota, and host energy metabolism.* Journal of lipid research, 2013. **54**(9): p. 2325-2340.
336. Smith, P.M., et al., *The microbial metabolites, short-chain fatty acids, regulate colonic Treg cell homeostasis.* Science, 2013. **341**(6145): p. 569-73.
337. Furusawa, Y., et al., *Commensal microbe-derived butyrate induces the differentiation of colonic regulatory T cells.* Nature, 2013. **504**(7480): p. 446-450.
338. Quigley, E.M.M. and P. Gajula, *Recent advances in modulating the microbiome.* F1000Research, 2020. **9**: p. F1000 Faculty Rev-46.
339. Azad, M.A.K., et al., *Probiotic Species in the Modulation of Gut Microbiota: An Overview.* BioMed research international, 2018. **2018**: p. 9478630-9478630.
340. Ianiro, G., et al., *Efficacy of different faecal microbiota transplantation protocols for Clostridium difficile infection: A systematic review and meta-analysis.* United European Gastroenterol J, 2018. **6**(8): p. 1232-1244.
341. Levy, A.N. and J.R. Allegretti, *Insights into the role of fecal microbiota transplantation for the treatment of inflammatory bowel disease.* Therapeutic advances in gastroenterology, 2019. **12**: p. 1756284819836893-1756284819836893.
342. Kamanaka, M., et al., *Expression of interleukin-10 in intestinal lymphocytes detected by an interleukin-10 reporter knockin tiger mouse.* Immunity, 2006. **25**(6): p. 941-52.
343. Komatsu, N., et al., *Heterogeneity of natural Foxp3⁺ T cells: A committed regulatory T-cell lineage and an uncommitted minor population retaining plasticity.* Proceedings of the National Academy of Sciences, 2009. **106**(6): p. 1903-1908.
344. Pearson, C., et al., *ILC3 GM-CSF production and mobilisation orchestrate acute intestinal inflammation.* Elife, 2016. **5**: p. e10066.
345. Gerner, M.Y., et al., *Histo-cytometry: a method for highly multiplex quantitative tissue imaging analysis applied to dendritic cell subset microanatomy in lymph nodes.* Immunity, 2012. **37**(2): p. 364-76.
346. Wershil, B.K. and G.T. Furuta, *4. Gastrointestinal mucosal immunity.* J Allergy Clin Immunol, 2008. **121**(2 Suppl): p. S380-3; quiz S415.
347. Esterhazy, D., et al., *Compartmentalized gut lymph node drainage dictates adaptive immune responses.* Nature, 2019. **569**(7754): p. 126-130.
348. Hamada, H., et al., *Identification of Multiple Isolated Lymphoid Follicles on the Antimesenteric Wall of the Mouse Small Intestine.* The Journal of Immunology, 2002. **168**(1): p. 57-64.

349. Fontenot, J.D., et al., *A function for interleukin 2 in Foxp3-expressing regulatory T cells.* Nat Immunol, 2005. **6**(11): p. 1142-51.
350. Alvarez, F., J.H. Fritz, and C.A. Piccirillo, *Pleiotropic Effects of IL-33 on CD4+ T Cell Differentiation and Effector Functions.* Frontiers in Immunology, 2019. **10**(522).
351. Pichery, M., et al., *Endogenous IL-33 is highly expressed in mouse epithelial barrier tissues, lymphoid organs, brain, embryos, and inflamed tissues: in situ analysis using a novel Il-33-LacZ gene trap reporter strain.* J Immunol, 2012. **188**(7): p. 3488-95.
352. Senn, K.A., et al., *T1-deficient and T1-Fc-transgenic mice develop a normal protective Th2-type immune response following infection with Nippostrongylus brasiliensis.* Eur J Immunol, 2000. **30**(7): p. 1929-38.
353. Hoshino, K., et al., *The absence of interleukin 1 receptor-related T1/ST2 does not affect T helper cell type 2 development and its effector function.* J Exp Med, 1999. **190**(10): p. 1541-8.
354. Louten, J., et al., *Endogenous IL-33 enhances Th2 cytokine production and T-cell responses during allergic airway inflammation.* Int Immunol, 2011. **23**(5): p. 307-15.
355. Oboki, K., et al., *IL-33 is a crucial amplifier of innate rather than acquired immunity.* Proc Natl Acad Sci U S A, 2010. **107**(43): p. 18581-6.
356. Pastorelli, L., et al., *Novel cytokine signaling pathways in inflammatory bowel disease: insight into the dichotomous functions of IL-33 during chronic intestinal inflammation.* Therapeutic Advances in Gastroenterology, 2011. **4**(5): p. 311-323.
357. Kolodin, D., et al., *Antigen- and cytokine-driven accumulation of regulatory T cells in visceral adipose tissue of lean mice.* Cell Metab, 2015. **21**(4): p. 543-57.
358. Molofsky, A.B., et al., *Interleukin-33 and Interferon-γ Counter-Regulate Group 2 Innate Lymphoid Cell Activation during Immune Perturbation.* Immunity, 2015. **43**(1): p. 161-74.
359. Vasanthakumar, A., et al., *The transcriptional regulators IRF4, BATF and IL-33 orchestrate development and maintenance of adipose tissue–resident regulatory T cells.* Nature Immunology, 2015. **16**(3): p. 276-285.
360. Schiering, C., et al., *The alarmin IL-33 promotes regulatory T-cell function in the intestine.* Nature, 2014. **513**(7519): p. 564-568.
361. Buettner, M. and M. Lochner, *Development and Function of Secondary and Tertiary Lymphoid Organs in the Small Intestine and the Colon.* Frontiers in Immunology, 2016. **7**(342).
362. Krummel, M.F., et al., *Paracrine costimulation of IFN-γ signaling by integrins modulates CD8 T cell differentiation.* Proceedings of the National Academy of Sciences, 2018. **115**(45): p. 11585-11590.
363. Gottschalk, R.A., E. Corse, and J.P. Allison, *Expression of Helios in Peripherally Induced Foxp3⁺ Regulatory T Cells.* The Journal of Immunology, 2012. **188**(3): p. 976-980.
364. Singh, K., et al., *Concomitant analysis of Helios and Neuropilin-1 as a marker to detect thymic derived regulatory T cells in naïve mice.* Scientific Reports, 2015. **5**(1): p. 7767.
365. Szurek, E., et al., *Differences in Expression Level of Helios and Neuropilin-1 Do Not Distinguish Thymus-Derived from Extrathymically-Induced CD4+Foxp3+ Regulatory T Cells.* PLoS One, 2015. **10**(10): p. e0141161.

366. Wohlfert, E.A., et al., *GATA3 controls Foxp3+ regulatory T cell fate during inflammation in mice.* The Journal of Clinical Investigation, 2011. **121**(11): p. 4503-4515.
367. Wohlfert, E.A., et al., *GATA3 controls Foxp3(+) regulatory T cell fate during inflammation in mice.* J Clin Invest, 2011. **121**(11): p. 4503-15.
368. Reboldi, A. and J.G. Cyster, *Peyer's patches: organizing B-cell responses at the intestinal frontier.* Immunological reviews, 2016. **271**(1): p. 230-245.
369. Pabst, O., et al., *Adaptation of Solitary Intestinal Lymphoid Tissue in Response to Microbiota and Chemokine Receptor CCR7 Signaling.* The Journal of Immunology, 2006. **177**(10): p. 6824-6832.
370. Pabst, O., et al., *Cryptopatches and isolated lymphoid follicles: dynamic lymphoid tissues dispensable for the generation of intraepithelial lymphocytes.* Eur J Immunol, 2005. **35**(1): p. 98-107.
371. Baptista, A.P., et al., *Colonic patch and colonic SILT development are independent and differentially regulated events.* Mucosal Immunol, 2013. **6**(3): p. 511-21.
372. Kanamori, Y., et al., *Identification of novel lymphoid tissues in murine intestinal mucosa where clusters of c-kit+ IL-7R+ Thy1+ lympho-hemopoietic progenitors develop.* Journal of Experimental Medicine, 1996. **184**(4): p. 1449-1459.
373. Moghaddami, M., A. Cummins, and G. Mayrhofer, *Lymphocyte-filled villi: comparison with other lymphoid aggregations in the mucosa of the human small intestine.* Gastroenterology, 1998. **115**(6): p. 1414-25.
374. Lochner, M., et al., *Microbiota-induced tertiary lymphoid tissues aggravate inflammatory disease in the absence of RORγt and LTi cells.* The Journal of Experimental Medicine, 2011. **208**(1): p. 125-134.
375. Bouskra, D., et al., *Lymphoid tissue genesis induced by commensals through NOD1 regulates intestinal homeostasis.* Nature, 2008. **456**(7221): p. 507-510.
376. Berg, R.D., *The indigenous gastrointestinal microflora.* Trends Microbiol, 1996. **4**(11): p. 430-5.
377. Fenton, T.M., et al., *Immune Profiling of Human Gut-Associated Lymphoid Tissue Identifies a Role for Isolated Lymphoid Follicles in Priming of Region-Specific Immunity.* Immunity, 2020.
378. Randall, T.D., D.M. Carragher, and J. Rangel-Moreno, *Development of Secondary Lymphoid Organs.* Annual Review of Immunology, 2008. **26**(1): p. 627-650.
379. Pabst, O., et al., *Cryptopatches and isolated lymphoid follicles: dynamic lymphoid tissues dispensable for the generation of intraepithelial lymphocytes.* European Journal of Immunology, 2005. **35**(1): p. 98-107.
380. Pearson, C., H.H. Uhlig, and F. Powrie, *Lymphoid microenvironments and innate lymphoid cells in the gut.* Trends in Immunology, 2012. **33**(6): p. 289-296.
381. Chan, B.C.L., et al., *IL33: Roles in Allergic Inflammation and Therapeutic Perspectives.* Frontiers in Immunology, 2019. **10**(364).
382. Liew, F.Y., N.I. Pitman, and I.B. McInnes, *Disease-associated functions of IL-33: the new kid in the IL-1 family.* Nat Rev Immunol, 2010. **10**(2): p. 103-10.
383. De Togni, P., et al., *Abnormal development of peripheral lymphoid organs in mice deficient in lymphotoxin.* Science, 1994. **264**(5159): p. 703-707.
384. Arpaia, N., et al., *A Distinct Function of Regulatory T Cells in Tissue Protection.* Cell, 2015. **162**(5): p. 1078-1089.
385. Gajardo, T., et al., *Exogenous interleukin-33 targets myeloid-derived suppressor cells and generates periphery-induced Foxp3(+) regulatory T cells in skin-transplanted mice.* Immunology, 2015. **146**(1): p. 81-8.

386. Olivier, B.J., et al., *Vagal innervation is required for the formation of tertiary lymphoid tissue in colitis.* Eur J Immunol, 2016. **46**(10): p. 2467-2480.
387. Kiss, E.A., et al., *Natural Aryl Hydrocarbon Receptor Ligands Control Organogenesis of Intestinal Lymphoid Follicles.* Science, 2011. **334**(6062): p. 1561-1565.
388. Fernandez-Salguero, P.M., et al., *Lesions of Aryl-hydrocarbon Receptor–deficient Mice.* Veterinary Pathology, 1997. **34**(6): p. 605-614.
389. Tsuji, M., et al., *Requirement for lymphoid tissue-inducer cells in isolated follicle formation and T cell-independent immunoglobulin A generation in the gut.* Immunity, 2008. **29**(2): p. 261-71.
390. Wang, C., et al., *Murine isolated lymphoid follicles contain follicular B lymphocytes with a mucosal phenotype.* American journal of physiology. Gastrointestinal and liver physiology, 2006. **291**(4): p. G595-G604.
391. Fung, T.C., et al., *Lymphoid-Tissue-Resident Commensal Bacteria Promote Members of the IL-10 Cytokine Family to Establish Mutualism.* Immunity, 2016. **44**(3): p. 634-646.
392. Ota, N., et al., *IL-22 bridges the lymphotoxin pathway with the maintenance of colonic lymphoid structures during infection with Citrobacter rodentium.* Nat Immunol, 2011. **12**(10): p. 941-8.
393. Pitzalis, C., et al., *Ectopic lymphoid-like structures in infection, cancer and autoimmunity.* Nature Reviews Immunology, 2014. **14**(7): p. 447-462.
394. Drayton, D.L., et al., *Lymphoid organ development: from ontogeny to neogenesis.* Nature Immunology, 2006. **7**(4): p. 344-353.
395. Takemura, S., et al., *Lymphoid Neogenesis in Rheumatoid Synovitis.* The Journal of Immunology, 2001. **167**(2): p. 1072-1080.
396. Chang, A., et al., *In Situ B Cell-Mediated Immune Responses and Tubulointerstitial Inflammation in Human Lupus Nephritis.* The Journal of Immunology, 2011. **186**(3): p. 1849-1860.
397. Armengol, M.-P., et al., *Chemokines Determine Local Lymphoneogenesis and a Reduction of Circulating CXCR4⁺ T and CCR7 B and T Lymphocytes in Thyroid Autoimmune Diseases.* The Journal of Immunology, 2003. **170**(12): p. 6320-6328.
398. Magliozzi, R., et al., *Meningeal B-cell follicles in secondary progressive multiple sclerosis associate with early onset of disease and severe cortical pathology.* Brain, 2007. **130**(4): p. 1089-1104.
399. Rangel-Moreno, J., et al., *Inducible bronchus-associated lymphoid tissue (iBALT) in patients with pulmonary complications of rheumatoid arthritis.* The Journal of Clinical Investigation, 2006. **116**(12): p. 3183-3194.
400. Dieu-Nosjean, M.C., et al., *Long-term survival for patients with non-small-cell lung cancer with intratumoral lymphoid structures.* J Clin Oncol, 2008. **26**(27): p. 4410-7.
401. de Chaisemartin, L., et al., *Characterization of Chemokines and Adhesion Molecules Associated with T cell Presence in Tertiary Lymphoid Structures in Human Lung Cancer.* Cancer Research, 2011. **71**(20): p. 6391-6399.
402. García-Hernández, M.d.l.L., et al., *A Unique Cellular and Molecular Microenvironment Is Present in Tertiary Lymphoid Organs of Patients with Spontaneous Prostate Cancer Regression.* Frontiers in Immunology, 2017. **8**(563).
403. Cabrita, R., et al., *Tertiary lymphoid structures improve immunotherapy and survival in melanoma.* Nature, 2020. **577**(7791): p. 561-565.

404. Helmink, B.A., et al., *B cells and tertiary lymphoid structures promote immunotherapy response.* Nature, 2020. **577**(7791): p. 549-555.
405. Petitprez, F., et al., *B cells are associated with survival and immunotherapy response in sarcoma.* Nature, 2020. **577**(7791): p. 556-560.
406. Smith, K., K.D. McCoy, and A.J. Macpherson, *Use of axenic animals in studying the adaptation of mammals to their commensal intestinal microbiota.* Seminars in Immunology, 2007. **19**(2): p. 59-69.
407. Helgeland, L., et al., *Regional phenotypic specialization of intraepithelial lymphocytes in the rat intestine does not depend on microbial colonization.* Scand J Immunol, 1997. **46**(4): p. 349-57.
408. Helgeland, L., et al., *Microbial colonization influences composition and T-cell receptor V beta repertoire of intraepithelial lymphocytes in rat intestine.* Immunology, 1996. **89**(4): p. 494-501.
409. Guy-Grand, D., C. Griscelli, and P. Vassalli, *The mouse gut T lymphocyte, a novel type of T cell. Nature, origin, and traffic in mice in normal and graft-versus-host conditions.* J Exp Med, 1978. **148**(6): p. 1661-77.
410. Theriot, C.M., A.A. Bowman, and V.B. Young, *Antibiotic-Induced Alterations of the Gut Microbiota Alter Secondary Bile Acid Production and Allow for Clostridium difficile Spore Germination and Outgrowth in the Large Intestine.* mSphere, 2016. **1**(1).
411. Fernández-Santoscoy, M., et al., *The Gut Microbiota Reduces Colonization of the Mesenteric Lymph Nodes and IL-12-Independent IFN-γ Production During Salmonella Infection.* Front Cell Infect Microbiol, 2015. **5**: p. 93.
412. Kinnebrew, M.A., et al., *Bacterial flagellin stimulates Toll-like receptor 5-dependent defense against vancomycin-resistant Enterococcus infection.* J Infect Dis, 2010. **201**(4): p. 534-43.
413. Brown, R.L., R.P. Sequeira, and T.B. Clarke, *The microbiota protects against respiratory infection via GM-CSF signaling.* Nat Commun, 2017. **8**(1): p. 1512.
414. Robak, O.H., et al., *Antibiotic treatment-induced secondary IgA deficiency enhances susceptibility to Pseudomonas aeruginosa pneumonia.* J Clin Invest, 2018. **128**(8): p. 3535-3545.
415. Deshmukh, H.S., et al., *The microbiota regulates neutrophil homeostasis and host resistance to Escherichia coli K1 sepsis in neonatal mice.* Nat Med, 2014. **20**(5): p. 524-30.
416. Izcue, A., et al., *Interleukin-23 restrains regulatory T cell activity to drive T cell-dependent colitis.* Immunity, 2008. **28**(4): p. 559-70.
417. Bluthmann, H., et al., *T-cell-specific deletion of T-cell receptor transgenes allows functional rearrangement of endogenous alpha- and beta-genes.* Nature, 1988. **334**(6178): p. 156-9.
418. Chiaranunt, P., et al., *T Cell Proliferation and Colitis Are Initiated by Defined Intestinal Microbes.* The Journal of Immunology, 2018. **201**(1): p. 243-250.
419. Xu, M., et al., *c-MAF-dependent regulatory T cells mediate immunological tolerance to a gut pathobiont.* Nature, 2018. **554**(7692): p. 373-377.
420. Levine, A.G., et al., *Continuous requirement for the TCR in regulatory T cell function.* Nat Immunol, 2014. **15**(11): p. 1070-8.
421. Szabo, P.A., M. Miron, and D.L. Farber, *Location, location, location: Tissue resident memory T cells in mice and humans.* Science Immunology, 2019. **4**(34): p. eaas9673.

422. Ashouri, J.F. and A. Weiss, *Endogenous Nur77 Is a Specific Indicator of Antigen Receptor Signaling in Human T and B Cells.* Journal of immunology (Baltimore, Md. : 1950), 2017. **198**(2): p. 657-668.
423. Moran, A.E., et al., *T cell receptor signal strength in Treg and iNKT cell development demonstrated by a novel fluorescent reporter mouse.* J Exp Med, 2011. **208**(6): p. 1279-89.
424. Mehling, M., et al., *FTY720 therapy exerts differential effects on T cell subsets in multiple sclerosis.* Neurology, 2008. **71**(16): p. 1261-7.
425. Demangel, C., P. Bertolino, and W.J. Britton, *Autocrine IL-10 impairs dendritic cell (DC)-derived immune responses to mycobacterial infection by suppressing DC trafficking to draining lymph nodes and local IL-12 production.* Eur J Immunol, 2002. **32**(4): p. 994-1002.
426. Schandené, L., et al., *B7/CD28-dependent IL-5 production by human resting T cells is inhibited by IL-10.* The Journal of Immunology, 1994. **152**(9): p. 4368-4374.
427. Joss, A., et al., *IL-10 directly acts on T cells by specifically altering the CD28 co-stimulation pathway.* Eur J Immunol, 2000. **30**(6): p. 1683-90.
428. De Togni, P., et al., *Abnormal development of peripheral lymphoid organs in mice deficient in lymphotoxin.* Science, 1994. **264**(5159): p. 703-7.
429. Taylor, R.T., et al., *Intestinal Cryptopatch Formation in Mice Requires Lymphotoxin α and the Lymphotoxin β Receptor.* The Journal of Immunology, 2004. **173**(12): p. 7183-7189.
430. Fagarasan, S., et al., *Adaptive Immune Regulation in the Gut: T Cell–Dependent and T Cell–Independent IgA Synthesis.* Annual Review of Immunology, 2010. **28**(1): p. 243-273.
431. Kroese, F.G.M., R. de Waard, and N.A. Bos, *B-1 cells and their reactivity with the murine intestinal microflora.* Seminars in Immunology, 1996. **8**(1): p. 11-18.
432. Tsuruta, T., et al., *The amount of secreted IgA may not determine the secretory IgA coating ratio of gastrointestinal bacteria.* FEMS Immunology & Medical Microbiology, 2009. **56**(2): p. 185-189.
433. van der Waaij, L.A., et al., *In vivo IgA coating of anaerobic bacteria in human faeces.* Gut, 1996. **38**(3): p. 348-354.
434. Zeng, M.Y., et al., *Gut Microbiota-Induced Immunoglobulin G Controls Systemic Infection by Symbiotic Bacteria and Pathogens.* Immunity, 2016. **44**(3): p. 647-658.
435. Hollister, K., et al., *Insights into the role of Bcl6 in follicular Th cells using a new conditional mutant mouse model.* J Immunol, 2013. **191**(7): p. 3705-11.
436. Eberl, G. and S. Sawa, *Opening the crypt: current facts and hypotheses on the function of cryptopatches.* Trends Immunol, 2010. **31**(2): p. 50-5.
437. Dohi, T., et al., *Elimination of colonic patches with lymphotoxin beta receptor-Ig prevents Th2 cell-type colitis.* J Immunol, 2001. **167**(5): p. 2781-90.
438. Browning, J.L., *Inhibition of the lymphotoxin pathway as a therapy for autoimmune disease.* Immunological Reviews, 2008. **223**(1): p. 202-220.
439. Chen, W., et al., *Conversion of peripheral CD4+CD25- naive T cells to CD4+CD25+ regulatory T cells by TGF-beta induction of transcription factor Foxp3.* The Journal of experimental medicine, 2003. **198**(12): p. 1875-1886.
440. Duell, B.L., et al., *Recent insights into microbial triggers of interleukin-10 production in the host and the impact on infectious disease pathogenesis.* FEMS Immunology & Medical Microbiology, 2012. **64**(3): p. 295-313.

441. Kamanaka, M., et al., *Expression of interleukin-10 in intestinal lymphocytes detected by an interleukin-10 reporter knockin tiger mouse.* Immunity, 2006. **25**(6): p. 941-52.
442. Moore, K.W., et al., *Interleukin-10 and the Interleukin-10 Receptor.* Annual Review of Immunology, 2001. **19**(1): p. 683-765.
443. Zigmond, E., et al., *Macrophage-Restricted Interleukin-10 Receptor Deficiency, but Not IL-10 Deficiency, Causes Severe Spontaneous Colitis.* Immunity, 2014. **40**(5): p. 720-733.
444. Pot, C., et al., *Cutting edge: IL-27 induces the transcription factor c-Maf, cytokine IL-21, and the costimulatory receptor ICOS that coordinately act together to promote differentiation of IL-10-producing Tr1 cells.* J Immunol, 2009. **183**(2): p. 797-801.
445. Spolski, R., et al., *IL-21 mediates suppressive effects via its induction of IL-10.* Journal of immunology (Baltimore, Md. : 1950), 2009. **182**(5): p. 2859-2867.
446. Worbs, T., et al., *Oral tolerance originates in the intestinal immune system and relies on antigen carriage by dendritic cells.* The Journal of experimental medicine, 2006. **203**(3): p. 519-527.
447. Huang, F.P., et al., *A discrete subpopulation of dendritic cells transports apoptotic intestinal epithelial cells to T cell areas of mesenteric lymph nodes.* J Exp Med, 2000. **191**(3): p. 435-44.
448. Spahn, T.W., et al., *Mesenteric lymph nodes are critical for the induction of high-dose oral tolerance in the absence of Peyer's patches.* Eur J Immunol, 2002. **32**(4): p. 1109-13.
449. Macpherson, A.J. and T. Uhr, *Induction of Protective IgA by Intestinal Dendritic Cells Carrying Commensal Bacteria.* Science, 2004. **303**(5664): p. 1662-1665.
450. Brinkman, C., J. Peske, and V. Engelhard, *Peripheral Tissue Homing Receptor Control of Naïve, Effector, and Memory CD8 T Cell Localization in Lymphoid and Non-Lymphoid Tissues.* Frontiers in Immunology, 2013. **4**(241).
451. Veiga-Fernandes, H., et al., *Tyrosine kinase receptor RET is a key regulator of Peyer's Patch organogenesis.* Nature, 2007. **446**(7135): p. 547-551.
452. Hampton, H.R. and T. Chtanova, *Lymphatic Migration of Immune Cells.* Frontiers in immunology, 2019. **10**: p. 1168-1168.
453. Miyasaka, M. and T. Tanaka, *Lymphocyte trafficking across high endothelial venules: dogmas and enigmas.* Nat Rev Immunol, 2004. **4**(5): p. 360-70.
454. Eberl, G. and S. Sawa, *Opening the crypt: current facts and hypotheses on the function of cryptopatches.* Trends in Immunology, 2010. **31**(2): p. 50-55.
455. Kanamori, Y., et al., *Identification of novel lymphoid tissues in murine intestinal mucosa where clusters of c-kit+ IL-7R+ Thy1+ lympho-hemopoietic progenitors develop.* J Exp Med, 1996. **184**(4): p. 1449-59.
456. Lügering, A., et al., *CCR6 identifies lymphoid tissue inducer cells within cryptopatches.* Clinical & Experimental Immunology, 2010. **160**(3): p. 440-449.
457. LORENZ, R.G. and R.D. NEWBERRY, *Isolated Lymphoid Follicles Can Function as Sites for Induction of Mucosal Immune Responses.* Annals of the New York Academy of Sciences, 2004. **1029**(1): p. 44-57.
458. Wang, C., et al., *Murine isolated lymphoid follicles contain follicular B lymphocytes with a mucosal phenotype.* American Journal of Physiology-Gastrointestinal and Liver Physiology, 2006. **291**(4): p. G595-G604.
459. Fagarasan, S., et al., *Critical roles of activation-induced cytidine deaminase in the homeostasis of gut flora.* Science, 2002. **298**(5597): p. 1424-1427.

460. Eberl, G., et al., *An essential function for the nuclear receptor RORγt in the generation of fetal lymphoid tissue inducer cells.* Nature Immunology, 2004. **5**(1): p. 64-73.
461. Lorenz, R.G., et al., *Isolated Lymphoid Follicle Formation Is Inducible and Dependent Upon Lymphotoxin-Sufficient B Lymphocytes, Lymphotoxin β Receptor, and TNF Receptor I Function.* The Journal of Immunology, 2003. **170**(11): p. 5475-5482.
462. McDonald, K.G., et al., *Dendritic Cells Produce CXCL13 and Participate in the Development of Murine Small Intestine Lymphoid Tissues.* The American Journal of Pathology, 2010. **176**(5): p. 2367-2377.
463. McDole, J.R., et al., *Goblet cells deliver luminal antigen to CD103+ dendritic cells in the small intestine.* Nature, 2012. **483**(7389): p. 345-349.
464. Kuehl, C.J., et al., *Colonization of the cecal mucosa by Helicobacter hepaticus impacts the diversity of the indigenous microbiota.* Infection and immunity, 2005. **73**(10): p. 6952-6961.
465. Victora, G.D., et al., *Germinal Center Dynamics Revealed by Multiphoton Microscopy Using a Photoactivatable Fluorescent Reporter.* Cell, 2010. **143**(4): p. 592-605.
466. Halle, S., et al., *Induced bronchus-associated lymphoid tissue serves as a general priming site for T cells and is maintained by dendritic cells.* The Journal of experimental medicine, 2009. **206**(12): p. 2593-2601.
467. van de Pavert, S.A. and R.E. Mebius, *New insights into the development of lymphoid tissues.* Nature Reviews Immunology, 2010. **10**(9): p. 664-674.
468. McLachlan, J.B., et al., *Dendritic cell antigen presentation drives simultaneous cytokine production by effector and regulatory T cells in inflamed skin.* Immunity, 2009. **30**(2): p. 277-88.
469. Hirota, K., et al., *Fate mapping of IL-17-producing T cells in inflammatory responses.* Nature immunology, 2011. **12**(3): p. 255-263.
470. Lüthje, K., et al., *The development and fate of follicular helper T cells defined by an IL-21 reporter mouse.* Nat Immunol, 2012. **13**(5): p. 491-8.
471. Lin, W., et al., *Regulatory T cell development in the absence of functional Foxp3.* Nat Immunol, 2007. **8**(4): p. 359-68.
472. Chinen, T., et al., *An essential role for the IL-2 receptor in T(reg) cell function.* Nat Immunol, 2016. **17**(11): p. 1322-1333.
473. Pasqual, G., et al., *Monitoring T cell-dendritic cell interactions in vivo by intercellular enzymatic labelling.* Nature, 2018. **553**(7689): p. 496-500.
474. Halle, S., et al., *Solitary Intestinal Lymphoid Tissue Provides a Productive Port of Entry for Salmonella enterica Serovar Typhimurium.* Infection and Immunity, 2007. **75**(4): p. 1577-1585.
475. Schenkel, J.M. and D. Masopust, *Tissue-resident memory T cells.* Immunity, 2014. **41**(6): p. 886-97.
476. Romano, M., et al., *Past, Present, and Future of Regulatory T Cell Therapy in Transplantation and Autoimmunity.* Frontiers in Immunology, 2019. **10**(43).
477. Yamazaki, S., et al., *Homeostasis of thymus-derived Foxp3+ regulatory T cells is controlled by ultraviolet B exposure in the skin.* J Immunol, 2014. **193**(11): p. 5488-97.
478. Delacher, M., et al., *Genome-wide DNA-methylation landscape defines specialization of regulatory T cells in tissues.* Nat Immunol, 2017. **18**(10): p. 1160-1172.

479. Malhotra, N., et al., *RORα-expressing T regulatory cells restrain allergic skin inflammation.* Science Immunology, 2018. **3**(21): p. eaao6923.
480. Fessler, J., V. Matson, and T.F. Gajewski, *Exploring the emerging role of the microbiome in cancer immunotherapy.* Journal for ImmunoTherapy of Cancer, 2019. **7**(1): p. 108.
481. Gopalakrishnan, V., et al., *Gut microbiome modulates response to anti–PD-1 immunotherapy in melanoma patients.* Science, 2018. **359**(6371): p. 97-103.
482. Routy, B., et al., *Gut microbiome influences efficacy of PD-1-based immunotherapy against epithelial tumors.* Science, 2018. **359**(6371): p. 91-97.
483. Togashi, Y., K. Shitara, and H. Nishikawa, *Regulatory T cells in cancer immunosuppression — implications for anticancer therapy.* Nature Reviews Clinical Oncology, 2019. **16**(6): p. 356-371.